A Modelling Study of the Impact of Surface Interactions on Indoor Air Quality

Magdalena Kruza

PhD

University of York

Environment

December 2017

Abstract

Although people in developed countries spend ~90% of their time indoors, indoor air quality has received little attention to date. The sparsity of measurements indoors, means that models are currently the best tool to provide insight into indoor air chemistry. This thesis examines the surface interactions indoors using a detailed chemical model, focusing on pollutant formation following ozone deposition on different indoor surfaces as well as from occupants.

The results from a simulated apartment show that ~80% of ozone indoors is deposited to surfaces, whereby subsequent interactions produce emissions of mainly oxygenated species (8-16 ppb) that were highest when ozone concentrations were enhanced outdoors. Replacing traditional furnishing materials with 'green' alternatives produced aldehyde concentrations that were 3 times lower.

Skin and breath emissions are also shown to impact indoor air quality depending on ventilation, volume and occupancy. The impact of breath emissions increases with decreasing ventilation rate, whereas that from skin emissions does the opposite. Human emissions are important in small areas (e.g. bedrooms) or high occupancy locations (such as classrooms). For instance, such emissions were 4-10 times higher in a bedroom compared to the whole apartment.

Experimental and modelling results in this dissertation show that there is significant variation in the concentrations of some pollutants following oxidation of different terpene mixtures. There is a potential for improving consumer product formulations using less reactive mixtures, resulting in less exposure to potentially harmful secondary products.

This study provides a valuable contribution to the understanding of indoor air chemistry. Ozone-derived surface emissions from materials and people, and also occupant activity indoors can impact chemical processing, through enhanced formation of secondary pollutants and decreased levels of oxidants. Consequently, there is a need for indoor air quality guidelines and policy regulation development.

List of Contents

List of Tables

List of Figures

Acknowledgements

Firstly, I would like to thank to my supervisor, Dr Nicola Carslaw, for her constant help and support. She always found time for me, taking care about my work and all the questions I had. I learned a lot from her and this knowledge is just priceless. Her encouragement, motivation, patience and great guidance were extremely helpful to complete my doctorate programme, even along with personal events like getting married! Also, I would like to thank to my second supervisor, Prof. Ally Lewis, for his support and useful advices he was providing during my doctorate programme.

I wish to thank to my family and friends. Particularly, I would like to thank to my husband, Jorge, for his love, patience and support during all the time of my research. His encouragement was invaluable during all of the ups and downs of my study. I would love to thank to my parents, Bogusia and Krzysztof, for their constant love and support, which last for over 30 years. Without their help and encouragement I would never achieve what I already did in my life.

I would like to show my gratitude to people who provided great help and support during my research. Particularly, I would like to thank to Dr Ray Wells and his group at NIOSH for their help with the experimental work, the comments on Chapter 6 of this work, and also for making my internship at NIOSH as fruitful time, during which I felt like part of the team. Also, I wish to thank to Prof. Glenn Morrison for his useful suggestions and comments he made in reference to the work published in the scientific journal Indoor Air (2017). I also appreciate support of Dr Paula Olsiewski and Alfred P. Sloan Foundation, who gathered the indoor air community together during great social events.

Finally, I would like to acknowledge the Cutting - Edge Approaches for Pollution Assessment in Cities (CAPACITIE) project, which has received funding from the European Union's Seventh Framework Programme (grant agreement no 608014), not only for the financial support but also for the research and personal experience I got during this Marie Curie doctoral training programme. Thank you to Prof. Alistair Boxall, who made it all happen, and to all the members of the CAPACITIE team, who made it unforgettable.

Declaration

I declare that this thesis is a presentation of original work and I am the sole author. This work has not previously been presented for an award at this, or any other, University. All sources are acknowledged as References.

The work of Chapter 4 has been published in the scientific journal Indoor Air (2017), for which I was the principal author.

To cite: *Kruza M., Lewis A.C., Morrison G.C. and Carslaw N., 2017. Impact of surface ozone interactions on indoor air chemistry: A modelling study. Indoor Air; 27(5):1001-1011.*

1. Introduction

1.1 General introduction

1.1.1 Indoor air quality

Since the 1970s, increasing attention has been paid to indoor air quality (Wolkoff et al., 2000; 2013). For decades the biggest focus was on outdoor air pollution, with relatively little for the indoor environment. The impact of higher energy costs following the oil crisis in the 1970s resulted in tighter building envelopes with reduced ventilation rates. New and retrofitted buildings had better insulation (e.g. double glazing, cavity wall and loft insulation), leading to better energy efficiency, but often poorer indoor air quality (Dimitroulopoulou, 2012). Over the same period, we have become a much more consumer driven society, driven to buy new things more frequently than previous generations. This increased consumerism can be a problem, because there are typically higher emissions of chemicals from new materials compared to older ones. For instance, VOC (Volatile Organic Compound) concentrations that were 1-2 orders of magnitude higher were noticed in newly installed buildings compared to older ones and these persisted for several weeks to months (Brown, 2002; Hodgson et al., 2002). Finally, we have become much more conscious of hygiene and clean ourselves, our homes and offices far more frequently than in the past. Coupled with these changes over the last 50 years, we also spend much more time indoors. It has been estimated that in developed countries, we spend approximately 90% of our time inside (i.e. at home, in the work place or commuting) and consequently most of our exposure to air pollution occurs indoors (Carslaw, 2007). To summarise, we are spending more time indoors in buildings that are more airtight than they used to be and with a much higher range of indoor chemical emissions.

Over the same time period, increased health effects have been reported for some building occupants (Ashmore and Dimitroulopoulou, 2009; Wolkoff, 2013). Indoor air pollutants have been reported to cause a range of adverse health effects such as skin and eye irritation, upper airway irritation, and even carcinogenic and mutagenic effects (Uhde and Salthammer, 2007; Wolkoff, 2013). The irritation effects are sometimes collectively referred to as 'sick building syndrome' (SBS) (Jurvelin et al., 2011). Such a phenomenon is defined when a building's occupants repeatedly suffer and complain about such health symptoms (Horvath, 1997). Notably, the symptoms improve or completely disappear when they leave

the building. The symptoms of SBS are usually reported in offices, but also in schools and homes: they are more common in modern energy-efficient buildings (Jones, 1999). Very often it is impossible to define the specific aspect responsible for health complaints (Lahtinen et al., 1998). The most frequently reported symptoms are headaches, tiredness and eye and upper airway irritation (Wolkoff et al., 2006; Wolkoff, 2013). Several studies (i.e. Berglund et al. 1992; Dimitroulopoulou, 2012; Tham, 2016) suggested that longer-term health symptoms such as allergy, asthma, skin irritation or immune system disease may be also associated with indoor air pollution.

Several guidelines for the indoor environment exist, such as from the World Health Organisation (WHO, 2010) and Scientific Committee on Health and Environmental Risk (SCHER, 2007) which provides limit values for indoor compounds or general recommendation on indoor air quality that can affect human health and can be used for toxicological risk assessment. For instance, a WHO guideline value for formaldehyde, which is recognised as a carcinogenic compound, is specified as a maximum concentration of 80 ppb for a 30 minute exposure. However, the INDEX (indoor exposure limits) report of the European Union gives a NOAEL (the no-observed-adverse-effect-level) value for formaldehyde of 30 μg m^{-3} (24 ppb).

Indoor air quality is recognised as a multi-disciplinary phenomenon and can be affected by many physical (e.g. lighting, heating), biological (e.g. mould and spores), chemical (e.g. emissions from personal care and cleaning products, furnishings and building materials) and building (location, ventilation regime, building operation) parameters (Tham, 2016). Such complexity often makes indoor air quality challenging to understand. Ideally, it would be valuable to measure the concentration of pollutants indoors and the personal exposure of indoor occupants to such pollutants. However, given the fact that indoor air often contains a complex mixture of pollutants, it is difficult to identify the many different components and even more challenging to quantify their concentrations analytically (Terry et al., 2014).

1.1.2 Sources of indoor air pollution

There are many different sources of indoor air pollution. Indoor air pollutants are generated through activities such as cooking, cleaning and smoking, as well as emitted from building materials like painted walls, ceilings and wood, and furnishing (Carslaw et al., 2012). For instance, the German Committee for Health Related Evaluation of Building Products (AgBB)

specified more than 150 compounds that can be distinguished from emissions from building products (Schripp et al., 2014). Consumer products such as cleaning agents, air fresheners and personal care products contain terpene species, such as limonene or α-pinene, frequently derived from plant oils with characteristic pleasant aromas (Singer et al., 2006). Along with that, the emissions of VOCs, semi-VOCs (SVOCs) or particular matter (PM) from building materials or indoor activities can increase the pollutant concentrations indoors and negatively impact indoor air quality (Trantallidi et al., 2015). As well as indoor emissions, indoor air pollutants can ingress from outdoors through open windows and doors as well as through cracks in the building fabric (Figure 1). Therefore, indoor environments often contain higher concentrations of air pollutants than outdoors (Brown, 2002; Wolkoff et al., 2013).
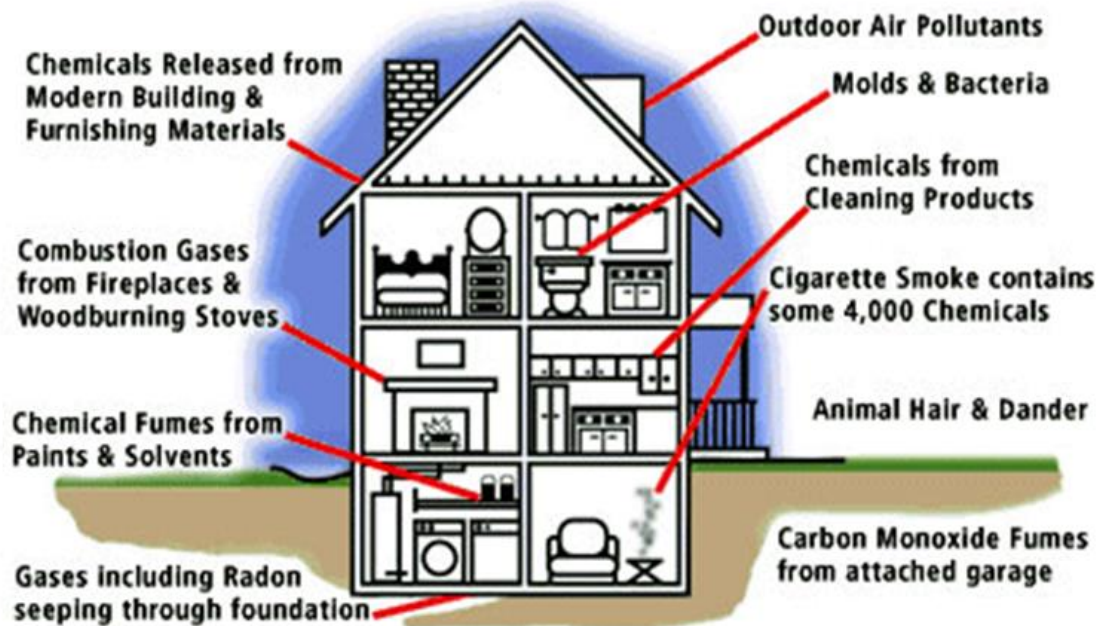
Figure 1: Sources of indoor air pollution (Source: Below Zero Heating and Air Conditioning, 2017).

It is generally accepted through measurements that there is a strong relationship between outdoor and indoor air pollutant concentrations (Blondeau et al., 2005). Outdoor ozone concentrations are highest downwind of highly polluted, densely populated areas with abundant sunshine. Given that the main source of ozone (O_3) indoors is from outdoors, O_3 concentrations indoors increase as outdoor concentrations increase (Weschler, 2000). It is estimated that 20-70% of ozone outdoors infiltrates indoors (Weschler and Shields, 1996;

Weschler, 2000). The typical indoor/outdoor ratio, calculated as the indoor concentration of ozone divided by the outdoor one, is in the range of 0.2 to 0.7 according to a review by Weschler (2000). This is because once indoors, ozone is lost rapidly on indoor surfaces through deposition, a key theme throughout this dissertation.

Once indoors, we also know that ozone is able to initiate indoor air chemistry. For instance, ozone-initiated reactions with other pollutants indoors (such as terpenes or aldehydes), both in the gas-phase as well as with the surface of indoor materials, contribute to the formation of secondary pollutants, which might be harmful to health (Wolkoff et al., 2006; Weschler, 2011; Wolkoff, 2013). There is a wealth of evidence for such interactions. For instance, Apte et al. (2008) found a correlation between the ambient ozone concentration and the indoor concentrations of some aldehydes, which suggests that ozone rich air was entering the building where measurements took place and undergoing chemical reactions which produced aldehydes (as discussed in Chapters 4 and 5). Therefore, it is important to know outdoor concentrations for a particular location. As well as ambient ozone concentrations, it is also important to know those of nitrogen oxides (NO_X) and VOCs. With some knowledge of the ventilation rate of the building, it is then possible to estimate how much of this ambient pollution can make its way into a building. This enables an investigation of the importance of indoor versus outdoor sources of pollution indoors. Clearly, an identical residential building with the same indoor activities could experience very different indoor air concentrations depending on its location (Carslaw et al., 2015). The chemistry that occurs indoors can be summarised using the schematic in Figure 2.
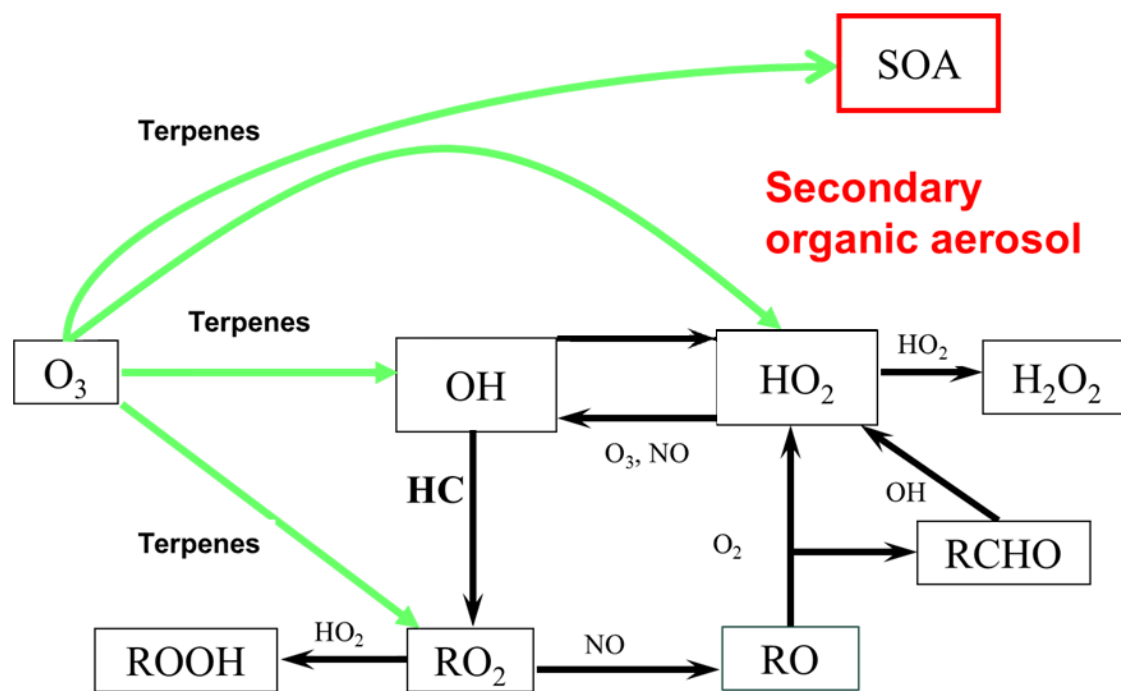
Figure 2: Chemical pathways of the pollutants formation indoors. ROOH denotes organic hydroperoxide, RO_2 peroxy radical, RO oxy radical, RCHO aldehyde, H_2O_2 hydrogen peroxide.

As seen in Figure 2, the chemistry indoors is initiated by ozone, which can react with terpenes. Given that terpenes are frequently used in consumer and personal care products, their indoor concentrations are often higher than those outdoors, particularly following indoor activities such as cleaning (Singer et al., 2006). Terpene-ozone reactions form a range of secondary products, including carbonyl compounds such as aldehydes, ketones, acids (Hodgson et al., 2002; Morrison, 2015), secondary organic aerosols (SOA) (Waring and Siegel, 2013), and radical species, including the hydroxyl (OH) radical, the hydroperoxy radical (HO_2) and organic peroxy radicals (RO_2). These species then participate in further reactions, some of which regenerate radicals and effectively catalyse further oxidation reactions.

Ventilation of buildings is key to preventing poor indoor air quality where indoor sources of pollution dominate. Ventilation is described as 'fresh air' introduced and circulated through the building (Dimitroulopoulou, 2012). Lower ventilation rates can increase the potential for poorer indoor air quality and higher concentrations of indoor air pollutants (Uhde and Salthammer, 2007). In addition, research has shown that lower ventilation rates can be associated with adverse health effects (Wargocki et al., 2000; Sundell et al., 2011). There is also evidence for a relationship between ventilation and comfort of the

indoor occupants as well as their work performance. For instance, in schools, inadequate ventilation has been associated with low performance of pupils (Seppanen et al. 2006; Shaughnessy et al., 2006). For instance, Bakó-Biró et al. (2012) studied the performance of children in a classroom. The results show that performance tasks were achieved significantly faster at higher ventilation rate conditions. On the other hand, a higher infiltration rate of air to the building may lead to energy waste and higher operational costs. Clearly, it is important to balance the ventilation requirements, energy usage and indoor air quality.

As well as pollutants that are directly emitted indoors and those that make their way indoors from outdoors, a third class of pollutants is formed indoors through chemical reactions indoors, including on surfaces. Such interactions often involve deposition of ozone, a surface reaction and then an emission of a VOC, commonly containing the carbonyl functional group (C=O). For instance, Weschler et al. (1992) found that with the presence of ozone in a freshly carpeted chamber, the gas-phase concentration of the total VOCs decreased whilst the concentration of aldehydes formed as secondary products increased. The primary emissions of VOCs that are emitted directly or evaporated from indoor materials and surfaces are non-bound, low weight compounds (Wolkoff, 1999). These emissions influence indoor air quality particularly during the initial period following installation. Over longer periods however, the secondary emissions following surface interactions become more important, as ozone uptake and consequent surface processing to produce secondary pollutants can continue for several years (Wang and Morrison, 2006).

A key focus is therefore to produce healthier building products. It has been recognised for many years that low emitting materials that are certified as such would be better for indoor use (Wolkoff and Nielsen, 2001). Such environmentally friendly 'green' materials are gaining more attention from consumers and manufacturers and are being suggested as alternative solutions for indoor air quality improvements (Cheng et al., 2015). Therefore, it is necessary to compare the impact on indoor air quality of emissions from green materials with those from conventional ones and this is investigated in Chapter 4.

There is evidence that the presence of human occupants indoors is highly correlated with ozone loss and enhanced secondary pollutant formation. Weschler et al. (2007) demonstrated that human skin and clothing materials are a major sink of ozone. Hence, Weschler and co-authors (2007) verified the presence of nonanal, decanal, acetone, 4-OPA, 6-MHO and geranyl acetone as the main products following the ozonolysis reaction of skin oils. Likewise, highly occupied indoor places, such as classrooms, are associated with higher human-related emissions that originate from skin and breath emissions. For instance,

emissions from occupants contributed to 57% of the total VOCs emitted in a well ventilated classroom (Tang et al., 2016).

Given the lack of measurements and challenges that exist with measuring many indoor air pollutants, particularly in a real building scenario, models are often used to predict indoor air concentrations and to provide insight into the underlying chemical processing. Also, models can be used to compare with existing measurement data, help to design experiments and provide predictions for the future. In order to represent indoor air chemistry in a model, Figure 4 summarises the different processes that occur indoors and hence should be considered in properly designed models.

Air Exchange with outdoors: exchange rate; infiltration through building envelope; outdoor concentrations

Building Physics: T; RH; lighting; heat and moisture flux; air flow; building location and operation; outdoor climate

Chemistry: chemical mechanisms; indoor pollutant concentrations; physical parameters; occupant activities; surface interactions

Aerosol: gas-to-aerosol partitioning; indoor pollutant concentrations; physical parameters; occupant activities; surface interactions

Physical influence

$X_{IN} + Y_{IN} = Z_{IN}$

X_{OUT}

X_{IN}

Surface emissions

Surface loss

Occupant exposure: Health effects: chemical and/or biological exposure; inhalation, dermal or ingestion; hot spots

Occupancy effects: Emissions from humans; transformation on human surfaces; human activities; building operation

Surface Chemistry: Deposition to surfaces; chemical transformation on surface; chemistry of films/coatings; emission from surfaces; surface composition; occupancy

Figure 3: Physical and chemical processes that impact indoor air chemistry.

As illustrated in Figure 3, a good model should include the different physical and chemical processes that have an impact on indoor air chemistry. Hence, the air exchange rate describes the exchange with outdoors. Likewise, the location of the building (and therefore outdoor concentrations), temperature, relative humidity and photolysis rates can impact

19

processes indoors. Using a good chemical mechanism and including different parameters and processes as described above, a model can then predict indoor air pollutant concentrations. Thus, it is possible to estimate occupant exposure to indoor air pollutants in different indoor environments.

Chemical mechanisms still require many improvements in order to accurately represent indoor environments. As highlighted by Morrison et al. (2017) future model development should include improved parameters that describe surface interactions indoors, both in terms of deposition rates to surfaces as well as formation rates of pollutants formed through such surface interactions. Another area of uncertainty is the fate of terpene mixtures indoors, such as that which may follow cleaning. This thesis will address some of these current uncertainties providing improved parametrization for surface interactions and a more thorough consideration of the impact of terpene mixtures on indoor air chemistry.

1.2 Research objectives

The aim of this thesis is to elucidate the indoor air chemistry that arises when surface interactions take place indoors, with a particular view to identifying products that might be harmful to health.

The specific objectives of this dissertation are:

1. To identify the key chemical species that are formed when indoor surfaces interact with indoor air pollutants.

2. To compare green building materials with conventional ones and their impact on indoor air chemistry.

3. To identify the impacts that human skin and breath emissions have on indoor air chemistry.

4. To evaluate the impact of different mixtures of terpenes (as a proxy for cleaning product formulation) on aspects of indoor air chemistry.

The research objectives of this study are addressed by using a detailed modelling approach. The model takes into consideration a real building scenario in two different cities, Milan and Seoul, representing average size and megacity examples respectively during typical and heatwave summer outdoor conditions. Also, the model is used to simulate cleaning activity indoors conducted in an experimental scenario.

The structure of the thesis is as follows:

Chapter 2: This Chapter provides a literature review with a focus on previous modelling studies of indoor air chemistry. It describes the evolution of indoor models and their scope up to the current study.

Chapter 3: This Chapter presents the methodology used in this research, including the processes and parameters used in the model employed together with description of the experimental designs of the studies in Chapters 4-6. Also, it includes a description of the simulated buildings and case study locations.

Chapter 4: This Chapter investigates surface processes on indoor materials and their impact on indoor air quality. It examines surface production following ozone deposition. The modelling results compare the formation of secondary pollutants following such surface interactions for different case study locations and for different conditions (such as varying ventilation rates). This chapter identifies the key chemical species that are formed when indoor surfaces interact with indoor air pollutants. Then, green building material emissions are compared to those from standard materials in terms of their impact on indoor air quality.

Chapter 5: This Chapter explores the impact of human occupancy on indoor air pollution. Namely, it investigates ozone loss onto human bodies (skin) for different indoor environments including an apartment, a bedroom and a classroom and then quantifies the production of various secondary pollutants following these processes. As well as these reactions at the skin surface the Chapter focuses on the consequent impact on indoor air chemistry and it also investigates the impact of breath emissions on indoor quality.

Chapter 6: This Chapter investigates cleaning as a source of indoor air pollution following human activities indoors. It describes experimental work, which simulates a cleaning event. It compares the results of single terpene experiments with those of mixtures of terpenes. It also presents some experimental results which investigated potential surface interactions on carpets and vinyl flooring following cleaning activities. Finally, this chapter presents the modelling results of a simulation of terpene mixture experiments, evaluates their impact on aspects of indoor air chemistry and discusses their potential relevance for modification of product formulation.

Chapter 7: This Chapter provides the overall conclusions of the study. It also considers the wider implications of this research and provides recommendations for further research.

2. Review of indoor air quality models

2.1 Introduction

Over recent years, models for indoor air chemistry have become increasingly complex. The first indoor air quality models, which described only basic processes indoors, have been developed to include much more complex representations of the chemistry. This chapter provides a review of the important models that have been developed to investigate aspects of indoor air chemistry that are relevant for this dissertation (focusing on those that investigate gas-phase chemistry and/or surface interactions).

2.2 Review of indoor air chemistry models

2.2.1 Gas-phase chemistry models

2.2.1.1 Simple chemical models

Nazaroff and Cass (1986) proposed the first indoor air chemistry model. A mathematical model was proposed to estimate the concentrations of chemically reactive compounds indoors. A single well-mixed zone model considered photochemistry (indoor lighting and infiltration of light from outdoors), exchange with outdoors, deposition, emission and filtration. The model was used to simulate conditions in a museum gallery, where the flow rate between the different 'chambers' (rooms) within the building varied with time.

A rather simple set of model equations considered the sum of all the possible sources for each pollutant (e.g. transport between the chambers, outdoor concentrations, the mechanical ventilation system, direct indoor emissions and products of chemical reactions) diminished by the loss of all considered sinks (e.g. chemical reactions, removal by surface processes indoors and the loss rate through transport from the chamber). The chemical mechanism following Falls and Seinfeld (1978), considered 31 species and 56 reactions and is presented in Figure 4.

no.	reaction	rate constant, ppm min K units
1	$NO_2 + h\nu \rightarrow NO + O(^3P)$	a
2	$O(^3P) + O_2 + M \rightarrow O_3 + M$	$0.346T^{-2} \exp(510/T)$
3	$O_3 + NO \rightarrow NO_2 + O_2$	$(9.245 \times 10^5)T^{-1} \exp(-1450/T)$
4	$NO_2 + O(^3P) \rightarrow NO + O_2$	$(3.99 \times 10^6)T^{-1}$
5	$NO + O(^3P) \rightarrow NO_2$	$(1.67 \times 10^5)T^{-1} \exp(584/T)$
6	$NO_2 + O(^3P) \rightarrow NO_3$	$(8.81 \times 10^5)T^{-1}$
7	$O_3 + NO_2 \rightarrow NO_3 + O_2$	$(5.19 \times 10^4)T^{-1} \exp(-2450/T)$
8	$NO_3 + NO \rightarrow 2NO_2$	$(8.81 \times 10^6)T^{-1}$
9	$NO + OH \rightarrow HNO_2$	$(5.07 \times 10^5)T^{-1}$
10	$HNO_2 + h\nu \rightarrow NO + OH$	a
11	$HO_2 + NO_2 \rightarrow HNO_2 + O_2$	$17.3T^{-1} \exp(1006/T)$
12	$HNO_2 + OH \rightarrow H_2O + NO_2$	$(2.91 \times 10^6)T^{-1}$
13	$NO_2 + HO_2 \rightarrow HNO_4$	$(1.73 \times 10^4)T^{-1} \exp(1006/T)$
14	$HNO_4 \rightarrow HO_2 + NO_2$	$1.80 \times 10^{15} \exp(-9950/T)$
15	$HO_2 + NO \rightarrow NO_2 + OH$	$(3.58 \times 10^6)T^{-1}$
16	$RO_2 + NO \rightarrow NO_2 + RO$	$(3.58 \times 10^6)T^{-1}$
17	$RCO_3 + NO (+O_2) \rightarrow NO_2 + RO_2 + CO_2$	$(1.13 \times 10^6)T^{-1}$
18	$NO_2 + OH \rightarrow HNO_3$	$(4.401 \times 10^{17})T^{-1} (280/T)^{1/2} 10^{(11.6T/(17.4+T))}$
19	$CO + OH (+O_2) \rightarrow HO_2 + CO_2$	$(1.31 \times 10^5)T^{-1}$
20	$O_3 + h\nu \rightarrow O(^3P) + O_2$	a
21	$HCHO + h\nu (+2O_2) \rightarrow 2HO_2 + CO$	a
22	$HCHO + h\nu \rightarrow H_2 + CO$	a
23	$HCHO + OH (+O_2) \rightarrow HO_2 + H_2O + CO$	13890
24	$RCHO + h\nu (+2O_2) \rightarrow HO_2 + RO_2 + CO$	a
25	$RCHO + OH (+O_2) \rightarrow RCO_3 + H_2O$	25680
26	$C_2H_4 + OH \rightarrow RO_2$	11660
27	$C_2H_4 + O(^3P) \rightarrow HO_2 + RO_2$	1219
28	$OLE + OH \rightarrow RO_2$	89142
29	$OLE + O(^3P) \rightarrow RO_2 + RCO_3$	22118
30	$OLE + O_3 \rightarrow 0.5\ RCHO + 0.5\ HCHO + 0.3\ HO_2 + 0.31$ $RO_2 + 0.14\ OH + 0.03\ RO$	0.136
31	$ALK + OH \rightarrow RO_2$	4700
32	$ALK + O(^3P) \rightarrow RO_2 + OH$	99.8
33	$ARO + OH \rightarrow RO_2 + RCHO$	16112
34	$RO \rightarrow HO_2 + 0.5HCHO + RCHO$	2.0×10^5
35	$RONO + h\nu \rightarrow RO + NO$	a
36	$RO + NO \rightarrow RONO$	$(4.38 \times 10^6)T^{-1}$
37	$RO + NO_2 \rightarrow RNO_3$	$(2.19 \times 10^6)T^{-1}$
38	$RO + NO_2 \rightarrow RCHO + HNO_2$	$(1.91 \times 10^5)T^{-1}$
39	$NO_2 + RO_2 \rightarrow RNO_4$	$(1.64 \times 10^6)T^{-1}$
40^b		
41	$RNO_4 \rightarrow NO_2 + RO_2$	$(1.80 \times 10^{15}) \exp(-9950/T)$
42	$RCO_3 + NO_2 \rightarrow PAN$	$(6.17 \times 10^5)T^{-1}$
43	$PAN \rightarrow RCO_3 + NO_2$	$(4.77 \times 10^{16}) \exp(-12516/T)$
44	$NO_2 + NO_3 \rightarrow N_2O_5$	$(7.48 \times 10^5)T^{-1}$
45	$N_2O_5 \rightarrow NO_2 + NO_3$	$(4.07 \times 10^{16}) \exp(-11080/T)$
46	$H_2O + N_2O_5 \rightarrow 2HNO_3$	$(5.66 \times 10^{-4})T^{-1}$
47	$O_3 + OH \rightarrow HO_2 + O_2$	$(6.62 \times 10^5)T^{-1} \exp(-1000/T)$
48	$O_3 + HO_2 \rightarrow OH + 2O_2$	$(4.85 \times 10^3)T^{-1} \exp(-580/T)$
49	$NO_3 + h\nu \rightarrow NO + O_2$	a
50	$HO_2 + HO_2 \rightarrow H_2O_2 + O_2$	$(3.4 \times 10^4)T^{-1} \exp(1100/T) + (5.8 \times 10^{-5})T^{-2} \exp(5800/T)[H_2O]^c$
51	$H_2O_2 + h\nu \rightarrow 2OH$	a
52	$RO_2 + RO_2 \rightarrow 2RO + O_2$	$(2.04 \times 10^4)T^{-1} \exp(223/T)$
53	$NO_3 + HCHO (+O_2) \rightarrow HNO_3 + HO_2 + CO$	0.86
54	$NO_3 + RCHO (+O_2) \rightarrow HNO_3 + RCO_3$	3.6
55	$NO_3 + h\nu \rightarrow NO_2 + O(^3P)$	a
56	$NO_3 + OLE \rightarrow RPN^d$	$3288T^{-1}$
57	$NO_2 + NO_3 \rightarrow NO_2 + NO + O_2$	$175T^{-1}$

[a] Rate depends on photon flux; see Table II. [b] Reaction in earlier mechanisms that was subsequently eliminated. [c] $[H_2O]$ is water vapor concentration in ppm. [d] Nitroxyperoxyalkyl nitrates and dinitrates, not considered to participate in further chemistry.

Figure 4: The list of the chemical mechanism reactions that were used in the Nazaroff and Cass (1986) model.

The rate of change of the concentration of each pollutant was described and included in the model as presented in equation 1.

$$\frac{dc}{dt} = S - L\,C \qquad (1)$$

where S is the sum of all the sources, such as emissions, transport from other chambers and production following chemical reactions; L describes the sum of all the sinks, such as loss by chemical reactions, surface loss and removal by transport; C stands for the concentration of a particular pollutant (molecule cm^{-3}).

The ventilation process considered the mechanical ventilation system that supplied and exchanged air with outside (the air exchange rate was 0.3-2.0 per hour), infiltration processes (air that infiltrated directly from outside) and mixing of air between the chambers. The air exchange rates were adopted from experimental data measured in the museum. The model considered both artificial indoor lighting and also, sunlight that is transmitted through the windows. The photolysis rate values were then calculated using a combination of measurements (outdoor photon fluxes) and laboratory derived data (e.g. for absorption cross-sections, quantum yields etc.) This method was adopted for the model used in this dissertation and is further described in Chapter 3.

The input values of outdoor concentrations were the hourly-averaged concentrations of species or groups of species such as ozone, nitrogen oxide (NO), nitrogen dioxide (NO_2), formaldehyde (HCHO), ethylene, higher aldehydes, olefins, alkenes, aromatics, H_2O_2, nitrous acid (HONO) and nitro compounds (RNO_2) measured on-site at the museum or adapted from other measurement studies carried out in California. Indoor concentrations of ozone, NO and NO_2 were measured in the museum. At the time of this research, little was known about surface reactions indoors and it was not possible to incorporate such heterogeneous chemistry into the model. However, the model included irreversible surface deposition for several species, such as O_3, NO, NO_2 and HCHO and the deposition velocities were obtained from literature.

The Nazaroff and Cass (1986) model was validated through comparison of the model results with measurements carried out in a newly constructed museum gallery in California, USA. The surface area of the building was 3060 m^2 and the volume was 2530 m^3. The model was parameterised with the characteristics of the museum. The comparison was conducted for O_3, NO, NO_2, nitrate (NO_3), HONO, nitric acid (HNO_3), dinitrogen pentoxide (N_2O_5), peroxyacyl nitrate (PAN), H_2O_2, HCHO and aldehydes (RCHO).

The predicted concentrations of ozone and nitrogen dioxide were in relatively good agreement with the measurement values but, the concentration of NO was underpredicted in the model simulations compared with the measurements. The Nazaroff and Cass model was constructed as a general tool for studying the reactive chemistry of the indoor environment. The results from this first indoor air chemistry model indicated the potential importance of

chemical transformations in indoor air, but also contained limitations. For instance, the model did not include surface processes indoors. Therefore, Nazaroff and Cass (1986) suggested further research on both mass transport and surface-reaction kinetics was necessary. In particular, they suggested that deposition velocity and loss rate processes as well as surface interactions, the rate of chemical reactions and detailed, heterogeneous chemistry indoors should be studied in detail in order to better understand chemical processes in indoor environments.

Weschler and Shields (1996) extended the scope of indoor air modelling. Their research focused on the production of hydroxyl radicals in indoor air, which previously had received little attention. Although, Nazaroff and Cass (1986) were first to model chemically reactive compounds in indoor air including reactions where the OH radical was recognised as a product, the research of Weschler and Shields (1996) focused more on this aspect using a simple mass balance model. In 1992 several studies (Paulson et al., 1992; Paulson and Seinfeld; 1992; Atkinson et al., 1992) reported that in the atmosphere, OH radicals were formed following the reactions of monoterpenes with ozone. Weschler and Shields (1996) examined the impact of such reactions indoors and developed a model which included the OH radical as a product of the reaction of alkenes with ozone. The model involved 13 reactions that formed OH as a product (the reaction of ozone with 13 indoor VOCs, i.e. d-limonene, α-terpinene, α-pinene, isoprene, styrene and camphene) and 39 reactions where OH reacted with the 13 VOCs (and other reactants) through a circular oxidation chain. The 13 VOCs selected for this study were those that were often found indoors and had the largest production rates of hydroxyl radicals. The OH sources and sinks were incorporated in a one-compartment mass balance model, which included indoor OH, NO_2, carbon monoxide (CO), O_3 and VOC concentrations, the outdoor OH concentration, chemical reactions, but also parameters such as the air exchange rate, the OH indoor deposition velocity (0.0007 m s^{-1}) and an indoor surface to volume ratio (2.8 m^{-1}). The indoor concentrations of VOCs and reactions rate constants were obtained from the literature. The values of NO_x and CO were based on measurements and the indoor concentration of ozone was set to 20 ppb. The OH production rates were calculated using the indoor concentrations of VOCs, the individual rate constants and the OH formation yield for each VOC, the latter two parameters from the literature. The concentration of OH indoors was calculated according to equation 2:

$$d[OH_{indr}]/dt = E_x[OH_{otdr}] + \sum y_i k_{O_{3i}}[O_3][VOC_i] -$$
$$E_x[OH_{indr}] - k_d(A/V)[OH_{indr}] - \sum k_{OH_i}[OH_{indr}][VOC_i] \tag{2}$$

where $[OH_{indr}]$ is the hydroxy radical concentration indoors (ppb), $[OH_{otdr}]$ is the hydroxy radical concentration outdoors (ppb), E_x is the air exchange rate (s^{-1}), y_i is the yield of the ozone-alkene reaction, k_{O3} is the rate constant of the ozone-alkene reaction (ppb^{-1} s^{-1}), $[O_3]$ is the ozone concentration indoors (ppb), $[VOC_i]$ is the VOC concentration indoors (ppb), k_d is the OH deposition velocity indoors (m s^{-1}), A/V is the surface to volume ratio (m^{-1}), k_{OHi} is the rate constant for OH/VOC reaction (ppb^{-1} s^{-1}).

The calculated production and loss rates for hydroxyl radical are presented in Figure 5. The model predicted an OH concentration indoors of 6.7 x 10^{-6} ppb (1.7 x 10^5 molecules cm^{-3}), smaller than a typical outdoor midday OH concentration, but approximately four times greater than the OH night time outdoor concentration (Weschler and Shields, 1996). For the input conditions, the reaction of d-limonene with O_3 was found to have the fastest OH production rate, followed by α-terpinene, 2-methyl-butene and α-pinene. Comparing the OH production rate via VOC ozonolysis with other potential sources such as outdoor to indoor transport, the photolysis of ozone or the reaction between HO_2 and NO, the production rate of OH was found to be highest from the VOC reactions with O_3. The research showed that the most significant sinks for OH radicals were with d-limonene, NO_2, ethanol, formaldehyde, CO and isoprene.

$$O_3 + \text{alkene} \rightarrow \text{intermediates} \rightarrow OH + \text{other products}$$
$$d[OH]/dt = (\text{yield})k[\text{alkene}][O_3]$$

alkene	typical indoor concn (ppb)		OH yield	rate constant $(O_3+\text{alkene})$ $(\text{ppb}^{-1}\,\text{s}^{-1})$	calcd OH production rate (ppb s^{-1})
	no O_3[a]	20 ppb O_3[b]			
d-limonene	4[c]	2.9	0.86	5.1×10^{-6}	2.6×10^{-4}
α-terpinene	0.5[c]	0.03	0.91	2.1×10^{-4}	1.2×10^{-4}
2-methyl-2-butene	0.4[d]	0.23	0.89	1.0×10^{-5}	4.2×10^{-5}
α-pinene	0.5[c]	0.43	0.85	2.1×10^{-6}	1.6×10^{-5}
trans-2-butene	0.3[d]	0.22	0.64	5.3×10^{-6}	1.5×10^{-5}
cis-2-butene	0.3[d]	0.24	0.41	3.2×10^{-6}	6.4×10^{-6}
isoprene	2[e]	2	0.27	3.0×10^{-7}	3.2×10^{-6}
isobutene	0.5[d]	0.49	0.84	2.8×10^{-7}	2.3×10^{-6}
styrene	0.5[c]	0.49	0.37	4.2×10^{-7}	1.5×10^{-6}
propene	0.5[d]	0.49	0.33	2.9×10^{-7}	9.4×10^{-7}
camphene	2.5[c]	2.5	0.15	2.2×10^{-8}	1.7×10^{-7}
ethene	1.5[d]	1.5	0.12	4.3×10^{-8}	1.5×10^{-7}
1,3-butadiene	0.3[f]	0.3	0.08	2.0×10^{-7}	9.5×10^{-8}
air exchange (i.e., $E_x[OH_{otdr}]$)	$[OH_{otdr}] = 2.0 \times 10^{-4}$			$E_x = 2.8 \times 10^{-4}\,\text{s}^{-1}$	5.6×10^{-8}

[a] Average VOC concentration in the absence of O_3. [b] VOC concentration in the presence of 20 ppb O_3.

$$OH_{indr} + \text{reactant} \rightarrow \text{products}$$
$$-d[OH]/dt = k[\text{reactant}][OH_{indr}]$$

reactant	rate constant $(OH_{indr}+\text{reactant})$ $(\text{ppb}^{-1}\,\text{s}^{-1})$	typical indoor concn (ppb)		calcd rate constant for OH removal (s^{-1})
		no O_3	20 ppb O_3	
d-limonene	4.2	4	2.9	12.3
nitrogen dioxide	0.30	30	30	9.0
ethanol	0.079	100	100	7.9
formaldehyde	0.24	30	30	7.2
carbon monoxide	0.0059	1000	1000	5.9
isoprene	2.5	2	2	5.0
camphene	1.3	2.5	2.5	3.2
acetaldehyde	0.39	5	5	2.0
1,2,4-trimethylbenzene	0.81	2	2	1.6
toluene	0.15	10	10	1.5
1,3,5-trimethylbenzene	1.4	1	1	1.4
m-xylene	0.62	2	2	1.2
o-xylene	0.37	3	3	1.1
styrene	1.5	0.5	0.49	0.74
p-xylene	0.37	2	2	0.74
isobutene	1.3	0.5	0.49	0.64
α-pinene	1.4	0.5	0.43	0.60
benzaldehyde	0.32	1.6	1.6	0.51
1,3-butadiene	1.65	0.3	0.3	0.50
2-methyl-2-butene	2.1	0.4	0.23	0.48
ethylbenzene	0.185	2	2	0.37
trans-2-butene	1.6	0.3	0.22	0.35
cis-2-butene	1.4	0.3	0.24	0.34
methane	0.00017	2000	2000	0.34
ethene	0.21	1.5	1.5	0.32
propene	0.64	0.5	0.49	0.31
n-undecane	0.295	1	1	0.30
α-terpinene	8.9	0.5	0.03	0.27
n-butane	0.063	4	4	0.25
methanol	0.023	10	10	0.23
n-pentane	0.10	2	2	0.20
benzene	0.032	5	5	0.16
acetone	0.0057	10	10	0.057
propane	0.027	1.5	1.5	0.041
ammonia	0.0039	10	10	0.039
ozone	0.0017	20	20	0.034
sulfur dioxide	0.022	1	1	0.022
ethane	0.0062	2.5	2.5	0.016
1,1,1-trichloroethane	0.00023	10	10	0.002
surface removal $(k_d(A/V))$	$k_d = 7 \times 10^{-4}\,\text{m s}^{-1}$	$A/V = 2.8\,\text{m}^{-1}$		0.002
air exchange (E_x)	$E_x = 2.8 \times 10^{-4}\,\text{s}^{-1}$			0.00028

Figure 5: Calculated OH production and loss rate constants for a number of reactants and for different ozone concentrations (Source: Weschler and Shields, 1996).

A sensitivity analysis for this model showed that the OH production did not scale linearly to the ozone concentrations indoors. Even for an ozone concentration of 1 ppb, there is sufficient oxidation to form OH radicals at concentrations similar to that representative for outdoors at night time (Weschler and Shields, 1996). For the simulated concentration of OH (1.7×10^5 molecules cm^{-3}), saturated organics will be oxidised 2-5 orders of magnitude faster by OH than by the 20 ppb of ozone also present. Weschler and Shields (1996) suggested that indoor oxidation products may be more irritating to human exposure and more corrosive to indoor materials than the parent VOCs. Weschler and Shields (1996) made recommendations for further research. They highlighted the importance of experimental confirmation of their predictions, including indoor OH measurements. They also highlighted the need to further improve the representation of chemical processes indoors in models.

2.2.1.2 Moderately complex chemical models

Sarwar et al. (2002) incorporated a more detailed set of chemical reactions applicable for the indoor environment in their model. Their model focused on predicting OH concentrations indoors using a new air quality model (ICEM – Indoor chemistry and Exposure Model). It included enhanced representation of the production and removal of OH radicals indoors and was developed using a modified version of the SAPRC-99 mechanism (Carter, 2000; 2003). Importantly, it included updated OH radical yields representative for alkene reactions with ozone (Paulson et al., 1999), which were not available for previous modelling studies.

The ICEM described the indoor setting as a single well-mixed environment with homogeneous chemistry and heterogeneous deposition processes. It included parameters describing the air exchange rate, chemical reactions, indoor emissions and internal deposition processes. Indoor and outdoor pollutant concentrations, as well as air exchange rates and deposition velocities were obtained from the experimental values found in the literature. On average, the indoor pollutant concentrations were higher than the outdoor values. Sarwar et al. (2002) noted the wide variations in VOC concentrations measured in different houses due to different sources such as cigarettes, use of cleaning agents or off-gassing from new building materials. While it is not possible to include all possible variation of indoor settings, Sarwar et al. (2002) used average VOC concentrations obtained from the literature to calculate indoor emission rates that were representative of background concentrations. The model included indoor emissions of 51 species (including 46 VOC compounds). This

study assumed that 50% of the light indoors came from outdoors and 50% from artificial indoor lighting. The air exchange rate used in this modelling study was 0.5 h^{-1}, relative humidity was assumed to be 50%, and the temperature was set to 297 K. The volume of the building was assumed to be 500 m^3 and surface area to be ~610 m^2.

The list of reactions considering OH production and consumption in the ICEM model are presented in Figure 6. The results of the model showed that for the base case scenario, the estimated OH radical concentration indoors was 1.2 x 10^5 molecule cm^{-3}. Comparing the ICEM model results with the previous predictions reported by Weschler and Shields (1996) for similar conditions, the predicted concentrations of the new model were within 0.3-12% of the estimates of the previous study. Again, a non-linear increase of the indoor concentration of OH was noticed with increased outdoor ozone concentration, air exchange rate and indoor VOC emission rates. Nevertheless, the photolysis rates, temperature, deposition velocity and direct transport from outdoors to indoors had at most, a moderate impact on predicted indoor OH concentrations.

No.	Reactions that produce OH$^{\bullet}$	No.	Reactions that consume OH$^{\bullet}$
3	$NO + HO_2^{\bullet} = OH^{\bullet} +$	23	$NO + OH^{\bullet} =$
4	$O_3 + HO_2^{\bullet} = OH^{\bullet} +$	24	$O_3 + OH^{\bullet} =$
5	$NO_3^{\bullet} + HO_2^{\bullet} = 0.8\ OH^{\bullet} +$	25	$NO_3^{\bullet} + OH^{\bullet} =$
6	$Ethene + O_3 = 0.18\ OH^{\bullet} +$	26	$Ethene + OH^{\bullet} =$
7	$Isoprene + O_3 = 0.25\ OH^{\bullet} +$	27	$Isoprene + OH^{\bullet} =$
8	$Propene + O_3 = 0.35\ OH^{\bullet} +$	28	$Propene + OH^{\bullet} =$
9	$Isobutene + O_3 = 0.72\ OH^{\bullet} +$	29	$Isobutene + OH^{\bullet} =$
10	cis-2-Butene $+ O_3 = 0.37\ OH^{\bullet} +$	30	cis-2-Butene $+ OH^{\bullet} =$
11	$trans$-2-Butene $+ O_3 = 0.64\ OH^{\bullet} +$	31	$trans$-2-Butene $+ OH^{\bullet} =$
12	2-Methyl 2-butene $+ O_3 = 1.0\ OH^{\bullet} +$	32	2-Methyl 2-butene $+ OH^{\bullet} =$
13	1,3-Butadiene $+ O_3 = 0.13\ OH^{\bullet} +$	33	1,3-Butadiene $+ OH^{\bullet} =$
14	3-Carene $+ O_3 = 1.0\ OH^{\bullet} +$	34	3-Carene $+ OH^{\bullet} =$
15	d-Limonene $+ O_3 = 0.86\ OH^{\bullet} + 0.04\ AMCYCHEX + 0.04\ IPOH + 0.19\ HCHO$	35	d-Limonene $+ OH^{\bullet} = 0.2\ AMCYCHEX + 0.29\ IPOH +$
		36	$AMCYCHEX + OH^{\bullet} =$
		37	$IPOH + OH^{\bullet} =$
16	Styrene $+ O_3 = 0.07\ OH^{\bullet} +$	38	Styrene $+ OH^{\bullet} =$
17	Criegee biradical 1 $= 0.8\ OH^{\bullet} + 0.3\ PINALD$	39	α-Pinene $+ OH^{\bullet} = 0.34\ PINALD +$
18	Criegee biradical 2 $= 0.8\ OH^{\bullet} +$	40	$PINALD + OH^{\bullet} =$
19	Methacrolein $+ O_3 = 0.20\ OH^{\bullet} +$	41	Methacrolein $+ OH^{\bullet} =$
20	Methyl vinyl ketone $+ O_3 = 0.16\ OH^{\bullet} +$	42	Methyl vinyl ketone $+ OH^{\bullet} =$
21	Lumped isoprene product species $+ O_3 = 0.285\ OH^{\bullet}$	43	Lumped isoprene product $+ OH^{\bullet} =$
22	Reactive aromatic fragmentation products $+ O_3 = 0.5\ OH^{\bullet} +$	44	Reactive aromatic fragmentation products $+ OH^{\bullet} =$
		45	$HONO + OH^{\bullet} =$
		46	$NO_2 + OH^{\bullet} =$
		47	$HNO_3 + OH^{\bullet} =$
		48	$CO + OH^{\bullet} =$
		49	$HO_2NO_2 + OH^{\bullet} =$
		50	$H_2O_2 + OH^{\bullet} =$
		51	$HO_2^{\bullet} + OH^{\bullet} =$
		52	$SO_2 + OH^{\bullet} =$

Figure 6: The list of reactions producing and consuming OH radicals (Source: Sarwar et al., 2002).

The production of OH radicals was dominated by the reaction of VOCs with ozone under the assumed conditions. For instance, the reaction between d-limonene and ozone constituted 40% of the total OH radical production rate. The significant sinks of OH radicals included reactions with VOCs, deposition to indoor surfaces and transport to outdoors. Both isoprene and d-limonene were expected to be the main sinks for OH radicals. However, OH radicals were predicted to reach the highest concentration indoors when both substrates and products are simultaneously present indoors at relatively high concentrations. Sarwar et al. (2002) suggested that indoor OH may have an adverse impact on indoor air quality. Their results showed that reactions of ozone with limonene formed a wide range of secondary compounds that may be of greater concern than the parent compounds. For instance, OH reactions with terpenes produce oxidized products, i.e. 3-isopropenyl-6-oxoheptanal (IPOH) and pinonaldehyde, that contain multifunctional groups ($=O$, $-OH$ and $-COOH$). Such products can cause adverse health effects including skin and eye irritation and occupational asthma (Nazaroff and Weschler, 2004). Also, such secondary products may contribute to the formation of fine particles (Wallace, 1996). Therefore further research was recommended to confirm the model predictions and particularly the formation of secondary pollutants following OH radical reactions with VOCs in real building scenarios. Sarwar et al. (2002) also pointed out the need for indoor air chemistry research and also verification of its impact on indoor air quality.

2.2.1.3 Near-explicit chemical models

Carslaw (2007) presented a new modelling approach. The detailed chemical box model included near-explicit chemical degradation schemes for the VOCs and inorganic species responsible for driving the indoor air chemistry. The INDCM model was constructed based on the master chemical mechanism (MCM v3.1) (Jenkin et al., 1997, 2003; Saunders et al., 2003). The comprehensive mechanism was modified and included 15,400 degradation reactions (with 2000 new reactions describing exchange with outdoors, emissions, deposition, surface reactions and gas-phase chemistry) and 4700 key indoor air pollutants.

Given that the MCM was adopted from use for outdoor atmospheric chemistry, some important species relevant for indoor air chemistry, such as limonene, camphene, terpinene and carene, were not available in the mechanism. The only two monoterpenes included in the mechanism at the time were α-pinene and β-pinene. The absent species were incorporated

in the model through consideration of the initial reactions with ozone, OH and NO_3, using rate coefficients found in the literature for each of the species. The products from these preliminary oxidation reactions were then mapped onto relevant existing species using the α- or β-pinene mechanism as most relevant (e.g. through consideration of the similarity rates of reactions with OH, NO_3 and O_3 and OH yields following reaction of the monoterpene with O_3). It was assumed that half of the limonene degradation products followed the α-pinene products and half the β-pinene products.

The model considered a single well-mixed environment representative of a typical urban residence in the UK. The surface to volume ratio was 3.0 m^{-1}, relative humidity 50%, temperature 293 K and the air exchange rate was a typical summer time value of 2.0 h^{-1} (Carslaw, 2007). The model included irreversible deposition to surfaces, with many of the deposition values adopted from Sarwar et al. (2002). Photolysis included both attenuated sunlight through windows and the artificial lighting contribution as outlined by Nazaroff and Cass (1986). Carslaw (2007) highlighted the potential importance of surface chemistry and its likely impact on indoor air chemistry and acknowledged its treatment in this model was likely inadequate and that more measurements of relevant input parameters were needed.

The predicted OH concentration indoors was up to 4.0 x 10^5 molecule cm^{-3}, a factor of 10-20 less than the outdoor concentrations, but still sufficient to drive the indoor air chemistry. In terms of radical chemistry, the focus was on OH, HO_2 and RO_2. The main initiation route for the OH and RO_2 radical formation was through ozone reactions with terpenes. Once OH was formed, it was possible to also produce HO_2 and RO_2 species. Cycling between OH and RO_2 radicals was dominated by the reaction with monoterpenes, and OH to HO_2 transformation was largely driven by reaction with alcohols. The indoor air chemical processes are presented in Figure 7.
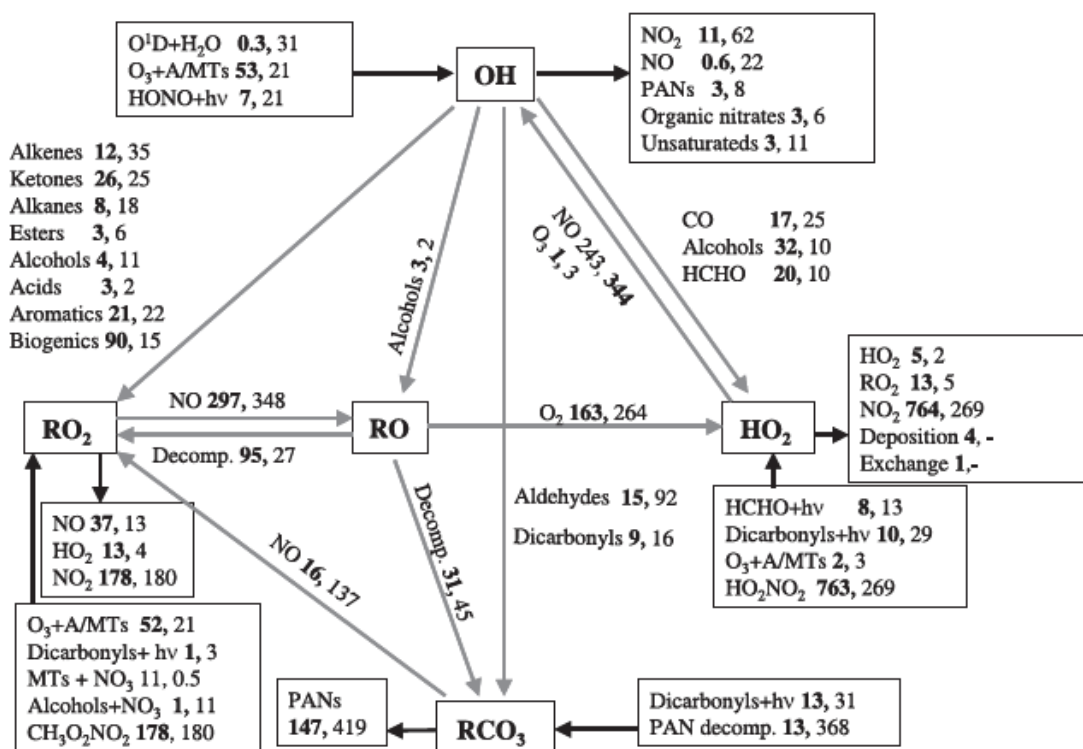
Figure 7: The chemical routes between radicals indoors including initiation, termination and propagation reactions. Numbers in bold indicate the reaction rates (in units of 10^5 molecule cm^{-3} s^{-1}) for indoors and in normal type for outdoors. Grey arrows denote propagation routes, the black arrows pointing in and out of the radical boxes – initiation and termination routes respectively (Source: Carslaw, 2007).

A sensitivity analysis verified that the most important parameters for OH concentration indoors were air exchange rate and the assumed photolysis values. Carslaw (2007) pointed out that indoor air chemistry results might have been very different for a similar residence in a different location, where outdoor concentrations will be different. Previous studies (Weschler et al., 1994) had focused on the US conditions where outdoor O_3 concentrations were higher (160 ppb indicated for the US, California conditions): indoor concentrations are likely to be different in suburban UK areas.

Carslaw (2007) noted that the concentrations of nitrated species such as PANs (RCO$_3$NO$_2$) and organic nitrates (RNO$_3$) could be significant indoors. Given that the results of this study showed that approximately 30% of PAN species and 72% of the total organic nitrates are expected to associate with the aerosol phase through the formation of secondary organic aerosols, the presence of the nitrated species indoors should be a concern. Therefore Carslaw (2007) suggested that measurements of radicals, nitrate species, and the secondary products of oxidation and photolysis reactions, should be carried out indoors to validate these

model findings. Nevertheless, the model presented by Carslaw (2007) was the first one to include detailed chemical reactions indoors and was important for improving our understanding of indoor air chemistry.

Within the scope of model development, Carslaw et al. (2012) presented an analysis of SOA formation indoors following cleaning activities. The improved model included additional reactions for gas to particle formation following the oxidation of limonene. The modelling results showed that in a typical suburban residence in the UK, the SOA concentration indoors is approximately 1 μg m^{-3}. The composition of SOA under such conditions is dominated by organic nitrates and PAN species (in total ~85%), peroxides, acids and carbonyls. A modelling simulation was also carried out for a cleaning event indoors. Then, the SOA concentration increased to 20 μg m^{-3} and the composition changed to be dominated by peroxides (~73%), with a smaller portion of organic nitrates and PANs (in total ~21%). The concentration and composition of modelled SOA indoors were found to depend most strongly on the outdoor concentration of ozone, the indoor concentration of VOCs, the deposition rates and the values assumed for the partitioning coefficients.

Clearly, the SOA composition will likely differ in a similar house placed in different locations and is dependent on frequency and duration of activities such as cleaning or cooking. Carslaw et al. (2012) highlighted the necessity for a detailed investigation of SOA composition indoors through measurements under realistic conditions: many of the experimental studies that have been carried out to date on SOA composition have been in chambers and typically in the dark or under low NO$_X$ conditions to simplify the chemistry. In addition, Carslaw et al. (2012) highlighted the need for more measurements of deposition rates on different indoor surfaces, which would help to validate the model and decrease the uncertainties in the model predictions.

Carslaw (2013) used the improved model to further investigate chemical composition indoors following cleaning, including the key species and their formation pathways. The results presented in this study show that the main gas-phase products are multi-functional carbonyl species such as limonaldehyde and 4-acetyl-1-methyl-1-cyclohexene (limona ketone). The particle-phase products were dominated by peroxide species. The exact secondary product formation depended on the competition between ozone and OH radicals. The simulated concentrations of the key gas-phase limonene oxidation products were compared with the few relevant health studies namely some human reference data values (Wolkoff et al. 2013). The modelled concentrations for IPOH, 4-AMOH and 4-OPA did not exceed the reference concentrations and were not a cause for concern for a typical indoor

environment. However, cleaning products contain not only limonene, but also a wide range of other terpenes that could enhance the formation of secondary pollutants such as formaldehyde, 4-OPA, glyoxal or PANs. Therefore, Carslaw (2013) suggested that further studies to measure carbonyl species indoors were required to help to validate and improve the models, and also to understand secondary pollutant formation in the real conditions of indoor environments. Further, more health studies were recommended as the toxicity of many species indoors was unknown at the time of the study (and this remains the case now).

Carslaw et al. (2015) investigated the impact of outdoor vegetation on office air indoors. The model was applied to simulate ozone and particulate matter ($PM_{2.5}$) concentration in offices in three European cities (Milan, Helsinki and Athens) during typical and heatwave summer time conditions. The model estimated the indoor $PM_{2.5}$ concentration, which included particles derived from outdoors and emitted from indoor sources. The results had significant implications for indoor air quality particularly when biogenic emissions are important outdoors, for instance for buildings with green walls.

Wong et al. (2017) used the INDCM model, adopted from Carslaw (2007), to predict gas-phase chlorine (Cl_2) and dichlorine monoxide (Cl_2O) concentrations, as well as radical formation indoors assuming different levels of illumination. Floor cleaning with products containing bleach, was demonstrated to lead to an increase of chlorinated gases and particles in the room. The INDCM model was able to show that the uptake of hypochlorous acid (HOCl) on indoor surfaces and the reaction with organics on the surface had an important impact on indoor air concentrations. It also showed that Cl_2 and HOCl photochemistry increased OH and Cl radical concentrations indoors. In general, using products that contain bleach enhance the oxidation rates both in the gas-phase and on surfaces.

Finally, Carslaw et al. (2017) used the INDCM to simulate concentrations of OH and HO_2 during surface cleaning with a limonene-containing cleaning product and also during the operation of an "air cleaning" device operation. The model results were in good agreement with measured values of the radical species (within 50% and often within a few percent) and also demonstrated that terpene reaction products (i.e. heptanal ~0.8 ppb, limonaldehyde ~0.1 ppb and limonaketone ~0.1 ppb) dominated the product composition following desk surface cleaning activity, whereas aromatics and other VOCs (i.e. methylglyoxal ~160 ppt and glyoxal ~100 ppt) were more important during the "air cleaning" device usage.

Although previous indoor chemistry research had focused mostly on ozone–terpene reactions, Waring and Wells (2015) investigated the importance of also including both OH

and NO_3 reactions with these species. Waring and Wells (2015) used a modelling analysis based on a Monte Carlo framework that varied input parameters probabilistically, to evaluate VOCs gas-phase conversion rates following ozone, OH and NO_3 oxidation in typical residences. The model was also able to determine the importance of sources of these oxidants indoors. The model included sources of the oxidants indoors mentioned previously, but also included the photolysis of nitrous acid (HONO) to generate OH radicals and the reactions of NO_2 with stabilized Criegee intermediates to form NO_3.

The time-averaged, mass-balance model presented by Waring and Wells (2015) assumed the indoor setting to be a single well-mixed environment with the air exchange rate calculated through a combination of natural ventilation and infiltration. The equations were used for four Monte Carlo operations, with 10,000 cases run for each. Each set of operations included stable indoor background VOC concentrations and variable outdoor NO_x and ozone concentrations. Additionally, one set included variable indoor limonene concentrations, then another set incorporated variable indoor emissions of NO_x and HONO. The final set incorporated both variable indoor limonene concentrations as well as variable indoor emissions of NO_x and HONO. Total VOC oxidation rates by ozone, OH and NO_3 were calculated using reaction rate coefficients and median VOC concentrations for a typical residential building were taken from the literature. In general, the modelling results showed that the oxidation rates of VOCs by ozone, OH and NO_3 were higher as outdoor ozone and NO_2 concentrations, indoor limonene concentration, HONO photolysis rate and the air exchange rate increased. The oxidation rates decreased as NO increased and as ozone deposition increased. OH formation following photolysis of HONO could be as important as ozonolysis of alkenes indoors under some conditions. VOC oxidation rates were dominated by the reactions of ozone and OH in the indoor environment. When the concentration of ozone outdoors was high (~142 ppb) and NO_x low (~0.3 ppb), the oxidation rates by OH and O_3 were similar. However, when the ozone concentration outdoors was low (~4 ppb) and NO_x high (~116 ppb) the oxidation rate by OH was the highest. In general, the oxidation reaction of limonene was the most important for ozone and NO_3, however OH loss was dominated by reactions with alcohols, aldehydes and aromatics.

Following the oxidation reactions, a variety of secondary products were formed such as alcohols, carbonyls, carboxylic acids and SOA. Since the model presented by Waring and Wells (2015) considered the simultaneous oxidation process of different oxidants, the study presented crucial findings for future indoor chemistry research development. Given that the research considered only limonene, Waring and Wells (2015) suggested that using

a variety of terpenes could enhance the model predictions. Therefore, further model development would be necessary. Also, detailed indoor air measurements would be challenging but definitely beneficial for validation and further model development.

Mendez et al. (2015) presented a new time-resolved INCA-Indoor model. The INCA-Indoor model was developed from a box model called the INteraction with Chemistry and Aerosols (INCA) (Hauglustaine et al., 2004; Folberth et al., 2006) model for outdoors. The aim of the INCA-Indoor model was to help understand field campaign data, but first, it was used to compare with previous modelling studies, focusing on the oxidant species. INCA-Indoor was used to estimate the major sources of OH radicals indoors, such as the photolysis of HONO and the ozonolysis of alkenes.

The INCA-Indoor model included photochemistry, deposition and emissions processes, as well as surface processes indoors. The surface interactions were described by exchange with outdoors, emissions from building materials, sorption processes and heterogeneous chemistry reactions at surfaces. The input values of the parameters describing such processes i.e. deposition velocities or emission rates were taken from the literature. The air exchange rate was assumed to be 2.0 h^{-1}, the volume of the room was 250 m^3 and the surface to volume ratio was 3.0 m^{-1}.

The model included the chemical mechanism based on the updated but simplified version of the SAPRC-07 mechanism (Carter, 2010), which consisted of 1400 oxidation reactions of 640 VOCs. The model did not include fluid mechanics, so the concentration of the pollutants was assumed to be spatially homogenous. However, for VOCs, the model considered three regimes: the bulk air, a boundary layer adjacent to a surface and the surface itself. VOCs species were assumed to adsorb reversibly on the material surface, so desorption also happened. Gases could also diffuse from the bulk air through the boundary layer to undergo direct uptake to the surface. They could also diffuse out of the boundary layer and back into the bulk air. The model also included deposition for inorganic species as an irreversible process, where the loss rate of the pollutant was calculated using the deposition velocity and the surface to volume ratio.

The model simulated cooking and cleaning indoors for different photolysis and air exchange rates, and NO_x and HONO concentrations. To assess the impact of indoor chemistry, the analysis focused on the production and loss pathways of formaldehyde and acetaldehyde (as potentially harmful species) and estimation of their concentrations indoors. The results showed that under the chosen conditions, formaldehyde had a high emission rate from building materials (88-99% of the total production), such that the chemical production

(2-11%) and deposition loss processes (~25%) became insignificant. However, the production of formaldehyde through chemistry increased (up to 6.5 ppb/h) with higher OH concentrations. Similarly, acetaldehyde was produced rapidly (~9 ppb/h) when the OH concentration is high.

As HONO is as an important OH precursor indoors (e.g. Figure 7), the concentration of the OH radical indoors varied with the HONO concentration. For higher air exchange rates, species like ozone, NO_x and VOCs were transported indoors more efficiently from outdoors. Thus, the resulting NO concentration enhances the conversion of HO_2 to OH. When the air exchange rate was high (AER = 2.0 h^{-1}), the formation of secondary species was limited by ventilation. On the contrary, low ventilation rates (AER = 0.2 h^{-1}) enabled efficient formation of secondary species as reaction time was effectively extended (i.e. acetaldehyde concentration was ~16.3 ppb).

The INCA-Indoor model was compared with the model presented by Carslaw (2007). The main differences were in the chemical scheme the models used, the photolysis rates and the outdoor concentrations. The Carslaw (2007) model was based on the MCM v3.1 scheme whereas the INCA-Indoor model was based on the SAPRC-07 scheme. The two models included similar parameters for the processes of ventilation, deposition and reaction with alkenes, so the ozone concentrations were similar (~ 4% difference) for both models. NO_2 and NO concentrations estimated by INCA-Indoor model were underestimated by 63% and 35% respectively compared to the model presented by Carslaw (2007). However, HO_2 and OH concentrations from the INCA-Indoor model were overestimated by 38% and 34% respectively. Although the INCA-Indoor model included a less detailed chemical mechanism in comparison with the model presented by Carslaw (2007), the mean relative difference for OH, HO_2, O_3, NO, NO_2, PANs, limonene and formaldehyde was in the range between 4.3% for ozone to 88% for PAN species.

However, there are still validation issues of the INCA-model. The INCA-model was developed to interpret the results of the experimental campaign MERMAID, which was aimed to study the indoor air quality of rooms in low energy buildings (Schoemaecker et al., 2014). On the other hand, the INCA-Indoor model predictions were different to those measured indoors. For instance, the predicted HONO and alkene concentrations were lower than those from the measurements (Alvarez et al., 2013). Therefore further studies should include the input data obtained from the field measurements to enhance the understanding of detailed chemistry indoors.

2.2.2 Related models

This section describes models that are at least partially relevant for the topic of this thesis but are not indoor air chemistry models. Those described include dermal uptake models, exposure models and kinetic skin models.

2.2.2.1 Dermal uptake models

There is strong evidence that dry cleaning solvents, such as naphthalene, dichlorobenzene or methamphetamine, can sorb to clothing materials and enhance dermal exposure owing to release of chemicals near the skin surface (e.g. Sherlach et al., 2011; Morrison et al., 2015). Partitioning of such chemicals and/or passive adsorption from indoor air can have an impact on exposure. Following the hypothesis presented by Weschler et al. (2015), which assumed that clothing materials absorb a great quantity of phthalates and release them close to the skin reducing the mass transfer resistance from indoor air to the skin. Morrison et al. (2015) measured the amount of airborne phthalates that could partition to clothing. The specific aim was to measure the mass of two phthalate esters, dibutyl phthalate (DnBP) and diethyl phthalate (DEP), that could accumulate on cotton clothing and to assess partition coefficients. The partitioning coefficients normalized by volume for DEP and DnBP for three different materials were in the range of $2.5 - 2.7 \times 10^5$ and $36 - 44 \times 10^5$ respectively and showed that phthalates could be highly concentrated closer to the skin. The concentrations of DnBP and DEP adsorbed on cotton clothing materials are function of air concentration (Figure 8).
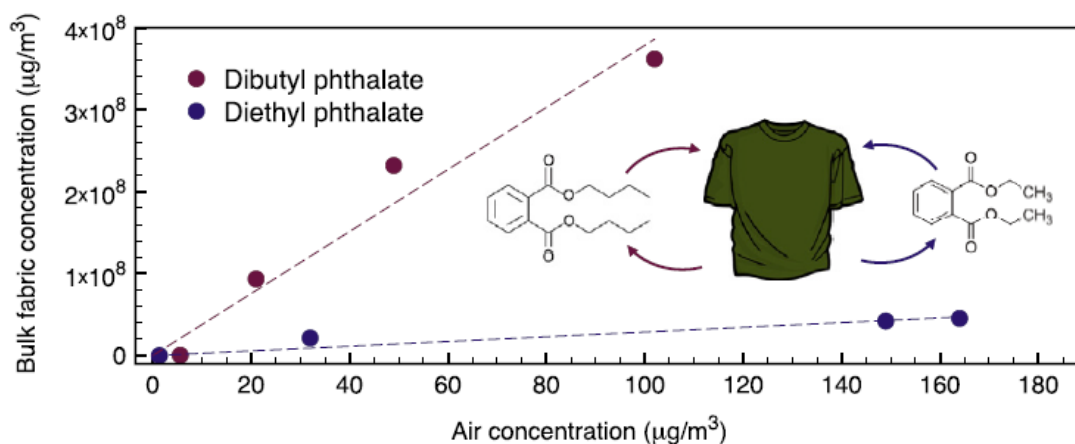
Figure 8: The concentrations of dibutyl phthalate (DnBP) and diethyl phthalate (DEP) adsorbed on cotton clothing materials as a function of air concentration (Source: Morrison et al., 2015).

Morrison et al. (2016) also noted that the uptake was higher for the subject wearing clothes compared to the bare-skinned person in the same experimental conditions and that freshly laundered clothes led to lower uptake than those exposed to the phthalates. The experimental work was followed by modelling studies (Morrison et al., 2016; 2017). Morrison et al. (2016) used a model to estimate the transdermal uptake for bare-skinned occupants, which showed relatively good agreement with the measurement results. The transdermal model included parameters describing transport of the phthalate compounds (DnBP and DEP) from the gas-phase (taking into consideration a gas-phase concentration) through the clothing layer by adsorption on the fabric material. Transport of the phthalates from the clothing layer to the skin lipids (a diffusion coefficient) occurred in the layer of air between the clothing material and the skin. The model also included parameters describing the mass transfer through the skin sub-layers (stratum corneum and viable epidermis). The layers of the clothing material, air between the clothing material and the skin, as well as skin surface lipids and the skin sub-layers were described by specific thicknesses (Figure 9).
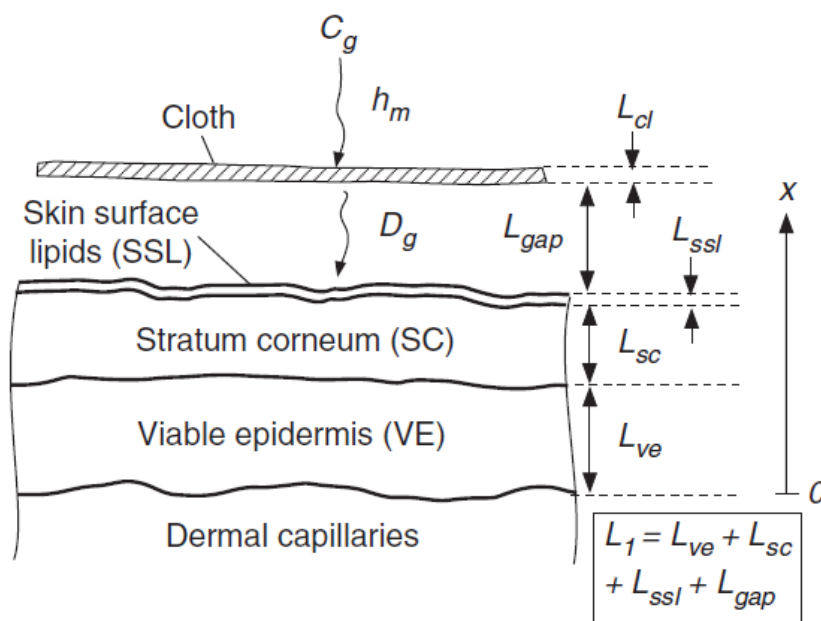
Figure 9: Schematic view of DnBP and DEP dermal uptake from the gas-phase through the gap of the air to the skin. C_g denotes gas concentration of the compound, D_g gas-phase diffusivity of the compound, L thickness of the layers (Source: Morrison et al., 2017).

Morrison et al. (2017) developed the model further to consider the transdermal uptake of SVOCs including the subjects wearing clothes. Therefore it was possible to estimate

the dermal uptake of DnBP and DEP more precisely than in the previous version of the model, as well as to evaluate the impact of clothing on the human subject. The model was used to simulate the experimental conditions reported by Morrison et al. (2016), where subjects wore either freshly laundered or exposed clothes for 6 hours, before dermal uptake was measured. The results of the model showed that a smaller gap between the clothing material and the skin led to higher dermal uptake of the phthalate compounds. For instance, the model predicted the uptake of DnBP and DEP as 13.8 mg and 7.6 mg respectively when the gap between cloth and skin was 0.2 mm, and 1.8 mg and 3.0 mg respectively when the gap was 10 mm. Higher dermal uptake was predicted for the compounds that have clothing-air partitioning coefficients within the range of 10^5 and 10^7. Also, the dermal uptake was higher for clothes that had been worn for longer without washing as the effect of phthalates accumulation.

In conclusion, the model proposed by Morrison et al. (2016) improved the estimation of dermal uptake of DnBP and DEP from clothing. The authors suggested that future models should include more SVOC compounds, not only DnBP and DEP, to expand the exposure prediction to a wider suite of compounds. Improved models should also include enhanced parameter values, such as partitioning coefficients, which would consider different types of materials, laundry habits and frequency or different environmental conditions.

2.2.2.2 Exposure model

Terry et al. (2014) proposed a new approach for indoor air models by combining a reduced indoor air chemistry model with a probabilistic and physical indoor − outdoor air exposure model. The new INDAIR–CHEM model was used to calculate exposure to secondary indoor air pollutants and to estimate indoor air quality in European offices under extreme, heat-wave conditions during the summer of 2003 and a more typical summer in 2009. Previous indoor air exposure models (Dimitroulopoulou et al., 2006) focused on primary pollutants, even though secondary pollutants were of increasing concern in terms of health impacts. On the contrary, the detailed indoor air chemistry models (i.e. Carslaw, 2007) included indoor air chemical degradation pathways, but did not focus on the exposure effect of the compounds. Hence, the INDAIR–CHEM model proposed by Terry et al. (2014) included both aspects and was used to evaluate exposure of indoor air pollutants taking into account different conditions indoors. The INDAIR-CHEM model used a simplified version of the model scheme which was previously presented by Carslaw (2007) and improved by

Carslaw et al. (2012). The chemical scheme was reduced to include only a few key indoor air pollutants, namely the reactions of ozone, NO_x, HCHO and CO with 19 chemical species (including limonene) incorporating 44 photolysis and chemical reactions. The INDAIR-CHEM model included also parameters describing air exchange rates between indoors and outdoors but also between different zones in the indoor environment, which would help to estimate personal exposure indoors. The new model investigated different outdoor and therefore indoor conditions focusing on ozone, NO_x, particulate matter and secondary pollutant concentrations that might be responsible for adverse health effect. The heat-wave summer (2003) (precisely the first two weeks in August 2003) conditions were chosen for the modelling study since measured ozone concentrations were extremely high and could contribute to poor indoor air quality. Such conditions are expected to arise more frequently in the future owing to climate change (Beniston, 2004). They were therefore chosen for comparison with the reference conditions for a more typical summer in 2009.

Eight different European cities (Amsterdam, London, Helsinki, Milan, Paris, Athens, Vienna and Lisbon) were chosen as study locations for air quality evaluation in office buildings. The model simulations assumed a naturally ventilated office (volume of 60 m^3 and surface area of 20 m^2) with an air exchange rate of 0.5 h^{-1} or 1.5 h^{-1} using the outdoor concentrations measured in each city. Since activities such as cleaning can have an impact on occupants' health and the exposure to the pollutants (Wolkoff et al. 2013), a 30-minute cleaning activity in the office was simulated, during which time, the limonene concentration was assumed to be 200 ppb based on Singer et al. (2006). The results of this modelling study showed that lower ventilation rates (AER = 0.5 h^{-1}) contributed to lower exposure to ozone indoors (4.2 ppb), however it also enhanced the formation of secondary indoor air pollutants since the time for reactions was prolonged. Thereafter, the cumulative exposure for indoor occupants increased when the ventilation rate was lower. For instance, formaldehyde concentration was 15.1 ppb when the air exchange rate was 0.5 h^{-1} and 8 ppb when the air exchange rate was 1.5 h^{-1}. Additionally, the indoor exposure increased when outdoor concentrations, particularly to ozone, here higher during heatwave summer conditions (i.e. an average outdoor ozone concentration in Milan during heatwave summer conditions was ~75 ppb). This research emphasized the need for further research on limonene oxidation products and their impact on the exposure of the occupants. Likewise, the authors recommended that additional work should be carried out for $PM_{2.5}$ measurements indoors, given that high concentrations were simulated following the cleaning activity indoors and may contribute to adverse health effect.

2.2.2.3 Kinetic skin model

Ozonolysis reactions with skin lipids can decrease ozone concentration indoors and increase the potential for secondary pollutant formation (e.g. Wisthaler and Weschler, 2010). A new model by Lakey et al. (2016) aimed to evaluate and quantify ozone – skin lipids reaction products, especially monocarbonyls and dicarbonyls which might cause skin or respiratory irritation, but also could be absorbed to the bloodstream over the time. Lakey and co-authors (2016) developed the Kinetic Multilayer model of SUrface and Bulk chemistry of the skin (KM-SUB-Skin), which included mass transport and chemical reactions at the skin-surface, in the near-surface gas phase and in the bulk gas-phase. The model was developed based on the kinetic multilayer for aerosol surface and bulk chemistry (KM-SUB) (Shiraiwa et al., 2010).

The surface layers included a sorption layer, a skin oil layer, bulk layers and a layer of blood vessels (Figure 10). Three sets of input data were used in the KM-SUB-Skin model (Lakey et al., 2016). Two of them used the data presented by Wisthaler and Weschler (2010), who measured the ozone and the ozonolysis volatile product (i.e. decanal, 6-MHO, 4-OPA or acetone) concentrations in a chamber in the presence of two people. The third set of data included VOC measurements, which was done for the purpose of this modelling study, placing an enclosure on the subject's forehead and being exposed to ozone flow. The effect of clothing on the chemistry processes, the mass transport between the skin and the gas-phase, including how skin oil content in clothing changes with time, different layers of materials and the different types of clothing materials, remains largely unknown and is a source of large uncertainty. Therefore, for simplicity, the model presented by Lakey et al. (2016) considered that skin oil exists solely on the skin and not on the clothing materials.
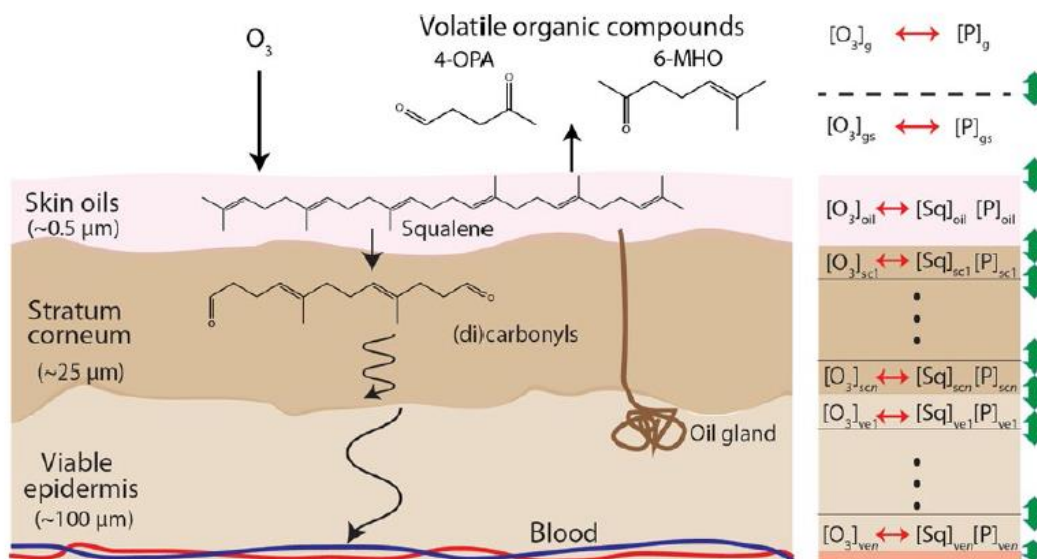
Figure 10: A schematic of ozone interactions with the skin taking into consideration gas-phase and different surface-phase layers (Source: Lakey et al., 2016).

The results of the model presented by Lakey and co-authors (2016) showed that the presence of people indoors decreases the ozone concentrations. Hence, two people in a 28.5 m^3 chamber reduced the concentration of ozone from ~33 ppb to ~16 ppb over 4 hours. In addition, as the ozone concentration decreased, the gas-phase concentrations of VOCs increased. For instance, 6-MHO increased to 2.5 ppb and 4-OPA up to 2 ppb both from a concentration close to zero. Increasing the number of people in the room (20 occupants, 28.5 m^3), the concentrations of ozone and the reaction products decreased, since each occupant was exposed to a lower concentration of ozone. An increase in the ventilation rate (higher than 1 h^{-1}) caused higher ozone concentrations indoors (~14 ppb), but a lower total concentration of carbonyl products (0.1-0.8 ppb) in the gas-phase and blood as they were flushed out more rapidly once formed.

In conclusion, skin oils can react very efficiently with ozone, though it should be noted that there are still uncertainties in terms of its chemical and physical production and removal. The number of occupants will also have an impact and the authors note that further research should include i.e. differences in the room temperature, which can impact the skin temperature and therefore potentially human body emissions. Also, the application of personal care products onto the skin could potentially enhance the chemical reactions. Likewise, the skin pH or the age of different individuals might affect the chemistry. Indeed, more measurement and further studies of the squalene ozonolysis reaction products in

the gas-phase as well as in the skin oil, skin and blood, such as the loss rate of the products, are required for better understanding and for future model development. Also following the recommendations of Lakey et al. (2016), it would be beneficial to assess the adverse health effect of the squalene ozonolysis products and their potential for skin and respiratory irritation.

2.3 Summary of indoor air chemistry model limitations

Indoor air chemistry is a complex subject which provides many challenges for modelling studies. One of the main issues is that measurements within indoor environments (for model validation) are very challenging. It is often difficult to measure in real buildings (noise, ventilation issues) and to do so in meaningful way that encapsulates the wide variety between different buildings. Thus, current measurement techniques are not able to provide all of the detailed results necessary to gain a broad understanding of chemistry indoors. Given that there are few measurements of indoor air pollutants, particularly with respect to the detailed chemistry such as concentrations of many secondary indoor air pollutants, the development of indoor air models is a substantial requirement for better understanding of the indoor air chemistry processes and to evaluate the impacts of indoor air pollution on human exposure.

Therefore, indoor air chemistry models should be properly designed to include the different sources and sinks of pollutants within a building envelope, such as indoor chemical reactions, material emissions and indoor surface interactions, human activity indoors for instance cleaning and cooking, exchange of the pollutants with outdoors, or transport of the pollutants within different zones of a building. Clearly, field and laboratory measurements can help to develop the model framework to improve chemical mechanisms or provide more accurate input parameters for the model, but detailed indoor air chemical models are likely to remain the most important tool to evaluate indoor air pollution for some time to come.

Current indoor air chemistry models use chemical mechanisms, such as the Master Chemical Mechanism (Jenkin et al., 1997), which were originally constructed for modelling outdoor atmospheric chemistry processes. Consequently, there are some aspects that could be improved to better represent processes indoors. For instance, the mechanisms should include more degradation schemes for terpenes, which are emitted during cleaning activities, or air freshener use. There are also fatty acids and esters emitted from indoor surfaces such as human skin. However, representation of these species in chemical mechanisms is currently

limited, largely owing to the chemical complexity. Likewise, current models include estimated photolysis rates indoors, since there are only a few measurements available. This is particularly a problem when considering the propagation of light indoors, such as the variation between the air close to a window and in the shadow on the far side of the room from the window.

There are also very few measurements of deposition rates of gas-phase species indoors. Those that exist are mainly for ozone, nitrogen dioxide and sulphur dioxide (Grontoft and Raychaudhuri, 2004) and are limited to relatively few surfaces. Measurements for gases such as formaldehyde and HONO are absent for indoors, but based on outdoor deposition rates, could potentially play a role indoors.

A major area for indoor model development is the representation of surface interactions. A wide range of materials exist indoors, each with different properties such as surface area and porosity. However, very few measurements of these properties have been made to date and those that have focus mainly on ozone. Nevertheless, some recent studies (e.g. Hodgson et al., 2002; Morrison and Nazaroff, 2000; 2002), have provided sufficient data such that model improvements can begin to be made. There are few existing surface-phase models and these typically focus on one type of surface, such as human skin. There is still a need to develop models, which include surface interactions in a real building case scenario. Therefore model development of surface interactions in a real indoor environment scenario is the focus of this dissertation.

3. Methodology

3.1 Introduction

In the absence of comprehensive indoor air measurements, the best way to quantify indoor air pollutant concentrations is through the use of an indoor air quality model. Modelling studies are necessary to provide insight into indoor air quality, as well as to inform focused measurements. An indoor air detailed chemical model (INDCM) developed by Carslaw (2007) and improved by Carslaw et al. (2012) has been used in this study to investigate indoor air chemistry and particularly that of surface interactions following deposition of ozone. Each component of the INDCM is now described in the following sections of this Chapter. This chapter describes the version of the model before the surface interactions developments described in subsequent chapters (Chapters 4-6) were employed. It describes the experimental framework used in Chapters 4-6 and also defines the case study locations, the case study apartment and the indoor and outdoor concentrations used for each study location.

3.2 The Master Chemical Mechanism

The model is based on a comprehensive chemical mechanism called the Master Chemical Mechanism, MCM v3.2 (MCM, University of Leeds). The MCM is a near-explicit chemical mechanism that describes in detail the gas phase chemical breakdown of a wide range of volatile organic compounds (VOCs) (Jenkin et al., 1997; Jenkin et al., 2003; Saunders et al., 2003). The MCM considers available information on the kinetics and products of the reactions related to VOC oxidation, aiming to construct a detailed representation of the atmospheric degradation mechanisms. For reactions where the kinetics and products have not yet been investigated experimentally (the vast majority), these parameters are defined based on analogy with the reactions that have already been studied following a defined protocol described by Jenkin et al. (1997) and in subsequent publications (Jenkin et al., 2003; Saunders et al., 2003).

The degradation of VOCs is initiated by reactions with O_3, OH, NO_3 and photolysis where relevant. The degradation routes are driven by the parent compound. For instance, carbonyls, organic nitrates etc. undergo photolysis whilst larger alkanes, alkenes and

alkynes will not. Initiation by photolysis reactions can form intermediate products of oxy and peroxy radicals (Jenkin et al., 1997).

All VOC species react with the OH radical to form peroxy radicals (RO_2). Examples for ethane, ethane and benzene are given in equations 3-5:

$$C_2H_6 + OH\ (+O_2) \rightarrow C_2H_5O_2 + H_2O \tag{3}$$

$$C_2H_4 + OH\ (+O_2) \rightarrow HOCH_2CH_2O_2 \tag{4}$$

$$C_6H_6 + OH\ (+O_2) \rightarrow BZBIPERO_2 \tag{5}$$

Alkanes react with OH via abstraction of the H atom from the carbon chain as shown in equation 3. Reactions of OH with alkanes, alkenes, alkynes and aromatics all produce RO_2 radicals, which can undergo a number of further reactions (Jenkin et al., 1997; Atkinson and Arey, 2003; Saunders et al., 2003). Alkenes undergo addition to the double bond by OH to form RO_2 radicals (equation 4). Aromatic species react with OH involving the addition of the OH radical to the aromatic ring (equation 5). Note that many of the reactions with NO_3 are similar to OH, but then nitrated products are formed.

RO_2 radicals react with NO_2, NO, NO_3, HO_2, itself and other peroxy radicals (Jenkin et al., 1997), to form oxygenated species, for instance carbonyl compounds (9) or alcohols (equation 8). The main fate outdoors is to react with NO_x/RO_2 to form oxy (RO) radicals such as C_2H_5O in equations 6-7:

$$C_2H_5O_2 + NO \rightarrow C_2H_5O + NO_2 \tag{6}$$

$$C_2H_5O_2 + RO_2 \rightarrow C_2H_5O \tag{7}$$

$$C_2H_5O_2 + RO_2 \rightarrow C_2H_5OH \tag{8}$$

$$C_2H_5O_2 + RO_2 \rightarrow CH_3CHO \tag{9}$$
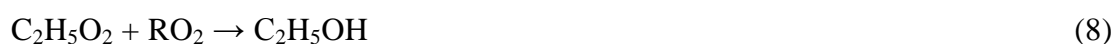
As each VOC will generate 3-4 peroxy radicals following oxidation by OH/NO_3, a large number of RO_2 radicals are generated in the chemical mechanism. Describing each of these reactions explicitly would be chemically and computationally complex, given that

each RO_2 radical can potentially react with all other RO_2 species, as well as with i.e. HO_2 and NO. A simplified approach is used in the MCM (Jenkin et al., 1997), whereby an RO_2 radical pool is assumed, where RO_2 is the sum of the concentrations of all peroxy radicals excluding HO_2. It can then be assumed that each RO_2 radical reacts with 'the pool' rather than individually with each of the RO_2 radicals.

For the majority of RO_2 reactions, kinetic data are unavailable and therefore generic rate coefficients are assigned. These rates and branching ratios are modified depending on the parent hydrocarbon. For instance, the rate coefficient for the reactions of RO_2 with NO_3 is assigned a value of 2.3×10^{-12} cm^3 $molecule^{-1}$ s^{-1} for the reactions with peroxy radicals and for the reactions of RO_2 with NO is assigned a temperature-dependent rate coefficient of 2.7×10^{-12} $e^{(360/T)}$ cm^3 $molecule^{-1}$ s^{-1} (MCM Protocol, University of Leeds).

The oxy radicals can then react with O_2, isomerise or thermally decompose depending on the parent VOC. Such reactions typically form HO_2 (e.g. equation 10) and then OH following reaction with NO (equation 11). For instance, for the relatively simple oxy radical C_2H_5O, the fate is shown in equation 10:

$$C_2H_5O + O_2 \rightarrow CH_3CHO + HO_2 \tag{10}$$

$$HO_2 + NO \rightarrow NO_2 + OH \tag{11}$$

Unsaturated species containing double bonds react with ozone as described by Atkinson (1997) and shown schematically in Figure 11. The initial attack of ozone on a double bond is followed by the formation of an ozonide, which decomposes rapidly to form a carbonyl compound and excited and stabilized Criegee biradicals (R'R''COO) (Murray, 1968; Criegee, 1975). The excited energy-rich Criegee biradicals may be stabilised or decomposed. Additionally, the OH radical can be formed. The stabilised Criegee biradicals react with NO, NO_2, SO_2, CO and water. However, the main fate is the reaction with water under most conditions outdoors and probably indoors too.
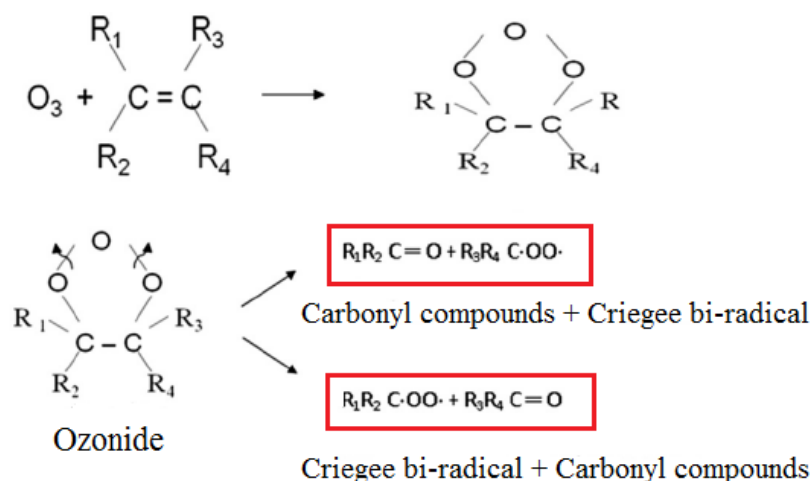
Figure 11: Ozonolysis of an alkene to form carbonyl and other products (Source: Cheng et al., 2015).

As well as the radical products described above, the degradation of VOC following initiation and propagation reactions leads to a wide range of more stable products, such as carbonyls, PANs (peroxyacetyl nitrates), organic nitrates ($RONO_2$), hydroperoxides (ROOH), percarboxylic acids (RC(O)OOH), carboxylic acids (RC(O)OH) and alcohols (ROH) (Saunders et al., 2003). Following the same methodology as described above, these products are degraded through reaction with OH, NO_3, O_3 and photolysis where relevant, until water and CO_2 are formed as final products (Jenkin et al., 1997). The schematic view of these processes is shown in Figure 12. The MCM also includes an inorganic scheme for ozone, NO_x and carbon monoxide, which contributes to the budget of radicals and species formation.
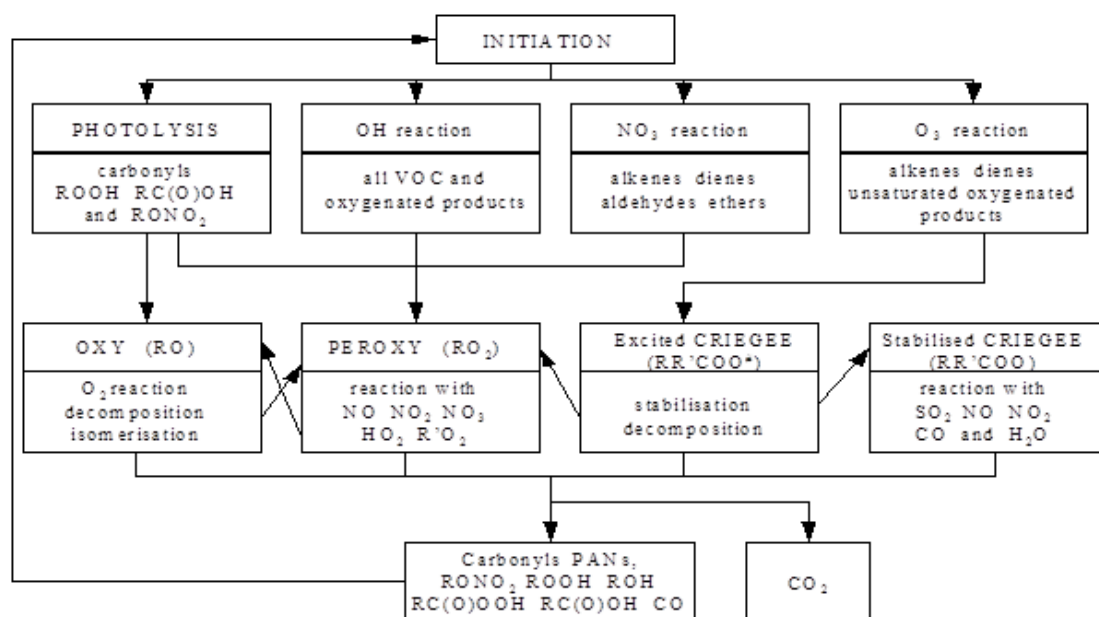
Figure 12: Flow chart describing the degradation process of VOCs reactions including initiation, propagation and termination reactions. Initiation reactions occur by reactions with O_3, OH, NO_3 and photolysis. Intermediate products, such as oxy (RO) and peroxy (RO_2) radicals, excited and stabilized Criegee (R'R''COO) species, undergo a variety of reactions to form final products, such as carbonyl species or organic nitrates until water and CO_2 is formed (Saunders et al., 2003).

3.3 Exchange with outdoors

The air exchange rate is the rate at which air passes into a building caused by its ventilation system or its leakage (Dimitroulopoulou et al., 2001). In general, the air exchange rate is calculated using the air flow rate through the indoor space divided by the volume of the indoor space. For naturally ventilated spaces, tracer gas measurements, such as CO_2, can be used to determine the average air exchange rate (Persily, 2006). Then, a mass balance analysis based on the indoor CO_2 concentration is estimated by calculating the reduction of the CO_2 concentration indoors over a period of time assuming no additional indoor sources (Coley and Beisteiner, 2002; Roulet and Foradini, 2002).

The air exchange rate depends on several factors, such as climatic conditions (degree of window opening), the behaviour of residents and building characteristics (e.g. natural versus mechanical ventilation, building filtration factor). There is often higher air exchange rate in a kitchen than in living rooms and bedrooms because of ventilation associated with cooking (Dimitroulopoulou et al., 2001). Also, different ventilation rates might be noted for

classrooms or offices compared to residential buildings. Furthermore, ventilation rates are expected to be higher during summer, when windows are open more frequently.

In a typical residential environment the air exchange rate may vary quite broadly from 0.2 h^{-1} (air changes per hour), which is considered as a representative value for tightly constructed, energy-efficient housing, to the value of 2.0 h^{-1} that is more typical for loosely constructed building, though in some cases it might exceed 5.0 h^{-1} (Weschler, 2000). An analysis of the data from approximately 2800 households in the US an average of air exchange rate as 0.76 h^{-1} (Murray and Burmaster, 1995). Similarly, following the review of Dimitroulopoulou et al. (2006) based on a data-base of approximately 470 UK dwellings the mean AER was ∼ 0.7 h^{-1}, with a range of 0.2-1.5 h^{-1}. Ventilation rates greater than 0.5 h^{-1} were reported in Mediterranean countries such as Portugal and Greece, whereas in the Nordic countries, values lower than 0.5 h^{-1} were more typical (Dimitroulopoulou, 2012). Furthermore, higher ventilation rates are measured in mechanically ventilated dwellings, where the air is recirculated, rather than in naturally ones.

Following the large-scale statistical analysis presented by Murray and Burmaster (1995), the base case model runs in this study were performed assuming an air exchange rate of 0.76 h^{-1}. However, to investigate the model sensitivity to this parameter, the model has been tested over the range of the commonly reported values (0.2 h^{-1} - 2.0 h^{-1}).

3.4 Deposition processes

One of the components used to describe deposition processes is the deposition velocity (Raunemaa et al., 1989). The deposition velocity is a mass transfer coefficient that describes the reactivity of surfaces (Wang and Morrison, 2006). The deposition velocity is associated with the loss rate K (h[-1]) of pollutants and a particular surface to volume ratio (A/V) of the indoor environment, which can be described by equation 12 (Dimitroulopoulou et al., 2001):

$$K = \upsilon_d \left(\frac{A_i}{V_i} \right) \tag{12}$$

where υ_d is the deposition velocity of indoor species (m h^{-1}), A_i the surface area indoors (m^2), V_i the volume of air in the indoor environment (m^3) .

The surface area in this case incorporates those of the floor, walls and all of the internal furnishings. It is assumed that each gas has a characteristic deposition velocity, which defines how likely it is to be lost to the internal surfaces in a building. The deposition velocities for common pollutants that were used in the model were calculated by Carslaw et al. (2012), and presented in Table 1. Carslaw et al. (2012) averaged the deposition velocity for 25 species measured by Zhang et al. (2002) for different outdoor surfaces ("mixed broadleaf and needle leaf trees", "grass", "shrubs and interrupted woodlands" and "urban") in summer conditions. These surfaces were meant to be representative of a typical suburban area outdoors.

For O_3 and NO_2, indoor values were available that took into consideration a range of deposition velocities on different surfaces indoors and were averaged to give the values 0.0345 and 0.0261 cm s^{-1} respectively (Grontoft and Raychaudhuri, 2004). Since the calculated outdoor suburban values for O_3 and NO_2 were factors of 17.6 and 21.7 respectively higher than those for indoors, the suburban outdoor values were all divided by 20 to give indoor deposition velocity values that were used in the model (Table 1). The deposition velocities presented in Table 1 were used in the study of Carslaw (2007) and therefore are adopted in the current study with the exception of ozone, the treatment of which is described in the subsequent chapters.

Table 1: Calculated average deposition velocities used in the INDCM model and derived from outdoor values measured by Zhang et al. (2002) (Carslaw et al., 2012).

Compound	Compound symbol	Deposition velocity [cm s^{-1}]
Ozone	O_3	0.0345
Sulphur dioxide	SO_2	0.029
Nitrogen dioxide	NO_2	0.0261
Nitrogen pentaoxide	N_2O_5	0.07
Nitric acid	HNO_3	0.176
Nitrous acid	HONO	0.065
Hydrogen peroxide	H_2O_2	0.045
Nitrate radical	$NO_3\bullet$	0.07
Hydroperoxy radicals	$HO_2\bullet$	0.07
Hydroxyl radicals	$OH\bullet$	0.07
Formaldehyde	HCHO	0.035
Acetaldehyde	CH_3CHO	0.0123
Acetone	CH_3COCH_3	0.005
Methanol	CH_3OH	0.0307
Ethanol	C_2H_5OH	0.0264
Methylglyoxal	CH_3COCHO	0.0153
Formic acid	HCOOH	0.0438
Acetic acid	CH_3COOH	0.0359
Higher aldehydes	RCHO	0.0103
Long chain alcohols	ROH	0.0162
Long chain acids	RCOOH	0.0292
Long chain ketones	RCOR	0.0103
PANs	RO_3NO_2	0.0197

The value for higher aldehydes was applied to all aldehydes with a chain longer than acetaldehyde. Also, the values for long chain alcohols and acids were used for all alcohols and acids with a chain longer than ethanol and acetic acid respectively.

3.5 Photolysis

Outdoor photolysis rates were calculated following the method described in detail by Carslaw (2007). Basically, a 2-stream isotropic scattering model uses the longitude, latitude, time of year and day to calculate location and time specific clear-sky photolysis rates, which will affect the light that can reach the surface from the sun (Jenkin et al., 1997). Such values must then be attenuated to be representative for indoors. Although there is limited information in the literature, recent measurements (Gandolfo et al., 2016) have shown that whilst light at the visible wavelengths needed to photolyse NO_2 and HONO is typically attenuated to 10-15% of that outdoors by the time it reaches indoors, for species photolysed in the UV (such as ozone to give excited oxygen state atoms), transmission is typically <1% of that outdoors. Nazaroff and Cass (1986) found that 0.7% and 0.15% of visible and UV light respectively were transmitted through museum skylights, whilst for two laboratories in Greece with large windows; 70-80% of the visible light was transmitted indoors compared to 25-30% in the UV (Drakou et al. 1998). Clearly, approximately 3-5 times more light is transmitted in the visible compared to the UV.

Fiadzomor (2002) measured indoor and outdoor photolysis coefficients for NO_2 and found the indoor to outdoor ratio was about 1:10. Therefore, a value of 10% for transmission of visible light was assumed for the INDCM model runs. Following the assumption that there is ~ 3 times more light transmitted in the visible compared to the UV, it was assumed that 3% of the outdoor UV light was transmitted through the windows (Carslaw, 2007). The values were adopted from Carslaw (2007) and were used in the current study.

The indoor lighting is considered as having two components, namely UV (300-400 nm) and visible (400-760 nm) (Carslaw, 2007). For each species, the photolysis coefficient (j) was calculated according to the equations 13-15:

$$j_i = h_{uv}I_{uv} + h_{vis}I_{vis},$$

(13)

where:

$$h_{uv} = (100\,\text{nm})^{-1} \int_{300\,\text{nm}}^{400\,\text{nm}} \sigma\varphi\,d\lambda,$$

(14)

$$h_{vis} = (360\,\text{nm})^{-1} \int_{400\,\text{nm}}^{760\,\text{nm}} \sigma\varphi\,d\lambda.$$

(15)

I_{uv} and I_{vis} stands for spherically integrated photon flux (photons cm^{-2} s^{-1}) in the UV and visible respectively, h_{uv} and h_{vis} are constants calculated according to the equations 14-15, where σ represents the absorption cross-section of the molecule (cm^2), φ the quantum yield and dλ the relevant wavelength interval.

The sensitivity of the model to these assumptions is tested in the following chapters. For the baseline model of this study, indoor photolysis is assumed to be driven only by light that comes from outdoors and penetrates through the windows.

3.6 Initial conditions

3.6.1 Case study locations

To compare the impact of outdoor pollutant concentrations on indoor air quality, two different locations were chosen: Milan, Italy and Seoul, South Korea (Figure 13 and 14 respectively).
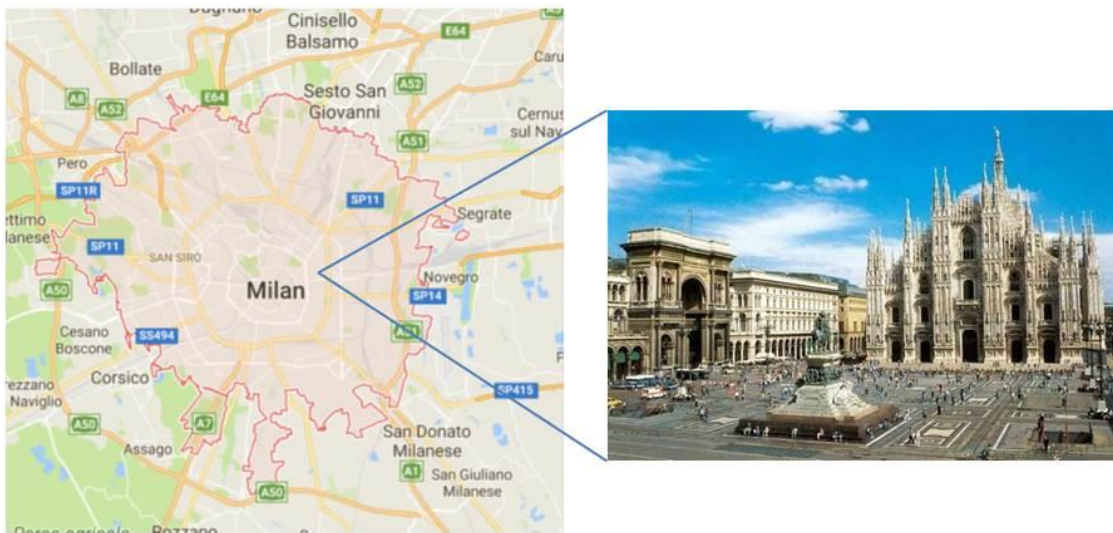
Figure 13: Schematic view of Milan (Source: Google Maps; TripAdvisor).
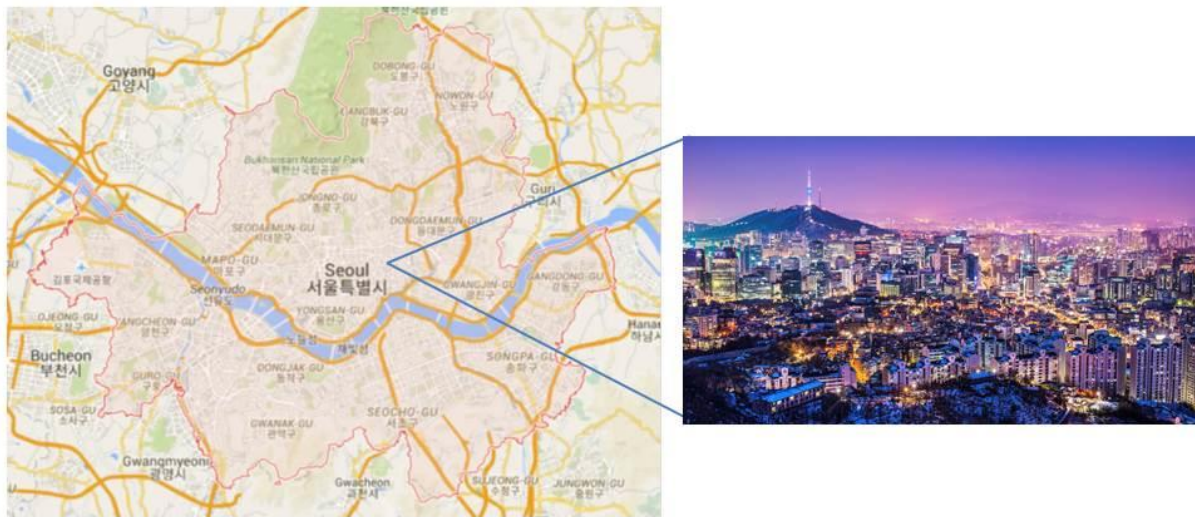
Figure 14: Schematic view of Seoul (Source: Google Maps; TripAdvisor).

Milan and Seoul were selected as study cities. Given that the selected cities are characterised by different sizes (Table 2), Seoul had approximately three times bigger area and was chosen as a megacity pollution example (the CAPACITIE project) and Milan as an average size but highly polluted city (Carslaw et al., 2015). The outdoor air pollutant concentrations vary between the case study cities (especially ozone and NO_x as shown in Table 3), which can potentially influence the formation of secondary pollutants indoors (Weschler, 2000). In particular, it is expected that the higher the outdoor ozone concentration, the more infiltrates indoors and impacts on the indoor air chemistry.

Table 2: Characteristics of the case study cities.

City	Area [km²]	Population size [inhabitants in 2013]	Density [inh/km²]	Latitude [°]	Longitude [°]	Average summer temp. [°C]	Annual average temp. [°C]
Milan	181.2	1 251 000	6 882	45.47 N	9.18 E	21 / 40*	11.4
Seoul	605.2	10 440 000	17 250	37.57 N	126.97 E	24	12

* Summer temperature in Milan during heatwave condition.

Table 3 shows the average summer outdoor concentrations of ozone, NO_2, NO and $PM_{2.5}$ in the case study cities. Also included for Milan are data during two weeks in August 2003 when there was a European heatwave, with many countries experiencing extreme temperatures and high ozone and PM concentrations (Terry et al., 2014). The outdoor NO_x and O_3 data for Milan were taken from the EU AirBase data set (Carslaw et al., 2015), for the 2 weeks during the heatwave in August 2003 and the same two weeks in August 2009 with more typical summer conditions (Carslaw et al. 2015). The averages for Seoul are presented for June-August of three years 2012-2014 (Professor Kyungho Choi, Seoul National University, South Korea, personal communication).

Table 3: Outdoor summer concentrations of ozone, NO_2, NO and $PM_{2.5}$ measured as an average for the heatwave period of 2 weeks in August 2003 and the same 2 weeks during typical summer conditions in August 2009 in Milan, and the outdoor concentration averages for June-August 2012-2014 in Seoul.

	Ozone [ppb]	NO₂ [ppb]	NO [ppb]	PM₂.₅ [μg m⁻³]
Milan August 2003	75.2	30.5	14.1	28
Milan August 2009	49.0	19.1	16.0	14
Seoul (summer 2012-2014)	34.4	25.0	9.2	19.9

The highest outdoor concentrations of ozone, NO_2 and $PM_{2.5}$ were recorded for Milan during summer time in 2003, when the heatwave conditions occurred. Thus, in respect of extreme conditions outdoors, the pollutant concentrations were higher than those measured in the typical summer conditions.

3.6.2 Case study residence

A typical apartment was used as a case study residence in this study. The size (70 m^2) and the plan of the apartment were adopted following Tae et al. (2011) who studied standard apartments in South Korea. Lim et al. (2011) in another study confirmed that small apartments in South Korea had typical surface areas less than 90 m^2, whilst Asdrubali et al. (2008) presented average surface areas of Italian apartments as ~73 m^2. Therefore this modelling study considers the size and the plan of the apartment suggested by Tae et al. (2011) as representative residence for both case study locations, Milan and Seoul. The apartment has 3-bedrooms each of 7.5 m^2 with an open plan kitchen/living room of 12.5 and 20.9 m^2 respectively, a small toilet (2.8 m^2), bathroom (7.8 m^2), corridor (3.9 m^2) and ceiling height of 2.4 m, giving a total surface area of 70 m^2 and a volume of 168 m^3. The plan of the apartment is shown in Figure 15.
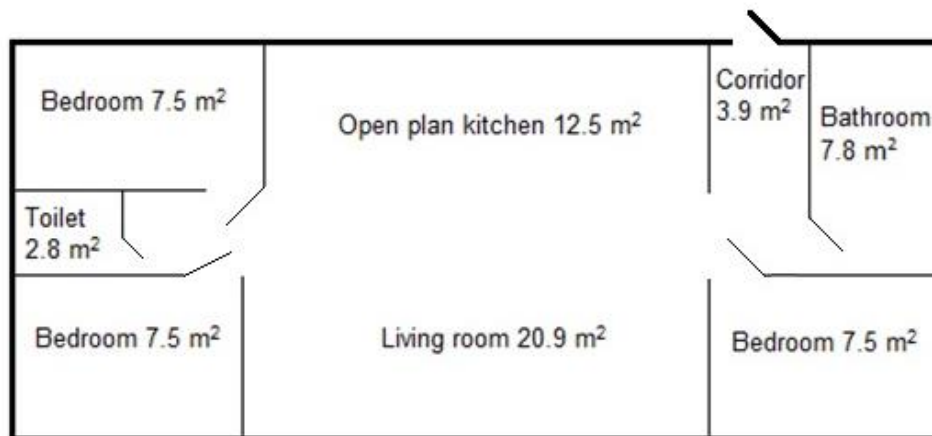
Figure 15: Schematic view of the case study apartment floor plan, with a total unfurnished surface area of 70 m^2 and a volume of 168 m^3 (Tae et al., 2011).

The case study apartment is assumed to have different types of internal surfaces for a typical residence, defined by different areas: hard furniture together with internal doors (22 m^2), soft furniture (35 m^2), wooden floors (51 m^2), painted walls and ceilings (199 m^2), linoleum including the kitchen, bathroom and toilet floors (11 m^2) and countertops, including those in the kitchen, toilet and bathroom and tiled toilet, bathroom and kitchen walls (19 m^2). This gives a total surface area for deposition of 337 m^2 (Singer et al., 2007; Cuéllar-Franca and

Azapagic, 2012). The proportions of surface size assumed for the apartment are shown in Figure 16.
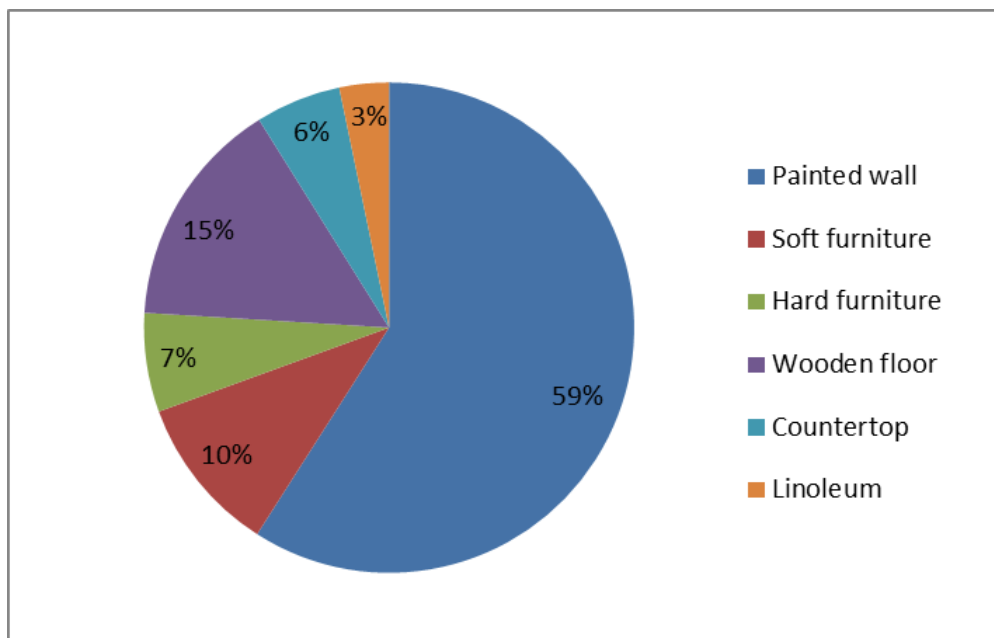
Figure 16: Surface type contribution to the total internal surface area in the apartment case study.

3.7 Outdoor and indoor VOC concentrations

The outdoor VOC values were assumed to be the same for each study location (Milan and Seoul) given the absence of detailed and representative measurements for these species outdoors. Outdoor VOC concentrations were available from the EU OFFICAIR project based on measurements in 3-5 buildings in Milan, Athens and Helsinki over 5 days in summer 2012 or set to typical outdoor values for an urban area (Sarwar et al., 2002; Carslaw et al., 2015). For C_6-C_{10} aldehydes, outdoor values of hexanal, heptanal, octanal, nonanal and decanal were assumed constant at 0.37, 0.15, 0.29, 1.0 and 0.11 ppb respectively for each location based on measurements outside US houses in residential areas (Hodgson et al., 2002). The outdoor VOC concentrations used in this study are presented in Table 4. The impact on model sensitivity of this assumption is discussed in later chapters.

Table 4: Mean outdoor VOC concentrations (µg m^{-3}) used in the model for all study locations (Hodgson et al., 2002; Sarwar et al., 2002; Carslaw et al., 2015).

Compound	Concentration [µg m^{-3}]
2-butoxyethanol	1.00
Acetaldehyde	5.20
Acrolein	4.60
α-pinene	1.60
Benzaldehyde	1.10
Benzene	0.77
Ethylbenzene	0.60
Formaldehyde	4.60
Limonene	4.30
n-hexane	1.30
Propionaldehyde	2.00
Styrene	0.98
Tetrachloroethylene	0.23
Toluene	3.10
Trichloroethylene	0.02
Xylenes	2.30
Cyclohexane	0.20
Ethane	1.04
Propane	0.91
Acetone	7.95
Methanol	4.40
Ethanol	63.70
2-propanol (isopropanol)	1.90
Isopropylbenzene	0.03
Phenol	7.81
Ethylene (ethane)	0.60
Propene	0.30
Isoprene	1.90
3-Carene	0.20
Hexanal	1.54
Heptanal	0.70
Octanal	1.54
Nonanal	5.90
Decanal	0.71

The mean indoor VOC concentrations used in the model are shown in the Table 5. For indoor VOC concentrations, the emission rates presented in Sarwar et al. (2002) for typical indoor environment or in Zhu et al. (2013) for Canadian homes were adjusted according to air

exchange rate and room dimensions and then used to provide background indoor concentrations representative for all of the case studies. The exception is those species for which indoor sources were explored in detail in later chapters (C_6-C_{10} aldehydes as for Chapter 4; species typical for skin and breath emissions as described in Chapter 5), where indoor emissions were set up as described.

Table 5: Mean indoor background VOC concentrations ($\mu g\ m^{-3}$) presented in the model for Milan and Seoul case studies (Sarwar et al., 2002; Zhu et al., 2015).

Compound	Concentration [$\mu g\ m^{-3}$]
2-butoxyethanol	3.0
Acetaldehyde	9.1
α-pinene	5.6
Benzaldehyde	2.8
Benzene	1.0
Ethylbenzene	1.4
Formaldehyde	25.0
Limonene	21.3
Styrene	0.7
Toluene	7.9
Xylenes	2.4
Cyclohexane	0.5
Ethane	3.1
Propane	2.7
Isopropylbenzene	0.1
Ethylene (ethene)	1.7
Propene	0.9
3-Carene	1.3

3.8 Running the Model

The INDCM includes approximately 20,000 gas-phase chemical and photolysis reactions, as well as a representation of indoor-outdoor exchange, VOC emissions and surface deposition (Carslaw, 2007). Moreover, the INDCM model includes an inorganic scheme for

ozone, NO_x, sulphur dioxide and carbon monoxide. Indoor temperature was assumed to be $27^{\circ}C$ and relative humidity (RH) 45% (Carslaw et al. 2015) unless stated otherwise.

The model considers a single well-mixed environment and assumes that the concentration of each species is calculated according to equation 16 (Carslaw et al., 2012):

$$\frac{dC_i}{dt} = -\upsilon_d \left(\frac{A}{V_i}\right) C_i + \lambda_r f C_o - \lambda_r C_i + \frac{E_i}{V_i} + \sum_{j=1}^{n} R_{ij} \qquad (16)$$

where C_i (C_o) is the indoor (outdoor) concentration of species (molecule cm^{-3}), υ_d its deposition velocity (cm s^{-1}), A the surface area indoors (cm^2), V_i the volume of air in the indoor environment (cm^3), λ_r the air exchange rate between indoors and outdoors (s^{-1}), f the building filtration factor, E_i the indoor emission rate for species i (molecule cm^{-3} s^{-1}) and R_{ij} the reaction rate between species i and j (cm^3 $molecule^{-1}$ s^{-1}).

The INDCM box model runs in FACSIMILE format using MCPA software. FACSIMILE works by solving differential equations (equation 16) for all species and through pragmatic time step selection with the focus on modelling the kinetics of chemical and physical systems. Figure 17 presents a screenshot of FACSIMILE modelling format to illustrate an example of the model code used for the INDCM model. The model takes approximately 30 minutes to perform a single model run on a powerful desktop PC. The model is run for 3 days and then output used from day 3 to ensure that the model has reached steady-state.
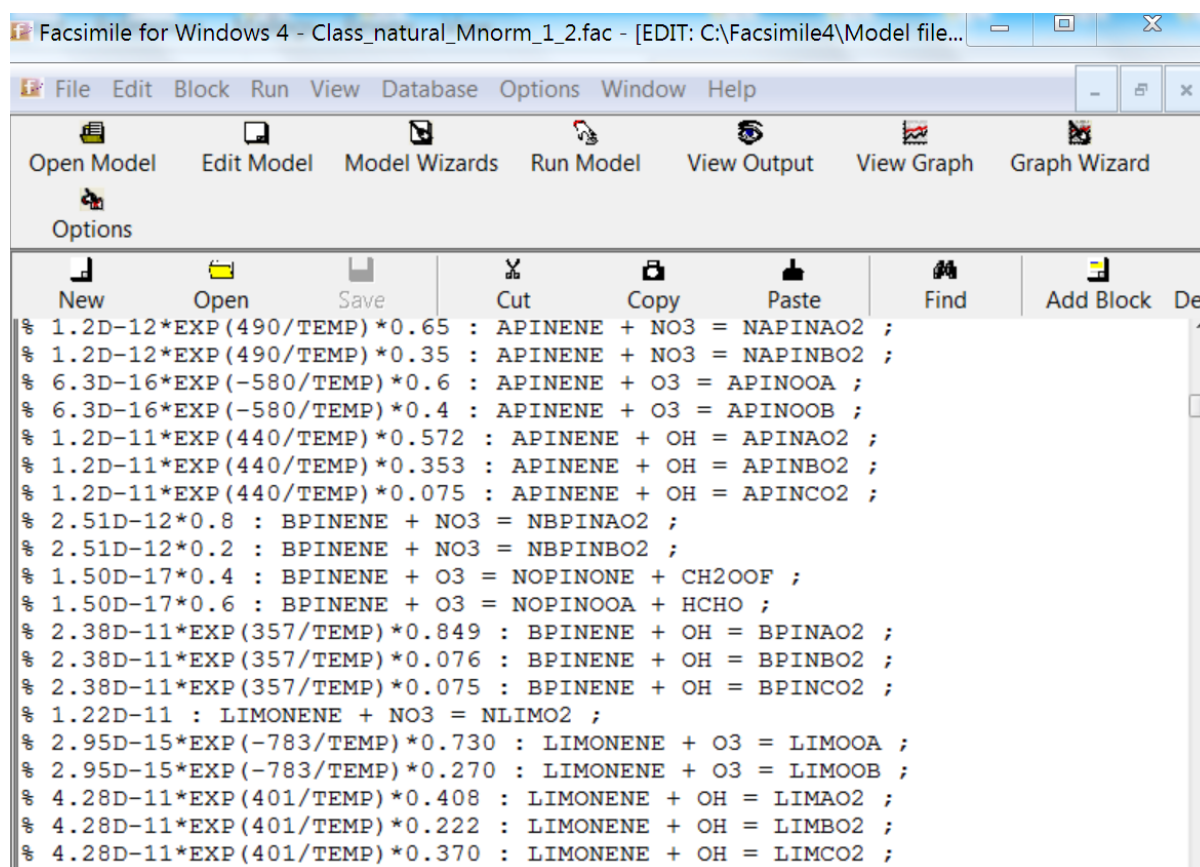
Figure 17: Screenshot of the FACSIMILE modelling format used in the INDCM model.

This chapter has described the methodology used in this dissertation. In the next 3 chapters, there is a description of how the model has been developed. The main area for development has been to add more detailed surface interactions as described in Chapters 4 and 5. In addition, new schemes have been developed for several higher aldehydes such as nonanal and decanal (Chapter 4). The model results have been performed and compared for the apartment scenario in Milan and Seoul during a heatwave (Milan 2003) and for typical (Milan 2009 and Seoul) summer time conditions (Chapter 4 and 5). Additionally, Chapter 5 compares the modelling results of human occupancy in the apartment scenario with a bedroom and a classroom scenario. Chapter 6 presents the modelling results of cleaning activity indoors.

4. Secondary pollutants formation following ozone-surface interactions

4.1 Background and introduction

Many sources contribute to indoor air pollution. Indoor contaminants can originate outdoors (i.e. ozone (O_3), nitrogen oxide (NO_x), particulate matter (PM)), however there are also significant sources indoors (Marchand et al., 2006). The main indoor air pollutant sources are indoor activities such as cooking (e.g. NO_x, PM) (Lee et al., 2002), smoking (such as formaldehyde (HCHO), PM) (Lin et al., 2007) or cleaning (e.g. terpenes) (Wolkoff et al., 1998). An increasingly active area of research for indoor air pollution is that driven by emissions from internal materials such as carpets, painted walls or furniture (Clausen et al., 2000; Nazaroff and Weschler, 2004; Coleman et al., 2008).

Species can be emitted directly from a surface (primary pollutants), but also following gas-phase transformations or interactions at surfaces (secondary pollutants) as shown in Figure 18. Furthermore these processes form an effective means of removing air pollutants prone to deposition, i.e. ozone, from indoor air, and consequently the concentrations of these species are much lower indoors than outdoors (Morrison, 2015).
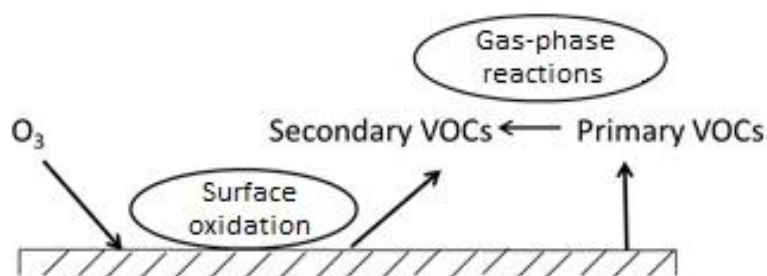
Figure 18: Primary and secondary VOC formation following surface deposition of ozone through oxidation processes and gas-phase transformations.

Following ozone deposition and surface oxidation, a wide range of primary and secondary pollutants can be formed. Furthermore, secondary pollutants from surface production can be more damaging for human health than the primary emissions, causing asthma and pulmonary infections (Mendell, 2007) and thus warrant further investigation. Porous and fleecy surfaces,

such as carpets and soft furniture are important sinks of ozone, and are also able to form a wide range of higher (C_6 and above) aldehydes (Lin and Hsu, 2015). According to the European Chemical Agency (ECHA), C_6-C_{10} aldehydes are expected to cause eye, skin and potential respiratory irritation. Therefore, emissions of higher aldehydes following surface interactions indoors may cause adverse health effects. The age of the material is also significant because emission rates tend to be higher for new materials and reduce as a material becomes older (Kim et al., 2006; Wang and Morrison 2006). Morrison and Nazaroff (2000) termed this process 'ozone aging'. Ozone can oxidize the available unsaturated bonds in a surface coating over time, leading to decreasing ozone uptake and also decreasing emission rates of secondary pollutants from this source. Examples of primary and secondary VOCs emissions following surface interactions are presented in Table 6. In terms of modelling studies, current indoor air models do not take into account surface interactions indoors, their impact on indoor air chemistry and secondary pollutants formation.

Table 6: Primary and secondary VOCs emissions from surface (Knudsen et al., 1999; Hodgson et al., 2002; Morrison and Nazaroff, 2002; Wang and Morrison, 2006).

Surface	Primary VOC	Secondary VOC
Carpet	C_{11}-C_{13} alkenes Cycloalkenes 4-phenylcyclohexane Dodecanol Branched alkenes Aliphatic aldehydes Benzene	Increased production of C_{11}-C_{13} aliphatic n-aldehydes Unsaturated aldehydes (mostly 2-nonanal, hexanal, heptanal, 2-octanal, decanal) Ketones: 2-butanone, 2-pentanone, 2-hexanone, 2-heptanone
Painted gypsum board	2-Butoxyethoxyethanol 1,2-Propandiol Texanol	Formaldehyde Acetone Acetaldehyde Higher aldehydes: octanal, nonanal, decanal Fatty acids
Plywood	α-pinene d-Limonene Aliphatic aldehydes	Formaldehyde Acetaldehyde Benzaldehyde Propionaldehyde Pentanal, Hexanal, Heptanal, Octanal, Nonanal
PVC/Linoleum	2-Butoxyethoxyethanol	2-Ethyl-1-hexanol Phenol Higher aldehydes: hexanal, heptanal, octanal, nonanal, decanal

Given the evidence for building material emissions indoors and the potential for adverse health effects to arise from secondary chemistry following their use, increasing attention is being paid to green building materials. Generally unconventional, green materials are designed for building occupants to live in a healthier environment, improve indoor air quality and reduce environmental impact (James and Yang, 2005). The green material attributes (e.g. recycling content, reduced humidity or emissions of VOCs) are then defined either by a guideline/certification organisation or by the manufacturer (Sharma and Mehta, 2014). Clearly, if green materials are used indoors, they are expected to have low emissions of VOCs and therefore there may be a significant improvement in indoor air quality (Lamble et al., 2011).

4.2 Aims of the Chapter

The principal aim of this Chapter is to investigate secondary pollutant formation following surface interactions indoors for the case-study indoor environments. The concentrations of several aldehyde species can reach appreciable concentrations indoors, particularly when outdoor ozone concentrations are enhanced such as during clear-sky, high pressure conditions (Apte et al., 2008). This is a concern, as there is the potential for an increased frequency of polluted episodes as the climate warms, particularly in big cities (Marlier et al., 2016). Currently, in the absence of measurements, detailed chemical models need to be developed to understand processes of surface interactions indoors and their impact on indoor air chemistry in a real building case scenario.

This chapter identifies the key chemical species that are formed when indoor surfaces interact with indoor air pollutants. Thus, this chapter first describes the model development including surface product formation following ozone deposition. Furthermore the chapter describes in detail key parameters used for the model improvements: the ozone deposition velocity and yields of the key surface products. Moreover it presents a sensitivity analysis test for the apartment in Milan during typical summer time conditions, considered as a base case scenario. Then, it describes the comparison of ozone deposition onto different types of surfaces in the case study scenarios in Milan and Seoul. Finally, this Chapter compares conventional surface emissions with those from so-called 'green' materials and therefore it evaluates their impact on indoor air chemistry.

4.3 Methodology

4.3.1 Model development

The INDCM has been developed based on previous work by Carslaw (2007) and Carslaw et al. (2012) as described in the previous chapter. In this study, the INDCM has been improved to consider ozone deposition onto different types of surface, as well as emissions of higher aldehydes following surface interaction. The ozone loss rate to a surface is calculated according to the equation 17:

$$F_{s1...n} = \upsilon_{dO_3} \, \frac{A_s}{V_i} \qquad (17)$$

where, $F_{s1...n}$ is the ozone deposition flux to the surface from 1 to n number of surfaces (s^{-1}), υ_{dO_3} is the total ozone deposition velocity to a surface (cm s^{-1}), A_s is the surface area (total area of a specific surface type) (cm^2), V_i is the total volume of the indoor environment (cm^3).

The emission of the surface products was calculated using equation 18 (Morrison and Nazaroff, 2002):

$$E_{sec,1...n} = \frac{A_s \, Y \, C_{O_3} \, \upsilon_{dO_3}}{V_i} \qquad (18)$$

where $E_{sec,1...n}$ is the relevant secondary product emission rate from 1 to n number of surfaces (molecule cm^{-3} s^{-1}), Y is the aldehyde yield of the emitted pollutant and C_{O_3} is the bulk indoor ozone concentration (molecule cm^{-3}).

4.3.2 Ozone deposition velocity

Surface deposition depends on two main processes: the transport of ozone to the surface and the uptake to the surface. Transport to the surface is determined by the thickness of a boundary layer (Reiss et al., 1994). The rate of ozone that is removed from indoor air (ozone loss) is proportional to the indoor ozone concentration, the air exchange rate, the surface area with a characteristic deposition velocity different for each surface

material and a total volume of indoor space that is taken into consideration (Fisher et al., 2013).

Ozone can undergo a number of loss processes depending on the conditions, but deposition usually dominates. Indoor surfaces range from highly reactive (i.e. carpet) to poorly reactive (i.e. glass). The deposition rate for materials like carpet is mostly limited by external mass transport, while deposition to glass is typically limited by surface reaction kinetics (Weschler, 2000). Each type of material has a different structure and therefore resistance to uptake of gases. The total surface resistance constitutes of the surface resistance and the air transport resistance (which also includes the boundary layer resistance). Thus the uptake of ozone from indoor air is different for each type of surface, characterised by a specific deposition velocity (Grontoft and Raychaudhuri, 2004). The deposition velocities, which are the inverse of the resistance, can be described by equation 19:

$$ \upsilon_{dO_3} = \frac{1}{\frac{1}{\upsilon_s} + \frac{1}{\upsilon_t}} \tag{19} $$

where υ_s is the surface deposition velocity defined for a specific material (cm s^{-1}) and υ_t is the deposition velocity at the air transport limit (cm s^{-1}) (Cano-Ruiz et al., 1993).

Based on a review of available literature (i.e. Klenø et al., 2001; Grontoft and Raychaudhuri, 2004; Nicolas et al., 2007), data distribution for characteristic velocities for ozone deposition on different type of materials was defined in terms of minimum, 25% of data distribution, median value, 75% of data distribution, and maximum values (Figure 19).
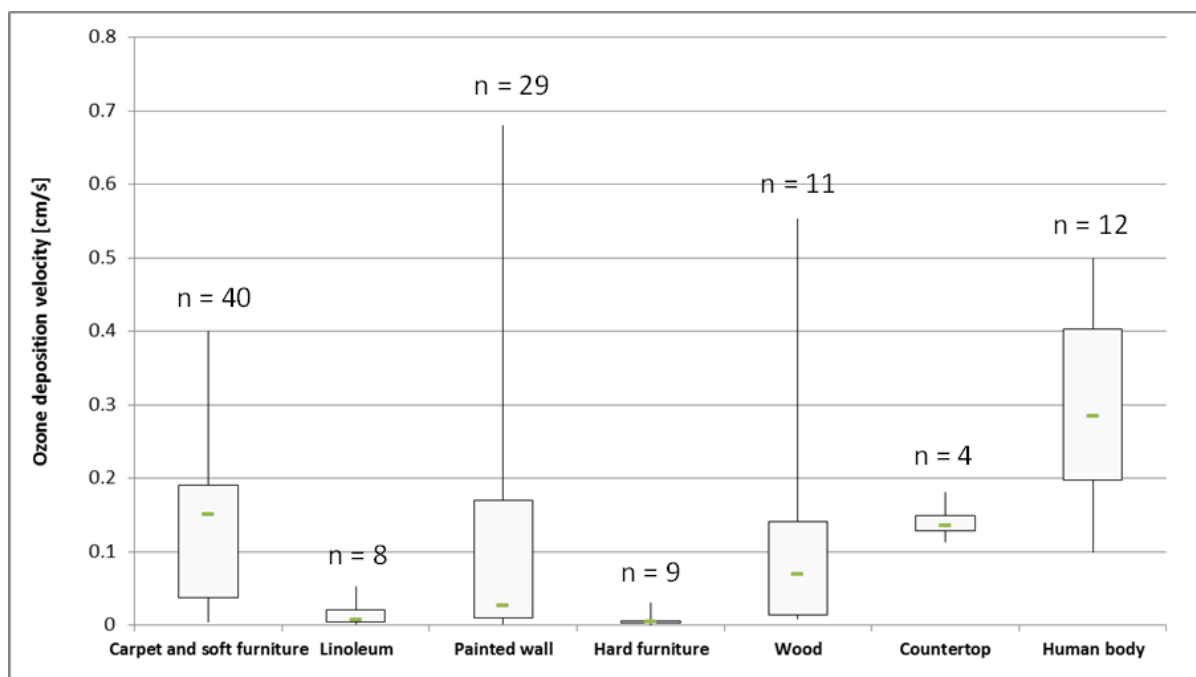
Figure 19: Ozone deposition velocity onto different indoor surfaces, considering minimum, 25% of data distribution, median value, 75% of data distribution and maximum value of ozone velocity deposition [cm/s]. 'n' symbol depicts number of measurements done for ozone deposition velocity at each type of the surface and green dash median value (Sabersky et al., 1973; Reiss et al., 1994; Morrison and Nazaroff, 2000; Klenø et al., 2001; Grontoft and Raychaudhuri, 2004; Tamás et al., 2006; Wang and Morrison, 2006; Nicolas et al., 2007; Poppendieck et al., 2007; Coleman et al., 2008; Hoang et al., 2009; Wang and Morrison, 2010; Wisthaler and Weschler, 2010; Lamble et al., 2011; Gall et al., 2013; Lin and Hsu, 2015; Rim et al., 2016).

The distribution of reported ozone deposition velocities onto different indoor surfaces (presented in Figure 19) shows that relatively large differences in the ozone deposition velocity exist both within and between surface types. Relatively big differences in ozone deposition velocity depend on the measurement technique, the conditions (e.g. near-surface air velocities) and the duration time of the measurements. For instance, Klenø et al. (2001) was using the Field and Laboratory Emission Cell (FLEC) as a measurement method and the ozone concentration was approximately 50 ppb. However, Wang and Morrison (2010) did the measurements in the field, where the ozone concentration was up to 150 ppb. Therefore, ozone concentration measured during the experiment could have an impact on the deposition velocity indoors. Moreover, differences in ozone deposition velocity within the same type of material are caused by the age of the material, the chemical composition of the surface coating, its gas permeability, the type and the porosity of the substrate material, as well as the presence of a film on the surface (Drakou et al., 1998; Klenø et al., 2001; Grontoft and

71

Raychaudhuri, 2004; Gall et al., 2015). For instance, latex paint shows the lowest ozone deposition velocity whereas painted gypsum board has the highest one for painted walls (Reiss et al., 1994; Klenø et al., 2001). Painted wood materials are characterized by 2-5 times larger values of ozone deposition velocities than the values on oiled or lacquered wood materials (Klenø et al., 2001). Lin and Hsu (2015) noted that fleecy and spongy materials are described by higher deposition velocities than plane and smooth surfaces. Finally, Abbass et al. (2017) noted that the fiber material used within carpets had a large effect on both ozone deposition and also subsequent oxidation-derived aldehyde emissions.

Figure 19 also shows ozone deposition velocity to human body to show the comparison within all the indoor surface materials. The ozone deposition velocity to a human body surface corresponds to the air movement around the human envelope (Wisthaler and Weschler, 2010). Therefore deposition velocity values depend on the measurement environment, for instance if the measurements were done in the real environment or in a chamber. For instance, due to a lower air exchange rate, a lower indoor ozone concentration and fewer occupants, the ozone deposition velocity onto people measured in an office was larger (0.4-0.5 cm s^{-1}) (Coleman et al., 2008) than those (0.20 − 0.23 cm s^{-1}) reported for passengers in a simulated aircraft cabin (Tamás et al., 2006). Note that human body surface included clothing in both cases.

4.3.3 C_6-C_{10} aldehydes yields

Molar yield is determined as the average molar emission rate of carbonyl compounds formed due to the reaction of the surface material with ozone, divided by the molar flux of ozone to the surface (Cheng et al., 2015). Hexanal, heptanal, octanal, nonanal and decanal are the carbonyls generated with the highest yields as secondary pollutants from building surfaces (Wang and Morrison, 2006). Although lower molecular weight carbonyl species are also emitted from surfaces, far less data are available. The indoor concentrations of the aldehyde species arise from emissions indoors, indoor-outdoor exchange and in some cases, additional gas-phase chemistry. Outdoor concentrations were based on Hodgson et al. (2002).

Degradation mechanisms were absent in the MCM for octanal, nonanal and decanal, so new schemes have been developed based on analogy with the existing heptanal scheme. The reaction rate coefficients for OH with higher aldehydes were taken from the literature,

with 3.2×10^{-11} cm^3 $molecule^{-1}$ s^{-1} used for octanal (Chacon-Madrid et al., 2010), 3.6×10^{-11} cm^3 $molecule^{-1}$ s^{-1} for nonanal (Bowman et al., 2003) and 3.6×10^{-11} cm^3 $molecule^{-1}$ s^{-1} was also assumed for decanal, based on the literature values for nonanal and undecanal both being this value (Bowman et al., 2003; Chacon-Madrid et al., 2010). For instance, for the nonanal scheme, the following code was added to the model (Figure 20):

```
* nonanal scheme ;
*;
% j15 : C8H17CHO = HO2 + CO + OCTO2 ;
% KNO3AL*5.5 : NO3 + C8H17CHO = C8H17CO3 + HNO3 ;
% 3.6D-11 : OH + C8H17CHO = C8H17CO3 ;

% KAPHO2*0.15 : C8H17CO3 + HO2 = C8H17CO2H + O3 ;
% KAPHO2*0.41 : C8H17CO3 + HO2 = C8H17CO3H ;
% KAPHO2*0.44 : C8H17CO3 + HO2 = OCTO2 + OH ;
% KAPNO : C8H17CO3 + NO = OCTO2 + NO2 ;
% KFPAN : C8H17CO3 + NO2 = C8H17PAN ;
% KRO2NO3*1.74 : C8H17CO3 + NO3 = OCTO2 + NO2 ;
% 1.00D-11*0.3*RO2 : C8H17CO3 = C8H17CO2H ;
% 1.00D-11*0.7*RO2 : C8H17CO3 = OCTO2 ;

% 9.89D-12 : OH + C8H17CO2H = OCTO2 ;
% j41 : C8H17CO3H = HEPTO2 + OH ;
% 1.33D-11 : OH + C8H17CO3H = C8H17CO3 ;
% 6.16D-12 : OH + C8H17PAN = C7H15CHO + CO + NO2 ;
% KBPAN : C8H17PAN = C8H17CO3 + NO2 ;
*;
```

Figure 20: Nonanal scheme from the model. Note that species names are all from the MCM protocol (MCM, University of Leeds).

Many of the species formed on the right hand side (e.g. OCTO2) were already in the model mechanism and hence their further degradation was automatically treated. For 'new' species (e.g. C8H17CO3), new degradation reactions were added as required, following the protocol defined in Jenkin et al. (1997).

Wang and Morrison (2006) measured aldehyde yields for different surfaces following uptake of ozone in four homes, calculated as a summer and a winter average as well as yields from two new (one and two years old) and from two old (12 and 14 years old, without refurbishment) homes in summer time. In order to calculate the oxidation-derived emissions of higher aldehydes from surfaces as defined in the Methodology section (Section 4.3),

average aldehyde yields were used. Table 7 shows aldehyde yields in summer from new and old homes surfaces and also calculated as an average of the two. New surfaces typically have higher yields than older ones, with the exception of painted walls, though few results exist for this surface.

Table 7: Aldehyde yields (calculated as average values adopted from measurements data) in summer for average age, new and old homes surface type (Wang and Morrison, 2010). Note that figures are rounded to 2 significant figures.

Surface type	Compound	No. of measurements (n)	Average age surface aldehyde yield (±SD)	New home surface aldehyde yield	Old home surface aldehyde yield
Carpet and soft furniture	Hexanal		0.03 (±0.03)	0.03	0.03
	Heptanal		0.01 (±0.01)	0.01	0.00
	Octanal	16	0.01 (±0.02)	0.01	0.01
	Nonanal		0.06 (±0.03)	0.08	0.04
	Decanal		0.03 (±0.03)	0.04	0.02
Painted wall	Octanal		0.01 (±0.02)	0.00	0.03
	Nonanal	3	0.13 (±0.18)	0.03	0.34
	Decanal		0.04 (±0.07)	0.01	0.12
Countertop	Hexanal		0.08 (±0.05)	0.09	0.06
	Heptanal		0.02 (±0.02)	0.03	0.02
	Octanal	12	0.01 (±0.01)	0.01	0.02
	Nonanal		0.26 (±0.15)	0.33	0.19
	Decanal		0.03 (±0.04)	0.04	0.03
Linoleum	Hexanal		0.07 (±0.06)	0.08	0.06
	Heptanal		0.01 (±0.01)	0.01	0.00
	Octanal	7	0.01 (±0.02)	0.02	0.01
	Nonanal		0.13 (±0.10)	0.20	0.04
	Decanal		0.03 (±0.04)	0.05	0.00

Since the data for aldehyde yields for wooden materials were not available, direct emission rates were calculated using literature data for different types of wooden materials following the results summarized by Hodgson et al. (2002), Nicolas et al. (2007) and Plaisance et al. (2014). Average emission rates measured for wooden floor and hard furniture, which were used in the model runs, are presented in Table 8.

Table 8: Average emission rates of higher aldehydes measured for wooden floor and hard furniture (Hodgson et al., 2002; Nicolas et al., 2007 and Plaisance et al., 2014).

Material	Hexanal ($\mu g\ m^{-2}\ h^{-1}$)	Heptanal ($\mu g\ m^{-2}\ h^{-1}$)	Octanal ($\mu g\ m^{-2}\ h^{-1}$)	Nonanal ($\mu g\ m^{-2}\ h^{-1}$)	Decanal ($\mu g\ m^{-2}\ h^{-1}$)
Wooden floor	62.2	3.7	7.2	40.4	1.3
Hard furniture	76.3	11	20	17	-

4.3.4 Surface to volume ratio

Following the methodology presented in Chapter 3, the case study apartment has different internal surfaces. Since different surfaces in the apartment (volume = 168 m^3) have different surface areas, each material is defined by a different surface to volume ratio. The surface to volume ratio for different surfaces in the apartment was calculated and is presented in Table 9. The biggest surface to volume ratio was for painted walls (and ceilings), given that they have the largest internal surface area in the apartment.

Table 9: Surface to volume ratio calculated for the surface types in the apartment.

	Carpet and soft furniture	Painted wall	Countertop	Linoleum	Wooden floor	Hard furniture
Surface to volume ratio (m^{-1})	0.21	1.18	0.11	0.07	0.30	0.13

4.4 Results and discussion

4.4.1 Model sensitivity analysis

Given the large uncertainty ranges in some of the input parameters, a series of sensitivity tests has been carried out to investigate the effect of changing key parameters on the predicted concentrations of C_6-C_{10} aldehydes. Key parameters were varied within uncertainty limits (e.g. rate coefficients) or within a typical observed range. Transmission of outdoor UV and visible light through the windows was varied between 0.15% and 25% for UV light and between 0.7% and 75% for visible light (Carslaw, 2007). Ozone deposition velocities were varied such that all values were set to the 25th percentile or the 75th percentile values of the range reported in the literature as indicated in Section 4.3.2. Selected rate coefficients were varied to the maximum values of their uncertainty range according to IUPAC (2016) as per the method reported by Carslaw et al. (1999). Key outdoor concentrations of ozone, NO_x and surface to volume ratio values were either increased or decreased by 50% and the effect of using the aldehyde yields for new and old materials instead of the average yields also investigated. The concentrations of the C_6-C_{10} aldehydes were then investigated between 09:00 and 17:00 h for the conditions described earlier in the Methods section. The results from the sensitivity analysis are shown in Table 10.

Table 10: Sensitivity test results: the % change in concentrations of C_6-C_{10} aldehydes in the apartment in Milan for typical summer conditions (AER = 0.76 h^{-1}) relative to baseline conditions. Baseline concentrations are hexanal as 2.7 ppb, heptanal 0.5 ppb, octanal 0.8 ppb, nonanal 6.5 ppb, decanal 1.7 ppb.

Scenario	Hexanal	Heptanal	Octanal	Nonanal	Decanal
UV=0.15%, VIS=0.7%	-4.9	-4.8	-4.7	-5.6	-6.0
UV=25%, VIS=75%	30.0	29.6	29.1	34.1	36.4
υ_d 25th percentile	-36.9	-17.8	-31.6	-21.4	-34.2
υ_d 75th percentile	-29.0	-36.2	15.5	38.1	50.5
k(OH+Nonanal)*1.19	-0.1	-0.1	-0.1	-0.6	0.1
Outdoor O_3*0.5	-53.5	-48.0	-46.8	-52.7	-55.2
Outdoor O_3*1.5	55.8	50.1	48.9	55.0	57.6
Outdoor NO_x*0.5	15.5	14.0	13.7	15.5	16.2
Outdoor NO_x*1.5	-16.5	-14.9	-14.6	-16.4	-17.2
Outdoor C_6-C_{10}*0.5	-3.3	-7.9	-8.9	-3.7	-1.5
Outdoor C_6-C_{10}*1.5	3.3	8.0	9.0	3.7	1.5
Surface-volume*0.5	5.2	9.9	10.4	7.4	7.4
Surface-volume *1.5	-11.1	-10.4	-10.3	-8.1	-7.4
Old materials	10.2	-18.7	10.5	5.0	6.3
New materials	-5.9	14.4	-24.5	4.0	-15.6

The model predictions are sensitive to a number of factors, particularly changes in deposition velocities, photolysis rates, outdoor ozone concentration and the age of

the materials considered. Uncertainties in deposition velocities are clearly key factors for model output. For instance, under baseline conditions, 26% of ozone deposition is to the walls, but this becomes 63% for the 75th percentile run and affects the resulting aldehyde concentration mix. Yields of hexanal and heptanal are reported to be very low from painted walls (Wang and Morrison, 2006; Liu et al., 2006), therefore increasing the rate of ozone deposition to walls does not lead to much increase in their concentrations. As Figure 19 shows, the median deposition velocity value is closer to the 25th percentile for some surfaces and 75th for others, reflecting the large range of values currently existing in the literature.

The age of the surface also affects the aldehyde yields, which in turn affects aldehyde production rates and concentrations. Table 7 shows that the relatively few measurements of aldehyde yields from walls suggest rates are higher from older materials. Consequently, in the sensitivity tests in Table 10, some aldehyde concentrations are higher for new materials whilst others are higher for older materials compared to the baseline. Clearly, far more information about these parameters in real world environments would reduce model uncertainties considerably.

The model predictions are less sensitive to the photolysis rates assumed, the outdoor NO_x concentrations and variations in the surface to volume ratio. For instance, increasing photolysis rates based on the upper bounds of transmitted light through windows (Drakou et al., 1998) increases the predicted aldehyde concentrations by ~30-36%. However either the increase or decrease of surface to volume ratio by 50% changes the C_6-C_{10} concentrations by only 5-10%. Doubling or halving outdoor NO_x concentrations decreased or increased respectively, the concentrations of C_6-C_{10} aldehydes by ~15%.

These sensitivity tests provide an estimate of the likely range of the model indoor aldehyde concentrations given the uncertainties in the input values. Clearly, the largest source of uncertainty in the model output, taking into consideration the analytically measured parameters only, is driven by the uncertainty in the deposition velocities. As model sensitivity to the 25th and 75th percentile values of this parameter was investigated, the uncertainties in the model estimates of aldehyde concentrations are estimated to be approximately double the sensitivity reported to the deposition velocities, so 80-100%.

4.4.2 Ozone surface deposition

The model results show that approximately 85% of the indoor ozone is deposited onto internal materials for both typical and extreme summer conditions (note that model inputs are

the same for the three runs except for outdoor ozone and NO_X concentrations). However different types of surface are more effective ozone sinks than others (Figure 21). In terms of total ozone deposition to each surface, most is deposited on the painted wall and ceilings and to the soft furnishings (both around 30% of the total). Bearing in mind that the painted wall surface in total is approximately 6 times larger than the soft furniture surface, the carpets and soft furniture are potentially the most efficient surface type (when human occupants are not included) for ozone removal in the indoor environment. The deposition velocities presented in Figure 19 suggest that carpets and soft furniture are expected to be highly reactive materials for the indoor environment with linoleum and hard furniture the least. Ozone deposition onto human bodies is described in detail in the next Chapter.
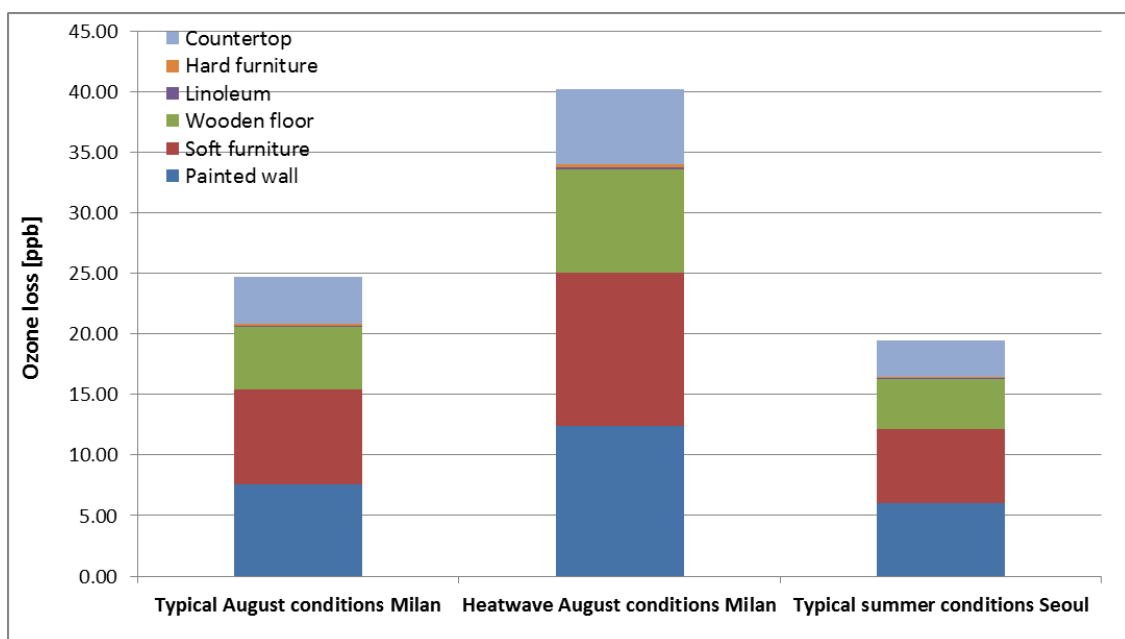
Figure 21: Ozone loss [ppb] onto different surface types in the apartment when different conditions occur outdoors and for two locations, Milan and Seoul.

The results show that approximately 75% of ozone indoors is deposited onto the surfaces in the apartment. The highest total ozone loss (~40 ppb) is estimated for the apartment in Milan when summer heatwave conditions occur. Since ozone loss is proportional to the ozone concentration indoors, the highest ozone concentration indoors is in Milan during heatwave conditions (~53 ppb with the absence of surface interactions indoors) and thus the highest ozone loss onto the surfaces takes place for these conditions.

4.4.3 Surface production

The average production rates of C_6-C_{10} aldehydes following surface interactions of ozone with different surfaces have been investigated as discussed in the Methods section. Note that the impact of human skin emissions on the total aldehyde concentrations in the apartment will be expanded in the Chapter 5. The concentrations of aldehydes formed following ozone deposition were analyzed and categorized by surface.

Figure 22 presents the C_6-C_{10} aldehyde mixing ratios in the apartment during typical summer conditions in Milan (AER = 0.76 h^{-1}). Painted walls, due to having the largest surface-volume ratio, made the biggest contribution to indoor nonanal and decanal concentrations, with countertops and soft furniture also providing a significant fraction of the total, given the high yields presented in Table 4.1. For hexanal, secondary emissions from wooden floors were most important.
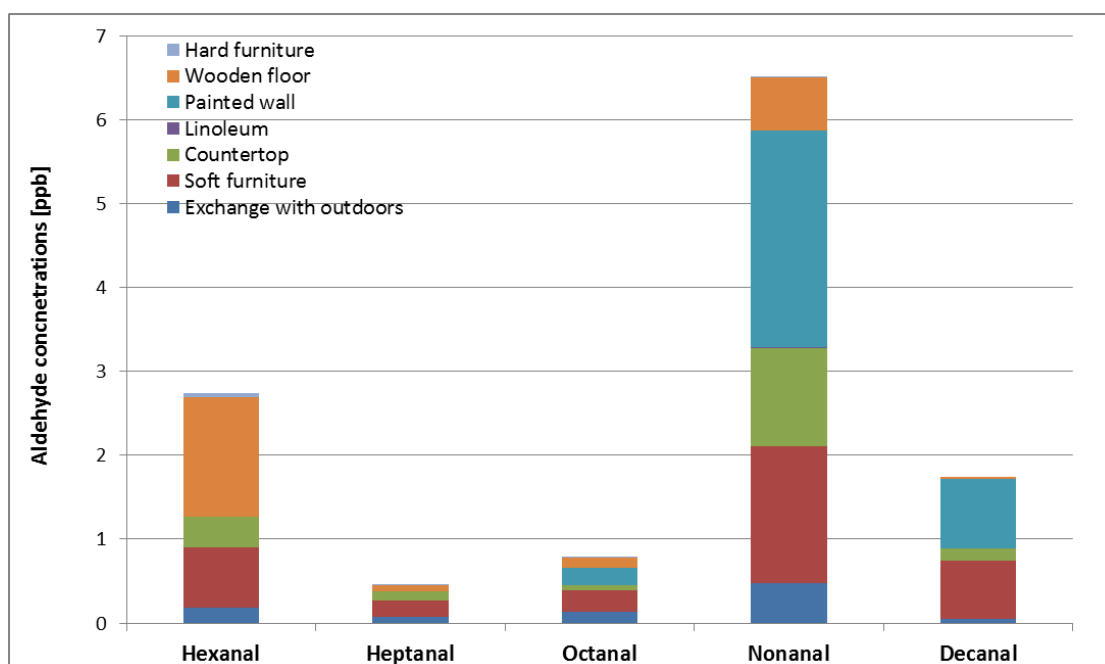
Figure 22: C_6-C_{10} aldehyde concentrations indoors following ozone surface deposition in the Milan apartment for typical summer conditions.

Similar tests of the model were performed for two other case studies, the apartment in Milan during heatwave conditions outdoors and the apartment in Seoul for typical summer conditions (Figure 23 and 24 respectively).
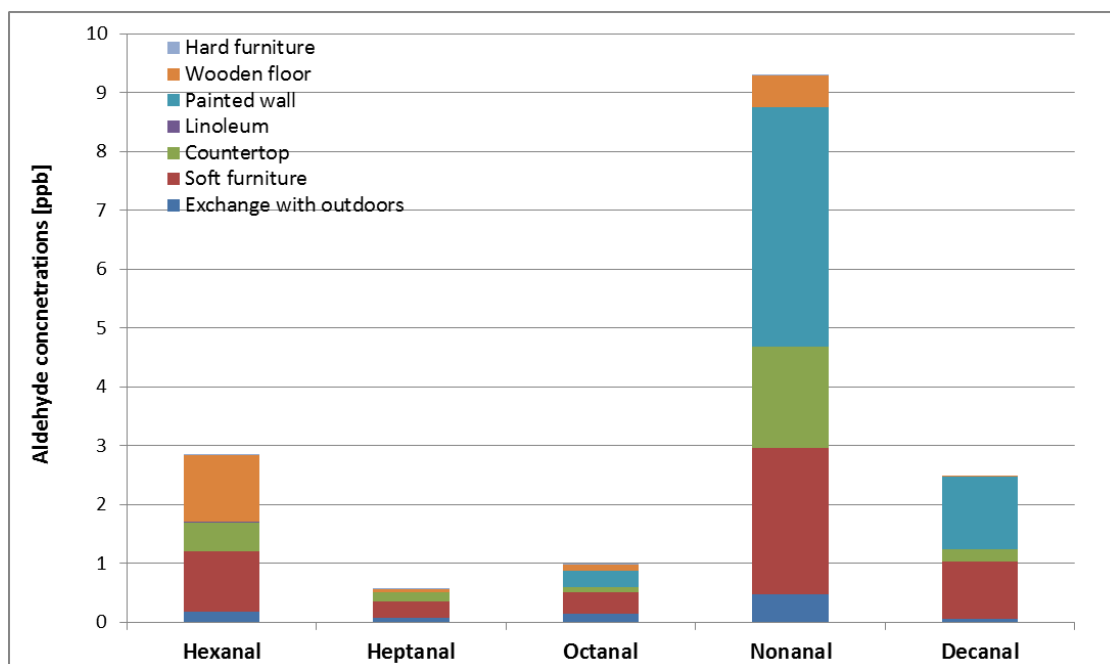
Figure 23: C_6-C_{10} aldehyde concentrations indoors following ozone surface deposition in the Milan apartment for heatwave summer conditions.
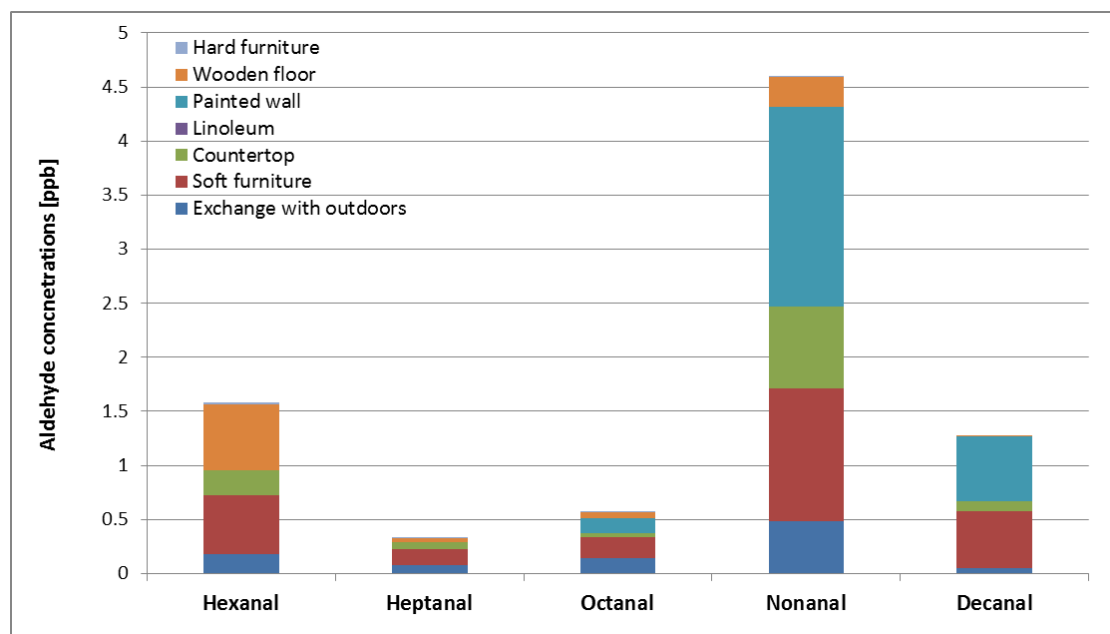
Figure 24: C_6-C_{10} aldehyde concentrations indoors following ozone surface deposition in the Seoul apartment for typical summer conditions.

Secondary pollutant formation following ozone – surface interaction is proportional to the ozone concentration indoors. The highest ozone concentration indoors is in Milan during heatwave summer conditions (~12 ppb). Nonanal, which shows the highest indoor

concentration for all of the higher aldehydes studied, reaches 9 ppb during the heatwave conditions in Milan, with the highest emission from the painted wall and the soft furniture. Much lower concentrations of the higher aldehydes were predicted for the apartment in Seoul, since the indoor ozone concentration was lowest (~5.5 ppb) out of the three study locations/conditions. Thus the nonanal concentration was only predicted to reach ~4.5 ppb. Likewise, higher aldehyde concentrations predicted for the apartment in Milan during typical summer conditions were proportional to the indoor ozone concentration (~8 ppb) and therefore the nonanal concentration was predicted to be ~6.5 ppb.

There are very few studies with which to compare these predictions of C_6-C_{10} aldehydes indoors and they are not directly comparable. However, the modelling results are in reasonable agreement with a study that reports measured values in ~4000 Canadian households (Zhu et al., 2013), though tend to be on the higher end of the measured ranges (75th-99th percentile) except for hexanal which is closer to the geometric mean. Likewise, both Reiss et al. (1995) and Marchand et al. (2006) report mean hexanal concentrations of ~2 ppb, whilst Liu et al. (2006, 2007) report mean concentrations of closer to 1 ppb. For nonanal, the predicted concentrations are relatively high compared to the measurements of Zhu et al. (2013), who report a 99th percentile value of ~2.5 ppb. However, the painted walls make a significant contribution to the predicted concentrations and the yield values used are based on relatively few measurements. Clearly, the assumptions made about the surfaces in the apartment used for this modelling study compared to those that existed in real buildings where measurements were made will be significant in any comparison. Whilst the predicted values appear to be representative of the magnitudes observed, there is a clear need for more measurements to help validate models results. Although indoor surfaces can be quite different in their initial reactivity, aging and soiling of surfaces may make indoor surfaces more similar than different over time (Nazaroff et al., 1993). In a study of four homes, Wang and Morrison (2006) showed that older carpet was less reactive than new carpet; but that kitchen countertops tended to remain reactive regardless of age and that this was probably due to continuous application of cooking oils and/or cleaning agents. Therefore, models will benefit from more extensive field measurements of ozone surface reactivity (deposition velocity and product yields) in occupied homes, as well as information on surface interactions for indoor pollutants other than ozone.

4.4.4 Impacts of oxidation-derived surface emissions on chemical processing indoors

The INDCM was used to investigate whether the oxidation-derived emissions of these aldehydes also have an impact on chemical processing indoors. In order to understand exactly how the chemistry changes when the oxidative production of these aldehydes are included, compared to when they are absent, a rate of production analysis was carried out for the Milan apartment during typical summertime conditions (Figure 25).

The modeled steady-state concentrations of OH, HO_2 and RO_2 for a model run with ozone deposition only (no subsequent emissions) were 4.8×10^5 molecule cm^{-3} and 4.9 and 6.0 ppt respectively. With surface production of aldehydes included, the same concentrations were 3.7×10^5 molecule cm^{-3} and 4.0 and 5.5 ppt respectively. Clearly, the internal emissions affect the subsequent radical concentrations indoors. Considering radical initiation processes first, production of HO_2 radicals via photolysis of aldehydes increases when ozone-derived surface aldehyde emissions and hence concentrations increase. Initiation rates of radical formation via O_3-terpene reactions remain similar with or without ozone-driven production of aldehydes on surfaces, but photolysis of dicarbonyl species becomes less important with the emissions included. Dicarbonyls are formed in numerous places in the model mechanism, such as through OH attack on alcohol species. The concentration of OH decreases by about 23% when oxidative production of aldehydes on surfaces is included and hence formation of dicarbonyls is also suppressed.
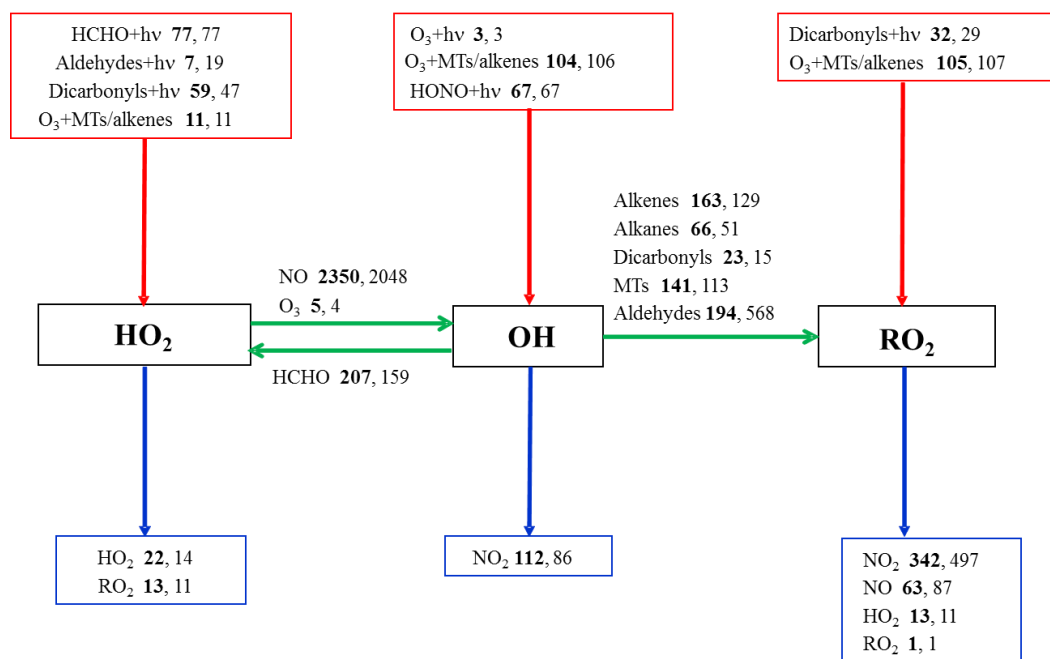
Figure 25: Simplified rate of production analysis for the major rates of reaction (10^4 molecule cm^{-3} s^{-1}) for: ozone deposition and no oxidation-derived aldehyde emissions (figures in bold) and with ozone deposition followed by ozone-driven aldehyde surface production (normal font). MT denotes monoterpenes (including isoprene). Red arrows denote radical initiation processes, blue arrows are termination processes with green arrows representing radical propagation.

In terms of radical propagation, increased aldehyde concentrations enable a higher production rate of acetyl peroxy radicals via reaction with OH, which more than offsets the decreased formation rate of peroxy radicals from other processes when oxidation-derived aldehyde emissions are considered. Perhaps the most interesting difference is when one considers the fate of the peroxy radicals through termination processes. Reactions of alkyl peroxy radicals with NO to form organic nitrates and of acetyl peroxy radicals with NO_2 to form PAN-type species dominate RO_2 loss whether ozone-driven aldehyde emissions are considered or not. The proportion of acetyl relative to alkyl peroxy radicals increases with higher aldehyde concentrations enhancing faster formation of PAN-type species. The overall concentration of RO_2 is similar for both scenarios, but the changed composition shifts the termination processes towards formation of the nitrated organic species. Interestingly, Weschler et al. (2007) found that the concentration of organic nitrates and PAN-type species increased by ~ a factor of 2 when soiled tee-shirts were introduced into an aircraft cabin with ozone, compared to when they were absent. Therefore, an important implication of surface processing indoors is that more nitrated organic species might be found indoors in

the presence of surface emissions, compared to the situation where there is no oxidative production of aldehydes on surfaces.

4.5 Emissions from green building materials

For a better understanding of the potential for ozone removal and secondary pollution formation, several experimental studies have investigated emissions from green materials. Hoang et al. (2009) showed that ozone deposition velocities and reaction probabilities are of the same order of magnitude for green materials as for the conventional ones. Similarly, Lamble et al. (2011) reported that there is no substantial difference between ozone uptake by green and conventional materials and emissions of secondary pollutants. However, Lin and Hsu (2015) reported that deposition velocities for green (unconventional materials defined in terms of low VOC emissions) building materials are lower than those for conventional ones. For instance, they measured an ozone deposition velocity for a wooden floor of 0.5 m h^{-1}, compared to 0.3 m h^{-1} for green wooden flooring material. Similarly, Cheng et al. (2015) found that green building materials, showing low chemical emission and negligible toxicity, typically have lower ozone deposition velocities and secondary emissions than conventional materials, especially for gypsum board and wooden floors. For instance, the primary emissions of carbonyls over 48 hours from a new conventional wooden floor were ~670 µg m^{-2} h^{-1} compared to ~150 µg m^{-2} h^{-1} for the new green wooden floor. Secondary emissions from conventional wooden flooring were measured to be ~90 µg m^{-2} h^{-1} compared to ~19 µg m^{-2} h^{-1} for the green version. Likewise, primary emissions over 48 hours from conventional gypsum board were ~500 µg m^{-2} h^{-1} compared to ~160 µg m^{-2} h^{-1} for the green gypsum board. Secondary emissions from conventional gypsum board were ~70 µg m^{-2} h^{-1} compared to ~40 µg m^{-2} h^{-1} for the green one.

These results vary depending on the study, but the more recent papers (e.g. Cheng et al., 2015) indicate that green building materials may have a lower impact on indoor air quality than the traditional materials. Several model runs were therefore performed to investigate the potential impact of replacing traditional building materials indoors with green equivalents for common VOC species indoors, assuming the results from Cheng et al. (2015) are representative of the more modern green materials now available.

4.5.1 Methodology

Following the results presented by Cheng et al. (2015), the comparison focuses on the selected internal surface types and the primary and secondary emissions of lower aldehydes they reported. Cheng et al. (2015) defined that in particular, formaldehyde, acetaldehyde, benzene, toluene and xylenes should be considered as priority pollutants emitted from building materials owing to health effects. Five different surface types were used for these model runs: countertop, linoleum, painted walls, wooden floor and hard furniture. Soft furniture is not included due to limited data available in the literature for green material emissions from these surfaces.

From the surface emitted carbonyls measured in Cheng et al. (2015), those that already exist in the model and are representative for all the surfaces were included in the modelling study. Therefore the model runs included C_1-C_4 aldehydes (formaldehyde, acetaldehyde, propionaldehyde and butyraldehyde) as primary and secondary carbonyl emissions for conventional and green materials. Primary emission rates were calculated as the sum of the emission rates from different types of surfaces for each compound, according to the surface area of each (as defined in Section 4.3.4). Primary emission rates of C_1-C_4 aldehydes for conventional and green materials including calcium silicate board, mineral fibre ceiling, gypsum board and wooden flooring, measured within 48 hours are presented in Table 11.

Table 11: Primary emissions rates of C_1-C_4 aldehydes [molecule cm^{-1} s^{-1}] measured for conventional and green surface materials measured within two days after installation (Source: Cheng et al., 2015).

Compounds	Conventional surface materials [molecule cm^{-1} s^{-1}]	Green surface materials [molecule cm^{-1} s^{-1}]
Formaldehyde	1.02×10^9	1.28×10^8
Acetaldehyde	4.43×10^8	1.45×10^8
Propionaldehyde	1.48×10^8	7.86×10^7
Butyraldehyde	1.40×10^8	6.74×10^7

James and Yang (2005) show that most of the total emissions take place during the first five days following installation with an exponential decay emissions profile. Similar conclusions

are presented by Cheng et al. (2015) who confirm that average primary emissions from building materials were high at the beginning of the experiment and then reduced over the subsequent 48 h. For these model runs, it has been assumed that the decay in emission rates is exponential. There is very little information on decay rates in emissions from green or traditional materials and this is clearly an area that warrants further research. Primary emissions of conventional materials were approximately 2-8 times higher than for the green ones. The highest difference of the selected compounds in primary emissions showed formaldehyde, which was approximately eight times higher for the conventional materials than for the green ones. The smallest difference was noted for propionaldehyde, approximately two times higher for conventional materials.

Secondary emission rates were calculated according to Equation 18 described previously in this Chapter. The surface to volume ratios for the materials were the same as described in Section 4.3.4. Carbonyl yields for the traditional countertop and linoleum surfaces were taken from Wang and Morrison (2010), whilst those for traditional painted walls, wooden floor and hard furniture as well as the carbonyl yields for all of the green materials were taken from Cheng et al. (2015). Yields for the production of carbonyls for different types of conventional and green surfaces are shown in Table 12. Molar yields of C_1-C_4 aldehydes were approximately 40-70% lower for green materials than for the conventional ones.

Table 12: Molar yields of C_1-C_4 aldehydes for conventional and green surface materials after 96 h after installation (Wang and Morrison, 2010; Cheng et al., 2015).

	Surface type	Formaldehyde	Acetaldehyde	Propionaldehyde	Butyraldehyde
Conventional materials	Countertop	0.019	0.003	0.014	0
	Linoleum	0.007	0	0.005	0
	Painted walls	0.56	0.25	0.15	0.12
	Wooden floor	0.72	0.39	0.19	0.19
	Hard furniture	0.72	0.39	0.19	0.19
Green materials	Countertop	0.0114	0.0018	0.0084	0
	Linoleum	0.0042	0	0.003	0
	Painted walls	0.2	0.1	0.09	0.05
	Wooden floor	0.23	0.14	0.11	0.08
	Hard furniture	0.23	0.14	0.11	0.08

Ozone deposition velocities for the conventional surface materials are used as described in Section 4.3.2. Following the results presented by Cheng et al. (2015), ozone deposition velocities for the green materials were estimated as approximately 60% of the values used for the conventional materials.

4.5.2 Results and discussion

The model runs were performed to investigate C_1-C_4 aldehyde concentrations indoors assuming either conventional or green building material surfaces in the apartment. Figure 26 presents a 24-hour profile of total (with no distinction between primary and secondary emissions) C_1-C_4 aldehyde concentrations in the apartment in Milan after material installation during typical summer conditions and for traditional building materials. Given that the diurnal profiles presented in Figure 26 include ozone dependent secondary emissions, there is an increase in concentrations during late afternoon hours. Within these hours ozone concentration indoors is the highest and therefore the emissions following ozone surface depositions are enhanced. The highest concentrations are for formaldehyde with a concentration up to 50 ppb in the late afternoon hours, with propionaldehyde the lowest (~17 ppb). The concentration of formaldehyde is below the WHO (2010) guideline value, which defines concentrations of formaldehyde below 80 ppb as safe for carcinogenic risk. Wolkoff and Nielsen (2010) reviewed the literature on formaldehyde concentrations and its heath effect in indoor environments. The review indicated that an average indoor air concentration of formaldehyde in residences in Europe and North America was ~40 ppb, while for new housing the average concentration exceeded ~80 ppb. Eye and airway irritation was reported at concentrations of ~480-800 ppb. Epidemiological studies reviewed by Wolkoff and Nielsen (2010) reported no increased cancer risk below a mean concentration of 1000 ppb.

Figure 27 shows the same conditions but for green materials. The aldehyde concentrations are much smaller than those from the traditional materials. For instance, the formaldehyde concentration is about 9 ppb, which is approximately 6 times lower than from traditional materials. The highest concentration indoors for green materials is for acetaldehyde, which is up to 17 ppb, though still lower than the equivalent run with traditional materials. Note that in both of these model runs, the highest concentration of the surface-generated aldehydes is when the ozone concentration is highest indoors (16:00-20:00 h).
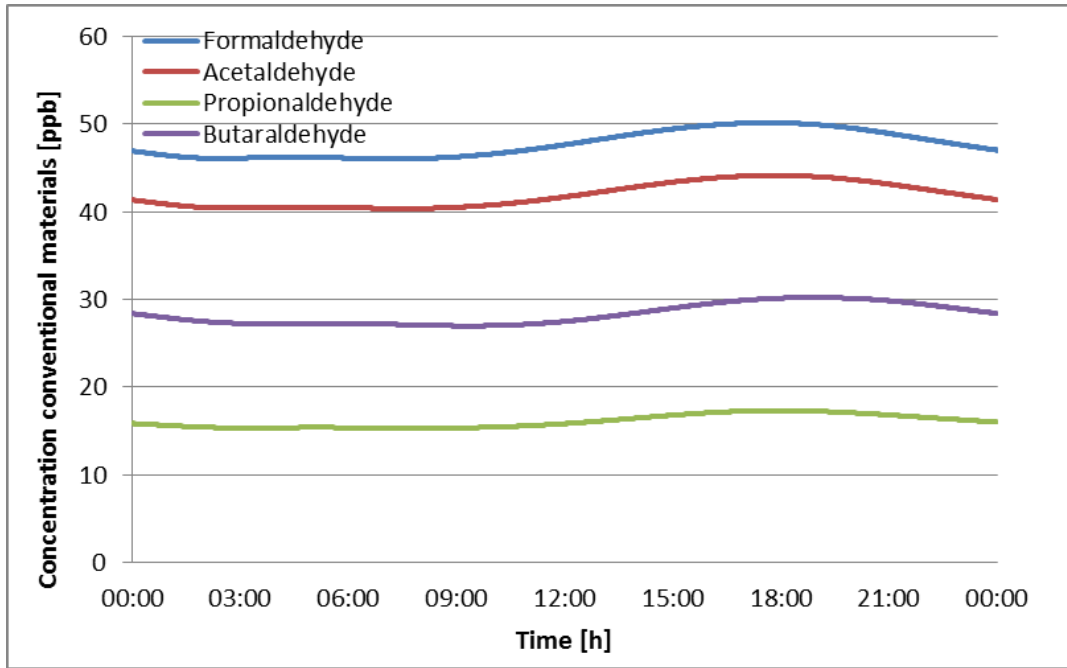
Figure 26: Average daily C_1-C_4 aldehyde concentrations indoors [ppb] after installation of traditional building materials in the apartment in Milan during typical summer conditions.
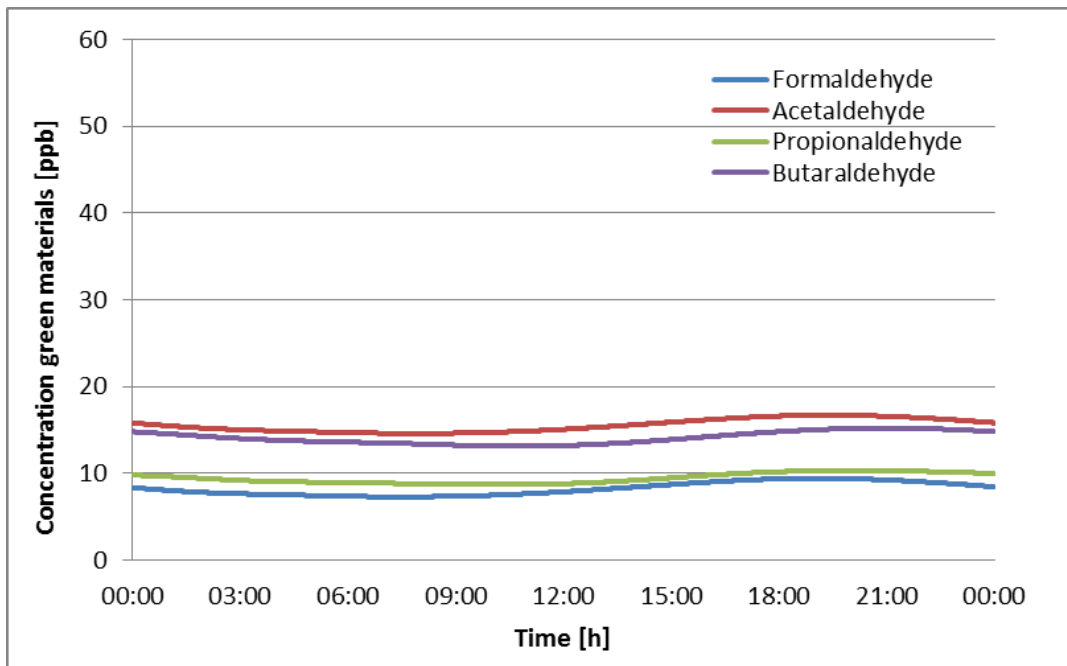
Figure 27: Average daily C_1-C_4 aldehyde concentrations indoors [ppb] after installation of green building materials in the apartment in Milan during typical summer conditions.

To investigate the emissions profile of the materials as they age, further model runs were carried out. Figure 28 and 29 show the concentrations that result from primary

emissions only, 0, three, six, nine and twelve months after installation. The model results reflect the exponential decay rates that were assumed for the material emissions.
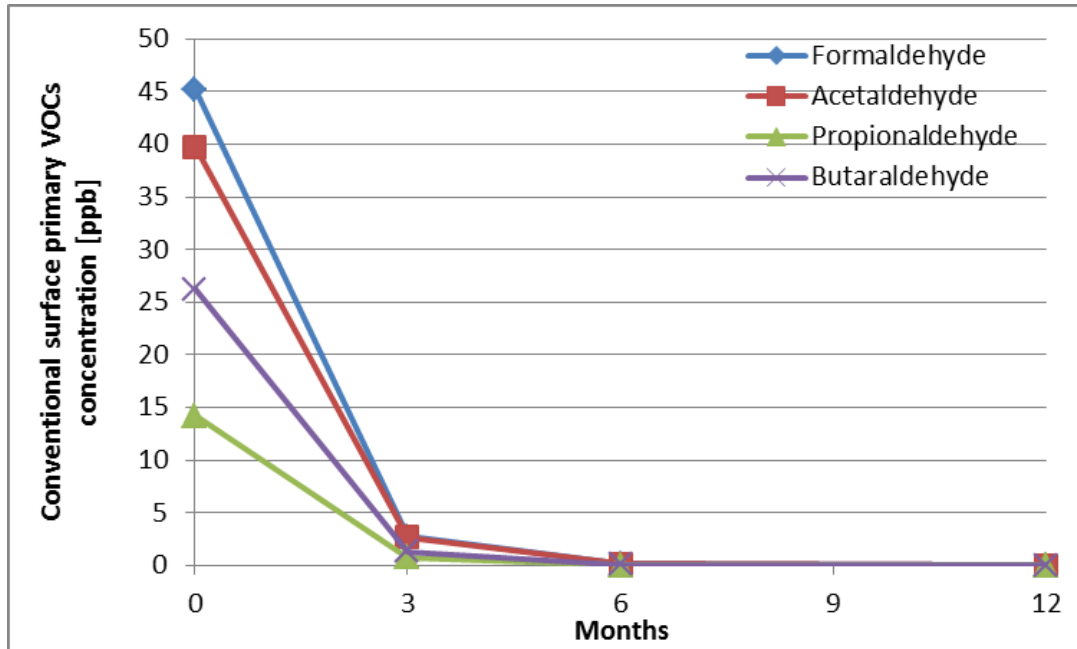
Figure 28: Annual C_1-C_4 aldehyde concentrations [ppb] that result from primary emissions from traditional building materials in the apartment in Milan during typical summer conditions.
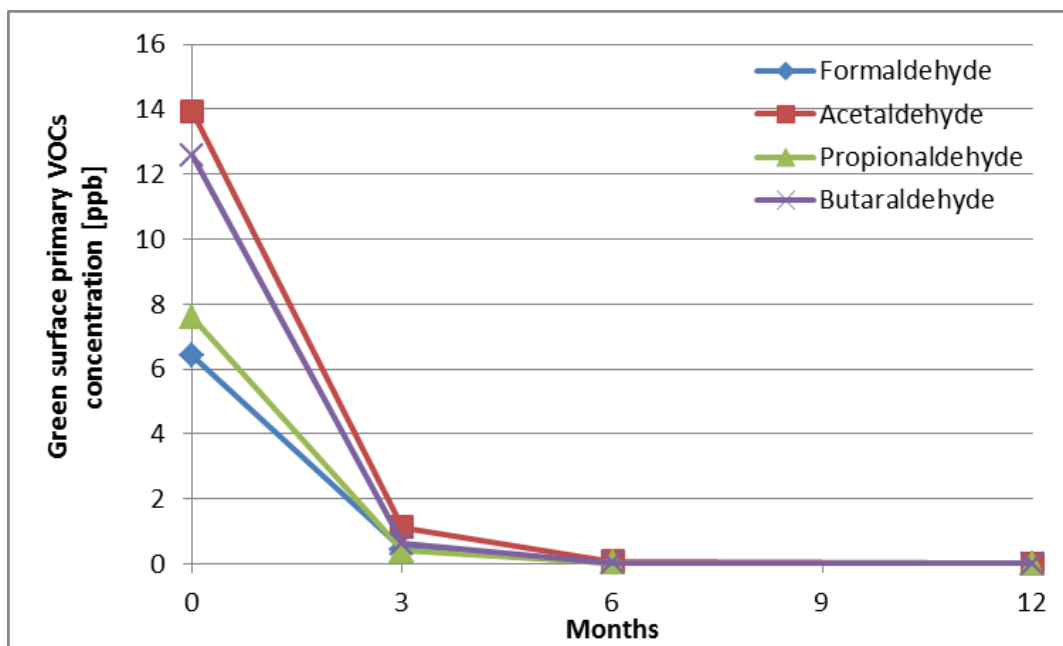
Figure 29: Annual C_1-C_4 aldehyde concentrations [ppb] from primary emissions only from green building materials in the apartment in Milan during typical summer conditions.

The biggest decrease in the aldehyde concentrations occurs during the first three months after installation. For instance, the concentration of formaldehyde decreases from ~45 ppb to ~3 ppb (Figure 28). Similarly, the acetaldehyde concentration from primary emissions from green materials decreases from 14 ppb to 1 ppb after 3 months (Figure 29). In general, C_1-C_4 aldehyde concentrations from primary emissions from traditional building materials directly after installation (0 months) were approximately 3 times higher than those from the green materials. It suggests that the use of green materials is important, particularly for the time period following installation of the materials. In the third month after the installation of materials, C_1-C_4 aldehyde concentrations in the apartment in Milan do not exceed 5 ppb for the conventional materials and 2 ppb for the green ones.

The highest concentration from the secondary emissions immediately following installation is for formaldehyde (Figures 30 and 31), for both the traditional and green building materials. The concentration in the apartment with traditional materials is ~2.5 ppb, and ~2 ppb for green materials. For the other aldehydes and for both types of materials, concentrations were ~1.5-2 ppb. However, the secondary emissions depend mostly on the availability of ozone and surface interactions indoors. In fact, secondary emission products from both conventional and green materials become more important after about 3-6 months (Figure 30 and 31 respectively), as primary emissions become less important and more ozone is available to react to produce secondary emissions. Nevertheless, the concentrations of the secondary VOCs for both conventional and green building materials were within the range of 2-3.5 ppb and 1.5-3 ppb respectively. Given that secondary emissions are ozone dependent, the range of secondary VOC concentrations is relatively small for both conventional and green materials, in contrast to the primary VOCs.
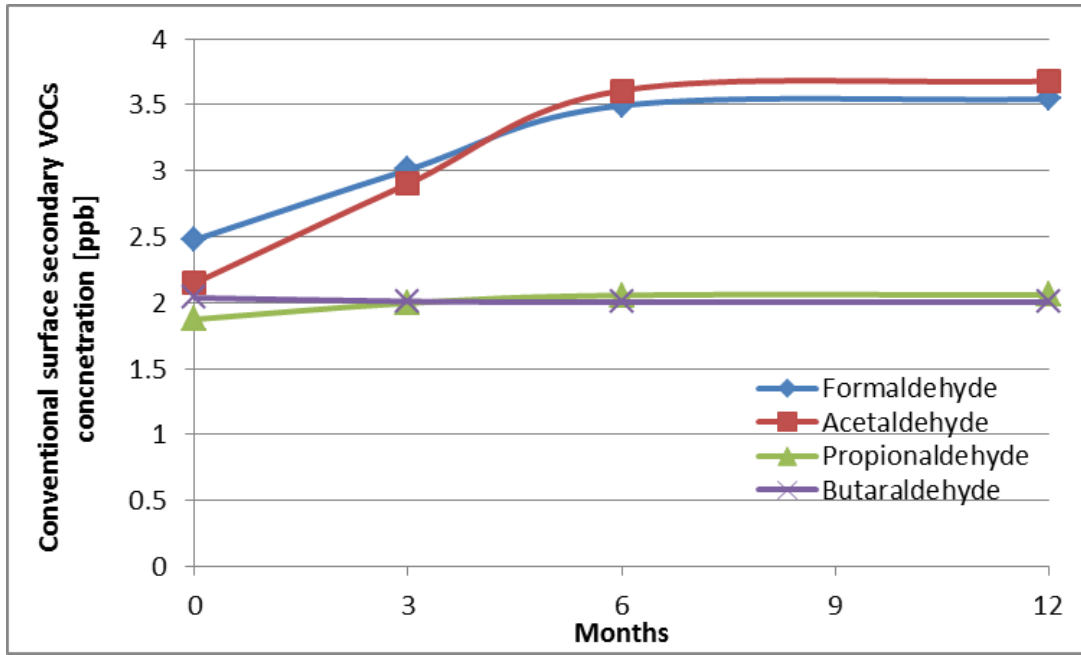
Figure 30: Annual secondary C_1-C_4 aldehyde concentrations [ppb] in the apartment following surface interactions of traditional building materials.
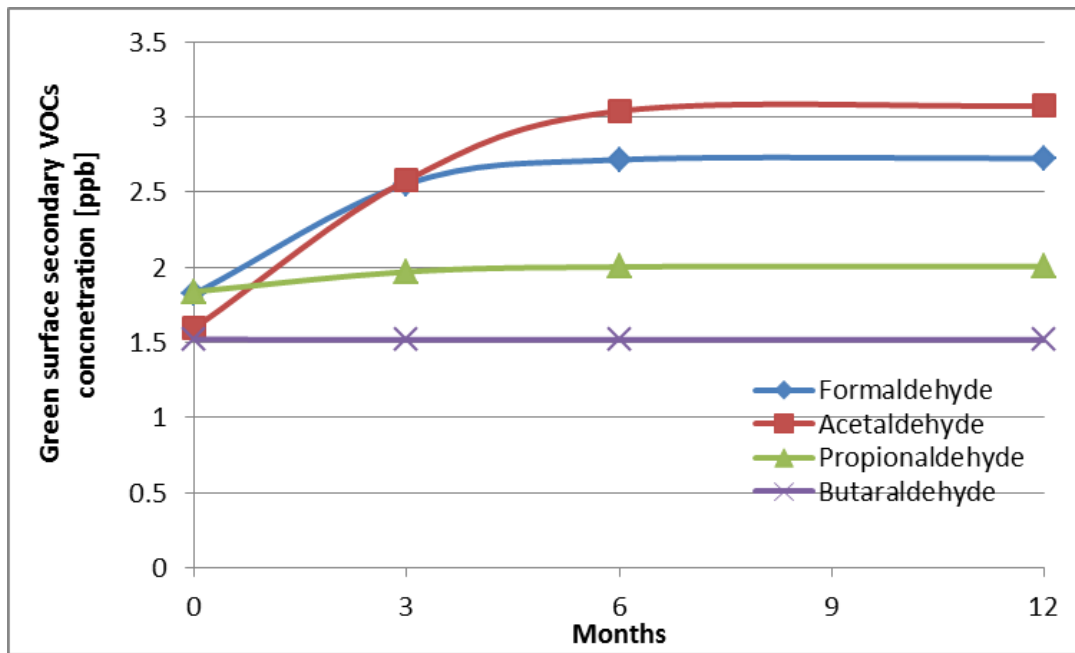
Figure 31: Annual secondary C_1-C_4 aldehyde concentrations [ppb] in the apartment following surface interactions of green building materials.

In general, the concentrations of aldehydes following secondary emissions for both types of materials are relatively stable with time (Figure 32), with a total average concentration of ~10 ppb for VOCs from traditional materials and ~8.5 ppb for the green materials. The biggest difference occurs in the concentrations of aldehydes following primary emissions. The total concentration of primary VOCs following conventional materials emissions is ~125 ppb whereas for green materials it is ~40 ppb.
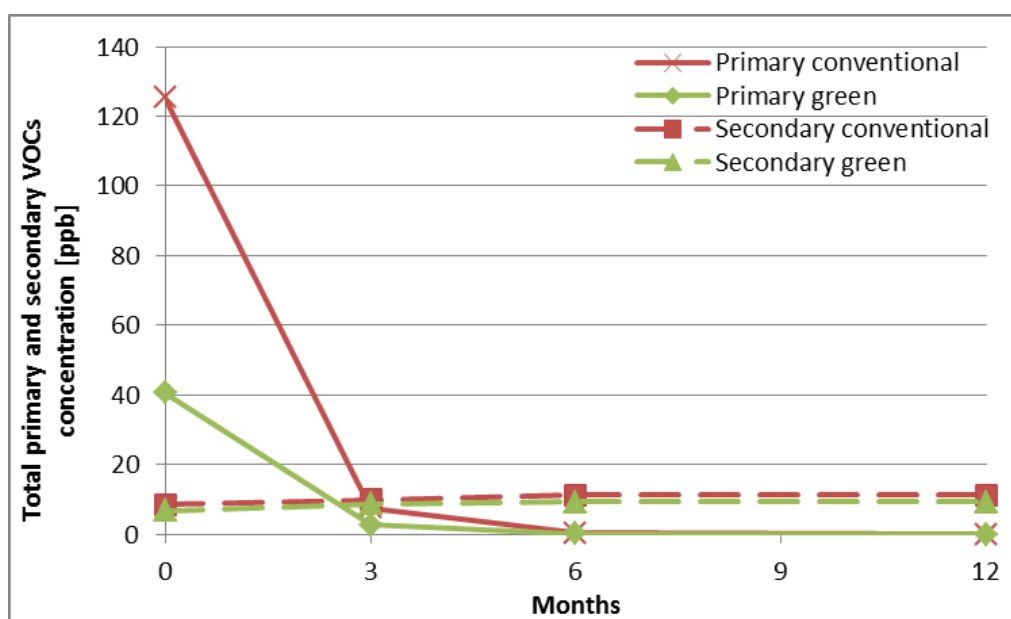
Figure 32: Total annual primary and secondary C_1-C_4 aldehyde concentrations [ppb] in the apartment for traditional and green building materials. VOC concentrations arising from primary emissions are marked with the solid lines and those from secondary emissions with the dashed lines. Red lines depict traditional materials, whilst green lines are for green materials.

4.6 Chapter summary

In this Chapter the surface interactions for typical furnished apartments for different outdoor pollution levels and in different locations (Milan and Seoul) was compared. Not surprisingly, ozone loss is proportional to the ozone concentration indoors. Therefore, the highest ozone loss (~40 ppb) occurs in the apartment in Milan during heatwave summer conditions. In general, the results show that approximately 75% of ozone indoors is lost onto the internal surfaces. Also, high outdoor ozone concentrations can enhance indoor air pollution and lead to higher emissions of C_6-C_{10} aldehydes. For instance, concentrations of nonanal increased by

~22% during polluted conditions when compared with more average conditions in Milan. Given that heatwaves may possibly become more frequent in future with climate change (Solomon et al., 2007), indoor ozone-derived surface aldehyde emissions may also increase. Furthermore, the modelling results clearly indicate the impact of surface processes indoors on indoor air chemistry. Hence, the concentration of oxidants decreases when surface emissions are included. For instance, OH, HO_2 and RO_2 concentrations decrease by approximately 23%, 18% and 8% respectively.

The comparison of traditional and green building materials showed that the green materials will likely produce lower concentrations of pollutants indoors. For instance, formaldehyde and acetaldehyde average daily concentrations when using green materials decrease by ~80% and 60% respectively by comparison with conventional materials. The total primary VOC concentrations in the apartment decrease by ~67% following installation of green materials. Interestingly, the model results show that the concentrations of aldehydes arising from primary emissions of both types of materials are much higher than those from secondary emissions over the first 3 months after the installation. After this period, secondary emissions become more important and lead to more similar concentrations from both sets of materials. The results show that the total secondary VOC concentrations for green and conventional materials are ~10 ppb for both green and conventional materials. Green materials therefore appear to have the biggest impact on avoiding very high concentrations immediately after installation and should be considered to improve indoor air quality indoors.

Given that there are very few measurement data, particularly in actual buildings, there is a clear need for more measurements to help validate model results as well as inform certification and standardization bodies and materials manufacturers.. Hence, models would benefit from more extensive field measurements of ozone surface reactivity (deposition velocity and product yields) in occupied homes with both traditional and green materials, as well as information on surface interactions for indoor pollutants other than ozone. Also, there is lack of health and epidemiological reference studies that would provide comprehensive information and allow the modelling results to be more informative for building occupants.

5. Human bodies as a source of indoor air pollutants

5.1 Chapter preview

This chapter estimates the ozone deposition rate onto human bodies for different indoor environments including an apartment, a bedroom and a classroom. Following the process of ozone deposition, secondary product formation from human skin is explored for the different environments and compared to the material emissions explored in Chapter 4. Finally, the impact of breath emissions on indoor air quality is explored.

5.2 Introduction

One surface receiving increasing attention indoors is the human body. Several studies (e.g. Tamas et al., 2006; Weschler et al., 2007; Coleman et al., 2008; Wisthaler and Weschler, 2010; Rai et al., 2014) have shown that presence of humans in the indoor environment decreases ozone concentrations, while VOC (e.g. mono and dicarbonyls) concentrations increase (Lakey et al. 2016). Therefore humans are recognized as a sink for ozone in the indoor environment and also, a source of secondary pollutants (Weschler, 2016).

The chemicals that constitute human skin oils can be classified as wax esters, glycerols, fatty acids, squalene, esters and sterols and contain unsaturated carbon bonds (C=C) which readily react with ozone (Wisthaler and Weschler, 2010). For instance squalene (a non-volatile triterpene) constitutes ~ 10 % and the fatty acids approximately 25% of human skin lipids (Fischer et al., 2013). Following reactions of such species with ozone, a wide range of secondary products can be formed, including aldehydes, ketones, acids and SOA, some of which might be harmful to health (Weschler et al. 2007; Wells et al. 2008; Wisthaler and Weschler, 2010; Mochalski et al. 2014; Nørgaard et al. 2014; Rai et al. 2014).

The main products of the ozone-squalene reaction (Figure 33) are 4-oxopentanal (4-OPA), 6-methyl-5-hepten-2-one (6-MHO), acetone and geranyl acetone (Fruekilde et al., 1998) Additionally, following ozonolysis of unsaturated fatty acids, higher aldehydes can be formed, namely hexanal, heptanal, octanal, nonanal, decanal, dodecanal and undecanal (Wisthaler and Weschler, 2010) (Table 13). Such compounds may be a concern particularly when the indoor ozone concentration is high. For instance, Wolkoff et al. (2013) showed that 4-OPA and 6-MHO formed through the squalene-ozone reaction are potential sensory and

pulmonary irritants and may cause airflow limitation. Furthermore, higher aldehydes such as nonanal and decanal might show an adverse health effect, as described in previous chapters (Chapter 4).
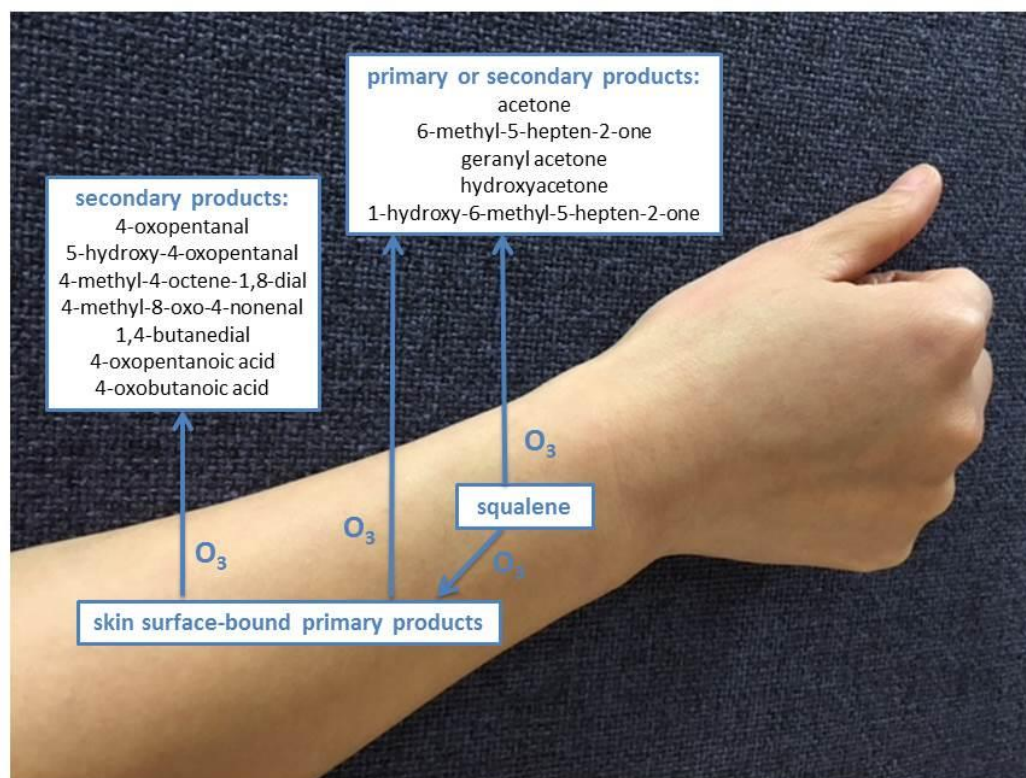
Figure 33: Production of surface-bound and gas-phase primary and secondary products following the reaction of squalene with ozone on the human skin. Following ozonolysis of squalene and other skin surface-bound primary products, additional gas-phase secondary compounds are produced (Source: Wisthaler and Weschler, 2010).

Lakey et al. (2016) developed a kinetic multilayer model of skin surface and chemistry, which included both the chemistry of squalene ozonolysis and the physical mass transport processes. The model investigated the concentrations of ozone indoors and the gas-phase products following ozonolysis of the skin. Considering different scenarios indoors (i.e. number of people, ventilation rate or the room size), the predicted results showed that the ozone concentration decreases while the concentration of gas-phase carbonyl species, such as 4-OPA and 6-MHO, increased. For instance, upon exposure of two adults to ~30 ppb

of ozone in the room, the concentrations of squalene ozonolysis products increased up to 2.0-2.5 ppb, whilst the ozone concentration decreased up to ~1.5 ppb.

Breath is also a significant source of pollutants emitted indoors, including alcohols, hydrocarbons, aldehydes and ketones (Fenske and Paulson, 1999). Several studies have quantified the major VOCs emitted in the exhaled breath of healthy individuals (within the range of weighted averages) such as isoprene (12-580 ppb), acetone (1.2-1880 ppb), ethanol (13-1000 ppb), methanol (1.3-2000 ppb) and isopropanol (50-260 ppb) (Conkle et al. 1975; Phillips and Greenberg, 1991; Hansel et al. 1995; Taucher et al. 1995; Warneke et al. 1996). The concentrations of the emitted compounds are in the range of ppb to ppm. However, their concentrations in the indoor environment depend on the volume of the indoor space, air exchange rate, number of individuals indoors and also individual variation such as dietary or smoking habits (Filipiak et al., 2012). For instance, a large number of VOCs are present in food and drinks, which may contribute to the VOCs detected in exhaled breath. Aldehydes can be used as flavoring agents and alcohols (i.e. ethanol) are typically found in coffee, tea, beverages and food (i.e. vegetables, fruits, cheese or meat) (Burdock, 2005). Filipiak et al. (2012) found 86 compounds in exhaled breath that are related to smoking habits: aromatic compounds, hydrocarbons and volatile nitrogen-containing compounds were detected with substantially higher peak areas for smokers rather than non-smoking participants in the study.

The rate of ozone deposition and subsequent pollutant formation clearly depends on the level and duration of occupancy in the indoor environment, given reactive chemistry processes occur on human skin, hair or soiled clothes (Fenske and Paulson, 1999; Zhou et al., 2016). Not surprisingly, in highly occupied and small indoor spaces, the emission rates of pollutants following skin and breath emissions and their impacts on indoor chemistry will be more important than for environments with fewer occupants (Petrick and Dubowski, 2009). Ventilation rate is, however, critical. Whilst high ventilation rates lead to higher ozone concentrations indoors to catalyse surface chemistry, ozone-derived surface emissions might be flushed out faster from the indoor environment than at a slower ventilation rate. The impact of skin and breath emissions on indoor air chemistry is still unclear, particularly for different occupancy and ventilation rates.

5.3 Aims

Since the human body is an important source of pollution indoors, this chapter aims to quantify the impact of occupancy for different indoor environments. The ozone deposition rate onto human bodies for various occupied indoor environments is quantified and then used to assess the impacts of subsequent pollutant emissions on indoor air chemistry through model simulations of a range of indoor environments.

This chapter first outlines the different indoor environments that have been considered: an apartment, a bedroom and a classroom in different locations (as defined in the previous chapter) such as Milan for typical and heatwave summer conditions and Seoul for typical summer conditions. The underlying assumptions made in the representation of breath and skin surface emissions are then described for relevant species (Table 13).

5.4 Methods

Since degradation schemes for many of the species emitted from skin are not currently available in the model mechanism (e.g. geranyl acetone and 6-MHO), this study focuses on those species that are the largest emitters and already represented in the model mechanism: acetone, nonanal, decanal, 4-OPA, formic and acetic acids as products of skin emissions, and acetone, methanol, ethanol, isoprene and isopropanol as products emitted from exhaled breath (Table 13).

Table 13: The most important gas phase reaction products from ozonolysis of human skin and emitted from human breath that are represented in the model.

Source of emissions	Product name	Product structure
Human skin emissions — squalene ozonolysis	Acetone	
	4-OPA	
	formic acid	
	acetic acid	
unsaturated fatty acids ozonolysis	nonanal	
	decanal	
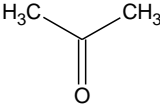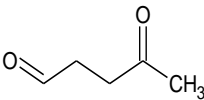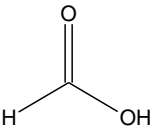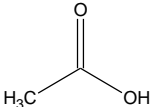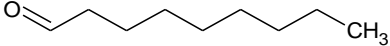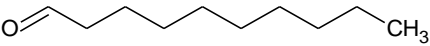
Source of emissions	Product name	Product structure
Breath emissions	acetone	H_3C $\diagdown$ CH_3, O
	methanol	H_3C——OH
	ethanol	H_3C $\diagup$ OH
	isoprene	CH_3, H_2C CH_2
	isopropanol	OH, H_3C CH_3
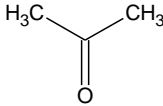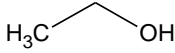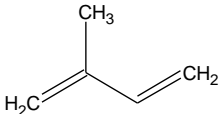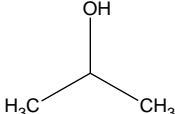
Based on the methodology described in previous chapters (Chapter 3 and 4), modelling was performed to investigate human occupancy in the indoor environment. The model framework, the case study cities, the air exchange rates, outdoor and indoor concentrations of O_3, NO_2 and NO, the outdoor VOCs concentrations reported for Milan and Seoul, the temperature, the humidity, the photolysis rates, and the defined types and surface

size indoors remain the same as described in the previous chapter. However to evaluate the impact of the human body on indoor air chemistry, new parameters were added.

The surface of the human body was defined as 2 m^2 for an adult and 1 m^2 for a child (Fisher, 2013). A median value (calculated based on 12 measurements) of ozone deposition velocity onto human bodies (0.29 cm/s) was derived from a literature review (Tamas et al. 2006; Coleman et al. 2008; Wisthaler and Weschler, 2010). Product yields of various species following human body − ozone interactions were measured by Weschler et al. (2007) in an aircraft cabin and were incorporated in this study (Table 14).

Table 14: Average yields of species from human body emission products following exposure to ozone with a stated uncertainty of 15-25%. Number of measurements is 4. (Weschler et al., 2007). Note that the yields of acetone, nonanal, formic and acetic acids have been halved (see text).

Compounds	Human body emission product yield
Acetone	0.049
Nonanal	0.018
Decanal	0.026
4-OPA	0.026
Formic acid	0.0085
Acetic acid	0.0065

The yields of decanal and 4-OPA reported by Weschler et al. (2007) derive almost exclusively from ozone-skin oil chemistry, but the yield of acetone, nonanal, formic and acetic acids also reflect emissions from internal surfaces in the aircraft cabin: the yields of the latter four species were therefore halved to represent emissions from the skin only (Professor Charles J. Weschler, EOHSI, Rutgers University, NJ, USA; personal communication). The ozone loss rate to the human body surface and the emission of the human body surface products were calculated according to equations 17 and 18 respectively, described in the previous chapter (4.3.1).

To calculate breath emissions, this study includes weighted averages of the major VOCs found in the exhaled breath, as reported by Fenske and Paulson (1999). These

weighted averages considered the results from several studies (Conkle et al., 1975; Phillips and Greenberg, 1991, Hansel et al., 1995; Taucher et al., 1995 and Warneke et al., 1996). Most of the measured values in human breath showed large variation, owing to variation between individual subjects, but also the sampling methods. For instance there is a significant difference in the concentration range of VOCs in exhaled breath when subjects of the study had different occupational exposure or habits (i.e. smoking).

The review of Fenske and Paulson (1999) summarises the weighted concentrations of numerous VOCs that can be found in the exhaled breath of adults. There is a substantial difference in metabolic processes between adults and children. Enderby et al. (2009) presented the analysis of VOCs detected in the exhaled breath of children. Note that the concentration of isopropanol was not included in the study of Enderby et al. (2009) and was calculated as 41 ppb for the purpose of the model runs. The concentration of isopropanol was calculated based on the correlation with other alcohol species concentrations identified in adults and children breath. Therefore the averages of the selected VOCs investigated in the model simulations are presented in Table 15.

Table 15: Weighted average concentrations of VOCs (ppb) in exhaled breath of adults and children (200 children were the subject of the study).

Compound	Adults		Children
	Weighted average concentration (concentration range) (ppb)	Number of subjects (n)	Median concentration (ppb)
Acetone	985 (1.2-1880)	24	297
Ethanol	770 (13-1000)	64	187
Methanol	330 (1.3-2000)	68	193
Isopropanol	150 (50-260)	94	41
Isoprene	210 (12-580)	107	37

The number of breaths per unit time and the volume of each breath vary according to the age of the individuals (Aurora et al. 2005 and Lechner et al. 2006). Recent research indicates that the tidal volume of a single exhaled breath of an adult is approximately 500 ml and that

the adult respiratory rate is 20 breaths per minute (Philip et al., 2015). This equates to 167 ml/sec of expired air.

Aurora et al. (2005) also presented information for children. For a healthy 10 year old child, the respiratory rate is typically 20 breaths per minute, with a tidal volume of approximately 10 ml/kg of body weight. The average weight of a 10-year old child is 31.2 kg (WHO report, 2007). Accordingly, the calculated expiration rate for a child is 104 ml/sec.

The emission of VOCs from exhaled breath in the indoor environment is calculated according to equation 20:

$$E_{VOC} = \frac{V_t * C_t * n * N_A}{V_m * V_i * 10^{18}} \tag{20}$$

where E_{voc} is the relevant VOC emission rate from an exhaled breath (molecule cm^{-3} s^{-1}), V_t is the breathing rate of an individual (ml s^{-1}), C_t is the weighted average concentration of a particular species in a single breath (ppb), n is number of people indoors, N_A is the Avogadro constant (6.02 x 10^{23} molecule mol^{-1}), V_m is the molar gas volume (22.4 litres mol^{-1} at room temperature), V_i is the volume of indoor air that the breath is emitted into (m^3) and 1x10^{18} provides the necessary unit conversion from m^3 to cm^3, litres to cm^3 and ppb to mixing ratio.

5.4.1 Apartment case study

The apartment was characterized in section 3.6.2 and it is assumed that all the dimensions and conditions are the same. However to evaluate the importance of human bodies for ozone loss and indoor surface interactions, it was assumed that two adults and one child were in the household. The surface area of humans in the apartment was ~ 5 m^2 and therefore, the human skin surface to volume ratio in the apartment was ~0.03 m^{-1}. The total surface area available for surface interactions, including the furnishing materials and the presence of people indoors, amounts to 342 m^2 and the total surface to volume ratio for the building is ~2.0 m^{-1}. Human skin emissions were calculated according to equation 18 using the average yields from the human body reported earlier in this chapter (Table 14).

Exhaled breath VOC emission rates were calculated according to equation 20 considering the 2 adults and child in the apartment and are presented in Table 16:

Table 16: Emission rates of VOCs [molecule cm^{-3} s^{-1}] calculated for exhaled breath of 2 adults and a child living in the apartment.

Compound	Emission rate of VOC [molecule cm^{-3} s^{-1}]
Acetone	5.76 x 10^7
Ethanol	4.43 x 10^7
Methanol	2.08 x 10^7
Isopropanol	8.70 x 10^6
Isoprene	1.18 x 10^7

As indicated in the previous chapter, the modelling study was carried out for Milan (during typical and heatwave summer conditions) and Seoul in summertime for a range of air exchange rates: 0.2; 0.76; 2.0 h^{-1}.

5.4.2 Bedroom case study

To estimate the impact of human emissions in a much smaller indoor space when emissions may be more significant, the indoor air quality for an occupied bedroom at nighttime was investigated. It was assumed that two adults (estimated surface of skin ~4 m^2) were in the room (7.5 m^2) continuously for 8 hours (23:00-07:00h). Thus the skin surface to volume ratio (A/V) in the bedroom was ~0.22 m^{-1}. The internal conditions were assumed the same as described in Chapter 3.

The internal surfaces in the bedroom included: soft furniture (5 m^2; A/V = 0.28 m^{-1}), painted walls and ceiling (30.6 m^2; A/V = 1.7 m^{-1}), wooden floor (7.5 m^2; A/V = 0.42 m^{-1}) and hard furniture (6.3 m^2; A/V = 0.35 m^{-1}). The volume of the bedroom was 18 m^3. The total surface area available for interactions, including the furnishing materials and 2 people in the room, amounts to 53.4 m^2 and the total surface to volume ratio for the bedroom was ~2.96 m^{-1}.

Internal surface emissions were calculated according to equation 18 described in the previous chapter including the average yields of aldehyde emissions from material surfaces presented in Table 7. Since the data for aldehyde yields for wooden materials were not available, direct emission rates were calculated using literature data (Nicolas et al., 2007). Emissions from hard furniture of hexanal, heptanal, octanal and nonanal in the bedroom were therefore assumed to be 3.89×10^7 molecule cm^{-3} s^{-1}; 8.37×10^5 molecule cm^{-3} s^{-1}; 8.06×10^5 molecule cm^{-3} s^{-1} and 1.81×10^7 molecule cm^{-3} s^{-1} respectively. The emissions from the wooden floor of hexanal, heptanal, octanal, nonanal and decanal in the bedroom were calculated as 4.63×10^7 molecule cm^{-3} s^{-1}; 9.98×10^5 molecule cm^{-3} s^{-1}; 9.61×10^5 molecule cm^{-3} s^{-1}; 2.16×10^7 molecule cm^{-3} s^{-1} and 5.65×10^5 molecule cm^{-3} s^{-1} respectively.

Human skin emissions were calculated according to equation 18 and included the average yields from human bodies presented in Table 14. Following the estimation of the internal surface size and the volume of the bedroom, emissions into this smaller volume were adjusted accordingly, whilst external conditions were kept the same as described in the Methodology. VOCs emission rates of exhaled breath were calculated according to equation 20 considering 2 adults in the bedroom and are presented in Table 17:

Table 17: Emission rates of VOCs [molecule cm^{-3} s^{-1}] calculated for exhaled breath of 2 adults in the bedroom.

Compound	Emission rate of VOC [molecule cm^{-3} s^{-1}]
Acetone	4.91×10^8
Ethanol	3.84×10^8
Methanol	1.65×10^8
Isopropanol	7.48×10^7
Isoprene	1.05×10^8

Again, the modelling study of human emissions in a bedroom was carried out for Milan and Seoul in summertime for air exchange rates of 0.2; 0.76 and 2.0 h^{-1}.

5.4.3 Classroom case study

Children inhale a higher air volume relative to their body weight when compared to adults (Suk et al., 2003). Thus special attention should be paid to children since they are at higher risk of exposure to air pollutants (WHO report, 2005). For this reason, indoor air pollution in classrooms has become a significant concern (Mendell and Heath, 2005). Some studies discuss the correlation between the ventilation rate and indoor air quality in schools (Godwin and Batterman, 2007; Chatzidiakou et al., 2015). Other studies report the relationship between the role of ventilation indoors and performance of the pupils (Shaughnessy et al., 2006; Wargocki and Wyon, 2007; Bakó-Biró et al., 2007, 2012; Twardella et al., 2012). For instance, Bakó-Biró et al. (2012) showed that more than 200 pupils in different classrooms at higher ventilation rates had an improved performance (by 2-15%) compared with low ventilation conditions.

Therefore to investigate the impact of human emissions in a highly occupied space within a school building, it was assumed that a classroom was occupied by thirty 10 year old pupils and one teacher. Since there are little detailed data available in the literature, this study adopted the measurements carried out in 51 French classrooms described by Canha et al. (2016). The median value of the classroom surface area was 58 m^2 and the volume 171 m^3. Given that there were 30 children and one adult in the classroom during the school hours (09:00-15:00 with an hour lunch break at noon), the total surface area of skin was 32 m^2. Thus the skin surface to volume ratio (A/V) within the classroom was ~0.19 m^{-1}.

The internal materials in the classroom considered as a source of ozone-derived surface emissions included: linoleum on the floor (58 m^2; A/V = 0.34 m^{-1}); painted wall (~138 m^2; A/V = 0.81 m^{-1}); wooden furniture such as the desks, chairs and the internal door (~25 m^2; A/V = 0.14 m^{-1}) (Canha et al., 2016). The total surface area available for ozone-initiated chemistry in the classroom including 30 children, the teacher and internal materials amounts to 252.6 m^2, with a total surface to volume ratio of ~1.48 m^{-1}.

Regarding the type of ventilation, Canha et al. (2016) indicated that 73% (n= 37) of the classrooms had natural ventilation and 27% (n=14) had a mechanical ventilation system. Following the methodology and the data presented by Canha et al. (2016), this study focuses on classrooms with natural ventilation. The mean value of the indoor temperature in this study was assumed as ~23.3^{o}C and the mean indoor relative humidity (RH) was 47%. The median air exchange rate was 1.2±0.6 per hour (Canha et al., 2016). Table 18 presents the mean concentrations of indoor background pollutants.

Table 18: Mean concentrations [μg/m^3] of indoor air pollutants (±standard deviation) measured in the classrooms.

VOC type	VOC concentration [μg/m^3]
Formaldehyde	28 (±16)
Acetaldehyde	6.9 (±2.1)
Butyraldehyde	15 (±11)
Hexaldehyde	13 (±8)
Benzene	2.2 (±2.4)
Toluene	5.8 (±5.5)
Ethylbenzene	2.4 (±1.4)
m,p-xylenes	5.0 (±3.7)
o-xylene	1.9 (±2.2)
Styrene	1.5 (±0.8)

Internal surface and skin emissions of classroom occupants were calculated according to equation 18 described in the previous chapter, including the average yields of material surface and human body products incorporated in Table 7 and 14 respectively. Since the data for aldehyde yields for wooden materials were not available, direct emission rates were calculated using literature data for different types of wooden materials (Hodgson et al. 2002, Nicolas et al. 2007, Plaisance et al. 2014). Therefore the emissions from hard furniture for hexanal, heptanal, octanal and nonanal were 1.56×10^7 molecule cm^{-3} s^{-1}; 3.35×10^5 molecule cm^{-3} s^{-1}; 3.23×10^5 molecule cm^{-3} s^{-1} and 7.25×10^6 molecule cm^{-3} s^{-1} respectively.

The breath emission rates of 30 children and one adult teacher were calculated according to equation 20 and are presented in Table 19.

Table 19: Emission rates of VOCs [molecule cm^{-3} s^{-1}] calculated for exhaled breath in the classroom.

Compound	VOC emission rate of 30 children [molecule cm^{-3} s^{-1}]	VOC emission rate of one adult teacher [molecule cm^{-3} s^{-1}]
Acetone	1.46 x 10^8	2.59 x 10^7
Ethanol	9.17 x 10^7	2.02 x 10^7
Methanol	9.46 x 10^7	8.66 x 10^6
Isopropanol	2.01 x 10^7	3.94 x 10^6
Isoprene	1.81 x 10^7	5.51 x 10^6

The modelling study of human emissions in a classroom with natural (air exchange rate = 0.6; 1.2; 1.8 per hour) ventilation system for the conditions described above was simulated for schools located in Milan (during typical and heatwave summer conditions) and Seoul in summertime.

5.5 Results and discussion

5.5.1 The apartment case study

5.5.1.1 Sensitivity analysis

To investigate the effect of changing key parameters on the predicted concentrations of ozone, radicals and carbonyl species indoors, a series of sensitivity tests have been carried out. The key parameters were varied within uncertainty limits or varied within a typical observed range. Transmission of outdoor UV and visible light through the windows was varied between 0.15% and 25% for UV light and between 0.7% and 75% for visible light (Carslaw, 2007). Air exchange rate was varied between 0.2 and 2.0 h^{-1} (Section 3.3). Furthermore, key outdoor concentrations of ozone, NO$_x$, carbonyl species and surface to volume ratio values were either increased or decreased by 50%.

The concentrations of the carbonyl species, ozone and radicals were then investigated between 09:00 and 17:00 h for the conditions described for the apartment in Milan during typical summer time conditions. The results from the sensitivity analysis, presented as % change in concentration relative to baseline conditions, are shown in Table 20.

Table 20: Sensitivity test results: the % change in concentrations of ozone, radicals and carbonyl products following skin and breath emissions in the apartment in Milan for typical summer conditions relative to baseline conditions (AER=0.76 h^{-1}).

Scenario	Nonanal	Decanal	4-OPA	Formic acid	Acetic acid	Acetone	Methanol	Ethanol	Isopropanol	Isoprene
UV=0.15%, VIS=0.7%	-5.3	-5.6	-4.0	-4.8	-4.7	-0.4	0.0	0.0	0.1	4.7
UV=25%, VIS=75%	31.3	32.9	23.9	30.8	29.5	2.5	-0.1	-0.3	-0.7	-22.1
AER = 0.2	-40.7	-39.8	-41.6	-55.0	-45.1	61.1	-18.3	-48.0	8.0	206.1
AER = 2.0	8.8	6.6	5.1	42.5	32.8	-33.5	23.4	57.7	-7.4	-43.5
Outdoor O_3*0.5	-53.3	-56.4	-57.9	-57.9	-57.1	-2.7	0.0	0.0	0.0	1.9
Outdoor O_3*1.5	56.2	59.4	60.1	60.2	58.4	2.7	0.0	0.0	0.0	-0.5
Outdoor NO_x*0.5	17.9	18.9	16.4	15.8	16.4	0.6	0.0	0.0	0.1	2.7

Scenario	Nonanal	Decanal	4-OPA	Formic acid	Acetic acid	Acetone	Methanol	Ethanol	Isopropanol	Isoprene
Outdoor NO$_x$*1.5	-18.3	-19.3	-17.5	-17.3	-17.2	-0.8	0.0	0.0	0.0	-0.2
Outdoor carbonyls*0.5	-4.4	-1.8	-0.1	-0.3	-0.1	-11.0	-22.8	-39.9	-15.8	-11.8
Outdoor carbonyls*1.5	4.4	1.8	0.1	0.3	0.1	11.1	22.9	40.0	15.8	11.8
A/V*0.5	16.3	14.8	-13.7	17.3	25.6	18.0	59.6	55.8	43.5	-2.0
A/V*1.5	-12.6	-12.0	-10.0	-21.2	-22.7	-13.7	-27.2	-26.4	-23.3	1.0
V$_d$ = 25th percentile	1.0	-2.0	-36.7	-35.2	-31.6	-1.5	0.0	0.0	0.0	-0.1
V$_d$ = 75th percentile	-1.3	2.3	44.1	42.5	38.0	1.8	0.0	0.0	0.0	0.1
Estimated error (%)	63	66	88	85	76	22	46	80	32	44

The model predictions are sensitive to a number of factors, particularly changes in photolysis rates, air exchange rate and outdoor ozone concentration as found for a similar analysis in Chapter 4. Again, it is clear that more experimental data would significantly reduce the model uncertainties and enable the model to become more accurate.

Not surprisingly, an increase in the ozone concentration outdoors, and therefore indoors, enhances the carbonyl emissions following skin ozonolysis. Doubling or halving outdoor O_3 concentrations decreased or increased respectively, the concentrations of these carbonyl species by ~50-60%. Moreover, the lower the air exchange rate is, lower the concentrations of carbonyl species following skin emissions are. However for lower air exchange rates, the concentrations of breath products (with the exception of methanol and ethanol) increase. For most breath emissions, a lower air exchange rate ensures that emissions can become more concentrated indoors. Also, the acetone concentration following both skin and breath emissions is dominated by breath emissions and therefore the concentration is higher when the air exchange rate is lower. Isoprene concentration indoors is dominated by breath emissions. Thus, isoprene concentration is higher when the air exchange rate is lower. The big change in isoprene concentration (an increase of ~206%) when the air exchange rate decreases from 0.76 h^{-1} to 0.2 h^{-1}, confirms that chemical processes indoors, such as the reaction with ozone and OH radicals, play a crucial role in terms of VOC oxidation. Therefore both lower exchange rate with outdoors and lower oxidant concentration indoors result in higher isoprene concentrations indoors. For methanol and ethanol exchange with outdoors is much more significant than emissions from breath, so clearly indoor concentrations are driven by influx from outdoors.

The model predictions are less sensitive to outdoor NO_x concentrations and variation in surface to volume ratio. For instance, doubling or halving outdoor NO_x concentrations decreased or increased respectively, the concentrations of carbonyls up to 20%. The estimated total error was calculated for each species (Table 20). Photolysis rates, secondary pollutant yields, deposition velocities and outdoor carbonyl concentrations were judged to be the most uncertain factors. As for Chapter 4, given the 25th-75th percentile values were used in the sensitivity analysis, the largest uncertainty for each species was doubled to give an estimate of the overall error (between 22-88%) in the model prediction for each species.

5.5.1.2 Ozone deposition

The deposition velocities presented in Figure 19 show that human bodies have the highest ozone median deposition velocity value and are expected to be the most reactive materials for the indoor environment. Darling et al. (2016) showed that ozone removal effectiveness increases along with a deposition velocity increase. Indeed, the highest loss rate per square

meter is to human bodies for all three sets of conditions. In total in each case, skin contributes to ~10% of ozone loss in the apartment. Although the surface-volume ratio of the skin surface is the lowest (0.03 m^{-1}) for all surfaces in the apartment, the ozone deposition velocity is the highest (Figure 19). Although ozone loss onto skin was only 2-3 ppb in each scenario, showing a relatively minor contribution to the overall ozone loss in the apartment, it still impact the indoor air chemistry. A comparison of the importance of skin for ozone loss rate with different type of surfaces in the apartment is shown in Figure 34.
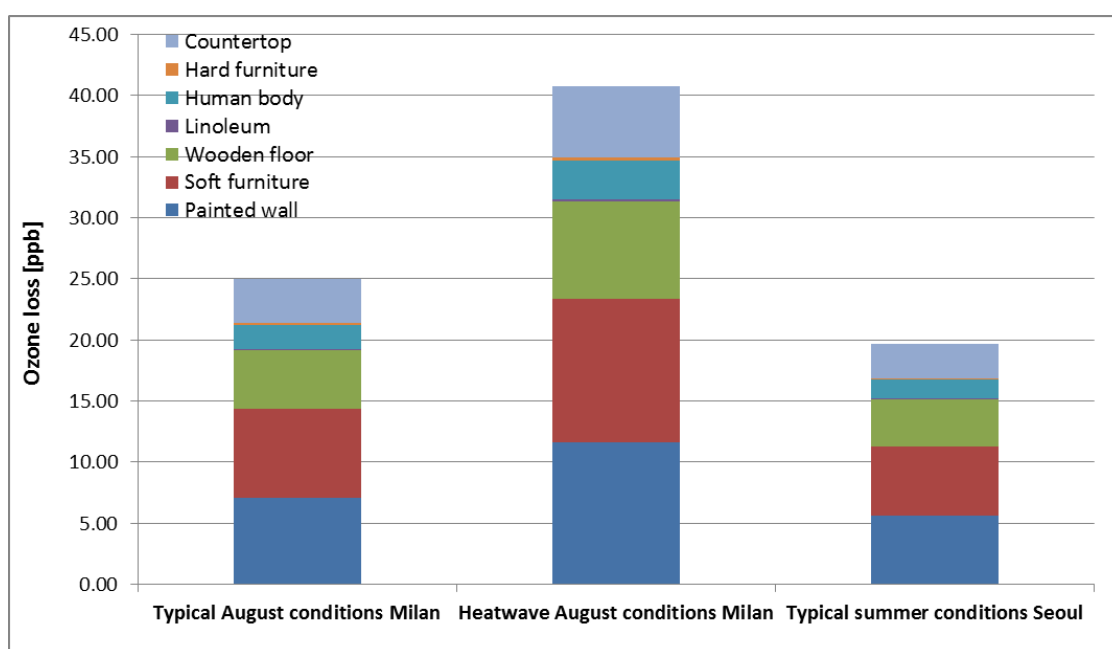
Figure 34: Total ozone removal rate [ppb sec^{-1}] onto different indoor surfaces (average age) in the Milan apartment during typical and heatwave conditions and in the Seoul apartment during typical summer time conditions.

Figure 35 compares the ozone concentration when occupants are present and absent indoors as well as when the apartment is unfurnished and unoccupied. Given that the highest outdoor ozone concentration is in the afternoon, infiltrated ozone indoors increases its concentration in the afternoon showing the highest concentration indoors around 4-5 p.m. Clearly, the ozone concentration is lower when the apartment is occupied, although owing to the relatively small surface area of skin relative to the overall volume, there is not a large difference when compared to an unoccupied apartment. A significant increase in the ozone concentration can be seen when the apartment is unfurnished and unoccupied, again reinforcing the fact that most ozone is lost to furnishing and building materials rather than to human occupants (for low occupancy). Wisthaler and Weschler (2010) measured ozone loss

when occupants are present in an unfurnished office. The results show that two occupants remove 55-56% of ozone in a 28.5 m^3 office over 1 h (AER = 1 h^{-1}). A single occupant removes 10-25% of ozone in a 30 m^3 room (AER = 0.9 h^{-1}). The results presented by Rim et al. (2018) show that a single occupant removes approximately 10% in an unfurnished 58 m^3 room (AER = 1.0 h^{-1}). However, Figure 35 shows that 3 occupants present in a furnished apartment (168 m^3) remove ~20% of ozone compared to an unoccupied apartment over 24h.
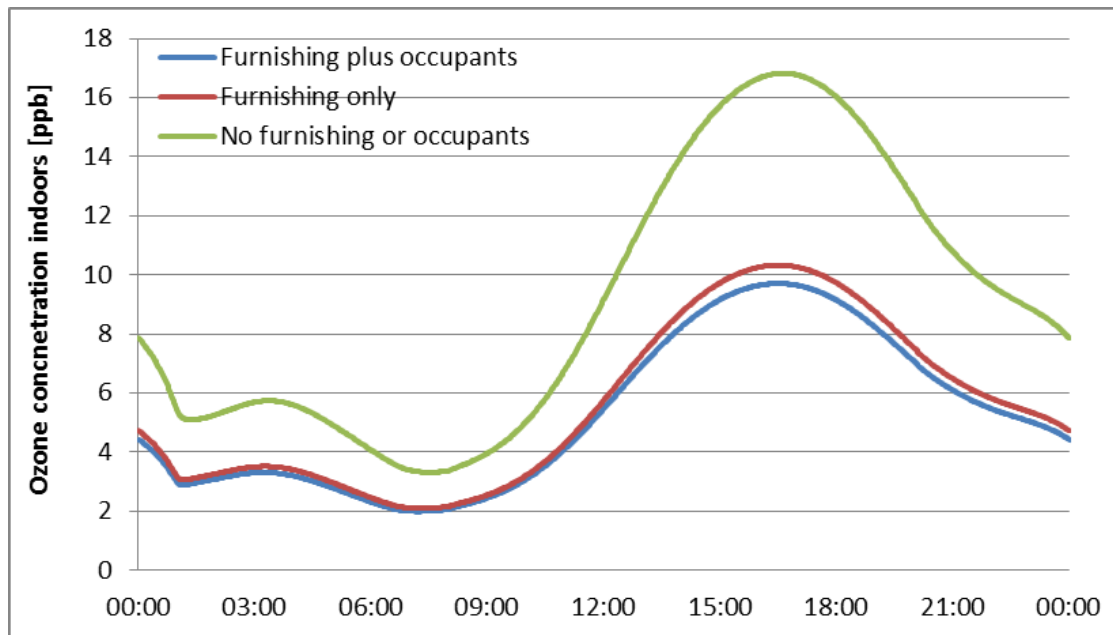
Figure 35: Ozone concentration diurnal profile [ppb] when the apartment is unfurnished (green line), the occupants are present (blue line), and absent (red line) indoors in the Milan apartment during typical summer conditions (air exchange rate = 0.76 h^{-1}).

5.5.1.3 Skin emissions

To compare the emissions of human skin with other surfaces present in the apartment, model runs were performed when 2 adults and a child were present in the apartment during the day (09:00-17:00). All the figures in this section (Section 5.5.1.3) show solely skin emissions in the apartment.

Figure 36 shows the concentrations of higher aldehydes (C$_6$-C$_{10}$) in the apartment and the contribution of different surfaces indoors. Given that nonanal and decanal are emitted both from surface materials and from human skin interactions, their importance can be compared. In the context of the results as whole apartment average values, emissions of pollutants from 3 human occupants are relatively small assuming a well-mixed environment.

The presence of 3 persons in the apartment for typical Milan summer conditions, when the air exchange rate is 0.76 h^{-1}, contributes only 0.1 and 0.2 ppb respectively to the total nonanal and decanal concentrations of 5.7 and 1.6 ppb. However, in the absence of occupants, nonanal and decanal concentrations were 5.9 and 1.6 ppb respectively. Without occupants, there is more deposition to surfaces other than skin, from which secondary emissions are more efficient. So for these aldehyde species and under these conditions, ozone-driven emissions from furniture and building materials generate higher concentrations than those when humans are present. The results confirm that the type of surface (and therefore ozone deposition velocity and consequent product yield), but also the surface to volume ratio, have a significant impact on secondary pollutant formation indoors.
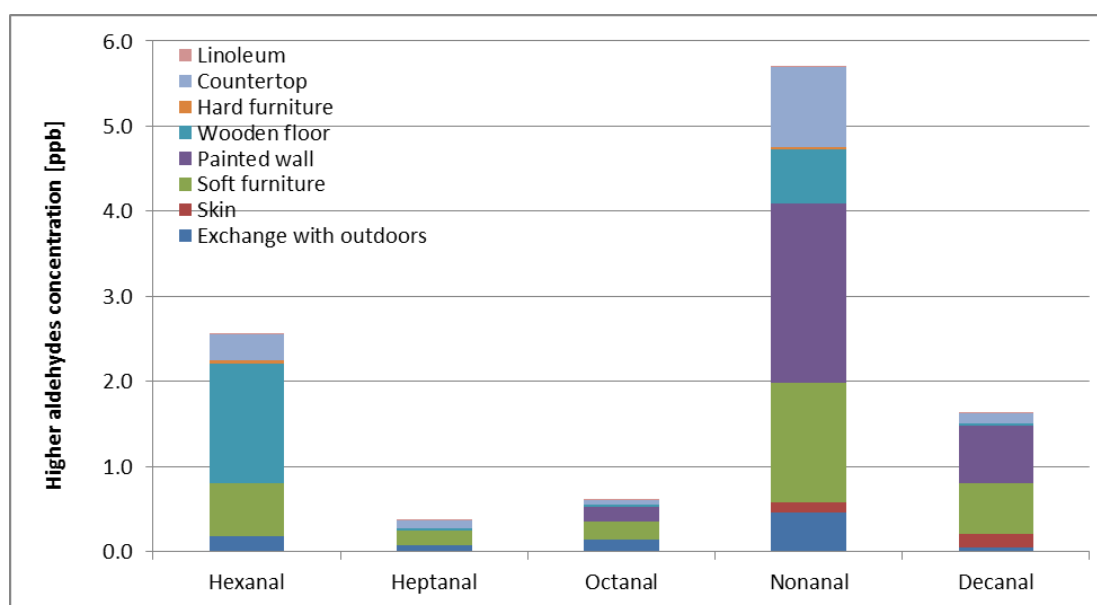
Figure 36: Concentration of higher aldehydes (C$_6$-C$_{10}$) [ppb] and their contribution from different type of surfaces in the apartment in Milan during typical summer conditions, when air exchange rate is 0.76 per hour (09:00-17:00 h).

Focusing only on the skin emission products, it should be emphasized that the air exchange rate has a great impact on the simulated concentrations indoors, as shown for Figure 37. Not surprisingly, the results show that carbonyl concentrations decrease at lower AERs, given less ozone is transported indoors under these conditions to drive the surface interactions. Acetone, 4-OPA and decanal are the most important compounds of the studied species. The concentration of acetone is relatively high, up to 0.45 ppb. 4-OPA and decanal only attain concentrations of up to 0.2 ppb in the apartment case study. The nonanal concentration is typically ~70% of the value of the decanal concentration.
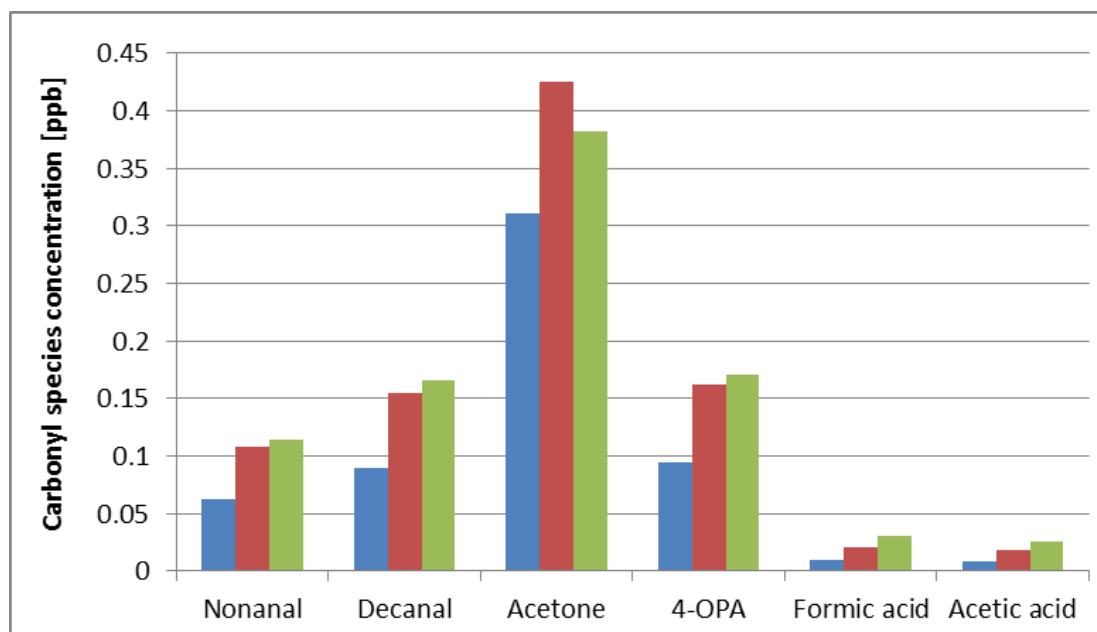
Figure 37: Concentration of carbonyl species following human skin emissions [ppb] in the apartment in Milan during typical summer conditions, when air exchange rates vary. Note that blue bars depict concentrations of the aldehydes when air exchange rate is 0.2 h^{-1}, red bars 0.76 h^{-1} and green bars 2.0 h^{-1} (09:00-17:00 h).

Figure 38 illustrates the concentrations of the carbonyls and acids in the apartment when the outdoor conditions are varied. The highest concentrations of carbonyls indoors are in Milan during summer heatwave conditions, owing to the high level of pollution outdoors and therefore indoors through enhanced skin (and material) emissions. In these conditions in Milan the concentrations of decanal and 4-OPA are up to ~0.2 ppb and for acetone ~0.6 ppb. In the apartment in Seoul during typical summer time conditions, the concentrations of emitted compounds are ~60% lower than during summer heatwave conditions in Milan. Wisthaler and Weschler (2010) measured skin emissions following ozone deposition onto a single occupant in a 30 m^3 unfurnished office (AER = 1.0 h^{-1}). Under the conditions of 50 ppb of ozone indoors, concentrations of acetone, decanal and 4-OPA were approximately 3 ppb, 1 ppb and 0.3 ppb respectively. Figure 38 shows the concentrations of selected carbonyl species from 3 occupants in the apartment in Milan during heatwave summer conditions (AER = 0.76 h^{-1}). These are lower than those presented by Wisthaler and Weschler (2010), but the current study has a larger volume (168 m^3) than the room (30 m^3) used in the reference study. Therefore, the skin surface to volume ratio is much lower than the one considered in the study of Wisthaler and Weschler (2010). Also, the results (Figure 38) are simulated for the occupants in a furnished apartment, which have an impact on the background chemistry and thus on the skin emissions following ozone interactions.

116
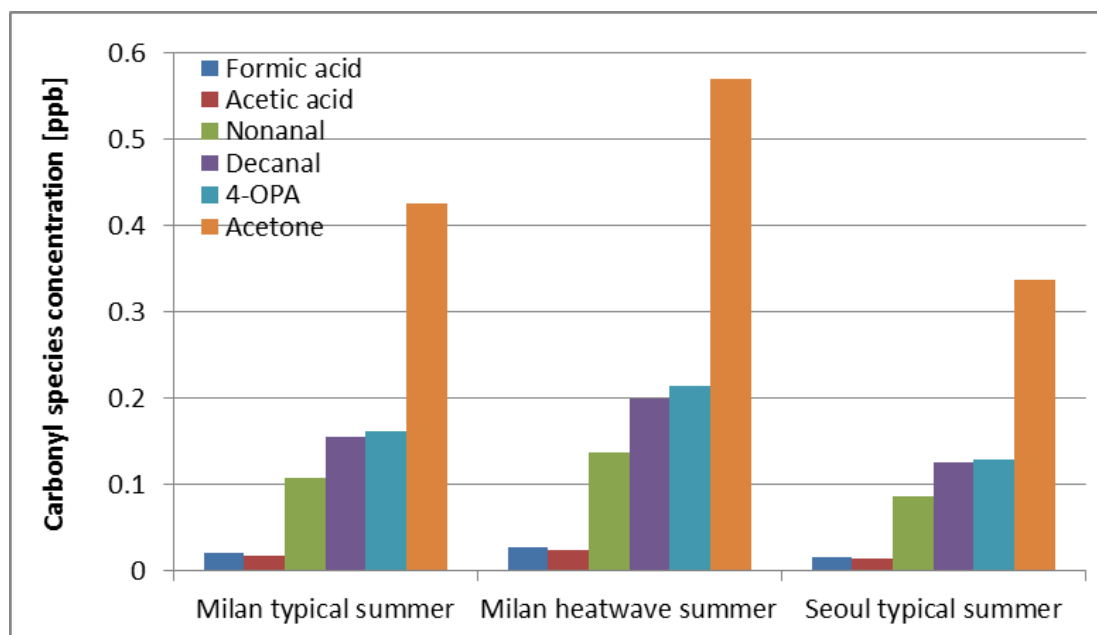
Figure 38: Concentration of carbonyl species following human skin emissions [ppb] in the apartment (AER = 0.76 per hour) when different outdoor conditions occur in Milan (during typical and heatwave summer conditions) and in Seoul during typical summer time (09:00-17:00 h).

As highlighted previously, lower concentrations of skin emission products are likely to be found indoors when the air exchange rate is lower. The model runs were repeated for the apartment scenario when outdoor conditions were different and the AER was 0.2 and 2.0 per hour (Figure 39 and 40 respectively). It can be inferred from Figure 39 that the concentration of the main ozone-derived skin products (nonanal, decanal and 4-OPA) in all the scenarios is diminished by ~50% when the air exchange rate decreases from 0.76 to 0.2 h^{-1}, though the concentration of acetone is only diminished by ~30% (more information about breath emissions will be given in the next section of this Chapter). Nevertheless acetone has the highest concentration in all three scenarios.

While the air exchange rate increases, higher concentrations of indoor ozone follow. Given that skin emissions are ozone dependent, higher concentrations of ozone indoors enhance skin emissions. Figure 40 shows that the skin emission products lead to higher concentrations by (~4-10%) when the air exchange rate increases from 0.76 to 2.0 h^{-1}. The acetone concentration decreases by 7-10% when air exchange rate is increasing from 0.76 to 2.0 per hour, as stated above. Acetone emissions derive from skin and breath. Its concentration depends on the balance between emission rates, ozone concentration and the air exchange rate (described in the next section of this Chapter).

117
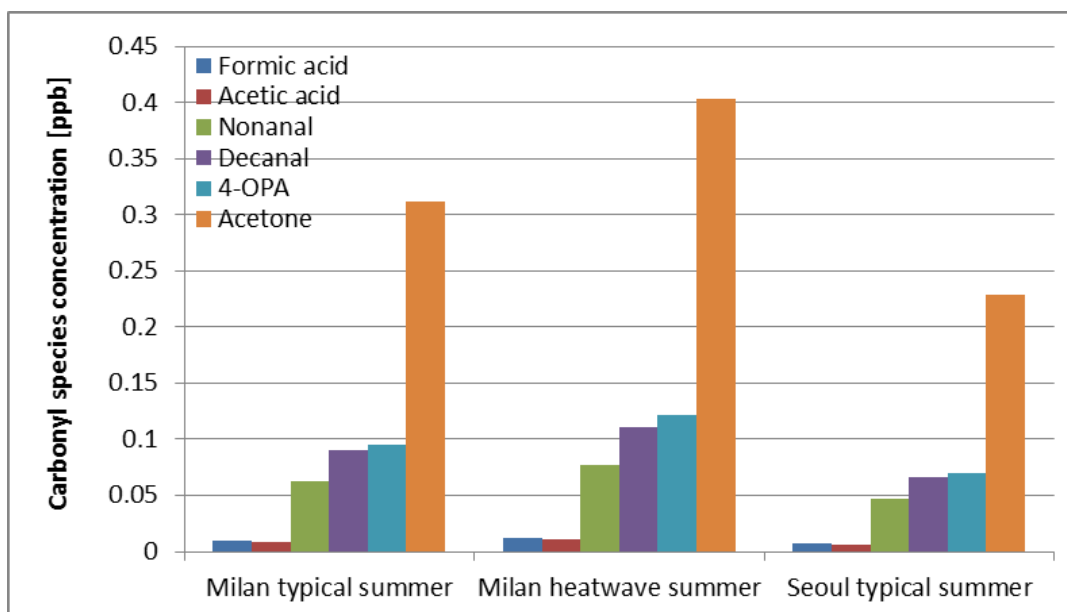
Figure 39: Concentration of carbonyl species following human skin emissions [ppb] in the apartment when different outdoor conditions occur in Milan (during typical and extreme summer conditions) and in Seoul during typical summer time; air exchange rate = 0.2 per hour (09:00-17:00 h).
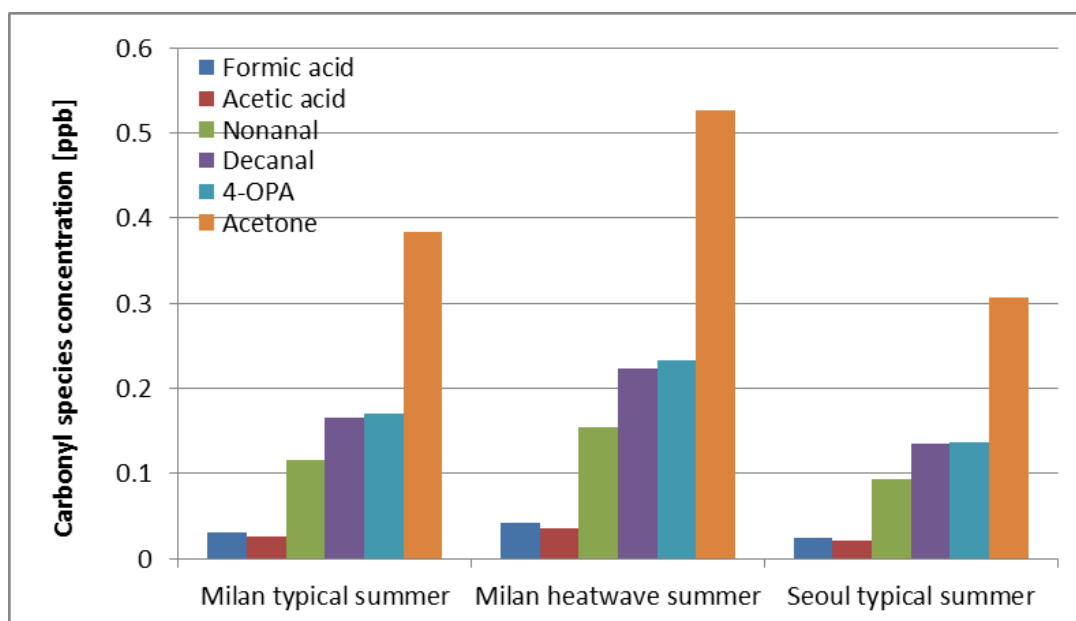
Figure 40: Concentration of carbonyl species following human skin emissions [ppb] in the apartment when different outdoor conditions occur in Milan (during typical and extreme summer conditions) and in Seoul during typical summer time; air exchange rate = 2.0 per hour (09:00-17:00 h).

5.5.1.4 Breath emissions

Figure 41 illustrates the predicted concentrations of breath emission products in the apartment scenario for different air exchange rates. The highest concentrations are for acetone and

118

isoprene, 7.3 and 1.9 ppb respectively for an AER of 0.76 h^{-1}. The concentrations decrease when the air exchange rate increases and ventilation effectively decreases their concentrations. For instance, the isoprene concentration decreases from 7.1 to 1.0 ppb when the air exchange rate increases from 0.2 to 2.0 h^{-1}. The concentrations deriving from breath emissions did not vary between the case study cities given the apartment/occupants were the same in each and that breath emissions are independent of other pollutant concentrations. However, perhaps could remove the emitted species but such process becomes less important than the emissions themselves.

It should be emphasized that acetone is emitted both from skin (as described in the previous section of this Chapter) and human breath. Although skin emissions become more important as AER increases, the opposite is true for breath emissions, which have greater importance at lower AERs. Therefore, there is a play off between breath and skin emissions and so the acetone relationship with AER is different to the other studied species.
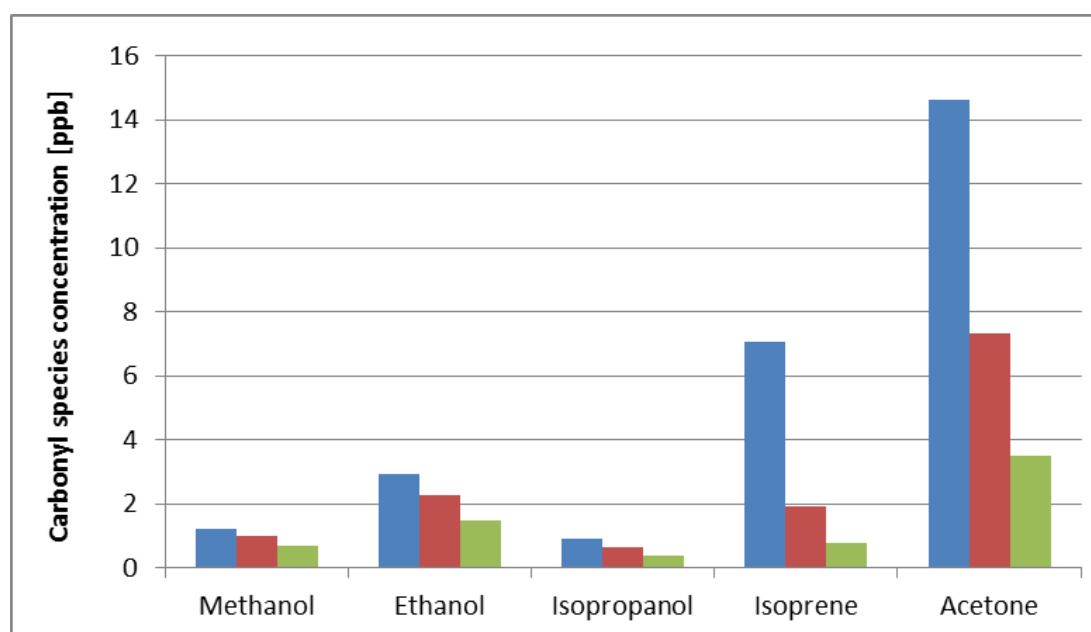
Figure 41: Concentration of carbonyl species emitted from human breath [ppb] in the apartment for different air exchange rates. Note that blue bars depict concentrations of the products when air exchange rate is 0.2 h^{-1}, red bars 0.76 h^{-1} and green bars 2.0 h^{-1}.

The model results shown in Figure 41 are the predicted values for breath emissions only. However, the total concentrations of the selected compounds modelled for the apartment in Milan during typical summer conditions are shown in Figure 42. The figure

represents the range of concentrations that might be expected indoors given variations in surface emissions, including from humans, and exchange with outdoors.
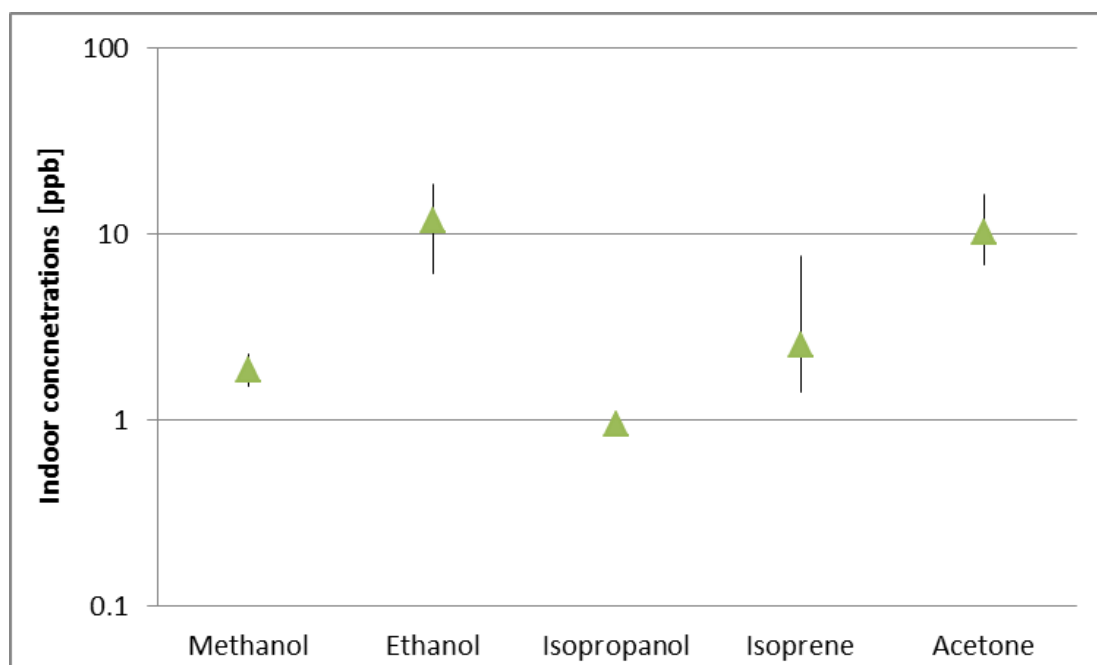
Figure 42: Indoor concentration of selected carbonyl species [ppb] modeled for the apartment in Milan during typical summer conditions. The range of the values represents predicted concentrations for different air exchange rates (0.2 h^{-1}; 0.76 h^{-1} and 2.0 h^{-1}). Triangles denote the concentrations when AER is 0.76 h^{-1}.

The concentrations of isopropanol, isoprene and acetone are the highest in the apartment when AER is 0.2 h^{-1} and the lowest when AER = 2.0 h^{-1}. However for methanol and ethanol, highest concentrations occur in the apartment when AER = 2.0 h^{-1} with lowest values when AER = 0.2 h^{-1}. Nevertheless, for methanol and isopropanol the range of the concentrations was still relatively small. For methanol and ethanol, exchange with outdoors is much more significant than emissions from breath, so outdoor concentrations have a large impact on indoor concentrations for this level of occupancy. On the other hand, the emissions of isopropanol, isoprene and acetone are more significant from breath emissions rather than from exchange with outdoors. The indoor concentrations are clearly dependent on the strength of indoor emissions as well as the exchange rate and outdoor concentrations, leading to different behaviour of these species indoors as ventilation rate changes.

The model predictions are in good agreement with measurements presented in the literature. For instance, Wang et al. (2017) measured concentrations of VOCs in UK

homes. Measured median values of isoprene concentrations were ~0.4 and 4.5 ppb in London and York houses respectively. The median concentration of isoprene measured in London is in the range of the values predicted by the model. Similarly, Bari et al. (2015) measured VOCs at 50 non-smoking homes in Canada during summer time. The measurements include isoprene, acetone, methanol and ethanol. The concentration of isoprene (median value of ~1 ppb) is comparable with the values predicted by the model (1-8 ppb).

Acetone, methanol and ethanol concentrations measured by Bari et al. (2011) (median values of 29; 71 and 151 ppb respectively) are higher than those predicted by the model. The study by Geiss et al. (2011) measured VOCs in private houses in eleven cities across Europe during different seasons. 88 samples were collected for acetone measurements with a median concentration value of ~20 ppb (within the range of 4-69 ppb). Again, the concentrations predicted by the model tend to be on the lower end of the measured ranges. The measurements presented in the literature were carried out in homes with occupants. Therefore, other indoor activities, i.e. cleaning, may enhance the concentrations of the alcohols and acetone (Carslaw et al., 2017). It should be noted that the modelled scenario for the apartment included surface emissions (including human body) and exchange with outdoors, however there are no additional emissions such as from cleaning and cooking included. The model also has not accounted for fragrance or personal care product use, which could add significantly to VOC load in a real environment (Tang et al. 2016; Stönner et al. 2017; Wang et al. 2017). This issue is addressed in section 5.5.3.2.

5.5.1.5 Impacts of human occupancy on chemical processing in the apartment

In order to compare how the indoor chemistry changes when occupants are present or absent in the apartment, a rate of production analysis was carried out for the Milan apartment during typical summertime conditions (AER = 0.76 h^{-1}). Table 21 shows the modeled steady-state concentrations of OH, HO$_2$ and RO$_2$ for a model run with ozone deposition only (no emissions) as well as with surface production included when the occupants are absent and present in the apartment.

Table 21: Concentrations of OH [molecule cm^{-3} s^{-1}], HO_2 [ppt] and RO_2 [ppt] modelled for the apartment in Milan in typical summer conditions (AER = 0.76 h^{-1}), for ozone deposition only, and ozone deposition together with surface production (with and without occupancy).

	OH [molecule cm^{-3}]	HO_2 [ppt]	RO_2 [ppt]
Ozone deposition only	4.78×10^5	4.90	6.02
Ozone deposition and surface production (no occupants)	3.77×10^5	3.71	5.78
Ozone deposition and surface production (with occupants)	3.60×10^5	3.83	5.82

As shown in Chapter 4, surface emissions reduce the oxidant concentrations indoors. The OH concentration is reduced by ~20% with surface emissions present compared to when they are not. HO_2 is reduced by a similar amount, though RO_2 concentrations are less affected. This is because the increased aldehyde concentrations following surface emissions permit more RO_2 to be produced; despite lower OH concentrations (see Figure 43).

Figure 43 presents the production rates with (i) ozone deposition and ozone-driven aldehyde surface production (without occupants) and (ii) with ozone-driven surface production including occupants (in units of 10^4 molecule cm^{-3} s^{-1}).
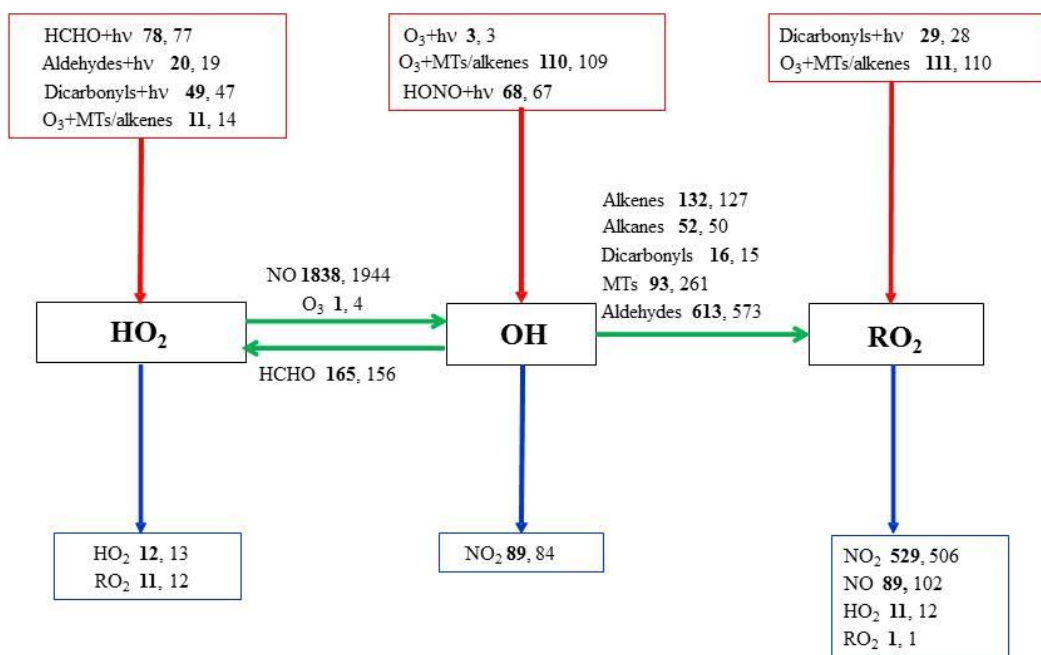
Figure 43: Simplified rate of production analysis for the major rates of reaction for a model run with ozone deposition followed by ozone-driven aldehyde surface production (with an absence of the occupants) (figures in bold) and with ozone deposition followed by ozone-driven surface production including occupants (2 adults and a child) (figures in normal font) in units of 10^4 molecule cm^{-3} s^{-1}. The model runs were performed for an apartment in Milan during typical summer conditions when air exchange rate was 0.76 h^{-1}. MTs denote monoterpenes, which also includes isoprene (strictly a hemiterpene). Red arrows denote radical initiation processes, blue arrows are termination processes with green arrows representing radical propagation.

The production of HO$_2$ radicals via photolysis of aldehydes decreases slightly when humans are in the room, compared with a furnished but unoccupied apartment. Human occupancy makes very little difference in this case. Initiation rates of HO$_2$ radical formation via O$_3$-terpene reactions become more important when occupant emissions are considered, but photolysis of dicarbonyl species becomes a little less important with the occupants present rather than with the surface emissions only.

In terms of radical propagation, the concentration of OH slightly decreases when occupants are present and causes lower production rates of peroxy radicals via reaction with aldehydes, alkenes, alkanes and dicarbonyls. Moreover, the formation of RO$_2$ radicals, following the reaction of OH radical with monoterpenes, becomes more important when

123

occupants are present indoors. Isoprene, which is emitted from breath, contributes to this increase.

The noteworthy difference is the fate of the peroxy radicals through termination. Reactions of alkyl peroxy radicals with NO increase formation of organic nitrates when humans are present at the expense of PAN formation, although formation of PANs still dominates overall termination routes. Hence it is expected that lower concentrations of oxidants and higher concentrations of organic nitrates might exist when humans are present indoors.

In conclusion, there are not many changes within the detailed chemistry when occupants are present indoors for these conditions. It might be explained by the fact that human emissions in the apartment are relatively small. One important difference might be observed for the production rate of RO_2 following the reaction of OH with isoprene, which is emitted from breath. Breath emissions were higher in comparison with skin emissions and therefore had a higher impact on the resulting chemistry.

5.5.2 The bedroom case study

To investigate a situation when human emissions can potentially be more important, the indoor air quality for an occupied bedroom at nighttime and for different ventilation rates was investigated. The assumption was that two adults (surface estimated as 4 m^2 in total; $A/V = 0.22$ m^{-1}) were in the bedroom (7.5 m^2) continuously for 8 hours (23:00-07:00h). The total surface to volume ratio was ~2.96 m^{-1}.

5.5.2.1 Skin and breath emissions

Figure 44 and 45 show the comparison of skin and breath-derived concentrations respectively in the bedroom for typical summer conditions in Milan (air exchange rate of 0.76 h^{-1}), with the predicted values for the whole apartment shown for comparison.

Figure 44: Concentration of oxygenated products following ozone-derived human skin emissions [ppb] in the apartment and in the bedroom when typical summer conditions occur in Milan (air exchange rate = 0.76 h^{-1}) for night time hours (23:00-07:00 h).

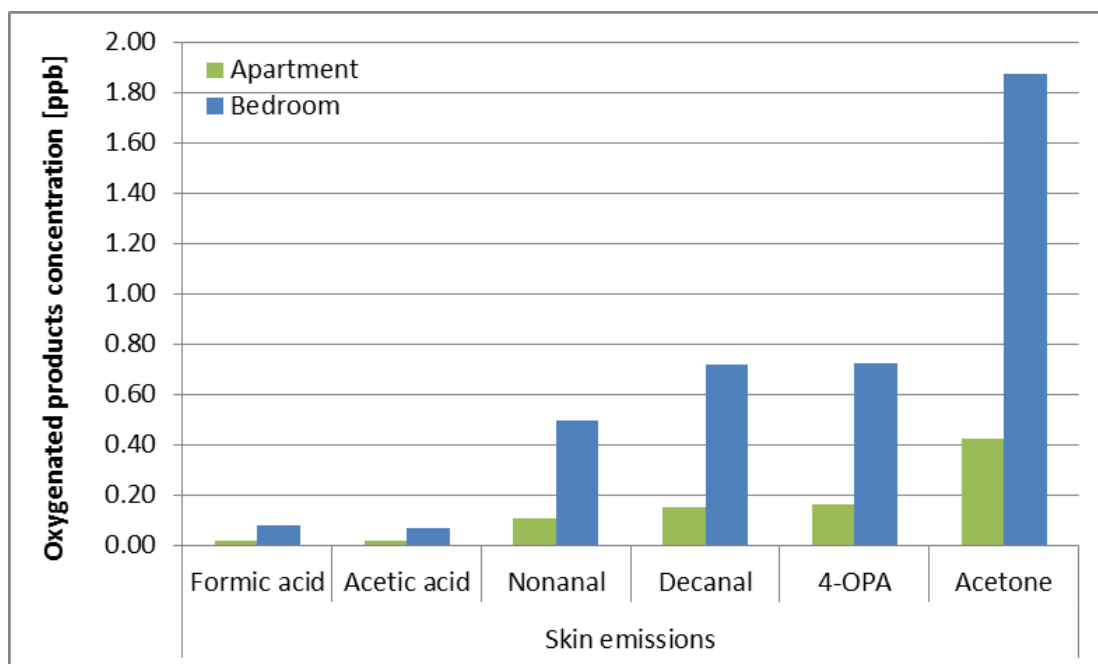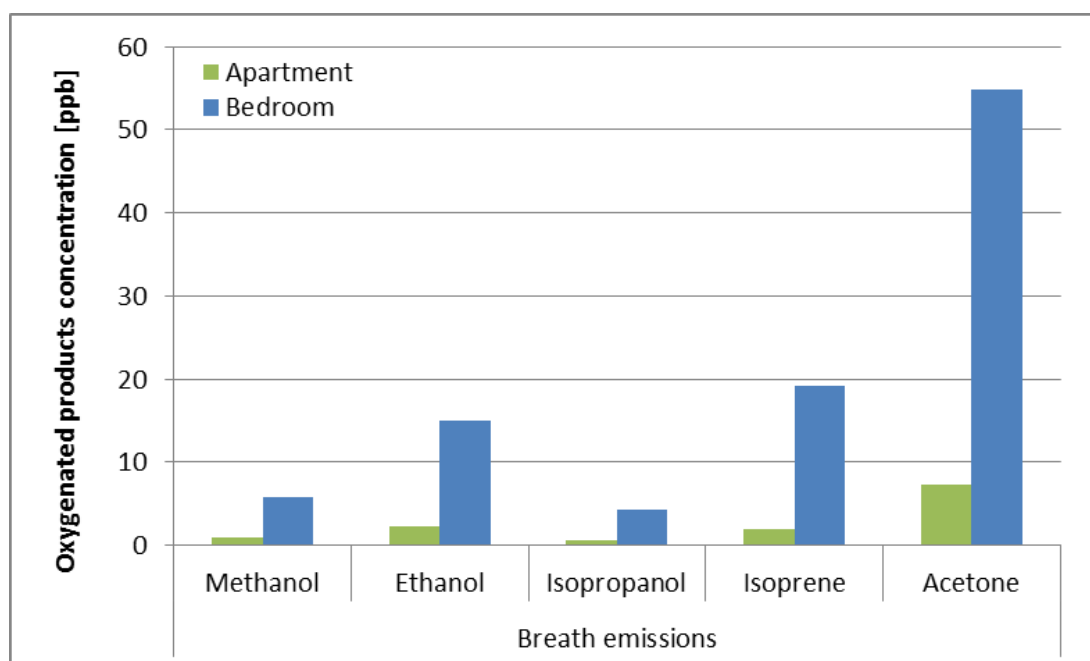**Figure 45:** Concentration of oxygenated products following breath emissions [ppb] in the apartment and in the bedroom when typical summer conditions occur in Milan (air exchange rate = 0.76 h^{-1}) for night time hours (23:00-07:00 h).

Not surprisingly, human emissions are more significant when the volume of the room is smaller. Hence, the concentration of 4-OPA following ozone-derived skin emissions in

the apartment was ~ 0.16 ppb compared to 0.73 ppb in the bedroom. For acetone, the concentration in the apartment is ~0.4 ppb and in the bedroom ~1.9 ppb from skin emissions. A similar conclusion can be drawn from the breath emission analysis. Much higher concentrations of the compounds emitted from breath are noticed in the bedroom scenario rather than in the apartment. For instance, the isoprene concentration increases from ~2.0 ppb in the apartment to 19.2 ppb for the bedroom.

The total concentrations of the compounds characteristic for breath and skin emissions during nighttime hours modelled for the bedroom in Milan during typical summer conditions are shown in Figure 46 and 47 respectively. The range of the concentrations takes into consideration surface emissions, including humans, and exchange with outdoors. Higher concentrations of methanol, ethanol, isopropanol, isoprene and acetone occur in the bedroom when AER is 0.2 h^{-1} and lower values when AER is 2.0 h^{-1}. However, the concentrations of nonanal, decanal, 4-OPA, formic and acetic acids are higher when AER is 2.0 h^{-1} and lower when AER is 0.2 h^{-1}. Again, the compounds presented in Figure 46 are the typical ones dominated by breath emissions. Therefore, higher concentrations occur when the air exchange rate is lower. The compounds presented in Figure 47 are formed following ozone-surface interactions. Nonanal and decanal are formed following material and skin surface emissions; however 4-OPA and carboxylic acids are dominated by skin surface emissions following ozone deposition. Thus, higher concentrations of these oxygenated products occur when the air exchange is higher and more ozone is available indoors. In general, ventilation rate plays an important role on indoor air chemistry and the total VOC concentrations in crowded or relatively small indoor spaces like in a bedroom.
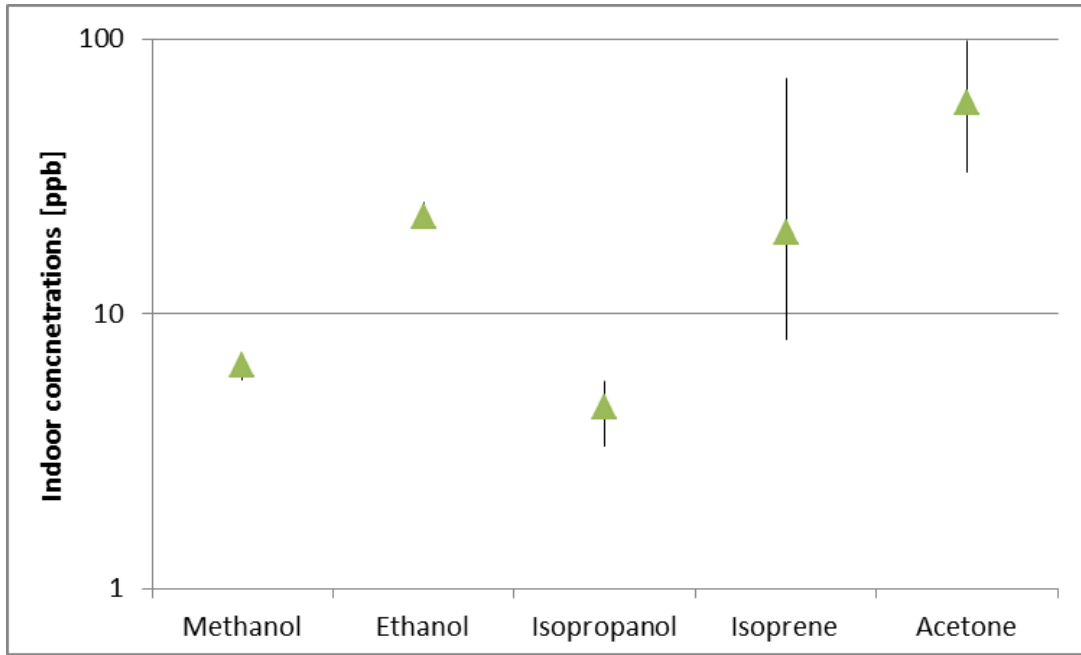
Figure 46: Indoor concentration of selected oxygenated products [ppb] modelled for the bedroom in Milan during typical summer conditions for night time hours (23:00-07:00 h). The range of the values represents the range of air exchange rates (0.2 h^{-1}; 0.76 h^{-1} and 2.0 h^{-1}). Triangles denote the concentrations when AER is 0.76 h^{-1}.
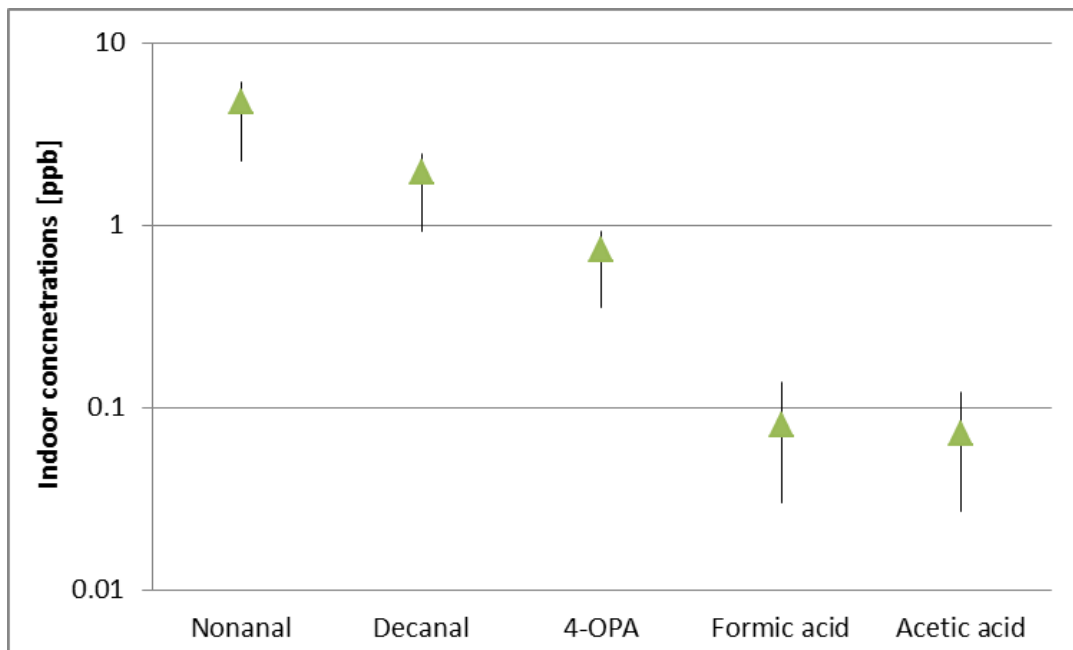
Figure 47: Indoor concentration of selected oxygenated products [ppb] modelled for the bedroom in Milan during typical summer conditions for night time hours (23:00-07:00 h). The range of the values represents the range of air exchange rates (0.2 h^{-1}; 0.76 h^{-1} and 2.0 h^{-1}). Triangles denote the concentrations when AER is 0.76 h^{-1}.

The predictions of the model are at the higher end of the results presented by Järnström et al. (2006) who measured mean annual concentrations of approximately 1.2 ppb and 0.8 ppb of nonanal and decanal respectively, in bedrooms of 12-month old Finnish homes with a mean AER of 0.9 per hour, though there is no information about the bedroom size.

Figure 48 shows the diurnal profiles of ozone, nonanal, decanal and 4-OPA concentrations in the bedroom in Milan when typical summer conditions occur (AER=0.76 h^{-1}). Nonanal and decanal concentrations originate both from skin and internal materials (i.e. soft furniture and painted wall) emissions. 4-OPA is only emitted from human skin. Clearly, there is dependence between the ozone concentration and the ozone-derived surface emissions. Following the increase of ozone concentration, the carbonyl concentrations increase.
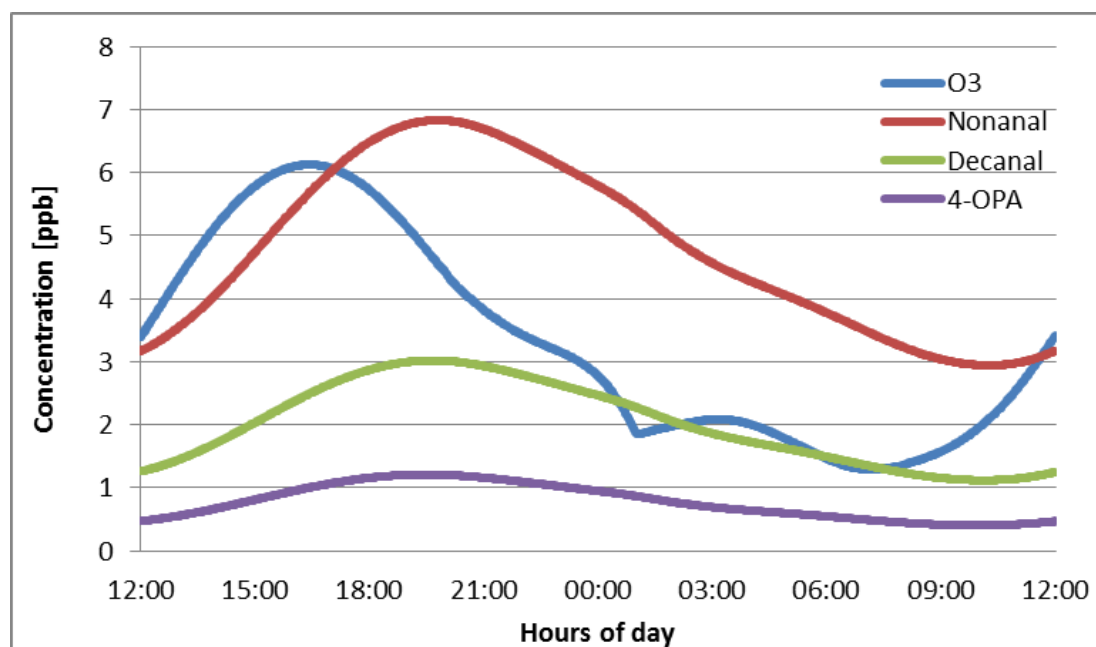
Figure 48: Hourly profile for O_3, nonanal, decanal and 4-OPA concentration modelled for the bedroom in Milan during typical summer time; AER = 0.76 h^{-1}.

Concentrations of oxygenated products formed following skin emissions increase when the air exchange rate and indoor ozone concentrations are higher. However VOCs emitted from breath originate as metabolic products and are not related to ozone concentration indoors. Therefore their concentration levels decrease in a room with higher ventilation. Figure 49 and 50 illustrate the VOC concentrations following skin and breath emissions respectively in the apartment located in Milan during typical summer time conditions when ventilation conditions vary (AER = 0.2; 0.76 and 2.0 h^{-1}).
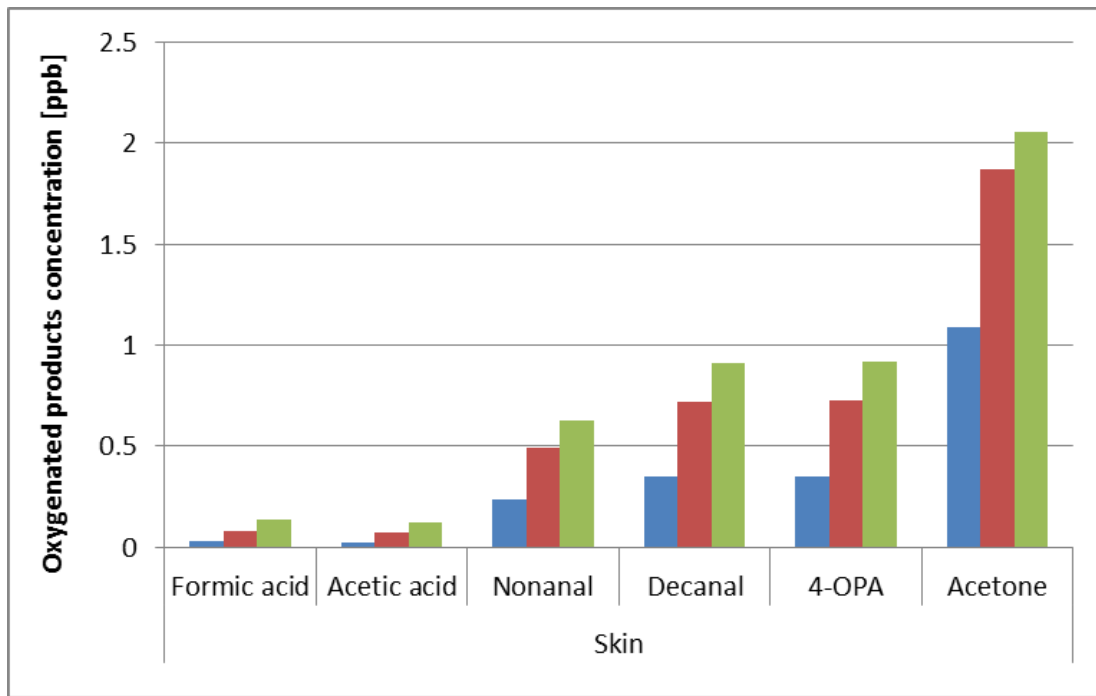
Figure 49: Concentration of oxygenated products following human skin emissions [ppb] in a bedroom when different ventilation conditions occur in the bedroom in Milan during typical summer conditions for night time hours (23:00-07:00 h). Blue bars depict concentrations of the products when air exchange rate is 0.2 h^{-1}, red bars 0.76 h^{-1} and green bars 2.0 h^{-1}.
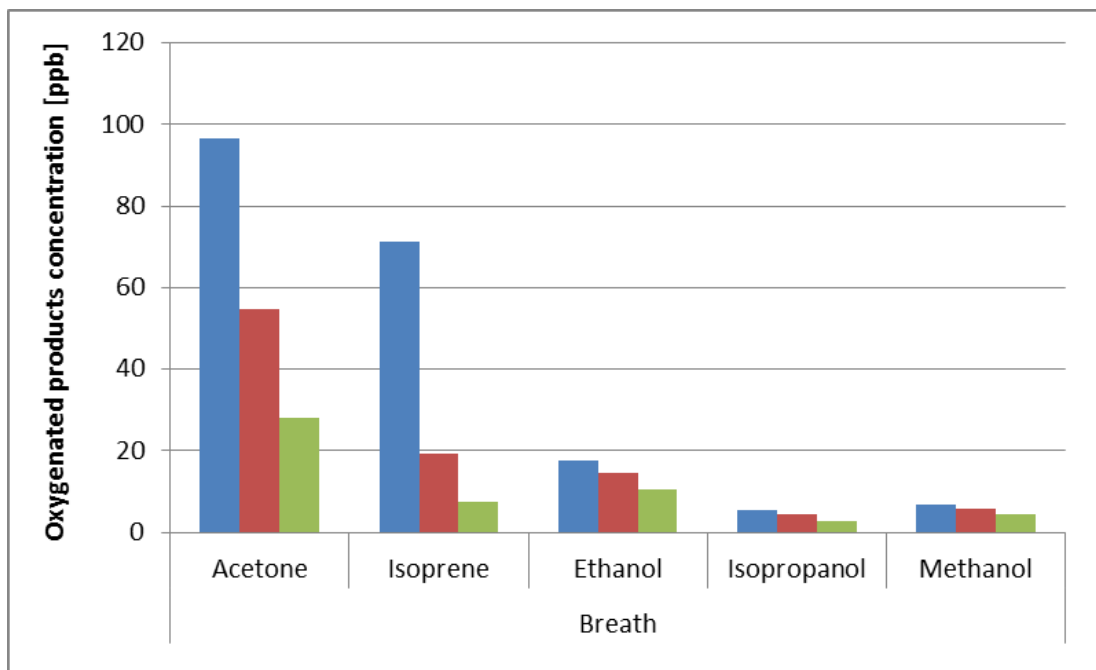
Figure 50: Concentration of oxygenated products following human and breath emissions [ppb] in a bedroom when different ventilation conditions occur in the bedroom in Milan during typical summer conditions for night time hours (23:00-07:00 h). Blue bars depict concentrations of the products when air exchange rate is 0.2 h^{-1}, red bars 0.76 h^{-1} and green bars 2.0 h^{-1}. Note that acetone was calculated separately for skin (Fig. 49) and breath (Fig. 50).

Figure 51 compares the differences in modelled oxygenated products concentrations following skin emissions in the bedroom, for Milan (during typical and heatwave summer) and Seoul during typical summer time conditions and for an air exchange rate of 0.76 h^{-1}. The concentrations of oxygenated products are lower for the bedroom in the Seoul apartment compared to Milan, owing to the lower ozone concentration indoors and therefore proportionally lower surface emissions. The concentration of the oxygenated products did not show a difference between the bedroom located in Milan during typical and summer heatwave conditions, since nighttime ozone concentration is similar (24.6 and 21.5 ppb respectively).
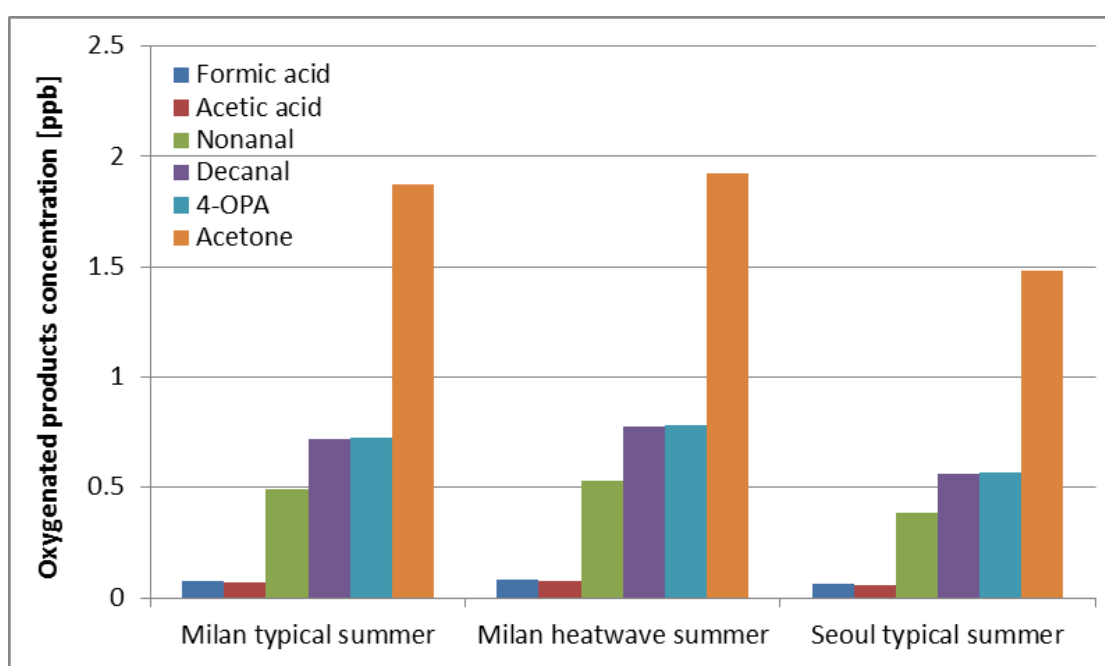
Figure 51: Concentration of oxygenated products following human skin emissions [ppb] in the bedroom placed in different locations, namely in Milan during typical and heatwave summer conditions, and in Seoul during typical summer conditions (air exchange rate = 0.76 h^{-1}) for night time hours (23:00-07:00 h).

5.5.2.2 Impacts of human occupancy on chemical processing in the bedroom

In order to evaluate the impact of occupancy on the chemical processing in the bedroom, a rate of production analysis was performed for night time hours (23:00-07:00), for typical summer conditions in Milan and for an AER of 0.76 h^{-1}.

Figure 52 presents the production rates for (i) ozone deposition and ozone-driven aldehyde surface production (no occupants) and (ii) ozone-driven surface production

130

including occupants (in units of 10^3 molecule cm^{-3} s^{-1}). The modeled steady-state concentrations of OH, HO_2 and RO_2 for a model run with ozone deposition and internal surface emissions only were 8.9 x 10^4 molecule cm^{-3}, and 0.4 and 0.9 ppt respectively. When the human emissions were included, the concentrations were 6.5 x 10^4 molecule cm^{-3} and 0.8 and 1.2 ppt respectively.

Not surprisingly, the production of the radicals via photolysis reactions is negligible at night time. In terms of radical propagation, concentrations of OH decrease leading to a lower production rate of acetyl peroxy radicals via reaction with aldehydes, alkenes, alkanes and dicarbonyls. Again, the 'O$_3$+MTs' production rate increases when the occupants are present given the increased isoprene emissions derived from breath. RO_2 is distributed more towards organic nitrates and therefore less PANs might be formed, although formation of PANs still dominates overall termination. This is because there are fewer aldehydes formed when occupants are present in the bedroom compared to when they are absent (emissions from furnishing are more important), but also, the OH concentration is lower compared to the unoccupied bedroom.
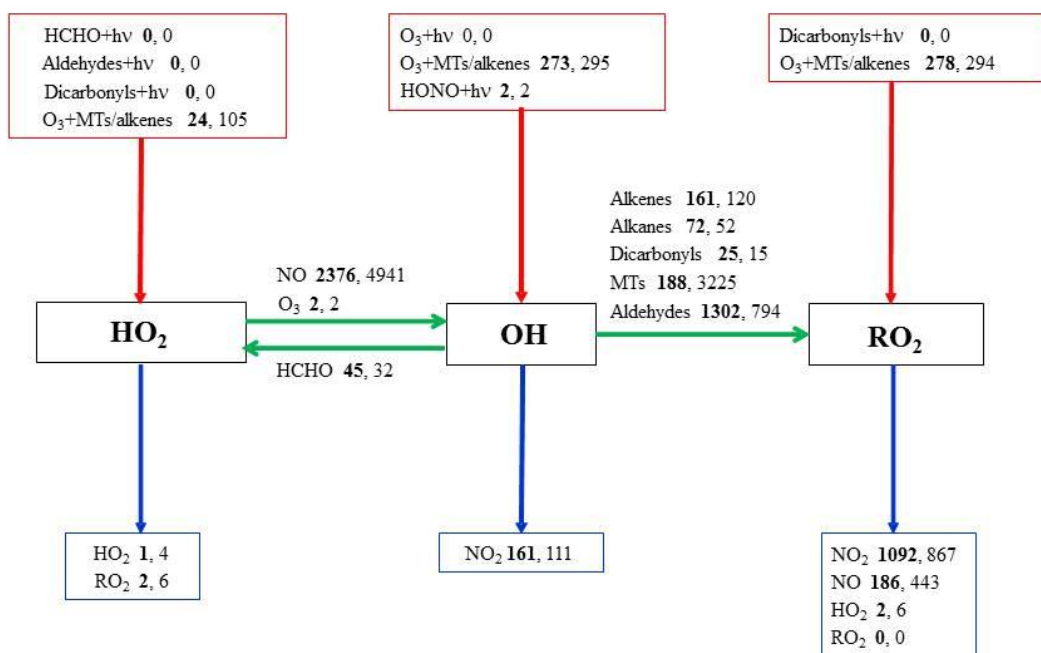
Figure 52: Simplified rate of production analysis for the major rates of reaction for a model run with ozone deposition followed by ozone-driven aldehyde surface production (no occupants) (figures in bold) and with ozone deposition followed by ozone-driven surface production including from human emissions (figures in normal font) in units of 10^3 molecule cm^{-3} s^{-1}. The model runs were performed for a bedroom in Milan during nighttime (23:00-07:00h) in typical summer conditions (AER = 0.76 h^{-1}). MT denotes monoterpenes including isoprene. Red arrows denote radical initiation processes, blue arrows are termination processes with green arrows representing radical propagation.

5.5.3 The classroom case study

5.5.3.1 Skin emissions

This section presents the modelling results from classrooms (defined in the Methodology section, earlier in this Chapter). The indoor air quality for a naturally ventilated occupied classroom during school-day hours (09:00-15:00h) with an hour break (12:00-13:00h) was investigated. It was assumed that 30 children and one teacher were present in the classroom. The results for different air exchange rates and for the three study locations/conditions are now discussed.

Figure 53 presents the diurnal profile of the concentrations of ozone and ozone-derived oxygenated products following skin emissions from the classroom occupants for Milan during a typical summer and with natural ventilation (AER 1.2 h^{-1}).
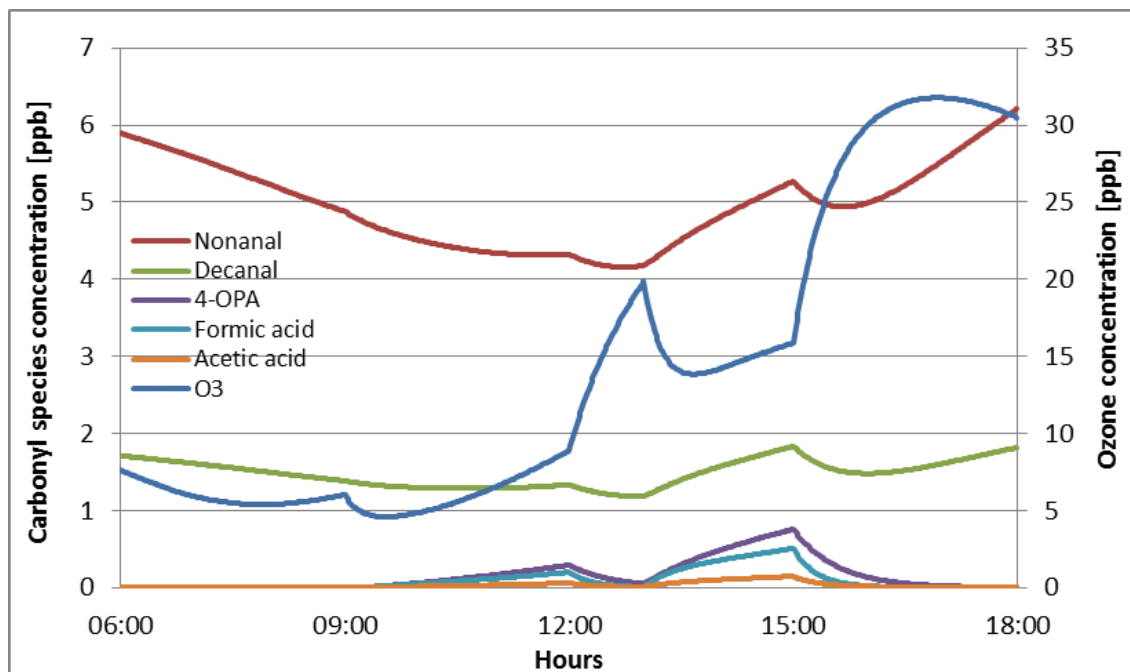
Figure 53: Diurnal profile of the concentration of ozone and carbonyl species following human skin emissions [ppb] in the classroom placed in Milan during typical summer conditions was applied (air exchange rate = 1.2 h^{-1}). All profiles include emissions from other internal surfaces where appropriate (i.e. nonanal and decanal) and exchange with outdoors.

As expected, skin emission products increase when occupants are in the classroom. Nevertheless carboxylic acids and 4-OPA are still at relatively low concentrations (up to ~0.1-0.5 ppb and 0.8 ppb respectively) when pupils are in the classroom. Nonanal and decanal show higher concentrations (on average up to 5.3 and 1.8 ppb respectively) with occupants, however, material emissions tend to dominate for these species: the profiles include emissions from internal surfaces (wooden materials, painted wall and linoleum), as well as contributions from outdoors.

There is substantial variation of the ozone concentration in the classroom. There is a significant increase of the O_3 concentration when the pupils are out for the lunch break (an increase of ~10 ppb). When the occupants return to the classroom after the break, the ozone concentration decreases from 20 to ~14 ppb. When the school day finishes at 3 p.m. there is again a significant increase of the ozone concentration in the classroom (up to 32 ppb by 5 p.m.), as ozone rich air from outdoors replenishes the supply indoors.

The model shows relatively good agreement with the results presented in the literature. Comparing the data presented in the literature for measurements carried out in Europe during summer, Blondeau et al. (2005) reported the mean ozone concentration measured in eight French schools in summer as ~5.8 ppb (with the median up to 9 ppb). Comparable median results of 2.3 ppb (with the range of 1.5-15.6 ppb) and 7.6 ppb (with the range of 2.5-19 ppb) were presented in the HESE (2006) study for 8 classrooms in Siena and in 7 classrooms in Udine (Italy) respectively. The modelling results show an ozone concentration in the range of ~5-16 ppb when the occupants are present in the classroom.

Model runs were also performed for the classroom in Milan during summer heatwave conditions and in Seoul during typical summer conditions (Figure 54 and 55 respectively). Air exchange rate (1.2 h^{-1}) and ventilation type (natural) were kept the same for all the case studies.
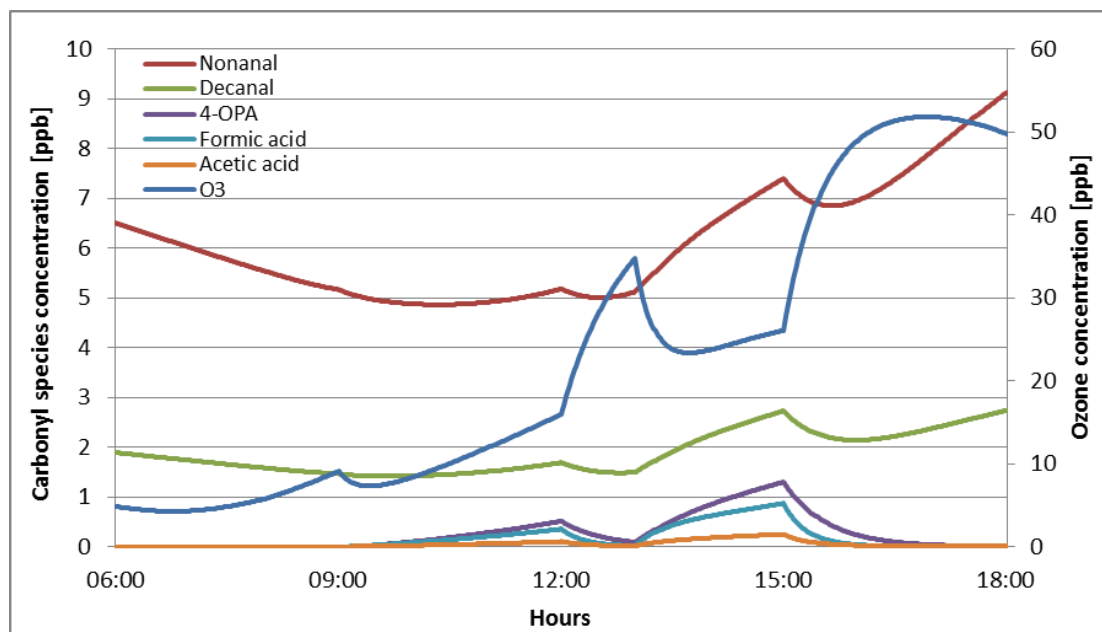
Figure 54: Diurnal profile of the modelled concentration of ozone and carbonyl species for the classroom in Milan during summer heatwave conditions; natural ventilation parameters were applied (air exchange rate = 1.2 h^{-1}). 30 children and a teacher stay in the classroom from 9:00-15:00 h with an hour lunch-break (12:00-13:00 h).
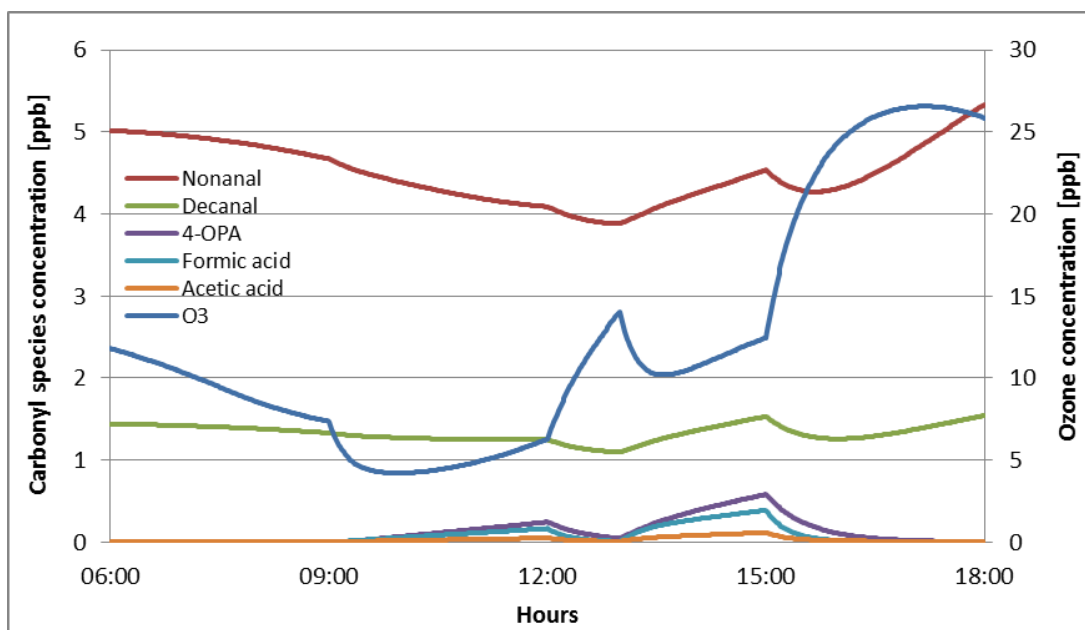
Figure 55: Diurnal profile of the modelled concentration of ozone and carbonyl species for the classroom in Seoul in typical summer time conditions; natural ventilation parameters were applied (air exchange rate = 1.2 h^{-1}). 30 children and a teacher stay in the classroom from 9:00-15:00h with an hour lunch-break (12:00-13:00 h).

Undoubtedly, ozone-derived skin emissions depend on the ozone concentration indoors. Comparing different locations and therefore different ozone concentration indoors, higher indoor ozone concentrations indoors cause an increase in secondary pollutant formation from skin. Therefore the highest concentrations of ozone-derived skin emission species are noted in Milan during summer heatwave conditions.

5.5.3.2 Breath emissions

Figure 56 shows the diurnal profile of modelled VOCs following breath emissions in the classroom in Milan during typical summer conditions with natural ventilation (air exchange rate = 1.2 h^{-1}). Again, the concentrations increase when the occupants enter the classroom at 9:00 a.m., then decrease when children leave the classroom for an hour lunch break. Then, the increase can again be noted at 1 p.m. until 3 p.m. when pupils leave the classroom.

Acetone shows the most significant variation in the concentration profile when the occupants are in and out of the classroom. Thus the acetone concentration increases from ~3 ppb before the children enter the classroom up to ~22 ppb. Note that the acetone

concentration profile in Figure 56 includes skin and breath emissions together, and breath emissions contribute ~90% to the total. The concentration of methanol and ethanol, increases from ~2 - 7 ppb and from ~16 - 21 ppb respectively when pupils are present.

Figure 56: Diurnal profile of the concentration of VOCs following breath emissions [ppb] in the classroom in Milan during typical summer conditions and with natural ventilation (average air exchange rate = 1.2 h^{-1}). Note that acetone originates from both skin and breath emissions. All profiles include emissions from other internal surfaces and outdoors.

Since breath emissions are not ozone-derived products, there is a strong negative relationship between the air exchange rate and VOC concentrations following breath emissions. There is a substantial difference in diurnal profiles of VOCs emitted from the breath between a poorly ventilated classroom (air exchange rate = 0.6 h^{-1}) (Figure 57) and a highly ventilated classroom (air exchange rate = 1.8 h^{-1}) (Figure 58) when the occupants are present. For example, with better ventilation of the classroom, the concentration of acetone decreases from ~30 to 18 ppb. Isoprene decreases from ~5 to 2 ppb, and methanol from ~7.5 to 6 ppb when the AER increases to 1.8 h^{-1}.

Surprisingly, the reverse trend can be noted for ethanol. The concentration of ethanol, which is one of the alcohols emitted from breath, increases from ~18 to 23 ppb when the AER increases to 1.8 h^{-1}. Under the model conditions and outdoor concentration of ~33 ppb, the deposition rate of ethanol is calculated as 1.3 x 10^8 molecule cm^{-3} s^{-1}, loss due to air exchange is calculated as 4.3 x 10^8 molecule cm^{-3} s^{-1} but the human breath emission rate is

1.1 x 10^8 molecule cm^{-3} s^{-1}. Therefore, deposition and exchange with outdoors are more important than breath emissions under these conditions and control the profile.

Figure 57: Diurnal profile of the concertation of VOCs following breath emissions [ppb] in the classroom placed in Milan during typical summer conditions when natural ventilation was applied and air exchange rate was 0.6 h^{-1}. Note that acetone originates from both skin and breath emissions. All profiles include emissions from other internal surfaces and outdoors.
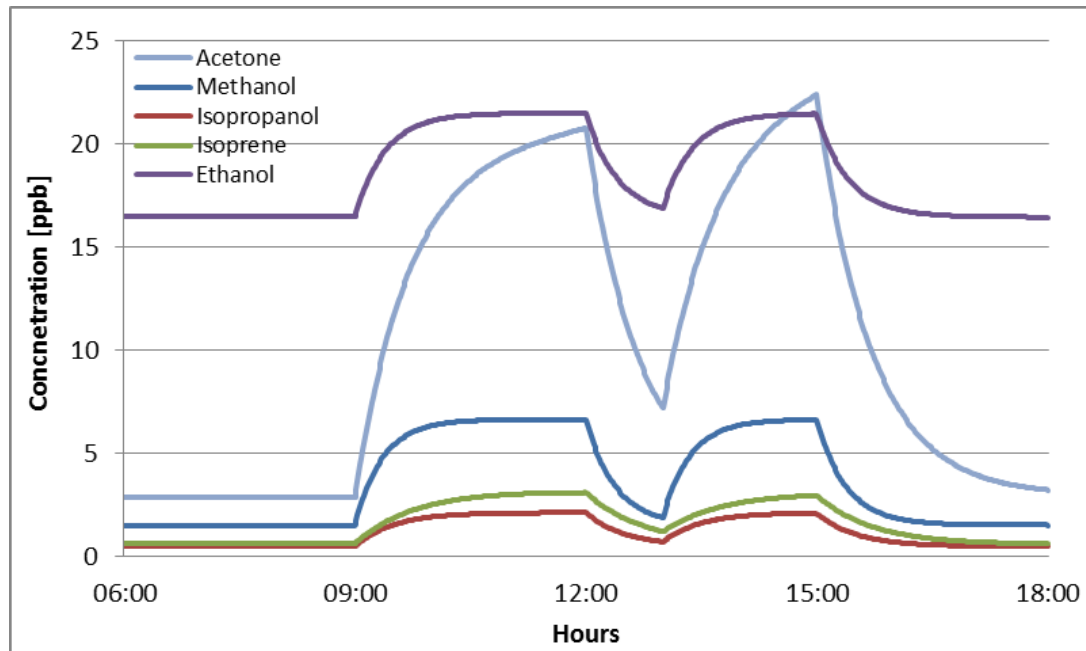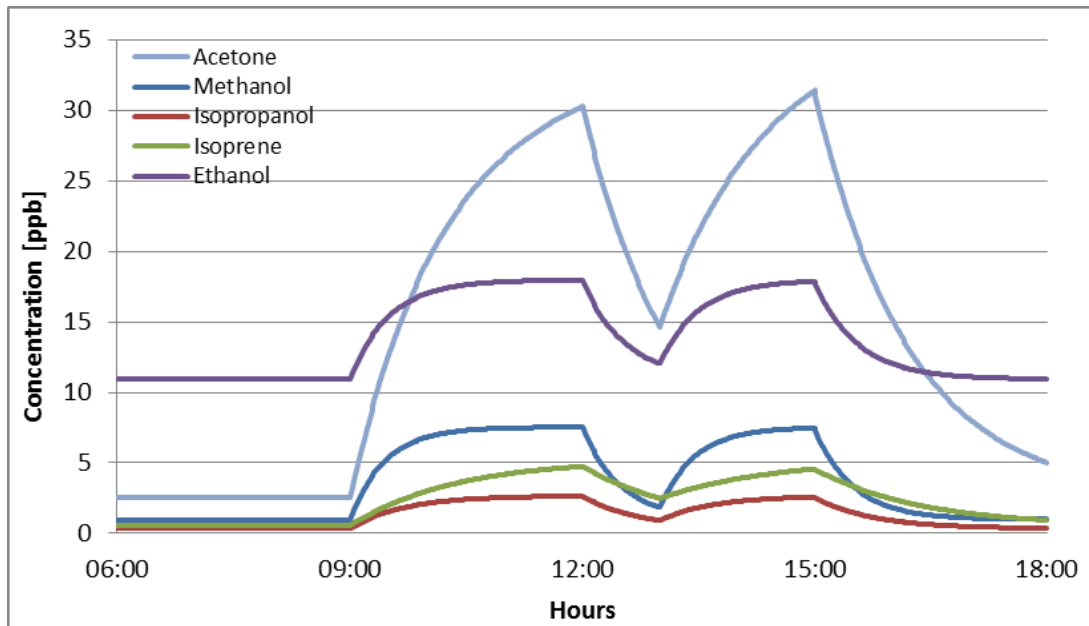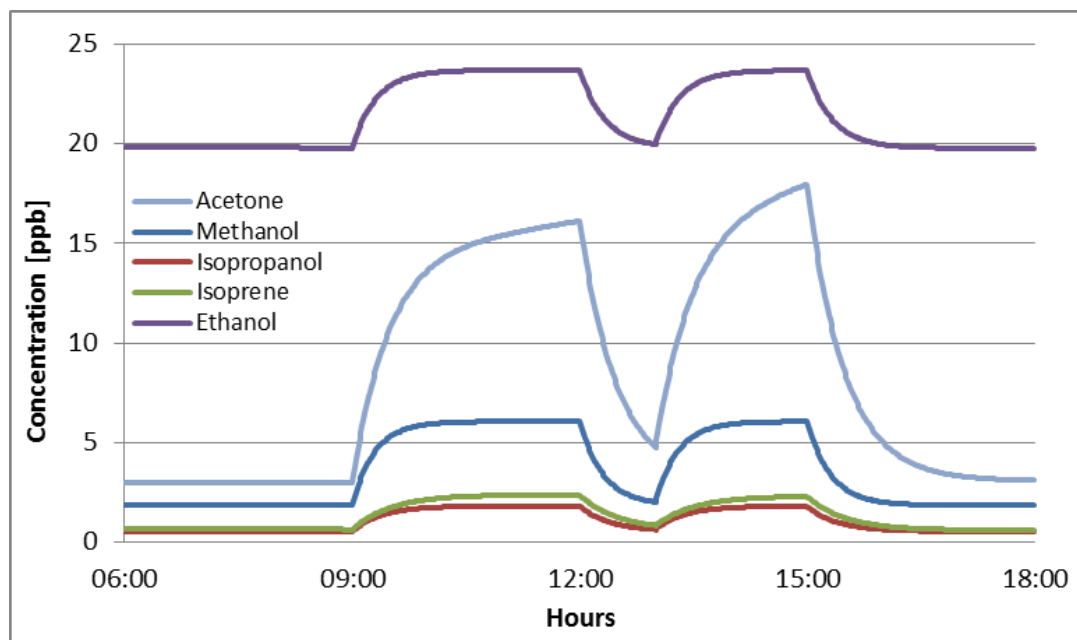

Figure 58: Diurnal profile of the concertation of VOCs following breath emissions [ppb] in the classroom placed in Milan during typical summer conditions when natural ventilation was applied and air exchange rate was 1.8 h^{-1}. Note that acetone originates from both skin and breath emissions. All profiles include emissions from other internal surfaces and outdoors.

137

The predicted values were compared with the few concentrations available in the literature. For instance, the model results show good agreement with the concentrations of carboxylic acids measured in a university classroom presented by Liu et al. (2017). The measured concentration of formic acid was in the range of 0.2-3.5 ppb, whereas the predicted average concentration from the model was 0.2 ppb.

Tang et al. (2016) measured indoor air mixing ratios of selected VOCs in a University classroom and also emission rates. The measurements were conducted over a two-week period on five weekdays (during 08:00-20:45h) when at least 17 adult occupants were present in the classroom. The volume of the classroom was 670 m^3 and air exchange rate with the use of mechanical ventilation was 5 ± 0.5 h^{-1}. The study considered the time-series measurements of VOCs, CO_2 and O_3, sampling the classroom and supply air six times per hour. The measured mixing ratios of isoprene, acetone and 4-OPA were ~1-2 ppb, ~10-13 ppb and ~0.4 ppb respectively. The indoor concentrations predicted by the model (when 30 children and 1 adult were present in the classroom in Milan during typical summer time conditions within 09:00-17:00h, AER = 1.2 h^{-1}) were ~2.5 ppb for isoprene, ~17 ppb for acetone and 0.3 ppb for 4-OPA. The two sets of results are not directly comparable as the classroom used in the study of Tang et al. (2016) was bigger than the one used for the modelling runs (171 m^3). Moreover, the air exchange rate of the experimental classroom was much higher than of the modelled one. Finally, the university classroom and its occupants were adults not children.

Recently, Stönner et al. (2017) measured emission rates in a cinema. The measurements were carried out over a month when three different movies were screened. The audience varied from 50-230 people (in total for adults and children) for various screenings of three movies. The volume of the screening room was 1300 m^3 and the room was constantly flushed with the outdoor air at a rate constant of 6500 m^3 h^{-1}. The measurements were made with the use of a steel ventilation channel, which transported the exhaust airstream from the cinema room to a separate room, where the measurement instruments (mass spectrometer and CO_2 analyzer) were placed. A comparison of the selected measured VOC emission rates in these two studies is presented in Table 22 and shows that there is some variation between the two studies and also the current study.

Table 22: Comparison of emission rates of selected VOCs for adults derived from this study and the studies of Tang et al. (2016) and Stönner et al. (2017).

VOC compound	This study ($\mu g\ h^{-1}\ p^{-1}$)	Tang et al. (2016) ($\mu g\ h^{-1}\ p^{-1}$)	Stönner et al. (2017) ($\mu g\ h^{-1}\ p^{-1}$)
Acetone	9	2796	419
Methanol	17	356	650
Isoprene	2	164	166
Ethanol	6	426	216

The emission rates used in the model are much lower than those presented by both Tang et al. (2016) and Stönner et al. (2017). According to the measurements, the total emissions could be approximately 50-100 times higher than those used to drive the model, mainly as those input into the model only included breath and skin emissions. The measurements were carried out in highly occupied places, but also included contributions from food (i.e. popcorn in a cinema) or personal care product emissions. In fact, in the University classroom study, there was a clear decline in emissions over the course of the day, as the personal care products worn by the students gradually degassed from their bodies (Tang et al., 2016).

To test the sensitivity of the model to higher emissions rates from occupants, the emissions from both skin and breath were increased by 10%, 50% and 100%. The results from the sensitivity analysis are shown in Table 23.

Table 23: Sensitivity test results: the % change in concentrations of carbonyl species following skin and breath emissions in the naturally ventilated classroom in Milan for typical summer conditions relative to baseline conditions (AER=1.2 h^{-1}) during school hours when the occupants were present.

Scenario	Nonanal	Decanal	4-OPA	Formic acid	Acetic acid	Acetone	Methanol	Ethanol	Isopropanol	Isoprene
Human emissions * 10%	0.5	1.1	7.7	7.6	7.1	8.2	7.6	2.5	7.5	7.6
Human emissions * 50%	2.4	5.2	35.1	34.6	32.4	40.6	38.1	12.7	37.7	38.1
Human emissions * 100%	4.4	9.4	63.6	62.5	58.6	80.9	76.2	25.3	75.5	76.3

The increase in human emissions enhances oxygenated products concentrations indoors. The model shows the highest sensitivity for species that are mainly derived from occupants, whilst those that are dominated by material emissions (nonanal, decanal) or outdoors (ethanol) are less sensitive to changes.

5.5.3.3 Impact of human occupancy on chemical processing in the classroom

In order to understand the impact on chemistry in a highly occupied indoor environment, an analysis of oxidant concentrations was carried out for a classroom in Milan during typical and heatwave summertime conditions and in Seoul during typical summer time for a range of air exchange rates (0.6; 1.2; 1.8 h^{-1}).

Table 24 presents a comparison of oxidant concentrations for the same hours of the unoccupied and occupied classroom during school day hours. The unoccupied classroom was just a furnished classroom without the occupants and modelling results are shown for the same hours as for the occupied classroom. As expected, the modelled steady-state

concentrations of O_3, OH, HO_2 and RO_2 for model runs with internal surface emissions only (no occupants in the classroom) were higher compared with the concentrations when occupants were present in the classroom. Weschler (2016) suggested that the presence of humans in a building would decrease the net level of oxidants, as ozone is deposited onto skin. However, these results also confirm that the OH, HO_2 and RO_2 radical concentrations decrease as more ozone-driven surface emissions (human skin) are included in the model. For instance, considering the classroom scenario in Milan during typical summertime conditions (air exchange rate = 1.2 h^{-1}), the concentration of O_3 decreases by about 40% and OH, HO_2, RO_2 by about 16%, 32% and 44% respectively when oxidative production of carbonyls on skin surfaces is included compared to when they are excluded (for the same ventilation conditions).

Table 24: Comparison of oxidants' concentrations when occupants are in and out of a classroom placed in Milan (during typical and extreme summer conditions) and Seoul (during typical summer conditions) when natural ventilation and different air exchange rates (0.6; 1.2; 1.8 h^{-1}) were applied. Note that concentrations were modelled for the hours when pupils are usually in the classroom (9:00-15:00 h) with an hour break (12:00-13:00 h). Ozone concentrations are given in ppb, OH in units of 10^5 molecule cm^{-3}, both HO_2 and RO_2 in ppt.

		Milan typical summer conditions			Milan extreme summer conditions			Seoul typical summer conditions		
		AER (h^{-1})			AER (h^{-1})			AER (h^{-1})		
		0.6	1.2	1.8	0.6	1.2	1.8	0.6	1.2	1.8
O_3	No occupants	12.4	15.9	18.3	20.3	27.8	33.2	9.9	12.4	14.0
	Occupants	6.6	9.6	11.9	10.7	16.4	20.6	5.3	7.5	9.1
OH	No occupants	4.0	4.5	4.7	4.4	5.0	5.2	3.7	4.1	4.2
	Occupants	3.2	3.8	4.0	3.6	4.2	4.5	2.9	3.4	3.6
HO_2	No occupants	5.4	3.4	2.8	7.3	5.1	4.3	5.4	3.1	2.4
	Occupants	3.6	2.3	1.9	5.1	3.6	3.1	3.5	2.1	1.7
RO_2	No occupants	10.6	6.1	4.7	16.3	10.5	8.6	9.5	5.0	3.8
	Occupants	5.6	3.4	2.8	8.4	5.6	4.8	5.1	2.9	2.4

The higher the air exchange rate is, the higher the concentration of O_3 is indoors. The concentrations of NO_2 and NO are also higher at higher AERs. The OH radical concentration increases along with the higher air exchange rate, as more OH can be formed through ozone oxidation of terpenes. However, the concentrations of HO_2 and RO_2 are suppressed by higher NO_X concentrations indoors as the AER increases. Therefore, the concentrations of HO_2 and RO_2 decrease, while those of ozone and OH radicals increase with AER.

Figure 59 presents the production rates for (i) indoor emissions when the classroom was occupied in Milan during typical summer conditions and for (ii) indoor emissions when the classroom was occupied in Milan during summer heatwave conditions (in units of 10^4 molecule cm^{-3} s^{-1}). The results are shown for the conditions of AER = 1.2 h^{-1}. The emission rates increase when photolysis and outdoor O_3 concentration is higher, which is the case during heatwave summer time conditions. Furthermore, during the summer heatwave period, NO_x concentrations are also higher. Therefore, the propagation and termination reactions involving NO and NO_2 are enhanced. For instance, following the RO_2 reaction with NO_2 more PANs, as the termination product are formed during the heatwave conditions.

HCHO+hν **21**, 21
Aldehydes+hν **22**, 26
Dicarbonyls+hν **91**, 176
O$_3$+MTs/alkenes **18**, 29

O$_3$+hν **4**, 7
O$_3$+MTs/alkenes **129**, 196
HONO+hν **104**, 129

Dicarbonyls+hν **39**, 40
O$_3$+MTs/alkenes **129**, 196

Alkenes **108**, 115
Alkanes **43**, 48
Dicarbonyls **23**, 34
MTs **273**, 301
Aldehydes **581**, 738

NO **1864**, 1976
O$_3$ **4**, 9

HCHO **44**, 50

HO$_2$ **OH**   **RO$_2$**

HO$_2$ **5**, 11
RO$_2$ **5**, 12

NO$_2$ **161**, 228

NO$_2$ **604**, 966
NO **93**, 95
HO$_2$ **5**, 12
RO$_2$ **0**, 1
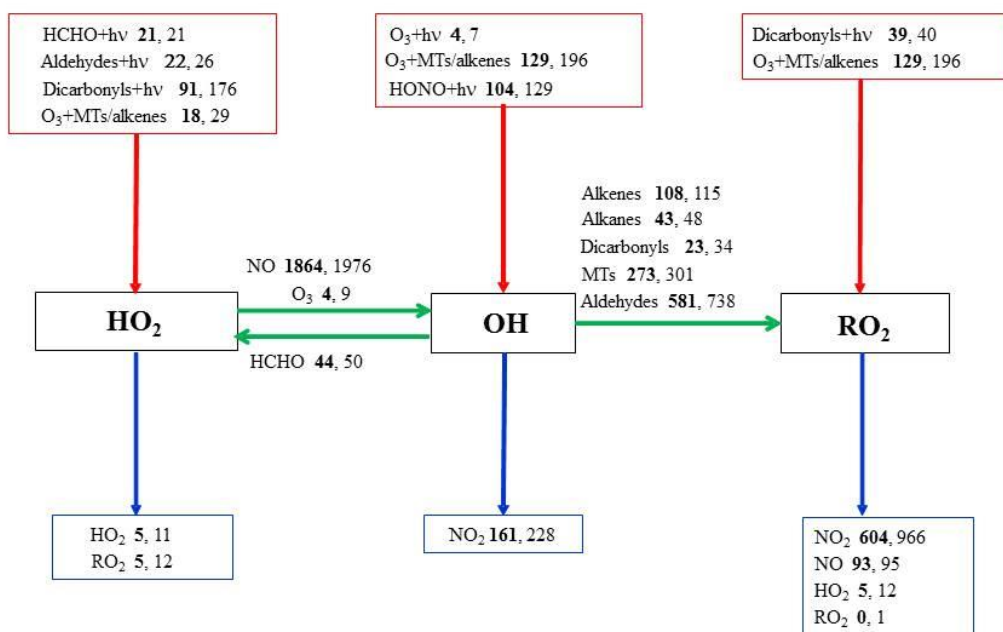
Figure 59: Simplified rate of production analysis for the major rates of reaction for a model run with ozone deposition followed by ozone-driven aldehyde surface production and breath emissions (with presence of the occupants) in Milan classroom scenario during typical summer conditions (figures in bold) and with ozone deposition followed by ozone-driven surface production including the human emissions in the classroom in Milan during heatwave summer conditions (figures in normal font) in units of 10^4 molecule cm^{-3} s^{-1}. The model runs were performed for a classroom when AER = 1.2 h^{-1}). MT denotes monoterpene. Red arrows denote radical initiation processes, blue arrows are termination processes with green arrows representing radical propagation.

5.6 Chapter summary

This Chapter has examined the role of human occupancy and the changes in indoor air chemistry when occupants are present. It quantifies the impact of human skin and breath emissions on oxidant levels and also the concentrations of various secondary pollutants that are formed. Among all the tested surfaces, the human body was shown to be the most efficient in terms of removing ozone from indoor air per square meter. However, when internal ozone-driven emissions of aldehydes are considered, soft furniture and painted walls become more important owing to their larger surface areas in a typical building. Ozone-initiated emissions from the human body can be important in smaller areas of a house (e.g. a bedroom at nighttime), when concentrations of various oxygenated products can become

significant. An important conclusion from this study is that inclusion of oxidation-derived surface emissions (from surfaces and/or people) within a detailed chemical model profoundly affects chemical processing. Ozone-driven surface emissions deplete oxidants, increase the importance of radical production from aldehyde photolysis indoors and shift formation of products towards nitrated organic carbon species.

The modelling results of human emissions indoors show that the emissions depend on the air exchange rate, size of the indoor space and indoor occupancy. When the air exchange rate is smaller, the impact of breath emissions is higher, but those from skin become less important. Skin emissions are ozone dependent. When the air exchange rate is smaller, there is less ozone indoors and so there is less potential for surface interactions and consequent formation of secondary pollutants from skin. Furthermore, the impact of human emissions indoors is subject to the size of indoor space. In general, the bigger the indoor space is, the lower the resulting concentrations of the compounds emitted from humans are. However, it is strongly dependent on the indoor occupancy. Finally, highly occupied indoor environments, such as classrooms or cinemas, might show relatively high concentrations of species derived from human emissions indoors.

6. Secondary pollutant formation following cleaning activities indoors

6.1 Chapter preview

The aim of this Chapter is to highlight the importance of cleaning on indoor air chemistry and in particular, the composition of mixtures on secondary product formation. First there is an explanation of the importance of such activity on chemical processes indoors including on the formation of secondary pollutants. The experimental procedures adopted are then described, for investigating both single compound oxidation processes, as well as of mixtures of compounds commonly used in cleaning products The results from some model simulations to further probe the experimental results are then detailed.

6.2 Introduction

There is evidence that cleaning indoors has a great impact on indoor air pollution (Wolkoff et al., 2000; Carslaw, 2013; Wolkoff, 2013). Cleaning products are used extensively in buildings, whether occupational or residential in use. Consumer cleaning products and air fresheners contain terpene hydrocarbons such as limonene, α-pinene, terpinolene, terpene alcohols and other unsaturated compounds. Such compounds, which often originate from plant oils, are widely used as active solvents and fragrance in air fresheners or cleaning products (Singer et al, 2006; Carslaw, 2013).

Reactions in the indoor environment between unsaturated VOCs such as these with reactive oxidants such as ozone, nitrate and hydroxyl radicals in the gas-phase or on indoor surfaces, can produce a wide range of intermediate and stable oxygenated secondary species (Jenkin et al., 1997; Walser et al., 2008). Such products include oxygenated organic species that contain carbonyl groups, such as aldehydes, ketones, carboxylic acids or di- and tricarbonyls and additionally, formaldehyde and acetaldehyde, hydrogen peroxide, SOA, peroxy and hydroxyl radicals (Fan et al. 2003; Forester and Wells, 2011; Ham et al. 2015; Ham et al., 2016; Nazaroff and Weschler, 2004). Indeed, there is evidence that these highly oxidized species are responsible for serious health effects including occupational asthma (Cartier 2015; Jarvis et al., 2005). Nazaroff and Weschler (2004) reported that cleaning products and air fresheners contain dermal and respiratory sensitizers and irritants, which can cause adverse health effects including skin and eye irritation and occupational asthma.

A large percentage of the general population is potentially at risk while cleaning their own homes (Medina-Ramon et al., 2005). Reilly and Rosenman (1995) showed in their study that the most frequent reason of hospital admission in the US for chemical related respiratory disease was from exposure to household cleaning products. However the highest risk of exposure is for professional cleaners. Epidemiological studies have shown the relationship of the various respiratory effects between cleaning work and asthma (Nazaroff and Weschler, 2004; Zock, 2005; Bello et al., 2009). Quirce and Barranco (2010) reviewed the available evidence and summarized that there is a substantially (30-50%) increased risk of asthma symptoms related to the weekly use of cleaning agent sprays and that the risk increases along with the number of products used for cleaning purpose, or with the frequency of use. In addition, respiratory health problems among 5000 surveyed cleaners in the UK were found to be higher than in other professions (Woods and Buckle, 2006).

Epidemiological studies have identified a need to pay special attention to the health effects of VOCs mixtures, which are widely used in cleaning consumer products (Wolkoff et al. 2000, 2013). There is evidence that irritative, unidentified compounds can be formed via ozonolysis reaction of terpene mixtures at concentrations typically observed in indoor air settings (Wolkoff et al. 2000; Fan et al., 2003). Reactions of VOC mixtures with ozone have been observed to produce short-lived, highly reactive species such as hydroxyl radicals and hydrogen peroxides, and more stable compounds for instance, ketones, aldehydes, organic acids, secondary aerosols and ultrafine particles (Fan et al., 2003; Fiedler et al., 2005).

Clearly, there is a need to study the oxidation products that are formed following cleaning activities and to evaluate the impact of mixtures of terpenes on indoor air chemistry. Additionally, it is important to use this understanding to aim to reduce the formation of harmful secondary pollutants and to remediate against their formation through such activities.

6.3 VOCs in consumer products

One of the main terpenes used in a large number of consumer products is limonene (1-methyl-4-(prop-1-en-2-yl)cyclohexene) (Figure 60). Household products (i.e. cleaning agents and air fresheners) contain limonene because of its orange/lemon-like fragrance and antimicrobial properties (Ham et al., 2016).
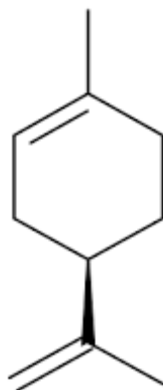
Figure 60: The chemical structure of limonene.

This cyclic terpene contains two double carbon-carbon bonds. The chemical structure makes limonene reactive with oxidants, to form a wide range of complex gas-phase reaction products (Wolkoff et al., 2012). Even when applying limonene to surfaces (e.g. through cleaning in bathrooms and kitchens), 7-70% of the compound can be emitted into the gas phase (Singer et al., 2006). The most important gas-phase products following cleaning activity are identified as carbonyl species, alcohols, peroxides and organic nitrates (Carslaw, 2013). Carslaw (2013) carried out a modelling study to determine the oxidation products of limonene following reaction with ozone and OH radical respectively (Figures 61 and 62). However, many of these products cannot be determined experimentally at present to confirm their predicted presence.

Figure 61: Major limonene gas phase ozonolysis routes. Species marked in grey are the major gas-phase products. Compounds marked in bold black are the key secondary aerosol species. The reaction rates are shown in units of 10^5 molecule cm^{-3} s^{-1} (Source: Carslaw, 2013).
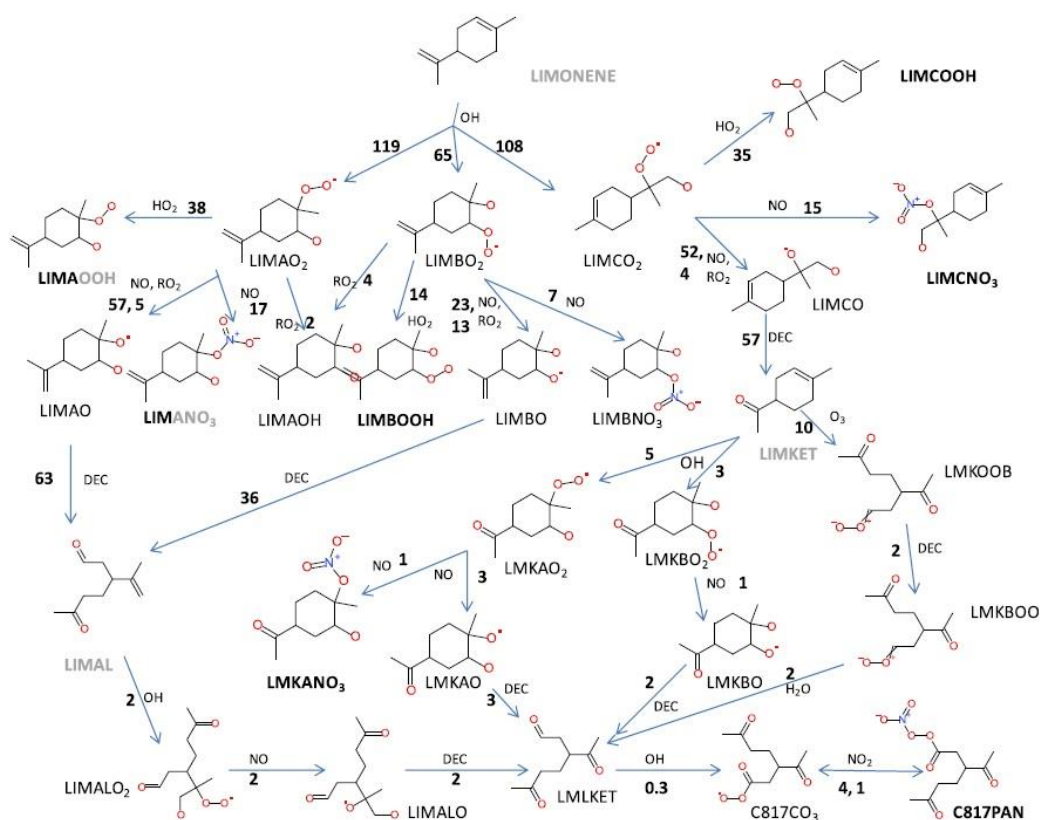
Figure 62: Major limonene gas-phase oxidation routes following a reaction with OH radical. Species marked in grey are the major gas-phase products. Compounds marked in bold black are the key secondary aerosol species. The reaction rates are shown in units of 10^5 molecule cm^{-3} s^{-1} (Source: Carslaw, 2013).

Similarly to limonene, α-pinene (Figure 63) is another common terpene frequently used in many consumer products. Alpha-pinene is a biogenic monoterpene and it can be detected from its pine scent (Rohr et al., 2003). Because of the fragrance, this monoterpene is widely used in numerous cleaning agents, detergents and air fresheners (Sarwar et al., 2004). For instance, Wallace et al. (1999) examined 31 fragrance products and α-pinene was detected in 12 of them.
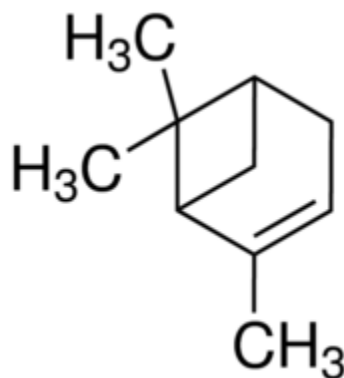
Figure 63: α-pinene chemical structure

The four-membered ring and also the double carbon bond in α-pinene make the hydrocarbon reactive like limonene. Therefore, α-pinene can also undergo oxidation reactions with ozone, NO_3 or OH radicals to form a wide range of secondary products. For instance, Rohr et al. (2003) summarized that the most important ozonolysis products of α-pinene are formaldehyde, acetone, pinonaldehyde, norpinonaldehyde, norpinone. Secondary organic aerosols were identified containing a range of carboxylic acid products: pinonic acid, ethanoic acid, methanoic acid, norpinonic acid, norpinic acid and pinic acid (Hoffmann et al., 1997; Rohr et al., 2003). However, pinonaldehyde was identified as the main gas phase product from a broad range of α-pinene reactions with O_3, OH and NO_3 radicals (Calogirou et al., 1999) (Fig. 64).
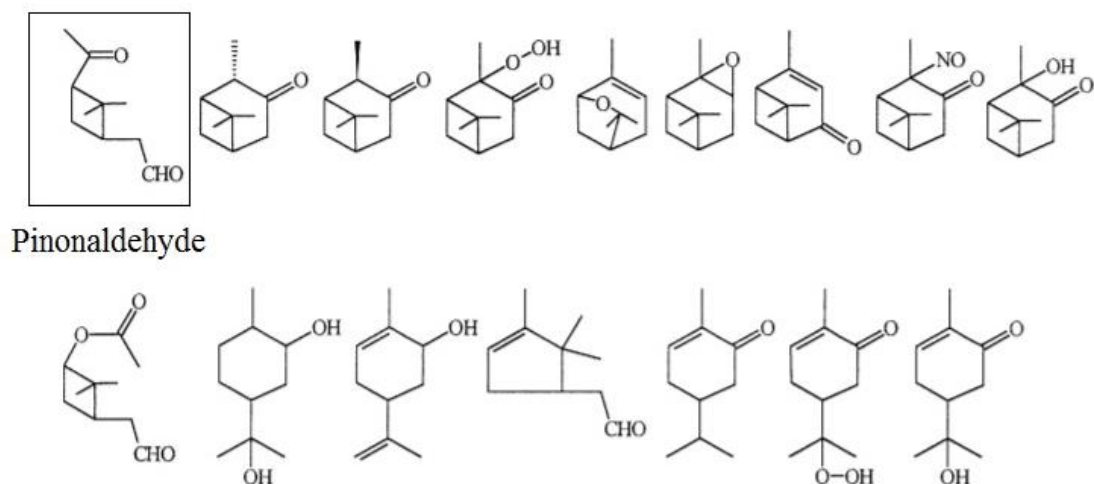
Figure 64: Secondary compounds formed via oxidation process following the reactions of α-pinene with O_3, OH and NO_3 radicals. Pinonaldehyde was found to be the main gas-phase product in the Calogirou et al. (1999) experimental conditions (Source: Calogirou et al., 1999).

6.4 Cleaning experiment

6.4.1 Introduction

Even though limonene is frequently detected at high concentrations indoors using sampling and laboratory methods, the numerous gas-phase oxidation products are difficult to detect via traditional techniques. For instance, gas chromatography is difficult as many of the oxidation products have low polarity (Yu et al., 1998). Other species are likely to be formed at relatively low concentrations such that detection is difficult with existing experimental techniques (e.g. organic nitrates) and reliable techniques to detect some species (such as peroxides) do not exist at all. However, Wells and coworkers have developed reliable techniques to detect and quantify a number of carbonyl species from terpene oxidation, as summarized by Forester and Wells (2009) for limonene and listed in Table 25.

Table 25: The gas phase reaction products from oxidation of limonene via OH radical and O_3 found using experimental methods (Forester and Wells, 2009).

Limonene oxidation product name	Product chemical structure
4-Acetyl-1-methylcyclohexene (4-AMCH)/Limonaketone	
2-hydroperoxy-3,4-dimethylpent-4-enal	
Dihydrocarvone	
Carvone	
2-(4-Methylcyclohex-3-en-1-yl)propanal	
Glyoxal	
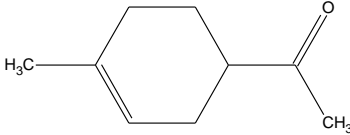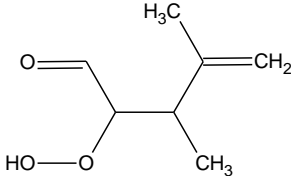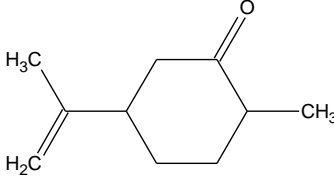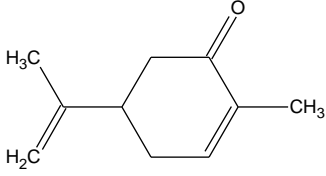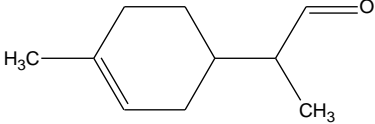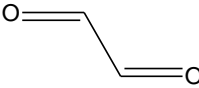
Limonene oxidation product name	Product chemical structure
4-Oxopentanal (4-OPA)	
3-Isopropenyl-6-oxoheptanal (IPOH)/ Limonaldehyde	
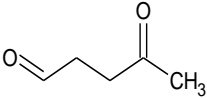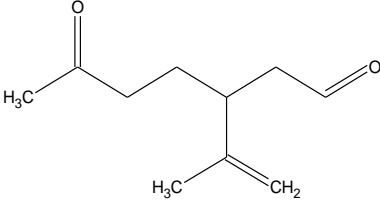
The carbonyl species are one of the most important groups that accumulate in the gas-phase following cleaning activity indoors (Carslaw, 2013). Such species have been noted as possibly responsible for adverse health effects and therefore they are relevant group of compounds for further studies (Wolkoff et al., 2000).

Wells and Ham (2014) presented a new method for derivatizing carbonyl compounds from gas-phase samples using aqueous solution. The method was achieved with the use of TBOX (O-tert-butyl-hydroxylamine hydrochloride). The advantages of using the TBOX derivatization agent technique include the ability to identify multi-carbonyl compounds and shortened oxime-formation reaction time (Wells and Ham, 2014). Wells and Ham (2014) more recently detected three additional limonene oxidation products, namely 7-hydroxyl-6-oxo-3-(prop-1-en—2yl)heptanal (7H6O), 2-acetyl-5-oxohexanal (2A5O) and 3-acetyl-6-oxopentanal (3A6O) using this novel technique to derivatize the carbonyl products. Interestingly, 3A6O but also other tricarbonyl products, that were not possible to quantify via conventional methods, were predicted by the model study of Carslaw (2013). Clearly, modelling studies can be a comprehensive tool to support and guide laboratory experiments.

6.4.2 Methods

6.4.2.1 Gas-phase experiments

To understand the fate of terpene hydrocarbons and their mixtures in indoor environments, an experiment was carried out to verify and compare the products from the reaction of ozone with single compounds (α-pinene and limonene) or a mixture of the two in the gas-phase. The experiment was conducted at the National Institute for Occupational Safety and Health (NIOSH) facility in the US, as the internship requirement of the CAPACITIE project fellowship.

To identify gas-phase carbonyl products, five different experiments were carried out in an 80-L Teflon® chamber (Fig. 65) at 50% relative humidity (RH). The experiments were carried out with an air exchange rate equal to zero and in the absence of NO_x. It was assumed that there was no deposition in the chamber.

Single compound experiments were carried out with a 20 µL injection of a 10% solution of the compound into the 80 L chamber. Thus, 60 ppb of ozone was added to 2.5 ppm of terpene, where the terpene component was either limonene or α-pinene, or a mixture in a 1:3 ratio (as limonene reacts approximately 3 times more quickly with ozone than α -pinene). Experiments were also carried out for 30 ppb and 100 ppb of ozone for the mixture of terpenes.

Figure 65: Teflon® reaction chamber (80 L).

Single compounds and then the mixture (all with a total gas-phase terpene concentration of 2.5 ppm) were added to the chamber and allowed to react with ozone for 30 minutes. Ozone was produced by photolyzing air in a separate Teflon® chamber prior to the experiments. After reaction with ozone, a sample was collected in 25 mL of deionized water, derivatized with 100 ml of O-tert-butylhydroxylamine hydrochloride (TBOX), and heated to 70°C for 2 hours in a water bath. After cooling, the samples were extracted with 500 µL of toluene and 100 µL of the toluene extract layer was analyzed using the gas chromatography-mass spectrometry (GC-MS) system to identify carbonyl species (Ham et al. 2015).

6.4.2.2 Surface-phase experiments

To simulate a surface cleaning activity indoors, two surface types (vinyl flooring tile and carpet) were used. A mixture of terpenes was prepared, similarly to the gas-phase experiment, using 3 µL of limonene and 8.58 µL of α-pinene, both 10% solutions in methanol (again in an ~ 1:3 ratio). Following the methodology presented by Ham and Wells (2011), prior to the experiment, a range of 0.40-0.45 g of the mixture was sprayed onto the vinyl and carpet

tiles. Each tile was sprayed for 16 seconds with an aluminum template on top (Fig. 66). The aluminum template had a 14.9 cm diameter hole in the center, which ensured that the sprayed area could be sampled accurately to investigate secondary emissions.
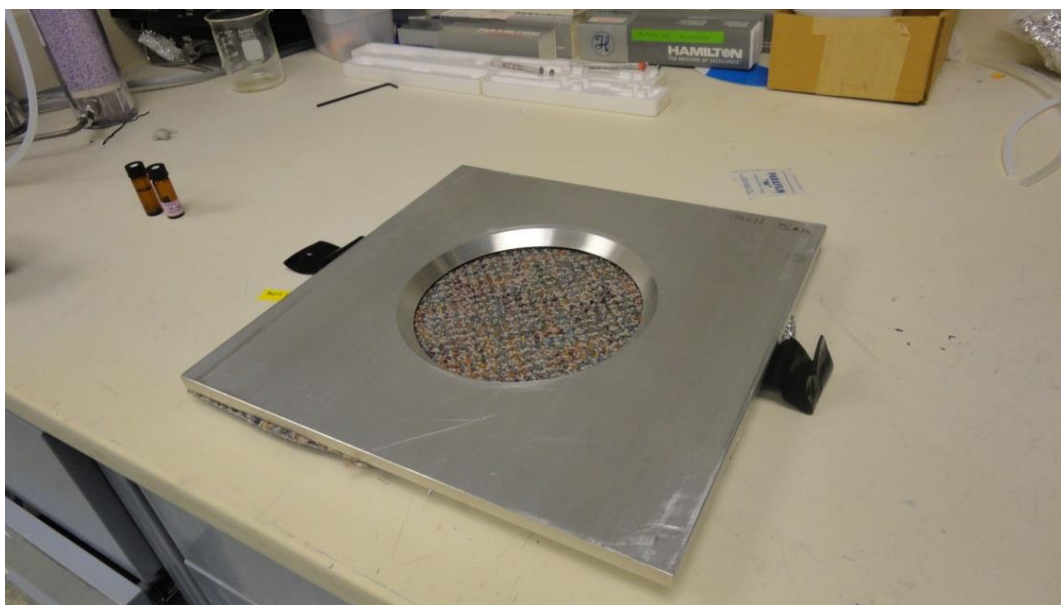
Figure 66: Surface preparation with the mixture of terpenes sprayed onto the surface prior to the experiment.

The instrument used for the experiment was the "Oxidant-Surface Chemistry Automated Reactor" (OSCAR) (Figure 67). This instrument is similar to FLEC, which is an emission test chamber and can be used to measure organic emissions from building materials and domestic products. The OSCAR instrument used in the experiment is composed of three stages: the air purification stage, the air humidification stage, and the reactant injection and delivery stage.
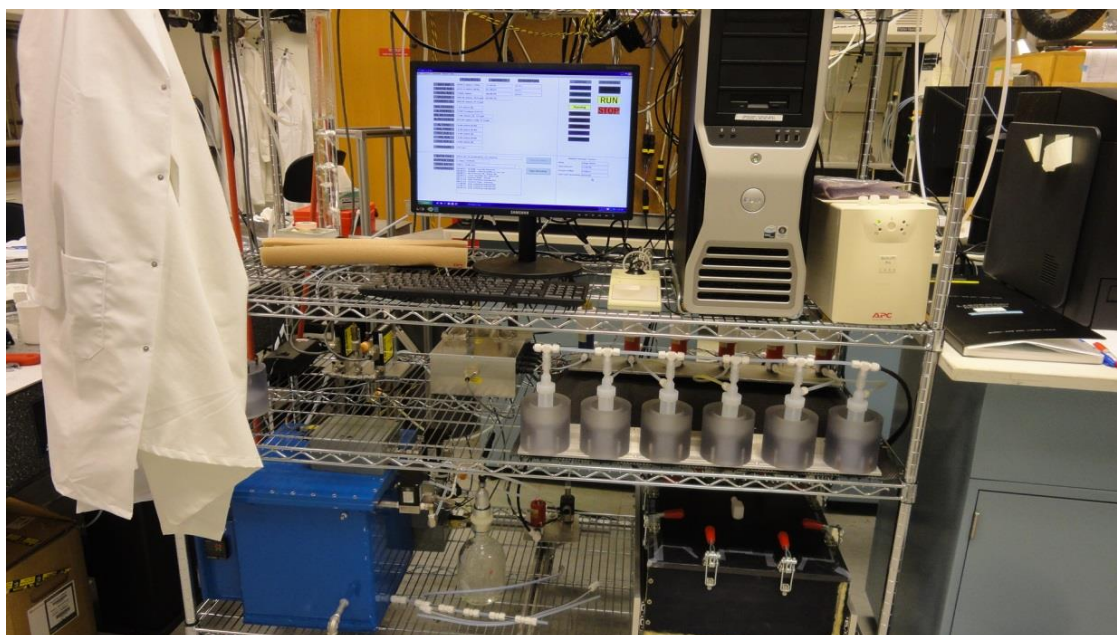
Figure 67: The OSCAR instrument used for the surface-phase emission experiment.

For each experiment the following parameters remain the same: the relative humidity was set to 50%, ozone concentration was set at 60 ppb and the flow rate through the instrument was 500 mL min^{-1}. Each experiment took 48 hours, during which time, emissions from the vinyl/carpet tiles following reaction with ozone were collected every 8 hours by impingers filled with 25 mL deionized water.

Then the samples were derivatized with 100 μL of O-tert-butylhydroxylamine hydrochloride (TBOX), and heated to 70°C for 2 hours in a water bath. After cooling, the samples were extracted with 500 µL of toluene and 100 μL of the toluene extract was analyzed using the gas chromatography-mass spectrometry (GC-MS) system to identify carbonyl species.

6.4.2.3 Model set-up

Different model runs were perform to verify reaction products and their formation profile within 30 minutes of the reaction following gas-phase ozonolysis of limonene, α-pinene and the limonene-α-pinene mixture. The experiments have been set up in the model to provide a qualitative understanding of the experimental data. Therefore, a model run time of 30 minutes was selected, given the experimental samples were extracted at this point. Similarly to the experiment described in the previous section of this Chapter, single terpenes were

subjects of the reaction with 60 ppb of ozone and the mixture of the terpenes with 30, 60 and 100 ppb of ozone. Both the single terpenes and the mixture were set to the concentration of 2.5 ppm. There was no NO$_x$ added to the system and the experiment was run in the dark and with zero air exchange. The relative humidity was set to 50%.

6.4.3 Results and discussion

6.4.3.1 Experimental results

6.4.3.1.1 Gas-phase experiments

The GC-MS results and carbonyl product identification are shown in Figure 68. Different coloured peaks correspond to the different mixtures used in each experiment.
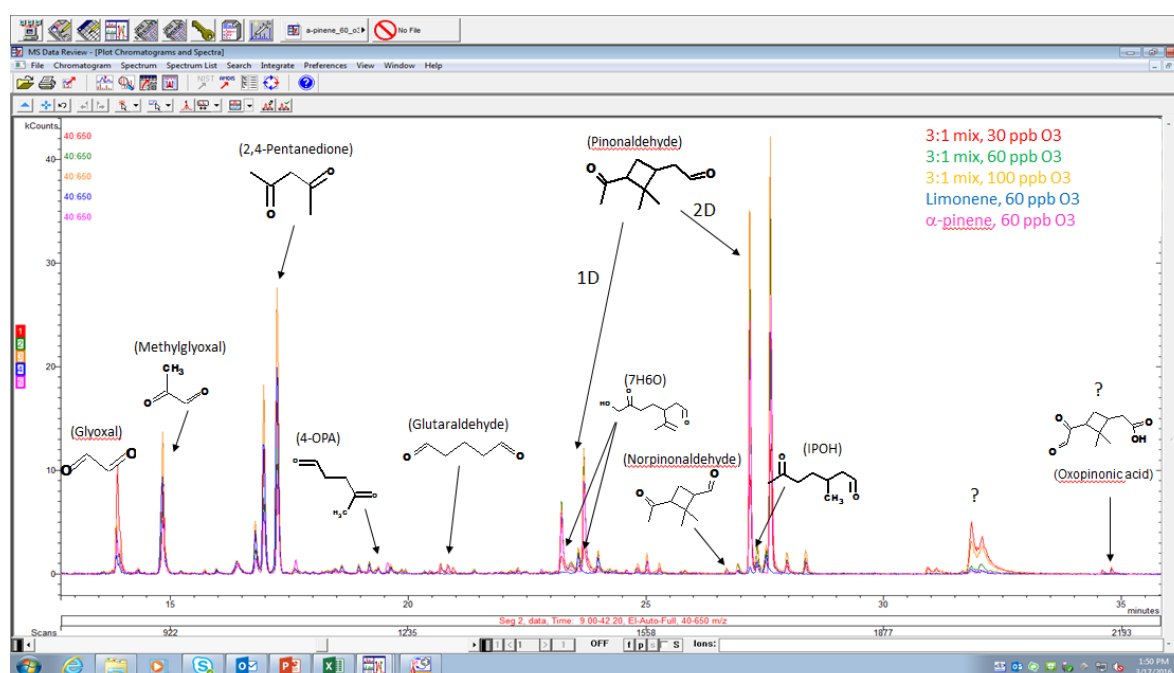
Figure 68: The GC-MS results and product identification following the gas-phase experiments of the ozonolysis reaction of 2.5 ppm of terpene with ozone. Red, green and yellow correspond to oxidation products of the mixture with 30, 60 and 100 ppb of ozone respectively. The blue colour depicts ozonolysis of limonene only and the pink one, α-pinene only. The latter two experiments were conducted with 60 ppb of O$_3$.

The results of the analysis show that a stronger signal was detected for some of the carbonyl compounds, such as glyoxal and methylglyoxal, following ozonolysis of the mixtures. Glyoxal, methylglyoxal and 2,4-Pentanedione, were all identified following

158

both limonene and α-pinene ozonolysis reaction but also in the mixtures. The carbonyls that were only observed as ozonolysis reaction products of limonene were 4-oxopentanal (4-OPA), 7-hydroxyl-6-oxo-3-(prop-1-en-2-yl)heptanal (7H6O) and 3-Isopropenyl-6-oxoheptanal (IPOH/Limonaldehyde), whilst those only from α-pinene ozonolysis were glutaraldehyde, pinonaldehyde and norpinonaldehyde. These species were also found in the terpene mixture experiments. It was not possible to identify all of the carbonyl species formed through this technique, but it is clear that there is a wide range of products formed following ozone reactions and that the exact composition depends on the starting terpene composition. This concept is explored further with the modelling studies in Section 6.4.3.2.

6.4.3.1.2 Surface-phase experiment

The results of the surface-phase experiment following the terpene mixture application are shown in Figure 69, which compares the gas-phase mixture experiment and surface-phase (a carpet tile) mixture experiment. All experiments were carried out in the presence of 60 ppb of ozone. There are a number of overlapping peaks in the two sets of experiments, showing that some species are formed in the gas phase and also on the surface following cleaning. Following the surface-phase mixture experiments, glyoxal, methylglyoxal, 4-OPA, glutaraldehyde, pinonaldehyde and IPOH were identified. 2,4-Pentanedione is also likely to be present, but this could not be confirmed. In general, the signal strengths from the surface-phase experiments were lower compared with the equivalent gas-phase experiments. This likely indicates that some of the carbonyl products were trapped on the surface and that the emissions were released more slowly over time.
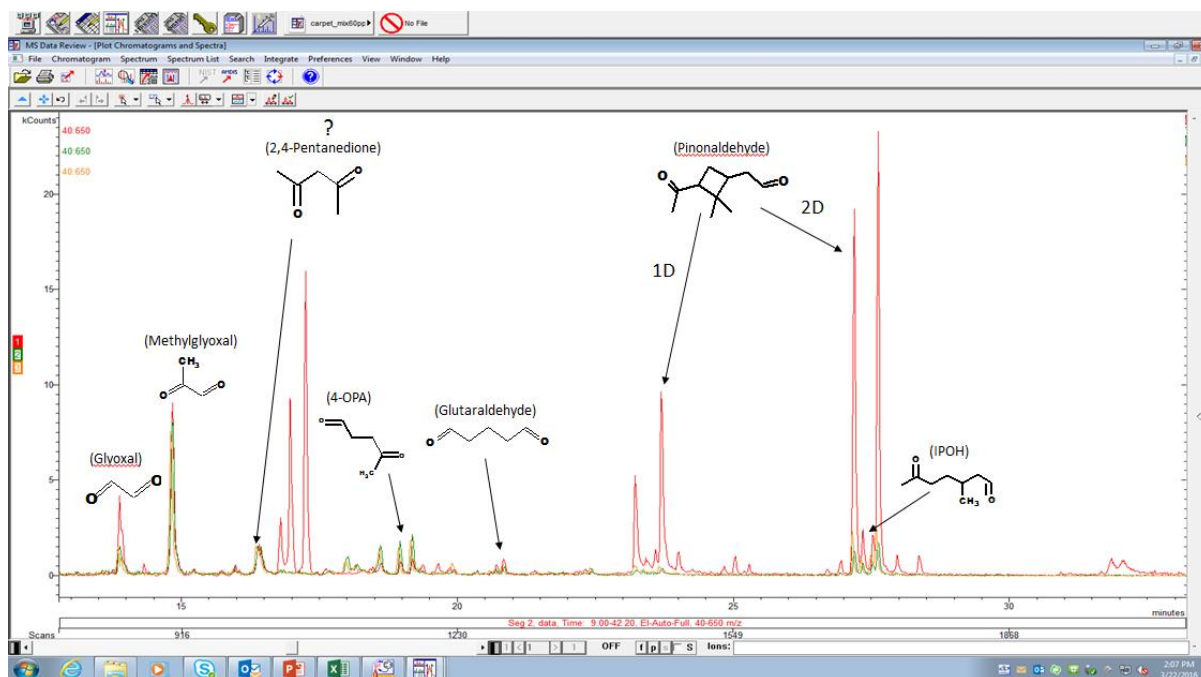
Figure 69: The GC-MS results and product identification following the gas-phase and surface-phase experiments. Red colour shows the ozonolysis reaction of 2.5 ppm of the mixture of limonene and α-pinene (in the 1:3 ratio) in a gas-phase. Green and yellow colour corresponds to surface-phase (a carpet tile) oxidation products of the limonene and α-pinene (in the 1:3 ratio) mixture with ozone.

The surface-phase experiment was repeated with a vinyl tile under the same experimental conditions. The results (Fig. 70) show that again, some of the same products are identified: glyoxal, methylgloxal, 4-OPA and pinonaldehyde. However there are also some unidentified compounds e.g. with mass-to-charge ratio (m/z) 176. This compound may be 2,4-Pentanedione, but it was difficult to confirm with the observed results and match with the results of the probable compounds. The biggest difference between carpet and vinyl tiles was observed for 4-OPA, with a much stronger signal for carpet sprayed with the mixture rather than for the vinyl tile.
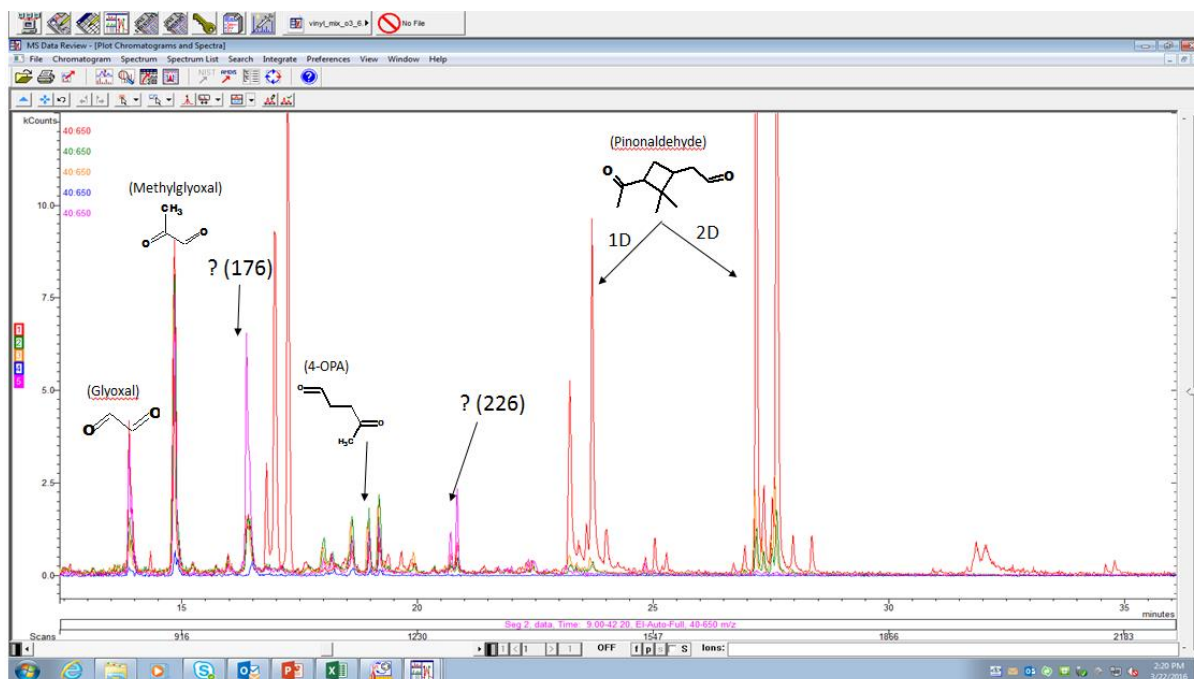
Figure 70: Comparison of the GC-MS results and product identification following the gas-phase and surface-phase experiments with the limonene and α-pinene mixture. Red colour shows the ozonolysis reaction in a gas-phase. Green and yellow colour corresponds to the repeated experiment of a surface-phase (a carpet tile). Blue and pink colour shows a repeated surface-phase (a vinyl tile) experiment.

These results are still at a very preliminary stage and further calibration is needed. There is insufficient quantitative data to attempt to model the results directly. However, the idea that different mixtures of terpenes in cleaning products may lead to quite different secondary pollutant composition indoors is now explored in more detail with the model in the next section.

6.4.3.2 Modelling test results

Figure 71 presents the modeled results for the predicted OH radical profile following the reactions of the terpenes with ozone in the gas-phase. The concentration of OH following α-pinene ozonolysis is much higher than for limonene ozonolysis. The peak modelled concentration of OH formed via α-pinene ozonolysis is ~1.4 x 10^6 molecule cm^{-3} whereas via limonene ozonolysis, it is ~7.4 x 10^5 molecule cm^{-3}. These results reflect the difference in the reaction rate of the terpenes with OH (according to Atkinson et al. (1986), 5.45 x 10^{-11} cm^3 molecule^{-1} sec^{-1} for α-pinene and 16.9 x 10^{-11} cm^3 molecule^{-1} sec^{-1} for limonene) and the efficiency of feedback of OH from the ozone-terpene reactions.

The OH concentration is also higher when the ozone concentration increases. In all cases, the OH is rapidly consumed within approximately 10 minutes and is near zero by 30 minutes (at the time when samples were extracted for the experiments described in previous sections).
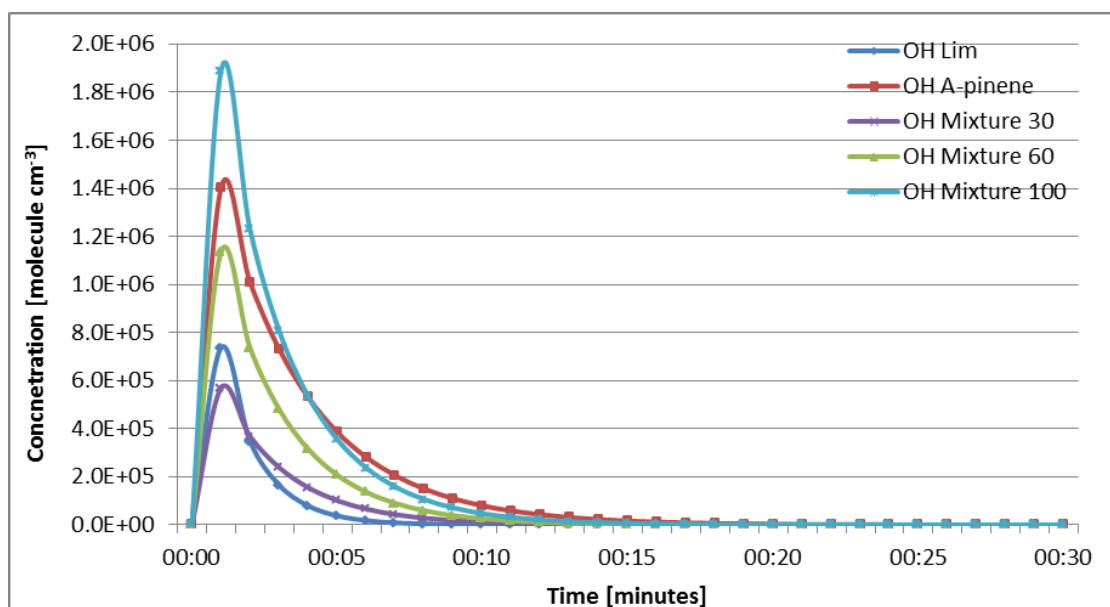
Figure 71: Modelled OH concentration [molecule cm^{-3}] following gas-phase oxidation of single terpenes (limonene and α-pinene) and limonene – α-pinene mixtures. Single terpene reactions are performed with 60 ppb of ozone, the mixture reactions are carried out for 30, 60 and 100 ppb of ozone.

Following the oxidation of each terpene by OH, RO$_2$ radicals are formed. Modelled predictions are shown in Figure 72, which shows that more RO$_2$ radicals are formed from the alpha-pinene only experiment when compared to limonene only, as more OH is available in this experiment (Fig. 71) to react and produce them.
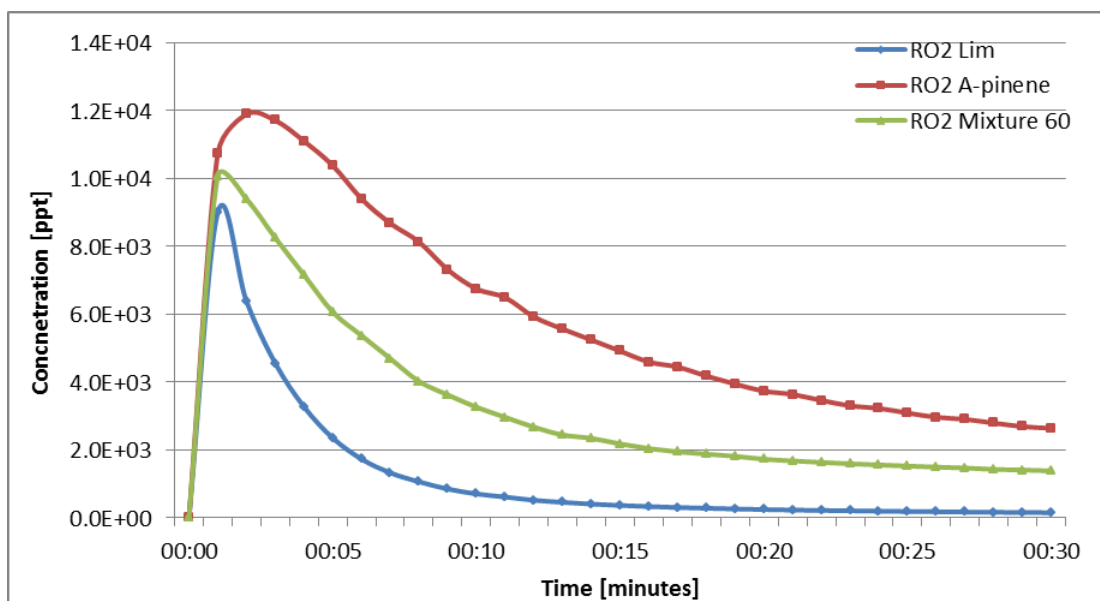
Figure 72: Modelled RO_2 concentration [ppt] following gas-phase oxidation of single terpenes (limonene and α-pinene) and limonene – α-pinene mixture. Blue, green and red lines depict the limonene, α-pinene and the terpene mixture oxidation reactions, respectively.

The RO_2 concentration decreases rapidly following the limonene only experiment, whereas the α-pinene only experiment has a broader, smoother decline, with significant RO_2 remaining after 30 minutes. The RO_2 concentration depends on the ozone concentration as shown in Figure 73. The higher the ozone concentration, the greater the production rate of OH and hence RO_2.
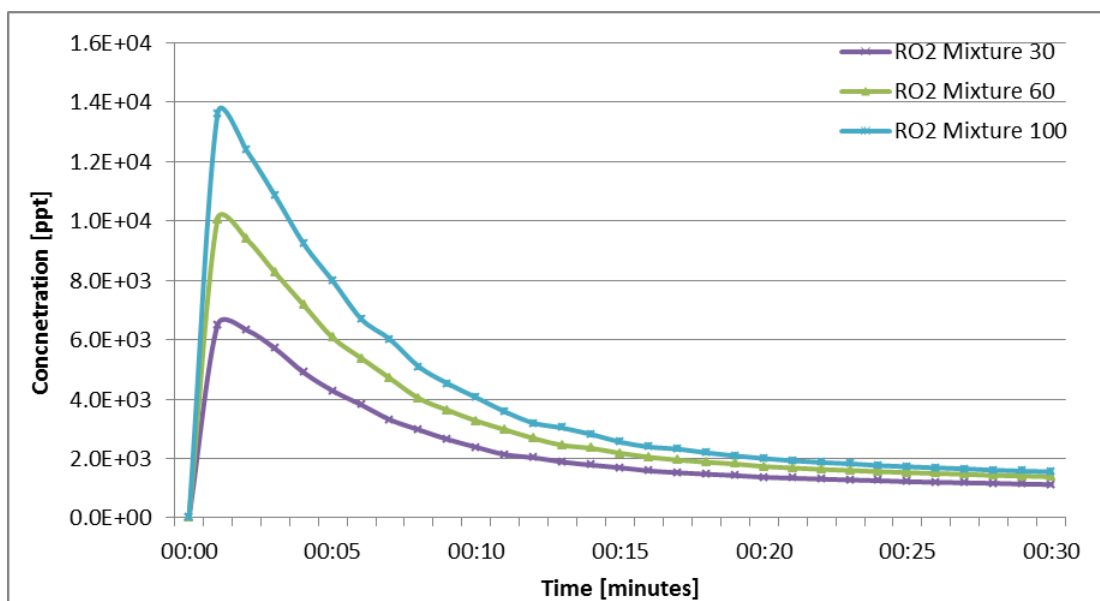
Figure 73: RO_2 concentration [ppt] profile following oxidation of the gas-phase of limonene – α-pinene mixture. Purple, green and blue lines depict the limonene - α-pinene mixture reactions with 30, 60 and 100 ppb of ozone respectively.

The detailed chemical mechanism used in the model, enables the user to follow gas phase degradation schemes for VOCs and identify different reaction products as they are formed along the oxidation chain (Saunders et al., 2003). Figure 74 shows the position in the oxidation chain for a number of RO_2 products formed following limonene and α-pinene oxidation reactions. For instance, for the α-pinene reaction with OH radicals, RO_2 radicals are formed: $APINAO_2$, $APINBO_2$, $APINCO_2$, which can be considered as first generation products. These undergo further reactions to form second, third, fourth (etc.) generation products.

Figure 74 presents this information for the limonene only and α-pinene only experiments. Following the limonene only experiment, ~100% of the RO_2 composition after 30 minutes is first generation products. However, for the α-pinene-only experiment, only ~9% of the RO_2 composition at 30 minutes is first generation products. Most are fourth generation (~53%), with contributions from fifth to eight generation products also. Since there are clear differences in the formation of the generation products between limonene and α-pinene, it is likely to lead to different oxidation products further down the oxidation chain.
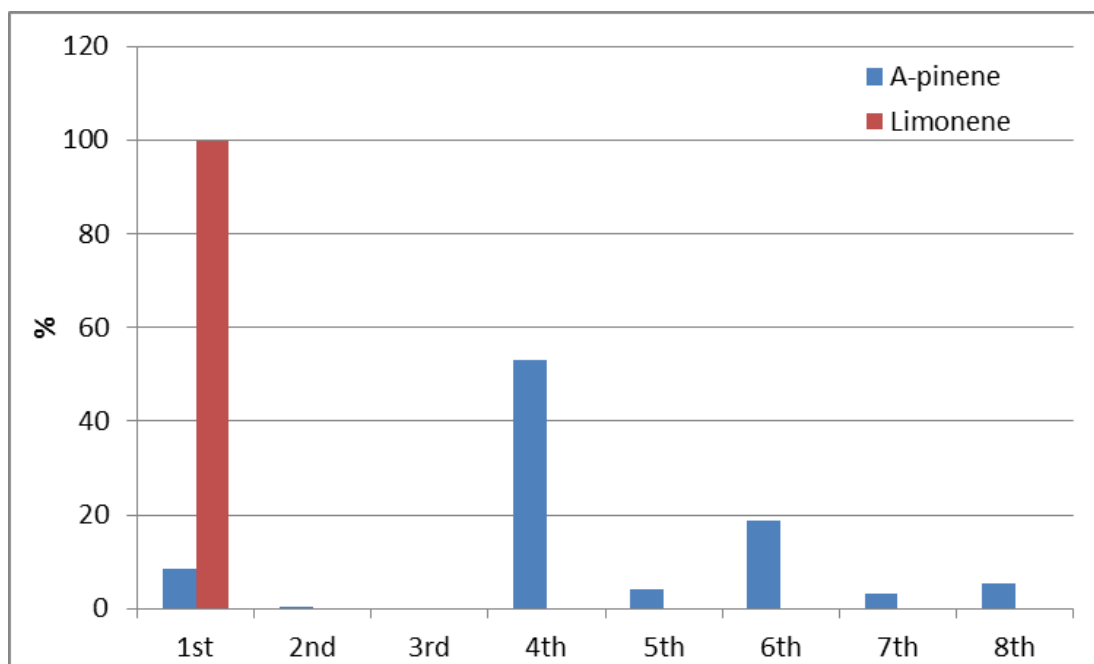
Figure 74: Percentage of RO_2 radicals as generations along the oxidation chain following the gas-phase reaction of limonene (red bars) and α-pinene (blue bars) with ozone. The bars depict first, second, third, fourth, fifth, sixth, seventh and eighth generation products.

Whilst α-pinene is more efficient for RO_2 production, limonene generates formaldehyde (HCHO) more effectively than α-pinene (Fig. 75). There are multiple pathways to generate HCHO following limonene degradation and Carslaw (2013) estimated that formaldehyde contributed ~6% to the overall composition of gas-phase limonene oxidation products. Wolkoff et al. (2008) suggested that gas-phase products, especially formaldehyde, are responsible for sensory health effects, though concentrations below 80 ppb should not lead to either acute or chronic sensory irritation in the airways (Wolkoff and Nielsen, 2010).
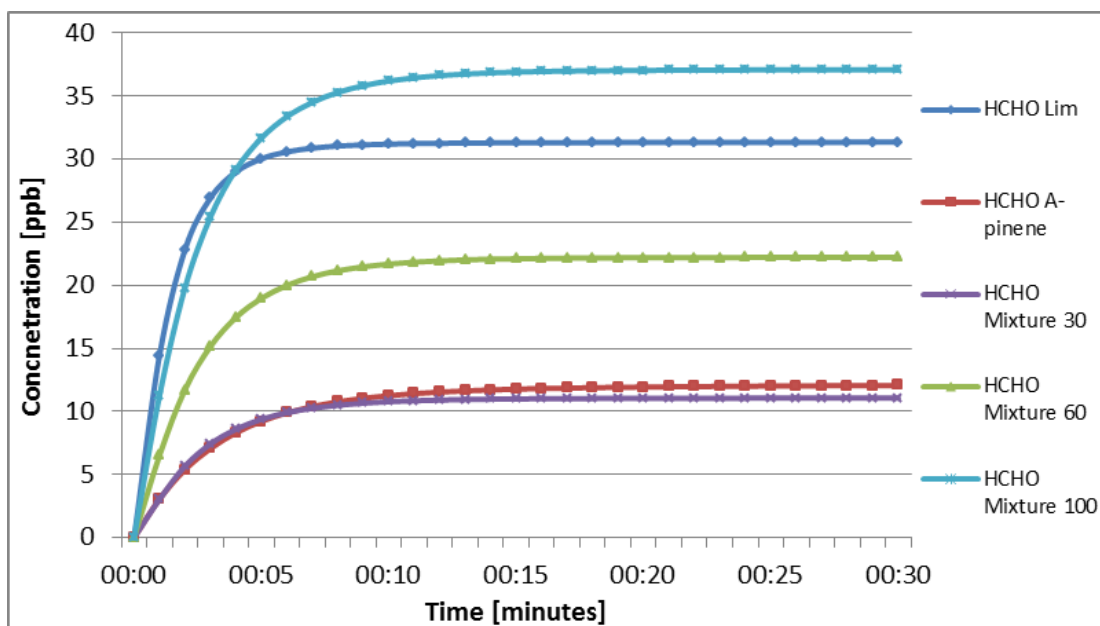
Figure 75: Modelled formaldehyde (HCHO) concentration [ppb] following the gas-phase oxidation of α-pinene only (red line), limonene only (dark blue line) and the limonene – α-pinene mixture oxidation for 30 ppb (purple line), 60 ppb (green line) and 100 ppb (light blue line) of ozone.

Glyoxal (Fig. 76) is one of the significant products from α-pinene oxidation under the conditions presented in the experiment. After 30 minutes of the experiment, the modelling results show that the concentration of glyoxal reached ~130 ppt. Similarly, methylglyoxal (Fig. 77) was an important product following α-pinene oxidation, however with a much smaller concentration than glyoxal –only 1.2×10^{-2} ppt after 30 minutes of the experiment.

Figure 76: Glyoxal concentration [ppt] profile product formation following the gas-phase of single α-pinene, limonene and the limonene – α-pinene mixture oxidation reaction. Purple, green and light blue lines depict the limonene - α-pinene mixture reactions with 30, 60 and 100 ppb of ozone respectively. Dark blue line represents the limonene oxidation and the red – α-pinene.
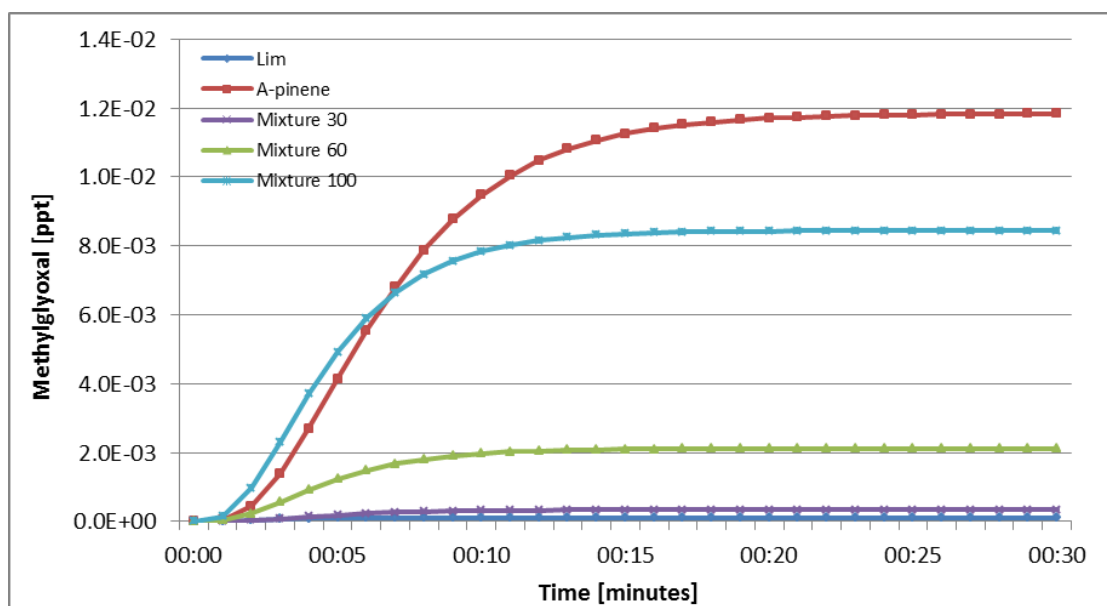
Figure 77: Methylglyoxal concentration [ppt] profile product formation following the gas-phase of single α-pinene, limonene and the limonene – α-pinene mixture oxidation reaction. Purple, green and light blue lines depict the limonene - α-pinene mixture reactions with 30, 60 and 100 ppb of ozone respectively. Dark blue line represents the limonene oxidation and the red – α-pinene.

2,4-Pentanedione has been identified as a product following both the single terpenes and the mixture oxidation. However the analysis of the measurement and modelling data do

167

not give a clear view of whether this compound can be confirmed as an oxidation product or it is just contamination in the measurement system (potentially in the α-pinene). Currently this issue is being investigated further at NIOSH to ascertain why it was present.

The highest concentration from the detected products following α-pinene oxidation was pinonaldehyde as found by Calogirou et al. (1999). Figure 78 shows that after 30 minutes of the experiment the concentration of this carbonyl compound reaches ~35 ppb. The concentration of pinonaldehyde following the reaction of the limonene - α-pinene mixture (60 ppb of ozone) is approximately half that for α-pinene only, since pinonaldehyde is not formed through limonene oxidation.
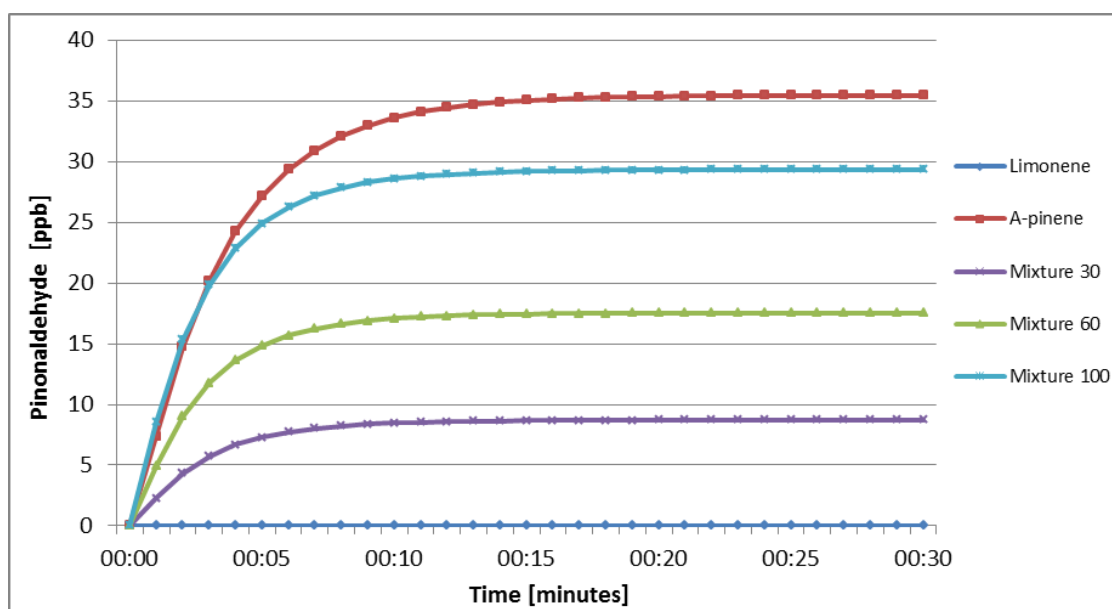
Figure 78: Pinonaldehyde concentration [ppb] profile product formation following the gas-phase of single α-pinene, limonene and the limonene – α-pinene mixture oxidation reaction. Purple, green and light blue lines depict the limonene - α-pinene mixture reactions with 30, 60 and 100 ppb of ozone respectively. Dark blue line represents the limonene oxidation and the red – α-pinene.

One of the major gas-phase species formed following oxidation of limonene is limonaldehyde (3-isopropenyl-6-oxo-heptanal, or IPOH). Limonaldehyde is formed via oxidation of limonene via OH and O_3. Carslaw (2013) showed that reaction with OH was approximately 1.4 times more important than the one with O_3 for typical cleaning conditions. The model results (Fig. 79) show that at the end of the experiment (30 min), limonaldehyde has the highest concentration (~20 ppb) for the limonene only experiment as expected. However, it is interesting that the 100 ppb O_3 experiment of the mixture produces almost as

much limonaldehyde as from the single terpene experiment, despite the lower limonene concentration. This observation is also true for pinionaldehyde production (Fig 78) and shows that the increased ozone concentration can compensate when it comes to the rate of production of the secondary product. Under these conditions, neither of the reactant concentrations are limiting.
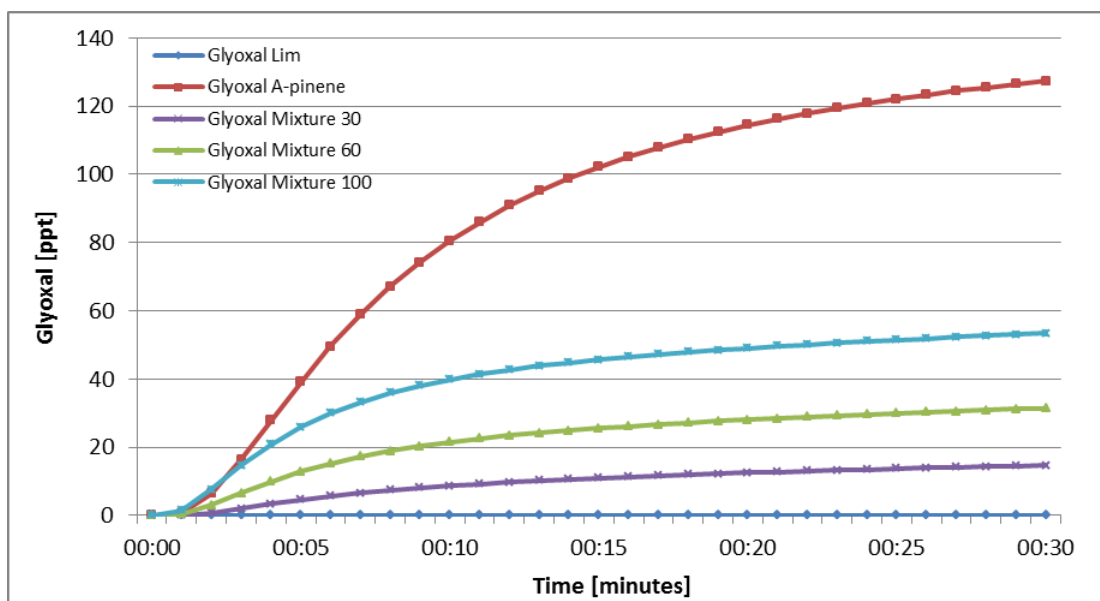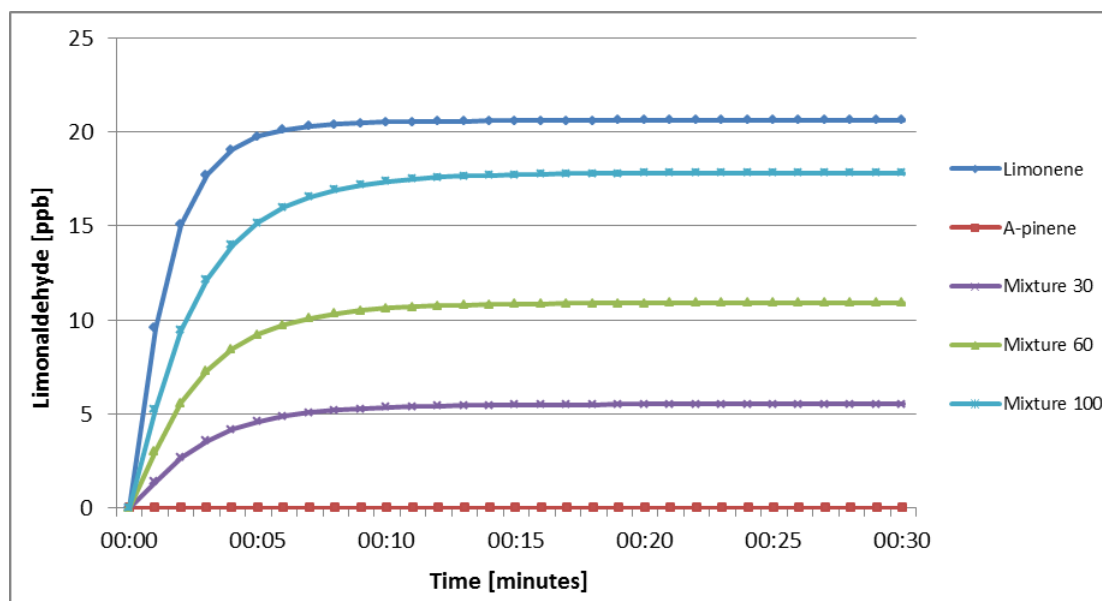

Figure 79: Limonaldehyde concentration [ppb] profile product formation following the gas-phase of single α-pinene, limonene and the limonene – α-pinene mixture oxidation reaction. Purple, green and light blue lines depict the limonene - α-pinene mixture reactions with 30, 60 and 100 ppb of ozone respectively. Dark blue line represents the limonene oxidation and the red – α-pinene.

When comparing the three experiments performed with 60 ppb of ozone, three species, 3-acetyl-6-oxopentanal, 4-oxopentanal (4-OPA), and 1-hydroxy-3-methyl-3-butene-2-one, were predicted to be formed at higher concentrations with the mixture of the terpenes rather than with the single compound runs. The chemical structures of these three identified compounds are shown in Figure 80.
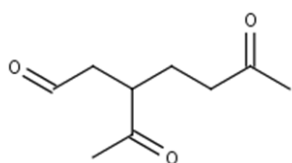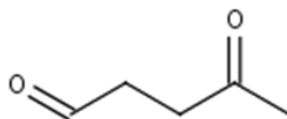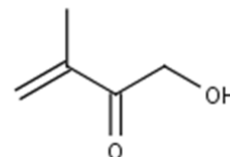
3-acetyl-6-oxopentanal   4-oxopentanal (4-OPA)   1-hydroxy-3-methyl-3-butene-
                                                                              2-one

Figure 80: Structures and names of carbonyl species predicted to be formed at higher concentrations for the mixture of terpenes compared to the single compound experiments.

Figure 81 shows the 4-OPA concentration profile over 30 minutes following oxidation of limonene only, α-pinene only and the terpene mixture, all with 60 ppb of ozone. 4-OPA is an important oxidation reaction product of limonene (Rossignol et al., 2012). The concentration of 4-OPA after 30 minutes of the reaction is relatively small for all the experiments, but interestingly, approximately 2.7 times higher for the mixture is than for the oxidation of limonene only.
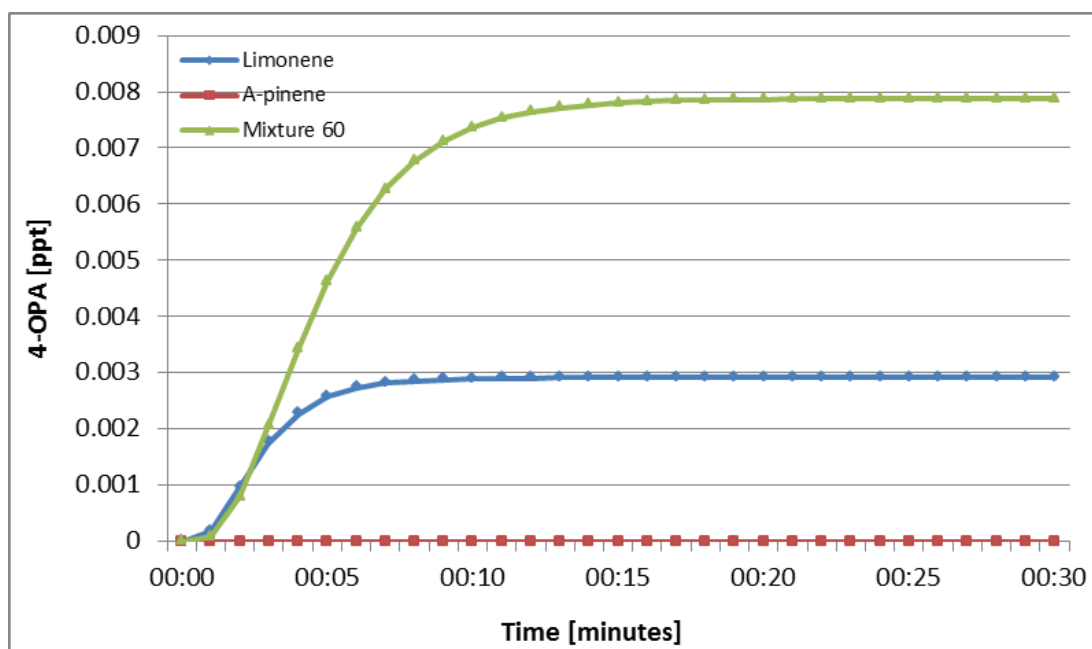
Figure 81: 4-OPA concentration [ppt] profile following the gas-phase oxidation of limonene (blue line), α-pinene (red line) and the mixture of the terpenes (green line).

4-OPA production indoors is determined by the OH concentration. The OH concentration was estimated to be higher following the ozonolysis of the terpene mixture compared to limonene only (Figure 81). Given that 4-OPA is formed following subsequent reactions of OH with the oxidation products, the 4-OPA concentration is higher following oxidation of the terpene mixture rather than the single terpene oxidation. Such results highlight the importance for investigating mixtures, which are commonly found in real indoor environments. Assuming that oxidation of a mixture is a summation of the reactions of the individual compounds will give erroneous results.

6.5 Chapter summary

This Chapter has highlighted the complex chemistry following terpene mixture oxidation. Since terpenes and their mixtures are widely used in consumer products such as cleaning agents or air fresheners, it is important to understand the fate of mixtures in terms of indoor chemistry and secondary species formation.

The laboratory experiments identified a number of the carbonyl products formed following gas-phase terpene oxidation, along with some unidentified species. Ongoing work at NIOSH (outside the scope of this PhD) involves quantification of more of the detected species.

Finally, some model runs have been performed to verify and understand the experimental results in terms of detailed chemistry and the pathways of the reactions. It is possible to identify more reaction products than using the laboratory methods, as the model is not limited to carbonyl species (though the results focus mainly on those). The concentrations of some of the products following oxidation of the mixtures may be higher than for oxidation of the single terpenes, despite the same overall terpene concentration. Further, the concentrations of secondary products change depending on the starting terpene mixture. However, the experiments and the model runs were performed for rather unrealistic indoor conditions. Concentrations of terpenes were high, the experiments were performed in the dark and there were no nitrogen oxides or air exchange with outdoors.

Nevertheless, the results point to the potential for improving consumer product formulations. Using less reactive mixtures might avoid exposure to potentially harmful secondary products. Clearly, such improved formulations would be beneficial for anybody using such products on a regular basis.

7. Conclusions

7.1 General conclusions

Over the last few decades, increasing attention has been paid to indoor air quality. It has been estimated that people spend most of their time indoors and consequently most of the exposure to air pollution occurs indoors (Carslaw, 2007). Different sources of indoor air pollution, such as building products emissions, cleaning and personal care products, cooking, smoking or outdoor air pollutants, together with more airtight buildings and consequently a higher range of different mixtures of chemicals indoors, have an impact on building occupants and increase the potential for adverse health effects. In the absence of detailed measurements, the INDCM model has been improved and developed throughout this dissertation to represent surface interactions indoors and to evaluate their impact on indoor air quality.

The INDCM model is a comprehensive tool, which enables the user to evaluate the impact of surface interactions on indoor air chemistry. The INDCM model development presented in this dissertation provides a wider understanding of air chemistry processes indoors, for a range of realistic conditions. The model now represents physical and chemical processes, such as exchange with outdoors, better parameterized deposition to surfaces, indoor emissions and photolysis reactions that impact indoor air chemistry. The explicit chemical mechanism that is used in the model has enabled ozone loss and secondary pollutant formation rates to be estimated following surface interactions indoors. It has also been used to compare green building materials with conventional ones and to evaluate their impact on indoor air chemistry and to simulate the impact of human occupancy indoors on indoor air quality, including human skin and breath emissions in different indoor environments. Comparing different locations for a building (Milan and Seoul were used as case study cities) and therefore outdoor and indoor concentrations, has also allowed the impact of outdoor air pollution on indoor concentrations to be investigated for a range of locations. Moreover, the INDCM model has been used to evaluate the impact of different mixtures of terpenes, widely used in cleaning and consumer products, on indoor air chemistry.

The results show that high outdoor pollutant concentrations can have a great impact on indoor air pollution. Higher concentrations of ozone outdoors, and therefore indoors, enhance oxidation processes and lead to higher emissions of secondary indoor air pollutants, for instance the C_6-C_{10} aldehydes. Thus, ozone loss onto all internal surfaces in the apartment in Milan during summer heatwave conditions (when outdoor ozone concentration was ~75

172

ppb) was approximately 40% greater than during typical summer conditions (outdoor ozone concentration was ~49 ppb). Following ozone deposition, nonanal was the most significant aldehyde species emitted from the surfaces (~4.5-9 ppb) and increased by ~22% during polluted conditions when compared with more average conditions in Milan. Since heatwaves may perhaps occur more frequently in the future along with climate change (Solomon et al., 2007), indoor ozone-derived surface aldehyde emissions may also increase. According to the European Chemical Agency (ECHA), C_6-C_{10} aldehydes are expected to cause eye, skin and potential respiratory irritation. Therefore, emissions of higher aldehydes following surface interactions indoors may cause increased adverse health effects. Furthermore, the modelling results show the impact of surface processes indoors on indoor air chemistry. Surface interactions indoors decrease the concentration of oxidants such as ozone or OH not only via deposition but also chemical reactions. For instance, OH concentration decreases by approximately 23% when the surface emissions were included in the model.

Nowadays, green materials are becoming more and more popular. A model comparison of emissions from traditional and green building materials showed that the green materials may lead to lower concentrations of pollutants indoors. For instance, the formaldehyde concentration directly after installation of conventional materials in a typical apartment was estimated as ~45 ppb, compared to 14 ppb for green materials. However, the concentrations of formaldehyde are below the WHO (2010) guideline value, which suggests concentrations below 80 ppb of formaldehyde do not cause cancer. The eye and airway irritation reported at concentrations of ~480-800 ppb (Wolkoff and Nielsen, 2010), was much higher than the formaldehyde concentrations presented both from conventional and green materials. The model results show that the concentrations of aldehydes arising from primary emissions from both types of materials are much higher than those from secondary emissions over the first 3 months based on model assumptions. The total aldehyde concentration following emissions from conventional and green materials directly after installation was ~130 ppb and ~40 ppb respectively. After the first three months, secondary emissions become more significant and lead to similar concentrations from both conventional and green materials (~10 ppb and 8.5 ppb total aldehyde concentrations respectively). Thus, green materials have the potential to have lower emissions immediately after installation indoors and can be considered as a better solution for buildings in terms of indoor air quality.

The limitation of this study indicates that input parameters rely on the few measurement results found in different literature studies. Undoubtedly, models would benefit

from more extensive field measurements of ozone surface reactivity, including deposition velocities and product yields (also for a larger set of species than studied here), in real and occupied homes. Such information would permit the more accurate prediction of indoor concentrations, reduce model uncertainty and validate modelling results. Likewise, the same information for indoor pollutants other than ozone is currently absent but would be interesting to explore.

Future studies should include aspects of the time history of surfaces i.e. ozone aging as well as prioritization of the type of surface for detailed studies. Also, in terms of green building materials more specific studies in terms of materials emissions are required. For instance, the profile of emissions with time from new materials is not well specified at present. The study of James and Yang (2005) showed that primary emissions of green materials decreased exponentially, but did not provide specific decay rates. Such information would be useful for more accurate modelling and for reducing the existing uncertainties in the model predictions.

Among all the tested surfaces, the human body is the most efficient in terms of removing ozone from indoor air per square meter. However, in terms of the total removal of ozone from typical apartments, soft furniture and painted walls are more important due to their large surface areas. The modelling results for human emissions indoors show that the air exchange rate, size of the indoor space and indoor occupancy are key factors. When the air exchange rate is lower, breath emissions become more important as dilution decreases, but skin emissions which are initialised by ozone (originally from outdoors) become less important. Furthermore, human emissions indoors are subject to the size of indoor space. For instance, the concentration of nonanal following skin emissions was ~0.1 ppb and ~0.5 ppb in the apartment and in the bedroom (during typical summer time conditions in Milan, AER = 0.76 h^{-1}) respectively. Given that skin surface to volume ratio was smaller in the apartment than in the bedroom, the concentrations of carbonyl species following skin emissions were also lower. However, the concentration of nonanal in the classroom during typical summer time conditions in Milan (AER = 1.2 h^{-1}) when occupants were present was up to ~5.3 ppb. Not surprisingly, highly occupied indoor environments, such as classrooms have high concentrations of some pollutants indoors. Nevertheless, breath emissions become more important when the air exchange rate is lower. For instance, the isoprene concentration in the apartment when the air exchange rate was 0.2 h^{-1} was ~7 ppb and decreased to ~1 ppb when the air exchange rate increased to 2.0 h^{-1}. However, comparing the concentrations of secondary products following breath emissions in the apartment and in the bedroom,

the results show that the concentrations are much higher in smaller indoor air spaces. For instance, the isoprene concentration was approximately ten times higher in the bedroom than in the apartment (~19.2 ppb and ~2 ppb respectively when AER = 0.76 h^{-1}).

Clearly, human emissions are important in terms of the overall indoor emissions. Subjects of a study might differ from one to another since each person has differences in metabolism, age, habits such as eating, drinking or smoking, and therefore can show different skin and breath emissions. Thus, it is difficult to choose appropriate inputs for models since each study presents different conditions and uses different subjects. Monte Carlo analysis, which relies on repeated random sampling, would potentially be useful to generate more wide ranging input parameters to enable exploring the results over a larger range of potential scenarios. Also, a wide range of secondary pollutants is formed following ozone – human body interactions, some of which may be harmful to health (Weschler et al., 2007). More health studies are necessary to provide guideline values, particularly given research indicates that surface-derived secondary pollutants can be more damaging for human health than the primary emissions, causing asthma and pulmonary infections (Mendell, 2007; Weschler et al., 2007).

Different activities indoors may enhance indoor air pollution. For instance, cleaning is one of the main sources contributing to higher pollutant concentrations indoors. Given that cleaning products or air fresheners contain a mixture of commonly found terpenes, this study has highlighted the complexity of chemical processes following terpene mixture oxidation. For instance, formaldehyde concentration was found to be highest (~32 ppb) when limonene underwent ozonolysis in isolation, whereas glyoxal, methylglyoxal and pinonaldehyde showed higher concentrations following α-pinene ozonolysis (130 ppt, 1.2×10^{-2} ppt and 35 ppb respectively). However, the 4-OPA concentration was highest following ozonolysis of the limonene - α-pinene mixture (~8×10^{-3} ppt) rather than limonene only (~3×10^{-3} ppt). There are more complex mixtures in use indoors and currently there are no guideline limits for a wide range of carbonyl species. There is a clear need for measurements of different mixtures of terpenes in real indoor scenarios, to quantify the concentrations of gas and particle-phase products that are formed, particularly those with known or suspected adverse health effects. It is important to understand these differences, as one can then consider changes to product formulation that might produce less harmful species as secondary products. Clearly, such improved formulations would decrease potential adverse health effects indoors, especially for those using the cleaning products regularly or who are more susceptible to adverse health effects from using them.

7.2 Future implications

In conclusion, future indoor air models should be more integrated, include real building scenarios and a wider range of different sources of indoor air pollution that may enhance chemical processes indoors. At the moment, indoor air models tend to focus on either chemistry or ventilation or surface interaction indoors, but very few consider all of the relevant aspects together. Future studies should include all of the different sources and processes indoors that have an impact on indoor air pollution. Likewise, the chemical mechanisms need to be developed to include more schemes for species commonly found indoors like α-terpinene or terpinolene. Also, to reduce model uncertainties, more experimental measurements are needed for gas-phase product yields, deposition velocities of a wider range of species, outdoor concentrations and photolysis rates.

Future cities will continue to aim to reduce energy use such as through the construction of energy efficient buildings (Asdrubali et al., 2015). Modern buildings are likely to become more airtight (with lower air exchange rates) and could potentially have worse indoor air quality than presently experienced (Stephen, 1998; Uhde and Salthammer, 2007; Sundell et al., 2011; Dimitroulopoulou, 2012). It is crucial to understand the causes of poor indoor air quality and the consequences it might bring, particularly in terms of human exposure effects. Thus, it is important to take into consideration adequate ventilation of indoor environments (higher than 0.5 h^{-1}, which is currently a standard in many European countries (Dimitroulopoulou, 2012)), the wider application of green materials instead of conventional ones, as well as educating consumers more widely about choosing and using cleaning or personal care products. Also, to evaluate more precisely any health effects of indoor air pollution, there is a need for cooperation between chemists, health and building scientists.

Currently, there is a lack of awareness of indoor air quality issues, the sources of indoor air pollution and the potentially better practice that could be implemented by building managers and occupants. Undoubtedly, future building design should be improved, not only thinking about minimisation of costs, but also improving the quality of the materials and products (Asdrubali et al., 2015). Indeed, application of non-toxic and renewable materials that passively remove gaseous pollutants, particularly ozone, may enhance the indoor air quality (Darling et al., 2016), which may be important for reducing pollutant formation indoors under some conditions. In addition, filtering particles from air inlets in mechanically

ventilated buildings (Jamriska et al., 2003) or improving formulation of cleaning and personal care products may improve the air quality indoors and diminish adverse health effects.

Smart cities of the future will need innovative technologies with intelligent design solutions to help to improve indoor air quality. For instance, developing digital concepts in a city, such as remote sensors and digital data application could improve information accessibility for inhabitants and also raise awareness about the potential problem (Nam and Pardo, 2011; Cimmino et al., 2014). Urban environmental monitoring may include further development in the areas of complex in situ miniaturised sensors, low cost user-friendly platforms, and innovative smartphone applications (Hancke and Hancke Jr, 2013). Hence, a fully functional system could contain self-configurable sensor units to constantly monitor air quality in buildings in cities, with the data transmitted and analysed in real time. Such systems would allow appropriate mitigation measures to be applied when concentrations of air pollutants reached detrimental concentrations indoor (Kitchin, 2014).

8. References

Abbass O.A., Sailor D.J., Gall E.T. 2017. Effect of fiber material on ozone removal and carbonyl production from carpets. Atmos. Environ.; 148:42-48.

Alvarez E.G., Amedro D., Afif C., Gligorovski S., Schoemaecker C., Fittschen C., Doussin J.F., Wortham H. 2013. Unexpectedly high indoor hydroxyl radical concentrations associated with nitrous acid. Proceedings of the National Academy of Sciences; 110(33):13294-13299.

Apte M.G., Buchanan I.S.H., Mendell M.J. 2008. Outdoor ozone and building related symptoms in the BASE study. Indoor Air; 18:156-170.

Asdrubali F., Bonaut M., Battisti M., Venegas M. 2008. Comparative study of energy regulations for buildings in Italy and Spain. Energ. Buildings; 40(10):1805-1815.

Asdrubali F., D'Alessandro F., Schiavoni S. 2015. A review of unconventional sustainable building insulation materials. Sust. Mater. Technol.; 4:1-17.

Ashmore M.R., Dimitroulopoulou C. 2009. Personal exposure of children to air pollution. Atmos. Environ.; 43:128-141.

Atkinson R., Aschmann S. M., Pitts J. N. 1986. Rate constants for the gas-phase reactions of the OH radical with a series of monoterpenes at 294 ± 1 K. Int. J. Chem. Kinet.; 18(3):287–299.

Atkinson R., Hasegawa D., Aschmann S. M. 1990. Rate constants for the gas-phase reactions of O_3 with a series of monoterpenes and related compounds at 296 ± 2K. Int. J. Chem. Kinet.; 22:871–887. doi:10.1002/kin.550220807

Atkinson R., Aschmann S. M., Arey J., Shorees B. J. 1992. Geophys. Res. 1992. 97:6065-6073.

Atkinson R. 1997. Gas-phase tropospheric chemistry of volatile organic compounds: 1. Alkanes and alkenes. J. Phys. Chem. Ref. Data; 26(2):215-290.

Atkinson R. and Arey J. 2003. Gas-phase tropospheric chemistry of biogenic volatile organic compounds: a review. Atmos. Environ.; 37:197-219.

Aurora P., Kozlowska W., Stocks J. 2005. Gas mixing efficiency from birth to adulthood measured by multiple-breath washout. Respir. Physiol. Neurobiol.; 148:125-139.

Bakó-Biró Z., Kochhar N., Clements-Croome D.J., Awbi H.B., Williams M. 2007. Ventilation rates in schools and learning performance. Proceedings of CLIMA (pp. 1434-1440).

Bakó-Biró Z., Clements-Croome D.J., Kochhar N., Awbi H.B., Williams M.J. 2012. Ventilation rates in schools and pupils' performance. Build. and Environ.; 48:215-223.

Bari M. A., Kindzierski W. B., Wheeler A. J., Héroux M. È., Wallace L. A. 2015. Source apportionment of indoor and outdoor volatile organic compounds at homes in Edmonton, Canada. Build. and Environ.; 90:114-124.

Bello A., Quinn M. M., Perry M.J., Milton D.K. 2009. Characterization of occupational exposures to cleaning products used for common cleaning tasks – a pilot study of hospital cleaners. Environ. Health; 8(11).

Below Zero Heating and Air Conditioning. 2017. Available online at: http://belowzerohvac.ca/indoor-air-quality-ottawa/ (date accessed January 2017).

Beniston M. 2004. The 2003 heat wave in Europe: a shape of things to come? An analysis based on Swiss climatological data and model simulations. Geophys. Res. Lett.; 31:1-4.

Berglund B., Brunekreef B., Knöppe H., Lindvall T., Maroni M., Mølhave L., Skov P. 1992. Effects of indoor air pollution on human health. Indoor Air; 2(1):2–25.

Bey I., Aumont B., Toupance G. 2001. A modelling study of the nighttime radical chemistry in the lower continental troposphere: 1. Development of a detailed chemical mechanism including nighttime chemistry. J. Geophys. Res.; 106(D9):9959–9990.

Blondeau P., Iordache V., Poupard O., Genin D., Allard F. 2005. Relationship between outdoor and indoor air quality in eight French schools. Indoor Air; 15(1):2‑12.

Bornehag C.G., Sundell J., Hagerhed-Engman L., Sigsgaard T. 2005. Association between ventilation rates in 390 Swedish homes and allergic symptoms in children. Indoor Air; 15:275.

Bowman J.H., Barket D.J., Shepson P.B. 2003. Atmospheric chemistry of nonanal. Environ. Sci. Technol.; 37(10):2218-2225.

Brown S.K. 2002. Volatile organic pollutants in new and established buildings in Melbourne, Australia. Indoor Air; 12(1):55-63.

Burdock G.A. (ed) 2005. Fenaroli's Handbook of Flavor. Ingredients 5th edn (London: CRC Press).

Calogirou A., Larsen B.R., Kotzias D. 1999. Gas-phase terpene oxidation products: a review. Atmos. Environ.; 33(9):1423-1439.

Canha N., Mandin C., Ramalho O., Wyart G., Ribéron J., Dassonville C., Hänninen O., Almeida S.M., Derbez M. 2016. Assessment of ventilation and indoor air pollutants in nursery and elementary schools in France. Indoor Air; 26:350-365.

Cano-Ruiz J.A., Kong D., Balas R.B., Nazaroff W.W. 1993. Removal of reactive gases at indoor surfaces: combining mass transport and surface kinetics. Atmos. Environ.; 27A(13):2039–2050.

Carslaw N., Jacobs P.J., Pilling M.J. 1999. Modelling OH, HO_2, and RO_2 radicals in the marine boundary layer: 2. Mechanism reduction and uncertainty analysis. J. Geophys. Res.; 104(D23):30257-30273.

Carslaw N. 2007. A new detailed chemical model for indoor air pollution. Atmos. Environ.; 41(6): 1164-1179.

Carslaw N., Mota T., Jenkin M.E., Barley M.H., McFiggans G. 2012. A significant role for nitrate and peroxide groups on indoor secondary organic aerosol. Environ. Sci. Technol.; 46:9290-9298.

Carslaw N., 2013. A mechanistic study of limonene oxidation products and pathways following cleaning activities. Atmos. Environ.; 80:507-513.

Carslaw N., Ashmore M., Terry A.C., Carslaw D.C. 2015. Crucial role for outdoor chemistry in ultrafine particle formation in modern office buildings. Environ. Sci. Technol.; 49(18):11011-11018.

Carslaw N., Fletcher L., Heard D., Ingham T., Walker H. 2017. Significant OH production under surface cleaning and air cleaning conditions: Impact on indoor air quality. Indoor Air; 00:1-10.

Carter W.P. 2000. Documentation of the SAPRC-99 chemical mechanism for VOC reactivity assessment. Contract; 92(329):95-308.

Carter W.P. 2003. The SAPRC-99 Chemical Mechanism and Updated VOC Reactivity Scales. California Air Resources Board.

Carter W.P.L. 2010. Development of the SAPRC-07 chemical mechanism. Atmos. Environ.; 44:5324-5335.

Cartier A. 2015. New causes of immunologic occupational asthma, 2012-2014. Curr. Opin. Allergy Clin. Immunol.; 15:117-123.

Chacon-Madrid H.J., Presto A.A., Donahue N.M. 2010. Functionalization vs. fragmentation: n-aldehyde oxidation mechanisms and secondary organic aerosol formation. Phys. Chem. Chem. Phys.; 12(42):13975-13982.

Chatzidiakou E., Mumovic D., Summerfield A.J., Altamirano H.M. 2015. Indoor air quality in London schools. Part 1:'performance in use'. Intell. Build Int.; 7(2-3):101-129.

Cheng Y.H., Lin C.C., Hsu S.C. 2015. Comparison of conventional and green building materials in respect of VOC emissions and ozone impact on secondary carbonyl emissions. Build. and Environ.; 87:274-282.

Cimmino A., Pecorella T., Fantacci R., Granelli F., Rahman T.F., Sacchi C., Carlini C., Harsh P. 2014. The role of small cell technology in future Smart City applications. T. Emerg. Telecommun. Technol., 25(1):11-20.

Clausen P.A., Wilkins C.K., Nielsen G.D. 2000. Formation of Strong Airway Irritants in Terpene/Ozone Mixtures. Indoor Air; 10(2):82–91.

Coleman B.K., Destaillats H., Hodgson A.T., Nazaroff W.W. 2008. Ozone consumption and volatile byproduct formation from surface reactions with aircraft cabin materials and clothing fabrics. Atmos. Environ.; 42(4):642-654.

Coley D.A. and Beisteiner A. 2002. Carbon dioxide levels and ventilation rates in schools. Int. J. Vent.; 1(1):45-52.

Conkle J.P., Camp B.J., Welch B.E. 1975. Trace composition of human respiratory gas. Arch. Enviorn. Health; 30: 290-295.

Cox S.S., Little J.C., Hodgson A.T. 2002. Predicting the emission rate of volatile organic compounds from vinyl flooring. Environ. Sci. Technol.; 36(4):709–714.

Criegee R. 1975. Mechanism of ozonolysis. Angewandte Chemie Int. Ed.; 14(11):745-752.

Cuéllar-Franca R.M. and Azapagic A. 2012. Environmental impacts of the UK residential sector: life cycle assessment of houses. Build. Environ.; 54:86-99.

Darling E., Morrison G.C., Corsi R.L. 2016. Passive removal materials for indoor ozone control. Build. Environ.; 106:33-44.

Dimitroulopoulou C., Ashmore M.R., Byrne M.A., Kinnersley R.P. 2001. Modelling of indoor exposure to nitrogen dioxide in the UK. Atmos. Environ.; 35(2):269-279.

Dimitroulopoulou C., Ashmore M.R., Hill M.T.R., Byrne M.A., Kinnersley R. 2006. INDAIR: a probabilistic model of indoor air pollution in UK homes. Atmos. Environ.; 40(33):6362-6379.

Dimitroulopoulou C. 2012. Ventilation in European dwellings: A review. Build. and Environ.; 47:109-125.

Drakou G., Zerefos C., Ziomas I., Voyatzaki M. 1998. Measurements and numerical simulations of indoor O3 and NOX in two different cases. Atmos. Environ.; 32(4):595-610.

Enderby B., Lenney W., Brady M., Emmett C., Španel P., Smith D. 2009. Concentrations of some metabolites in the breath of healthy children aged 7–18 years measured using selected ion flow tube mass spectrometry (SIFT-MS). J. Breath Res.; 3(3):036001.

EU AirBase dataset. Available online at: http://www.eea.europa.eu/data-and-maps/data/airbase-the-european-air-quality-database-3 (Date accessed September 2016).

Falls A. and Seinfeld J. 1978. Continued development of a kinetic mechanism for photochemical smog. Environ. Sci. Technol.; 12:1398-1406.

Fan Z., Lioy P., Weschler C., Fiedler N., Kipen H., Zhang J. 2003. Ozone-Initiated Reactions with Mixtures of Volatile Organic Compounds under Simulated Indoor Conditions. Environ. Sci. Technol.; 37:1811-1821.

Fenske J.D. and Paulson S.E. 1999. Human Breath Emissions of VOCs. J. Air Waste Manag. Assoc.; 49(5):594-598.

Fiadzomor P. 2002. Industrial placement report. Gas standards for indoor and in-car air. VAM 1.8 project, DTI ITT Number GBBK/C/14/26.

Fiedler N., Laumbach, R., Kelly-McNeil, K., Lioy, P., Fan, Z.-H., Zhang, J., Ottenweller J., Ohman-Strickland P., Kipen H. 2005. Health Effects of a Mixture of Indoor Air Volatile Organics, Their Ozone Oxidation Products, and Stress. Environ. Health Perspect.; 113(11):1542–1548.

Filipiak W., Ruzsanyi V., Mochalski P., Filipiak A., Bajtarevic A., Ager C., Denz H., Hilbe W., Jamnig H., Hackl M., Dzien A., Amann A. 2012. Dependence of exhaled breath composition on exogenous factors, smoking habits and exposure to air pollutants. J. Breath Res.; 6(3):36008.

Fischer A., Ljungström E., Langer S. 2013. Ozone removal by occupants in a classroom. Atmos. Environ.; 81:11-17.

Folberth G.A., Hauglustaine D.A., Lathiere J., Brocheton F. 2006. Interactive chemistry in the Laboratoire de M_et_eorologie Dynamique general circulation model: model description and impact analysis of biogenic hydrocarbons on tropospheric chemistry. Atmos. Chem. Phys.; 6:2319.

Forester C.D. and Wells J.R. 2011. Hydroxyl radical yields from reactions of terpene mixtures with ozone. Indoor Air; 21:400-409.

Fruekilde P., Hjort J., Jensen N.R., Kotzias D., Larsen B. 1998. Ozonolysis at vegetation surfaces: a source of acetone, 4-oxopentanal, 6-methyl-5-hepten-2-one, and geranyl acetone in the troposphere. Atmos. Environ.; 32:1893-1902.

Gall E.T., Darling E., Siegel J.A., Morrison G.C., Corsi R.L. 2013. Evaluation of three common green building materials for ozone removal, and primary and secondary emissions of aldehydes. Atmos. Environ.; 77:910-918.

Gall E.T., Siegel J.A., Corsi R.L. 2015. Modelling ozone removal to indoor materials, including the effects of porosity, pore diameter, and thickness. Environ. Sci. Technol.; 49(7):4398-4406.

Gandolfo A., Gligorovski V., Bartolomei V., Tlili S., Alvarez E.G., Wortham H., Kleffmann J., Gligorovski S. 2016. Spectrally resolved actinic flux and photolysis frequencies of key species within an indoor environment. Build. Environ.; 109:50–57.

Geiss O., Giannopoulos G., Tirendi S., Barrero-Moreno J., Larsen B. R., Kotzias D. 2011. The AIRMEX study-VOC measurements in public buildings and schools/kindergartens in eleven European cities: Statistical analysis of the data. Atmos. Environ.; 45(22): 3676-3684.

Godwin C. and Batterman S. 2007. Indoor air quality in Michigan schools. Indoor Air; 17(2):109-121.

Google Maps. Available online at: https://maps.google.com/ (date accessed September 2017).

Grontoft T. and Raychaudhuri M.R. 2004. Compilation of tables of surface deposition velocities for O_3, NO_2 and SO_2 to a range of indoor surfaces. Atmos. Environ.; 38(4):533-544.

Ham J.E., Jackson S.R., Harrison J.C., Wells J.R. 2015. Gas-phase reaction products and yields of terpinolene with ozone and nitric oxide using a new derivatization agent. Atmos. Environ.; 122:513-520.

Ham J.E., Harrison J.C., Jackson S.R., Wells J.R. 2016. Limonene ozonolysis in the presence of nitric oxide: Gas-phase reaction products and yields. Atmos. Environ.; 132:300-308.

Hancke G.P. and Hancke Jr G.P. 2012. The role of advanced sensing in smart cities. Sensors; 13(1):393-425.

Hansel A., Jordan A., Holzinger R., Prazeller P., Vogel W., Lindinger W. 1995. Proton transfer reaction mass spectroscopy on-line trace gas analysis at the ppb level. Int. J. Mass Spec. Ion Proc.; 149/150:609-619.

Hauglustaine D.A., Hourdin F., Jourdain L., Filiberti M.A.,Walters S., Lamarque J.F., Holland E.A. 2004. Interactive chemistry in the Laboratoire de M_et_eorologie Dynamique general circulation model: description and background tropospheric chemistry evaluation. J. Geophys. Res. Atmos. 109.

Health Effects of School Environment (HESE). 2006. Final scientific report [online]. Available online at: http://ec.europa.eu/health/ph_projects/2002/pollution/pollution_2002_04_en.htm (Date accessed May 2017).

Hoang C.P., Kinney K.A., Corsi R.L. 2009. Ozone removal by green building materials. Build. Environ.; 44(8):1627-1633.

Hodgson A. T., Beal D., McIlvaine J.E.R. 2002. Sources of formaldehyde, other aldehydes and terpenes in a new manufactured house. Indoor Air; 12(4):235-242.

Hoffmann T., Bandur R., Seinfeld J.H. 1997. Experimental and theoretical studies on the aerosol formation potential of natural VOCs. Workshop on Biogenic Hydrocarbons. American Meteorological Society. University of Virginia 24—27 August; 131—134.

Horvath E.P. 1997. Building-related illness and sick building syndrome: from the specific to the vague. Cleve. Clin. J. Med.; 64(6):303-309.

IUPAC (2016). Task Group on Atmospheric Chemical Kinetic Data Evaluation. Available online at: http://www.iupac-kinetic.ch.cam.ac.uk/ (Date accessed June 2016).

James J.P. and Yang X. 2005. Emissions of volatile organic compounds from several green and non-green building materials: a comparison. Indoor Built Environ.; 14(1):69-74.

Jamriska M., Morawska L., Ensor D.S. 2003. Control strategies for sub-micrometer particles indoors: model study of air filtration and ventilation. Indoor Air; 13(2):96-105.

Järnström H., Saarela K., Kalliokoski P. E. A., Pasanen A. L. 2006. Reference values for indoor air pollutant concentrations in new, residential buildings in Finland. Atmos. Environ.; 40(37): 7178-7191.

Jarvis J., Seed M.J., Elton R.A., Sawyer L., Agius R.M. 2005. Relationship between chemical structure and the occupational asthma hazard of low molecular weight organic compounds. Occup. Environ. Med.; 62:243-250.

Jenkin M.E., Saunders S.M., Pilling M.J. 1997. The tropospheric degradation of volatile organic compounds: a protocol for mechanism development. Atmos. Environ.; 31(1):81-104.

Jenkin M.E., Saunders S.M., Wagner V., Pilling M.J. 2003. Protocol for the development of the Master Chemical Mechanism, MCM v3 (Part B): tropospheric degradation of aromatic volatile organic compounds. Atmos. Chem. Phys.; 3(1):181-193.

Jones A.P. 1999. Indoor air quality and health. Atmos. Environ.; 33(28):4535-4564.

Kim S., Kim J.A., Kim H.J., Do Kim S. 2006. Determination of formaldehyde and TVOC emission factor from wood-based composites by small chamber method. Polym. Test.; 25(5):605-614.

Kitchin R. 2014. The real-time city? Big data and smart urbanism. GeoJournal; 79(1):1-14.

Klenø J.G., Clausen P.A., Weschler C.J., Wolkoff P. 2001. Determination of ozone removal rates by selected building products using the FLEC emission cell. Environ. Sci. Technol.; 35(12):2548-2553.

Knudsen H.N., Kjaer U.D., Nielsen P.A., Wolkoff P. 1999. Sensory and chemical characterization of VOC emissions from building products: impact of concentration and air velocity. Atmos. Environ.; 33:1217-1230.

Kotzias D., Koistinen K., Kephalopulos S., Schlitt C., Carrer P., Maroni M., Jantunen M., Cochet C., Kirchner S., Lindvall T., McLaughlin J., Molhave L., de Oliveira Fernandez E., Seifert B. 2005. The INDEX project – Critical appraisal of the setting and implementation of indoor exposure limits in the EU. European Commission – Joint Research Centre, Ispra.

Lahtinen M., Huuhtanen P., Reijula K. 1998. Sick building syndrome and psychosocial factors } a literature review. Indoor Air; (Suppl 4):71-80.

Lakey P.S.J., Wisthaler A., Berkemeier T., Mikoviny T., Pöschl T., Shiraiwa M. 2016. Chemical kinetics of multiphase reactions between ozone and human skin lipids: Implications for indoor air quality and health effects. Indoor Air; 00:1-13.

Lamble S.P., Corsi R.L., Morrison G.C. 2011. Ozone deposition velocities, reaction probabilities and product yields for green building materials. Atmos. Environ.; 45(38):6965-6972.

Langford V.S., Graves I., McEwan M.J. 2014. Rapid monitoring of volatile organic compounds: a comparison between gas chromatography/mass spectrometry and selected ion flow tube mass spectrometry. Rapid Commun. Mass Spectrom.; 28(1):10-18.

Lechner M., Moser B., Niederseer D., Karlseder A., Holzknecht B., Fuchs M., Colvin S., Tilg H., Rieder J. 2006. Gender and age specific differences in exhaled isoprene levels. Res. Physiol. Neurobiol.; 154:478-483.

Lee S.C., Li W.M., Ao C.H. 2002. Investigation of indoor air quality at residential homes in Hong Kong - case study. Atmos. Environ.; 36(2):225-237.

Lim S., Lee K., Seo S., Jang S. 2011. Impact of regulation on indoor volatile organic compounds in new unoccupied apartment in Korea. Atmos. Environ.; 45(11):1994-2000.

Lin H.H., Ezzati M., Murray M. 2007. Tobacco Smoke, Indoor Air Pollution and Tuberculosis: A Systematic Review and Meta-Analysis. PloS Med.; 4(1):173-189.

Lin C.C. and Hsu S.C. 2015. Deposition velocities and impact of physical properties on ozone removal for building materials. Atmos. Environ.; 101:194-199.

Liu W., Zhang J., Zhang L., Turpin B.J., Weisel C.P., Morandi M.T., Stock T.H., Colome S., Korn L.R. 2006. Estimating contributions of indoor and outdoor sources to indoor carbonyl concentrations in three urban areas of the United States. Atmos. Environ.; 40(12):2202-2214.

Liu W., Zhang J.J., Korn L.R., Zhang L., Weisel C.P., Turpin B., Morandi M., Stock T., Colome S. 2007. Predicting personal exposure to airborne carbonyls using residential measurements and time/activity data. Atmos. Environ.; 41(25):5280-5288.

Liu S., Thompson S.L., Stark H., Ziemann P.J., Jimenez J.L. 2017. Gas-phase carboxylic acids in a university classroom: abundance, variability, and sources. Environ. Sci. Technol.; 51(10):5454-5463.

Marchand C., Bulliot B., Le Calvé S., Mirabel Ph. 2006. Aldehyde measurements in indoor environments in Strasbourg (France). Atmos. Environ.; 40(7):1336-1345.

Marlier M.E., Jina A.S., Kinney P.L., DeFries R.S. 2016. Extreme air pollution in global megacities. Current Clim. Change Rep.; 2(1):15-27.

MCM, University of Leeds. Available online at: http://mcm.leeds.ac.uk/MCM/ (date accessed March 2017).

Medina-Ramon M., Zock J.-P., Kogevinas M., Sunyer J., Torralba Y., Borrell A., Burgos F., Antó J.M. 2005. Asthma, chronic bronchitis, and exposure to irritant agents in occupational domestic cleaning: a nested case-control study. Occup. Environ. Med.; 62(9):598-606.

Meininghaus R., Salthammer T., Knöppel H. 1999. Interaction of volatile organic compounds with indoor materials—a small-scale screening method. Atmos. Environ.; 33(15):2395-2401.

Mendell M.J. and Heath G.A. 2005. Do indoor pollutants and thermal conditions in schools influence student performance? A critical review of the literature. Indoor Air; 15(1):27-52.

Mendell M.J. 2007. Indoor residential chemical emission as risk factors for respiratory and allergic effects in children: a review. Indoor Air; 17(4):259-277.

Mendez M., Blond N., Blondeau P., Schoemaecker C., Hauglustaine D.A. 2015. Assessment of the impact of oxidation processes on indoor air pollution using the new time-resolved INCA-Indoor model. Atmos. Environ.; 122:521-530.

Mitragotri S. 2002. A theoretical analysis of permeation of small hydrophobic solutes across the stratum corneum based on scaled particle theory. J. Pharm. Sci.; 91:744−752.

Mochalski P, King J, Unterkofler K, Hinterhuber H, Amann A. 2014. Emission rates of selected volatile organic compounds from skin of healthy volunteers. J. Chromatogr. B; 959:62-70.

Morrison G.C. and Nazaroff W.W. 2000. The Rate of Ozone Uptake on Carpets: Experimental Studies. Environ. Sci. Technol.; 34(23):4963–4968.

Morrison G.C. and Nazaroff W. 2002. Ozone Interactions with Carpet: Secondary Emissions of Aldehydes. Environ. Sci. Technol.; 36:2185-2192.

Morrison G.C., Li H., Mishra S., Buechlein M. 2015. Airborne phthalate partitioning to cotton clothing. Atmos. Environ.; 115:149-152.

Morrison G.C., Shakila N.V., Parker K. 2015. Accumulation of gas-phase methamphetamine on clothing, toy fabrics, and skin oil. Indoor Air; 25(4):405-414.

Morrison G.C. 2015. Recent Advances in Indoor Chemistry. Curr. Sust/Renew Energ. Rep.; 2(2):33-40.

Morrison G.C., Weschler C.J., Bekö G. 2016. Dermal uptake directly from air under transient conditions: advances in modelling and comparisons with experimental results for human subjects. Indoor Air; 26(6):913-924.

Morrison G.C., Weschler C.J., Bekö G., Koch H.M., Salthammer T., Schripp T., Toftum J., Clausen G. 2016. Role of clothing in both accelerating and impeding dermal absorption of airborne SVOCs. J. Expo. Sci. Environ. Epidemiol.; 26(1):113-118.

Morrison G.C., Weschler C.J., Bekö G. 2017. Dermal uptake of phthalates from clothing: Comparison of model to human participant results. Indoor Air; 27(3):642-649.

Murray R.W. 1968. Mechanism of ozonolysis. Acc. Chem. Res.; 1(10):313-320.

Murray D.M. and Burmaster D.E. 1995. Residential air exchange rates in the United States: empirical and estimated parametric distributions by season and climatic region. Risk Analys.; 15(4):459–465.

Nazaroff W.W. and Cass G.R. 1986. Mathematical modelling of chemically reactive pollutants in indoor air. Environ. Sci. Technol.; 20(9):924-934.

Nazaroff W.W. and Weschler C.J. 2004. Cleaning products and air fresheners: exposure to primary and secondary air pollutants. Atmos. Environ.; 38:2841-2865.

Nam T. and Pardo T.A. 2011. Conceptualizing smart city with dimensions of technology, people, and institutions. In Proceedings of the 12th annual international digital government research conference: digital government innovation in challenging times. ACM; 282-291.

Nguyen H.T.-H., Takenaka N., Bandow H., Maeda Y., de Oliva S.T., Botelho M.M.f., Tavares T.M. 2001. Atmospheric alcohols and aldehydes concentrations measured in Osaka, Japan and in Sao Paulo, Brazil. Atmos. Environ.; 35(18):3075-3083.

Nicolas M, Ramalho O, Maupetit F. 2007. Reactions between ozone and building products: Impact on primary and secondary emissions. Atmos. Environ.; 41(15):3129-3138.

Nørgaard A.W., Vibenholt A., Benassi M., Clausen P.A., Wolkoff P. 2013. Study of ozone-initiated limonene reaction products by low temperature plasma ionization mass spectrometry. J. Am. Soc. Mass Spectrom.; 24(7):1090-1096.

Nørgaard A.W., Kudal J.D., Kofoed-Sørensen V., Koponen I.K., Wolkoff P. 2014. Ozone-initiated VOC and particle emissions from a cleaning agent and an air freshener: Risk assessment of acute airway effects. Environ. Int.; 68:209-218.

Paulson S.E., Flagan R.C., Seinfeld J.H. 1992. Atmospheric photooxidation of isoprene part I: The hydroxyl radical and ground state atomic oxygen reactions. Int. J. Chem. Kinet.; 24(1):79-101.

Paulson S.E. and Seinfeld J.H. 1992. Development and evaluation of a photooxidation mechanism for isoprene. J. Geophys. Res.: Atmos.; 97(D18):20703-20715.

Paulson S.E., Sen A.D., Llu P., Fenske J.D., Fox M.J. 1997. Evidence for formation of OH radicals from the reaction of O3 with alkenes in the gas phase. Geophys. Res. Lett.; 24:3193-3196.

Paulson S.E., Chung M.Y., Hasson A.S. 1999. OH radical formation from the gas-phase reaction of ozone with terminal alkenes and the relationship between structure and mechanism. J. Phys. Chem. A; 103:8125-8138.

Perera E. and Parkins L. 1992. Airtightness of UK buildings: status and future possibilities. Environ. Policy Pract.; 2:143–160.

Petrick L. and Dubowski Y. 2009. Heterogeneous oxidation of squalene film by ozone under various indoor conditions. Indoor Air; 19:381-391.

Philip K.E.J., Pack E., Cambiano V., Rollmann H., Weil S., O'Beirne J. 2015. The accuracy of respiratory rate assessment by doctors in a London teaching hospital: a cross-sectional study. J. Clin. Monit. Comput.; 29(4):455-460.

Phillips M. and Greenberg J. 1991. Method for the collection and analysis of volatile compounds in the breath. J. Chrom.; 564:242-249.

Plaisance H., Blondel A., Desauziers V., Mocho P. 2014. Hierarchical cluster analysis of carbonyl compounds emission profiles from building and furniture materials. Build. Environ.; 75:40-45.

Poppendieck D., Hubbard H., Ward M., Weschler C.J., Corsi R.L. 2007. Ozone reactions with indoor materials during building disinfection. Atmos. Environ.; 41(15):3166-3176.

Persily A. 2006. What we think we know about ventilation. Int. J. Vent.; 5(3):275-290.

Proffesor Charles J. Weschler, The State University of New Jersey, USA, personal communication.

Quirce S., Barranco P. 2010. Cleaning agents and asthma. J. Investig. Allergol. Clin. Immunol.; 20:542-550.

Rai A.C., Guo B., Lin C.-H., Zhang J., Pei J., Chen Q. 2014. Ozone reaction with clothing and its initiated VOC emissions in an environmental chamber. Indoor Air; 24:49-58.

Raunemaa T., Kulmala M., Saari H., Olin M., Kulmala M.H. 1989. Indoor Air Aerosol Model: Transport Indoors and Deposition of Fine and Coarse Particles. Aerosol Sci. Technol.; 11(1):11-25.

Reilly M.J and Rosenman K.D. 1995. Use of hospital discharge data for surveillance of chemical-related respiratory disease. Arch. Environ. Health; 50:26–30.

Reiss R., Ryan P.B., Koutrakis P. 1994. Modelling ozone deposition onto indoor residential surfaces. Environ. Sci. Technol.; 28(3):504-513.

Reiss R., Ryan P.B., Tibbetts S.J., Koutrakis P. 1995. Measurement of organic acids, aldehydes, and ketones in residential environments and their relation to ozone. J. Air Waste Manag. Assoc.; 45(10):811-822.

Rim D., Gall E.T., Maddalena R.L., Nazaroff W.W. 2016. Ozone reaction with interior building materials: Influence of diurnal ozone variation, temperature and humidity. Atmos. Environ.; 125:15-23.

Rim D., Gall E.T., Ananth S., Won Y. 2018. Ozone reaction with human surfaces: Influences of surface reaction probability and indoor air flow condition. Build. Environ.; 130:40-48.

Rohr A., Weschler C.J., Koutrakis P., Spengler J.D. 2003. Generation and Quantification of Ultrafine Particles through Terpene/Ozone Reactions in a Chamber Setting. Aerosol Sci. Technol.; 37:65-78.

Rossignol S., Chiappini L., Perraudin E., Rio C., Fable S., Valorso R., Doussin J.F. 2012. Development of a parallel sampling and analysis method for the elucidation of gas/particle partitioning of oxygenated semi-volatile organics: a limonene ozonolysis study. Atmos. Meas. Tech.; 5(6):1459-1489.

Roulet C.A. and Foradini F. 2002. Simple and cheap air change rate measuring using CO_2 concentration decays. Int. J. Vent.; 1(1):39-44.

Rudd A. 2008. Volatile organic compound concentrations and emission rates in new manufactured and site-built houses. Build. Sci. Corp.

Sabersky R.H., Sinema D.A., Shair F.H. 1973. Concentrations, decay rates, and removal of ozone and their relation to establishing clean indoor air. Environ. Sci. Technol.; 7(4):347–353.

Salthammer T., Mentese S., Marutzky R. 2010. Formaldehyde in the indoor environment. Chem. Rev.; 110(4):2536-2572.

Sarwar G., Corsi R., Kimura Y., Allen D., Weschler C.J. 2002. Hydroxyl radicals in indoor environments. Atmos. Environ.; 36(24):3973-3988.

Sarwar G., Olson D.A., Corsi R.L., Weschler C.J. 2004. Indoor fine particles: the role of terpene emissions from consumer products. J. Air Waste Manag. Assoc.; 54(3):367-377.

Saunders S.M., Jenkin M.E., Derwent R.G., Pilling M.J. 2003. Protocol for the development of the Master Chemical Mechanism, MCM v3 (Part A): tropospheric degradation of non-aromatic volatile organic compounds. Atmos. Chem. Phys.; 3(1):161-180.

SCHER. 2007. Scientific Committee on Health and Environmental Risks. Opinion on Risk Assessment on Indoor Air Quality. European Commission: Health & Consumer Protection Directorate e General, Brussels; 1-33.

Schoemaecker C., Verriele M., Hanoune B., Petitprez D., Leclerc N., Dusanter S., Le Calve S., Millet M., Bernhardt P., Mendez M., Blond N., Hauglustaine D., Clappier A., Blondeau P., Abadie M., Locoge N. 2014. Characterization of the IAQ in low energy public buildings in France through a dual experiment and modelling approach. In: Proceedings of the 13th International Conference on Indoor Air Quality and Climate. Hong-Kong; 000-008.

Schripp T., Etienne S., Fauck C., Fuhrmann F., Märk L., Salthammer T. 2014. Application of proton-transfer-reaction-mass-spectrometry for indoor air quality research. Indoor Air; 24(2):178-189.

Sharma B. and Mehta G. 2014. Selection of Materials for Green Construction: A Review. J. Mech. Civil Eng.; 11(6):80-83.

Shaughnessy R.J., Haverinen-Shaughnessy U., Nevalainen A., Moschandreas D. 2006. A preliminary study on the association between ventilation rates in classrooms and student performance. Indoor Air; 16(6):465-468.

Sherlach K.S., Gorka A.P., Dantzler A., Roepe P.D. 2011. Quantification of perchloroethylene residues in dry-cleaned fabrics. Environ. Toxicol. Chem.; 30:2481-2487.

Shiraiwa M., Pfrang C., Pöschl U. 2010. Kinetic multi-layer model of aerosol surface and bulk chemistry (KM-SUB): the influence of interfacial transport and bulk diffusion on the oxidation of oleic acid by ozone. Atmos. Chem. Phys.; 10:3673‑3691.

Seppänen O., Fisk W.J., Lei Q.H. 2006. Ventilation and performance in office work. Indoor Air; 16:28–36.

Shaughnessy R.J., Haverinen-Shaughnessy U., Nevalainen A., Moschandreas D. 2006. A preliminary study on the association between ventilation rates in classrooms and student performance. Indoor Air; 16(6):465-468.

Singer B.C., Destaillats H., Hodgson A.T., Nazaroff W.W. 2006. Cleaning products and air fresheners: emissions and resulting concnetrations of glycol esthersand terpenoids. Indoor Air; 16(3):179-191.

Singer B.C., Hodgson A.T., Hotchi T., Ming K.Y., Sextro R.G., Wood E.E., Brown N.J. 2007. Sorption of organic gases in residential rooms. Atmos. Environ.; 41(15):3251-3265.

Stephen R.K. 1998. Airtightness in UK dwellings: BRE's test results and their significance. BRE Report BR 359; CRC Ltd.

Stönner C., Edtbauer A., Williams J. 2017. Real world volatile organic compound emission rates from seated adults and children for use in indoor air studies. Indoor Air.

Suk W.A., Murray K., Avakian M.D. 2003. Environmental hazards to children's health in the modern world. Mutation Res./Rev. in Mutation Res.; 544(2-3):235-242.

Sundell J., Levin H., Nazaroff W.W., Cain W.S., Fisk W.J., Grimsrud D.T., Gyntelberg F., Li Y., Persily A.K., Pickering A.C., Samet J.M. 2011. Ventilation rates and health: multidisciplinary review of the scientific literature. Indoor Air; 21(3):191-204.

Tae S., Shin S., Woo J., Roh S. 2011. The development of apartment house life cycle CO_2 simple assessment system using standard apartment houses of South Korea. Renew Sust. Energ. Rev.; 15(3):1454-1467.

Tamás G., Weschler C.J., Bakó-Biró Z., Wyon D.P., Strøm-Tejsen P. 2006. Factors affecting ozone removal rates in a simulated aircraft cabin environment. Atmos. Environ.; 40(32):6122-6133.

Tang X., Misztal P.K., Nazaroff W.W., Goldstein A.A. 2016. Volatile Organic Compound Emissions from Humans Indoors. Environ. Sci. Technol.; 50(23):12686-12694.

Taucher J., Lagg A., Hansel A., Vogel W., Lindinger W. 1995. Methanol in human breath. Alcohol Clin. Exp. Res.; 19(5):1147-1150.

Terry A.C., Carslaw N., Ashmore M., Dimitroulopoulou S., Carslaw D.C. 2014. Occupant exposure to indoor air pollutants in modern European offices: An integrated modelling approach. Atmos. Environ.; 82:9-16.

Tham K.W. 2016. Indoor air quality and its effects on humans—A review of challenges and developments in the last 30 years. Energ. Buildings; 130:637-650.

The CAPACITIE project. Available online at: https://www.york.ac.uk/yesi/projects/capacitie/ (date accessed July 2017).

The EU OFFICAIR project. Available online at: http://www.officair-project.eu/ (date accessed September 2017).

The European Chemicals Agency (ECHA). Available online at: https://echa.europa.eu/ (date accessed December 2017).

The MCPA Software. Available online at: http://www.mcpa-software.com/ (date accessed August 2017).

Trantallidi M., Dimitroulopoulou C., Wolkoff P., Kephalopoulos S., Carrer P. 2015. EPHECT III: Health risk assessment of exposure to household consumer products. Sci. Total Environ.; 536:903-913.

TripAdvisor. Available online at: http://www.tripadvisor.com/ (date accessed September 2017).

Twardella D., Matzen W., Lahrz T., Burghardt R., Spegel H., Hendrowarsito L., Frenzel A.C., Fromme H. 2012. Effect of classroom air quality on students' concentration: results of a cluster-randomized cross-over experimental study. Indoor Air; 22(5):378-387.

Uhde E. and Salthammer T. 2007. Impact of reaction products from building materials and furnishings on indoor air quality—a review of recent advances in indoor chemistry. Atmos. Environ.; 41(15):3111-3128.

Wallace L., Nelson C.W., Pellizzari E., Raymer J.H., Thomas K.W. 1991. Identification of Polar Volatile Organic Compounds in Consumer Products and Common Microenvironments. In Proceedings of the Air and Waste Management Association's. Annual Meeting, Vancouver, British Columbia, Canada; 91:62-64.

Wallace L. 1996. Indoor particles: a review. J. Air Waste Manag. Assoc.; 46:98–126.

Walser M.L., Desyaterik Y., Laskin J., Laskin A., Nizkorodov S.A. 2008. High-resolution mass spectrometric analysis of secondary organic aerosol produced by ozonation of limonene. Phys. Chem. Chem. Phys.; 10(7):1009-1022.

Wang H. and Morrison G.C. 2006. Ozone-Initiated Secondary Emission Rates of Aldehydes from Indoor Surfaces in Four Homes. Environ. Sci. Technol.; 40:5263-5268.

Wang H. and Morrison G.C. 2010. Ozone-surface reactions in five homes: surface reaction probabilities, aldehyde yields, and trends. Indoor Air; 20(3):224-234.

Wang C.M., Barratt B., Carslaw N., Doutsi A., Dunmore R.E., Warda M.W., Lewis A.C. 2017. Unexpecedly high concentrations of monoterpenes in a study of UK homes. Environ. Sci.: Processes Impacts; 19:528.

Wargocki P., Wyon D.P., Sundell J., Clausen G., Fanger P. 2000. The effects of outdoor air supply rate in an office on perceived air quality, sick building syndrome (SBS) symptoms and productivity. Indoor Air; 10(4):222-236.

Wargocki P. and Wyon D.P. 2007. The effects of moderately raised classroom temperatures and classroom ventilation rate on the performance of schoolwork by children (RP-1257). Hvac&R Res.; 13(2):193-220.

Waring M.S. and Siegel J.A. 2013. Indoor secondary organic aerosol formation initiated from reactions between ozone and surface-sorbed d-Limonene. Environ. Sci. Technol.; 47(12):6341-6348.

Waring M.S. and Wells J.R. 2015. Volatile organic compound conversion by ozone, hydroxyl radicals, and nitrate radicals in residential indoor air: magnitudes and impacts of oxidant sources. Atmos. Environ.; 106:382-391.

Warneke C., Kuczynski J., Hansel A., Jordan A., Vogel W., Lindinger W. 1996. Proton transfer reaction mass spectrometry: propanol in breath. Int. J. Mass Spec. Ion Proc.; 154: 61-70.

Warren P.R. and Webb B.C. 1980. Ventilation measurements in housing. Paper by BRE in CIBS Conference on Natural Ventilation by Design, 2 December 1980.

Wells J.R., Morrison G., Coleman B. 2008. Kinetics and reaction products of ozone and surface-bound squalene. J. ASTM Int.; 5:1–12.

Wells J.R. and Ham J.E. 2014. A new agent for derivatizing carbonyl species used to investigate limonene ozonolysis. Atmos. Environ.; 99:519-526.

Weschler C.J, Hodgson A.T., Wooley J.D. 1992. Indoor chemistry: ozone, volatile organic compounds and carpets. Environ. Sci. Technol.; 26:2371-7.

Weschler C.J., Shields H.C., Nalk D.V. 1994. Indoor chemistry involving O_3, NO, and NO_2 as evidenced by 14 months of measurements at a site in southern California. Environ. Sci. Technol.; 28:2120–2132.

Weschler C.J. and Shields H.C. 1996. Production of the hydroxyl radical in indoor air. Environ. Sci. Technol.; 30:3250–3258.

Weschler C.J. 2000. Ozone in indoor environments: concentration and chemistry. Indoor Air; 10(4):269–288.

Weschler C.J. 2006. Ozone's impact on public health: contributions from indoor exposures to ozone and products of ozone-initiated chemistry. Environ. Health Perspect.; 114:1489‑1496.

Weschler C.J., Wishaler A., Cowlin S., Tamás G., Strøm-Tejsen P., Hodgson A.T., Destaillats H., Herrington J., Zhang J., Nazaroff W.W. 2007. Ozone-Initiated Chemistry in an Occupied Simulated Aircraft Cabin. Environ. Sci. Technol.; 41(17):6177-6184.

Weschler C.J. 2011. Chemistry in indoor environments: 20 years of research. Indoor Air; 21(3):205-218.

Weschler C.J. and Nazaroff W.W. 2013. Dermal uptake of organic vapors commonly found in indoor air. Environ. Sci. Technol.; 48(2):1230-1237.

Weschler C.J., Bekö G., Koch H.M., Salthammer T., Schripp T., Toftum J., Clausen G. 2015. Transdermal uptake of diethyl phthalate and di (n-butyl) phthalate directly from air: experimental verification. Environ. Health Perspect.; 123(10):928.

Weschler C.J. 2016. Roles of the human occupant in indoor chemistry. Indoor Air; 26:6-24.

Wilke O., Jann O., Brödner D. 2004. VOC- and SVOC-emissions from adhesives, floor coverings and complete floor structures. Indoor Air; 14(8):98–107.

Wisthaler A. and Weschler C.J. 2010. Reactions of ozone with human skin lipids: Sources of carbonyls, dicarbonyls, and hydroxycarbonyls in indoor air. PNAS; 107(15):6568-6575.

Wolkoff P., Schneider T., Kildesø J., Degerth R., Jaroszewski M., Schunk H. 1998. Risk in cleaning: chemical and physical exposure. Sci. Total Environ.; 215(1):135-156.

Wolkoff P. 1999. How to measure and evaluate volatile organic compound emissions from building products. A perspective. Sci. Total Environ.; 227:197‑213.

Wolkoff P., Clausen P.A., Wilkins C.K., Nielsen G.D. 2000. Formation of Strong Airway Irritants in Terpene/Ozone Mixtures. Indoor Air; 10(2):82–91.

Wolkoff P. and Nielsen G.D. 2001. Organic compounds in indoor air—their relevance for perceived indoor air quality?. Atmos. Environ.; 35(26):4407-4417.

Wolkoff P., Wilkins C.K., Clausen P.A., Nielsen G.D. 2006. Organic compounds in office environments – sensory irritation odor measurements and the role of reactive chemistry. Indoor Air; 16:7‑19.

Wolkoff P., Clausen P.A., Larsen K., Hammer M., Larsen S.T., Nielsen G.D. 2008. Acute airway effects of ozone-initiated d-limonene chemistry: importance of gaseous products. Toxicol. Lett.; 181:171-176.

Wolkoff P. and Nielsen G.D. 2010. Non-cancer effects of formaldehyde and relevance for setting an indoor air guideline. Environ. Int.; 36(7):788-799.

Wolkoff P., Clausen P.A., Larsen S.T., Hammer M., Nielsen G.D. 2012. Airway effects of repeated exposures to ozone-initiated limonene oxidation products as model of indoor air mixtures. Toxicol. Lett.; 209:166-172.

Wolkoff P. 2013. Indoor air pollutants in office environments: assessment of comfort, health, and performance. Int. J. Hyg. Environ. Health; 216(4):371-394.

Wolkoff P., Larsen S.T., Hammer M., Kofoed-Sørensen V., Clausen P.A., Nielsen G.D. 2013. Human reference values for acute airway effects of five common ozone-initiated terpene reaction products in indoor air. Toxicol. Lett.; 216:54-64.

Wong J.P.S., Carslaw N., Zhao R., Zhou S., Abbatt, J.P.D. 2017. Observations and impacts of bleach washing on indoor chlorine chemistry. Indoor Air.

Woods V. and Buckle P. 2006. Musculoskeletal ill health amongst cleaners and recommendations for work organisational change. Int. J. Ind. Ergon.; 36(1):61-72.

World Health Organisation (WHO). 2005. Effects of Air Pollution On Children's Health and Development – A Review of the Evidence, WHO Regional Office for Europe, Denmark, WHO Press.

World Health Organization (WHO). 2007. Available online at: http://www.who.int/growthref/who2007_weight_for_age/en/ (Date accessed February 2017).

World Health Organization (WHO). 2010. WHO guidelines for indoor air quality: selected pollutants.

Yu J.Z., Flagan R.C., Seinfeld J.H. 1998. Identification of products containing -COOH, -OH, and –CdO in atmospheric oxidation of hydrocarbons. Environ. Sci. Technol.; 32:2357–2370.

Zhang L., Moran M. D., Makar P. A., Brook J. R., Gong S. 2002. Modelling gaseous dry deposition in AURAMS: A unified regional air quality modelling system. Atmos. Environ.; 36(3):537−560.

Zhu J., Wong S.L., Cakmak S. 2013. Nationally representative levels of selected volatile organic compounds in Canadian residential indoor air: population-based survey. Environ. Sci. Technol.; 47(23):13276-13283.

Zhou S., Forbes M.W., Katrib Y., Abbatt J.P.D. 2016. Rapid Oxidation of Skin Oil by Ozone. Environ. Sci. Technol. Lett.; 3:170-174.

Zock J.P. 2005. World at work: Cleaners. Occup. Environ. Med.; 62(8):581-584.